

# UC San Diego

## UC San Diego Electronic Theses and Dissertations

### Title

Synthesis of electron-poor bifunctional ligands and their use in catalysis

### Permalink

<https://escholarship.org/uc/item/7td1t749>

### Author

Sattler, Daniel J

### Publication Date

2023

Peer reviewed|Thesis/dissertation

UNIVERSITY OF CALIFORNIA SAN DIEGO

SAN DIEGO STATE UNIVERSITY

Synthesis of electron-poor bifunctional ligands and their use in catalysis

A dissertation submitted in partial satisfaction of the requirements for the degree of Doctor of  
Philosophy

in

Chemistry

by

Daniel James Sattler

Committee in charge:

San Diego State University

Professor Douglas B. Grotjahn, Chair

Professor Thomas Cole

University of California San Diego

Professor Katherine Barbeau

Professor Guy Bertrand

Professor Jerry Yang

2023

Copyright

Daniel James Sattler, 2023

All rights reserved

The dissertation of Daniel James Sattler is approved, and it is in acceptable quality and form for publication on microfilm and electronically.

---

---

---

---

---

---

---

(Chair)

University of California San Diego

San Diego State University

2023

## **Dedication**

I would like to dedicate this work to my family, Roger, Betsy, and Jenny Sattler, without whose support and love I never would have made it this far.

## Table of Contents

Dissertation Approval Page .....	iii
Dedication .....	iv
Table of Contents .....	v
List of Figures .....	viii
List of Schemes .....	x
List of Tables .....	xii
Acknowledgements .....	xiii
Vita .....	xiv
Abstract of the Dissertation .....	xiv
Chapter 1 Background and introduction .....	1
1.1 Introduction .....	1
1.2 Addition of polar hydroxyl groups to an alkene .....	1
1.2.1 Addition of water to form an alcohol with the same number of carbon atoms .....	1
1.2.1.1 Previous Methods .....	1
1.2.1.2 Overall addition using a triple relay metal catalyst .....	3
1.2.2 Addition of carboxylic acids and alcohols .....	3
1.2.2.1 Previous methods .....	3
1.3 Addition of N-H .....	3
1.3.1 Previous Methods .....	4
1.4 Addition of less polar X-H bonds (B, Si) .....	4
1.4.1 Addition of B-H bonds to an alkene .....	4
1.4.1.1 Non metal-catalyzed .....	4
1.4.1.2 Metal Catalyzed .....	5

1.4.2 Addition of Si-H bonds to alkenes.....	5
1.5 Bifunctional Ligands.....	6
1.6 Electron-poor ligands.....	8
1.6.1 Definition and methods to determine donation strength.....	8
1.6.2 Determination of electron donating strength of phosphine ligands.....	9
1.6.3 Phosphites and phosphonates in catalysis.....	10
1.6.4 Changing a catalytic cycle.....	10
1.6.5.1 Increased rate of reductive elimination.....	10
1.6.5.2 Lower rate of oxidative addition.....	11
1.7 Summary of electron-poor and bifunctional ligand properties and potential uses.....	11
Chapter 2 Bidentate hybrid electron-poor phosphonate.....	12
Chapter 3 Imidazole based electron-poor ligands.....	20
3.1 Background and goals.....	20
3.2 Strategy and reasoning.....	22
3.3 Initial testing for catalytic activity.....	26
3.4 Catalytic investigation involving high-throughput experimentation in collaboration with the University of Pennsylvania.....	29
3.4.1 Hypothesis and design of experiments.....	29
3.4.2 Results.....	31
Figure 3.4.2.1 An example of one gas chromatographic trace showing the complexity of one reaction.....	31
Chapter 4 Phenol- and anisole-based ligands.....	32
4.1 Oxidative addition of water to platinum complexes.....	32
4.2 Synthesis of monodentate electron-poor bifunctional ligands.....	38
4.2: Addition of carbon monoxide and either H <sub>2</sub> , H <sub>2</sub> O, or ROH.....	42

4.2.1 Hydroformylation/Reduction .....	44
4.2.2 Hydroesterification/Alkoxy carbonylation .....	45
4.2.3 Alcohol carbonylation.....	45
4.2.4 Lucite Alpha process.....	45
4.2.5 Oxidative carbonylation.....	45
4.2.6 Addition of a new functional group using carbonylative cross-coupling of aryl halides 46	
4.3 Electron-poor bifunctional ligands and their use in carbonylative cross-coupling of aryl halides .....	46
4.3.1. Preliminary results of carbonylative cross coupling using electron-poor bifunctional ligands.....	47
4.4 Initial results from carbonylative cross-coupling using electron-poor ligands.....	49
Table 4.4.1 Initial results from carbonylative cross-coupling experiments.....	50
Chapter 5.....	52
Coordinating-ion-spray mass spectroscopy as a method for the analysis of poorly ionizable or highly air- and acid-sensitive phosphines .....	52
5.1 CIS-MS spectroscopy as an analytical method.....	52
5.1.1 Original development, usage, and transition away from elemental analysis .....	52
5.1.1.1 Development and usage .....	52
5.1.1.2 Transitions away from elemental analysis.....	52
5.2 Use of CIS-MS for analysis of compounds synthesized in this work.....	53
5.2.1 High-resolution mass spectrometry without the use of a coordinating ion .....	53
Chapter 6. Future directions.....	59
References.....	60
Appendices.....	68



## List of Figures

Figure 2.1 Target bidentate hybrid electron-poor phosphonate.....	12
Figure 3.1.1 Representative Togni reagent for use in trifluoromethylation .....	21
Figure 3.2.1 4- <i>t</i> -butyl <i>N</i> -methyl imidazole (Im'H).....	23
Figure 3.3.1 X-Ray diffractometry structure of Cp*IrCl <sub>2</sub> (Im'P(CF <sub>3</sub> ) <sub>2</sub> ).....	27
Figure 3.3.2 X-Ray diffractometry structure of Cp*RhCl <sub>2</sub> (Im'P(CF <sub>3</sub> ) <sub>2</sub> ).....	28
Figure 3.3.3 Compound 31 .....	29
Figure 4.1 More favorable hydrogen-bonding with phenols than with the NH imidazole.....	32
Figure 4.1.1. Pt complex with hydrogen bonding from pendant hydroxyl group on a phosphine ligand.....	33
Figure 4.1.2 Calculated structure using two phenolic phosphines with an electron withdrawing CF <sub>3</sub> para to OH, showing bond geometry and H-Pt distance (2.175 Å) of OH---Pt interaction. ....	36
Figure 4.1.3 Calculated structure using two phenolic phosphines with an electron donating <i>i</i> -Pr para to P, showing bond geometry and H-Pt distance (2.156 Å) of OH---Pt interaction.....	37
Figure 4.1.4 Calculated structure using two phenolic phosphines with two electron withdrawing CF <sub>3</sub> on P, showing bond geometry and H-Pt distance (2.255 Å) of OH---Pt interaction.....	38
Figure 4.2.1. Mono-and bidentate ligands synthesized.....	39
Figure 4.2.2. Two possible ways a pendant group could increase rate of acyl attack .....	41
4.3.1. Structure of 1,2-bis(di- <i>tert</i> -butylphosphinomethyl)benzene, a ligand commonly used in carbonylation reactions .....	47
Figure 5.2.2.1 1,1'-bis(dimethylamino pentafluorophenyl phosphino)ferrocene.....	54
Figure 5.2.1 Mass spectrum of 1,1'-bis(dimethylamino pentafluorophenyl phosphino)ferrocene without Ag <sup>+</sup> ion.....	54
Figure 5.2.2 Mass spectrum of 1,1'-bis(dimethylamino pentafluorophenyl phosphino)ferrocene with Ag <sup>+</sup> ion added.....	55
Figure 5.2.3 Phenylbis(trifluoromethyl)phosphine with AgNO <sub>3</sub> addition.....	56
Figure 5.2.5 Mass spectrum of phenylbis(trifluoromethyl)phosphine (C <sub>8</sub> H <sub>5</sub> F <sub>6</sub> PAuCH <sub>3</sub> CN) with	

addition of  $\text{Me}_2\text{SAuCl}$ ..... 57

## List of Schemes

Scheme 1.1.1 Markovnikov and anti-Markovnikov addition to an alkene.....	1
Scheme 1.2.1.1.1 A few possible useful transformations for primary alcohols .....	2
Scheme 1.2.1.1.2 Acid catalyzed addition of water to an alkene .....	2
Scheme 1.3.1.1 Markovnikov addition of an amine to an alkene.....	4
Scheme 1.4.1.1.1 Hydroboration of an alkene followed by oxidation to the primary alcohol .....	5
Scheme 1.5.1 Alkene zipper catalyst and representative reaction .....	7
Scheme 1.5.2 Monoisomerization using a bifunctional ligand on ruthenium .....	8
Scheme 3.1.1 Alternate route to formation of perfluoro- alkyl and aryl phosphines .....	21
Scheme 3.1.2 General reaction for Ruppert Prakash reagent and a phosphite or phosphonite ....	22
Scheme 3.2.1. Synthetic route to bis(trifluoromethyl)phosphines.....	24
Scheme 3.2.2 Synthesis of bis(trifluoromethyl) N-methyl imidazolyl phosphine.....	25
Scheme 3.2.3 Methods for substitution of a dimethylamide for a chloride on a phosphine.....	25
Scheme 3.2.4 Formation of phosphonites directly from dimethylamino-substituted phosphines	26
Scheme 3.2.5 Cleavage of P-N and P-C bonds under mild acidic conditions .....	26
Scheme 3.3.1 Coordination of Im'P(CF <sub>3</sub> ) <sub>2</sub> and PhP(CF <sub>3</sub> ) <sub>2</sub> to Rh and Ir.....	27
Scheme 3.3.2 Synthesis of N-methylimidazolyl bis(pentafluorophenyl)phosphine.....	29
Scheme 4.1.1. Addition of hydroxyl containing molecules to a Pt center.....	33
Scheme 4.1.2 Investigations into alkene addition using Pt-H complexes .....	34
Scheme 4.2.1. Synthetic route to bis(trifluoromethyl) aryl phosphines before demethylation with BBr <sub>3</sub> .....	39
Scheme 4.2.2. Demethylation of anisoles using BBr <sub>3</sub> .....	39
Scheme 4.2.1. General mechanism for carbonylative cross-coupling of aryl halides .....	43
Scheme 4.2.2. General mechanism for alkoxy carbonylation of an alkene .....	44
Scheme 4.3.1. Synthesis of bidentate electron-poor bifunctional phosphines with a ferrocene	

backbone ..... 48

## List of Tables

Table 4.4.1 Initial results from carbonylative cross-coupling experiments.....	50
--	----

## Acknowledgements

I would like to thank my family, Roger, Betsy, and Jenny Sattler for all of their support. Without it I never would have made it this far.

I would like to thank my advisor, Dr. Grotjahn for all of his advice and mentoring over the years, and for helping me get across the finish line.

I would like to thank my group members for their help in working through many issues and keeping me sane. I'd like to thank Kevin, Anthony, Ashley and Mark for their incredible support during this last bit. Dave and Charlie, breakfast is on me. And to North Park Men's, I'd be crazier than I already am without you all to keep me alive.

Chapter two, in full, is a reprint of the material as it appears in *Polyhedron*. Sattler, Daniel J., Bailey, Jake, Grotjahn, Douglas B., vol. 228, December 2022. The dissertation author was the primary investigator and author of this paper.

Chapter five, in part contains work that is currently being prepared for submission for publication of the material. Sattler, Daniel J., Elliott, Gregory, Grotjahn, Douglas B. The dissertation author was the primary investigator and author of the material.

## **Vita**

1999 Bachelor of Science in Chemistry, North Dakota State University

2023 Doctor of Philosophy in Chemistry, University of California San Diego and San Diego State University

## **Abstract of the Dissertation**

Synthesis of electron-poor bifunctional ligands and their use in catalysis

By

Daniel James Sattler

Doctor of Philosophy in Chemistry

University of California San Diego 2023

San Diego State University 2023

Professor Douglas Grotjahn, Chair

Electron-poor ligands that also contain a pendant basic or acidic functional group should provide improved conditions and catalytic performance in a variety of reactions, such as anti-Markovnikov addition of O-H compounds such as water, alcohols, and carboxylic acids to terminal alkenes, a highly-sought reaction for which there is no good general solution. A second application is alkoxycarbonylation reactions of aryl halides to make esters. A strategy to synthesize electron-poor monophosphines or (bis)phosphines was developed. The analysis of the electron-poor

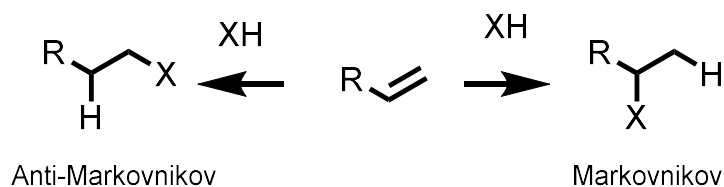


phosphines using coordinating-ion-spray high resolution mass spectrometry was developed due to the inability of the ligands (or water- and air-sensitive precursors) alone was often not successful. Initial results in testing electron-poor phosphines with either pendant OH or OCH<sub>3</sub> functionality as part of a metal complex for alkoxyacylation catalysis is reported.

## Chapter 1 Background and introduction

### 1.1 Introduction

Catalysis has long been used in chemistry. One reaction that is still an unsolved issue is the catalytic addition of a nucleophile to an alkene in an anti-Markovnikov fashion<sup>1</sup>. (**Scheme 1.1.1**)



**Scheme 1.1.1 Markovnikov and anti-Markovnikov addition to an alkene.**

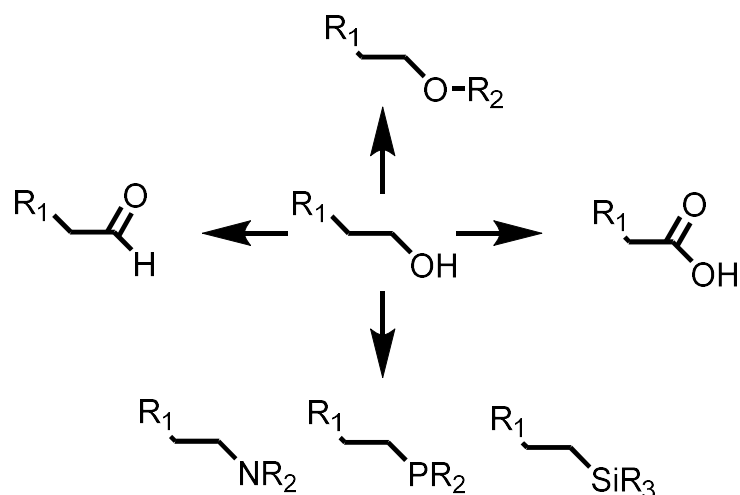
Addition in an anti-Markovnikov fashion would create more valuable compounds that have a variety of different uses in synthesis and industry. Some examples are given in the following sections. There are other organic transformations such as alkoxy carbonylation and hydroformylation that are used to add a carbon atom or a functional group onto an alkene, that are considered in Chapter 4. Addition of a carbon to ethylene is used on considerable scale in industrial facilities, and further improvements to the conditions required for the reaction are possible. The ultimate goal of the work in this dissertation is to contribute to enabling an effective catalyzed anti-Markovnikov addition of a hydroxyl group to an alkene.

### 1.2 Addition of polar hydroxyl groups to an alkene

#### 1.2.1 Addition of water to form an alcohol with the same number of carbon atoms

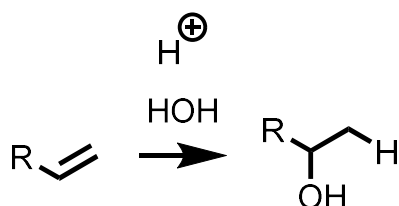
##### 1.2.1.1 Previous Methods

Alcohols are used throughout chemistry because they are valuable reagents or starting materials for the production of other functional groups.



**Scheme 1.2.1.1.1 A few possible useful transformations for primary alcohols**

Markovnikov addition of water has been a solved problem for a considerable length of time, with the acid catalysis addition of water to an alkene being widely used, though the reaction gives the Markovnikov product. (Scheme 1.2.1.1.1).



**Scheme 1.2.1.1.2 Acid catalyzed addition of water to an alkene**

Production on an industrial scale can be achieved using as well. Ring opening of epoxides to form the primary alcohol has also been developed using terminal alkenes as the starting alkene. Development of the production of terminal alcohols has continued whether the starting alkene is terminal or internal. While all of these methods are effective, each has drawbacks and further investigation into performing this reaction in a more efficient manner is a worthy goal and a major challenge in catalysis. Primary alcohols can be transformed into other useful functional groups (Scheme 1.2.1.1.2).

One of the most sought-after nucleophiles for anti-Markovnikov addition to an alkene is water to directly form a primary alcohol. There has been considerable work done to perform this reaction catalytically, though to date an efficient method has not been discovered.

#### **1.2.1.2 Overall addition using a triple relay metal catalyst**

Overall addition of a water molecule to an alkene has been achieved on a laboratory scale by Grubbs using a triple relay method with three different metals<sup>2</sup>, though this is only an indirect addition of water to a molecule. Selectivity and yields with substrates that were not styrene was limited with the selectivity dropping from >20:1 for anti-Markovnikov addition to a styrene to 1:1.4 for addition to 1-octene, and the yield dropping from 83% to 56%. The catalyst system also generates a considerable amount of waste and has a very low atom economy, limiting its use to laboratory scale.

### **1.2.2 Addition of carboxylic acids and alcohols**

Esters and ethers are also useful functional groups, but we are not aware of any metal-catalyzed or acid catalyzed anti-Markovnikov additions of alcohols or carboxylic acids to alkenes.

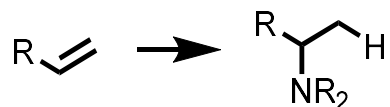
#### **1.2.2.1 Previous methods**

Other types of catalysts have been applied to realize anti-Markovnikov additions. If an alkene is electron-rich and can be oxidized by a suitable excited state of a photocatalyst, the method of Nicewicz can be used.<sup>3</sup> Cyclizing an alkenol to an ether via photocatalysis has also been used by Nicewicz<sup>4</sup> and by Knowles<sup>5</sup>, but intramolecular anti-Markovnikov O-H addition happens only because the reactions are cyclizations. The Knowles chemistry differs from that of Nicewicz in that the O-H component is oxidized, not the alkene.

## **1.3 Addition of N-H**

### 1.3.1 Previous Methods

Production of primary amines is also a major portion of the chemical industry, and primary amines have a variety of synthetic uses. Catalytic addition to an alkene or alkyne can be accomplished with a variety of catalysts including cobalt<sup>6</sup>, lanthanides<sup>7</sup>, both early<sup>8</sup> and late transition metals<sup>9</sup>, base-assisted using inorganic bases such as KOH and CsOH<sup>10</sup> and has advanced to the ability to add them in a chiral fashion<sup>11</sup>. Many of the additions are in a Markovnikov sense (Scheme 1.3.1.1), but aryl-substituted alkenes often give the anti-Markovnikov product. A breakthrough in anti-Markovnikov addition of NH bond to alkenes came from the Knowles group, who rely on oxidation of the amine nitrogen using photocatalysis, and radical addition to the alkene, followed by H-atom transfer from a very hindered thiol<sup>12-14</sup>. Unfortunately the strategy will not likely work for intermolecular additions of alcohol O-H bonds to alkenes because of the propensity for the alkoxy radical to abstract weak allylic C-H bonds, but it has succeeded in an intramolecular sense (see above).



**Scheme 1.3.1.1 Markovnikov addition of an amine to an alkene**

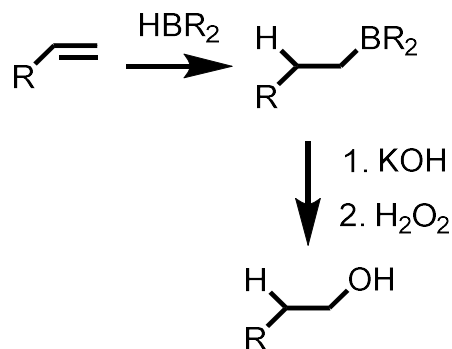
## 1.4 Addition of less polar X-H bonds (B, Si)

### 1.4.1 Addition of B-H bonds to an alkene

#### 1.4.1.1 Non metal-catalyzed

Hydroboration of terminal alkenes followed by oxidation to form the primary alcohol (Scheme 1.4.1.1.1) has been widely used since its discovery in 1959<sup>15</sup>. Hydroboration using this

method is



**Scheme 1.4.1.1.1 Hydroboration of an alkene followed by oxidation to the primary alcohol**

very effective, however one of the main downsides to using this method on a larger scale is the production of a considerable amount of waste.

#### 1.4.1.2 Metal Catalyzed

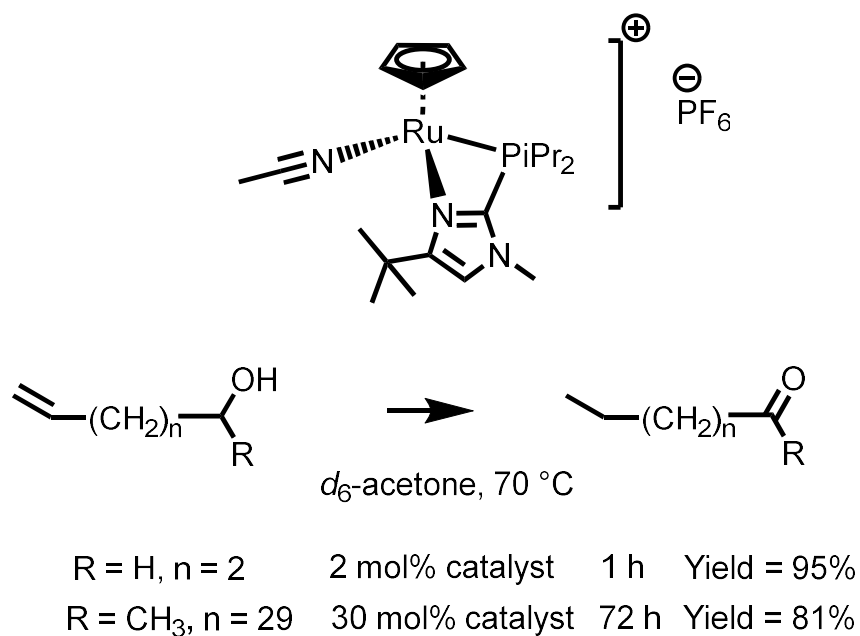
The metal-catalyzed reaction was first reported in 1980<sup>16</sup>, with significant improvements being made in 1985<sup>17</sup> with the use of Wilkinson's catalyst. While the addition of borane can be accomplished using metal catalysis to give a particular stereoisomer<sup>18-20</sup>, formation of the alcohol still requires an additional waste generating oxidation step.

#### 1.4.2 Addition of Si-H bonds to alkenes

Silanes are also used in industry as additives to improve the qualities of a variety of substances<sup>21, 22</sup>. Silanes have found use in medicinal chemistry<sup>23</sup> and organic synthesis as well<sup>24</sup>. Addition of a silane to an alkene is accomplished using metal catalysis with either Spiers or Karstedt's catalyst<sup>25</sup>, and the use of chiral ligands<sup>26</sup> or directing groups<sup>27</sup> has made possible the asymmetric addition of a silane to an alkene.

## 1.5 Bifunctional Ligands

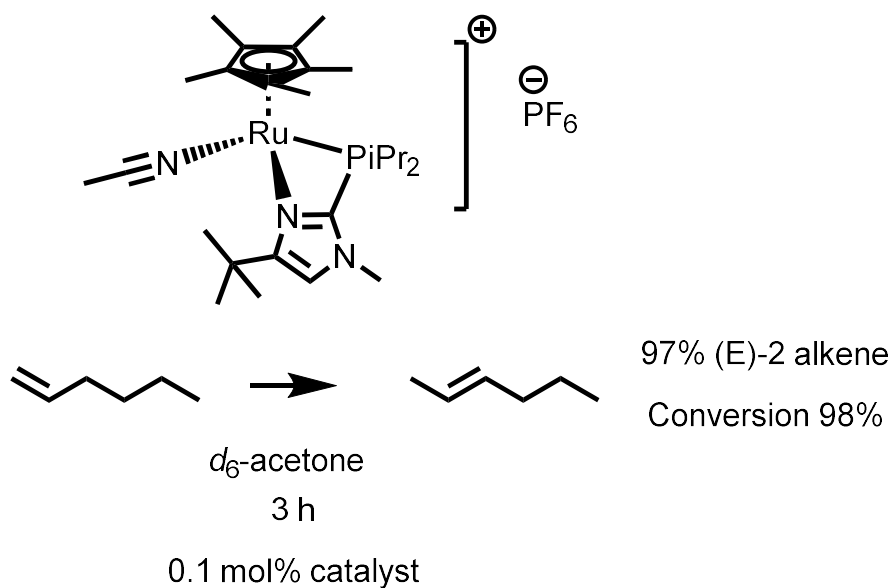
How a bifunctional ligand is defined is important, as the functions can be different depending on the role they play during the catalytic cycle. The first role of all types of ligands is to coordinate to the metal center and modify its steric and electronic properties which in turn changes what catalysis occurs at the metal center, along with its rate, efficiency, and the conditions necessary for the reaction to occur. The second role of the ligand can vary, with the functional group acting as a proton shuttle, e.g. as a pendant base to deprotonate the substrate, as a way to affect the regio- or stereoselectivity of the reaction, or to modify the nucleophilicity or electrophilicity of an incoming reactant. Bifunctional ligands can also be hemilabile<sup>28</sup>, which has been shown to be effective in improving catalyst functionality<sup>29</sup>. Ligands containing a bifunctional substituent have been used for several purposes such as asymmetric hydrogenation by Noyori<sup>30</sup> and Schvo<sup>31,32</sup>, and Sigman<sup>33</sup> and Stoltz's<sup>34</sup> work involving kinetic resolution. Ligands containing a pendant base can be capable of doing more than one of these things and so remain an active area of research.



**Scheme 1.5.1 Alkene zipper catalyst and representative reaction**

Previous work in the Grotjahn lab on pendant base-containing ligands has focused so far on two different areas. One is the isomerization of an alkene, either very quickly<sup>35</sup> (Scheme 1.5.1) or in a selective monoisomerization<sup>36, 37</sup> (Scheme 1.5.2); another is the hydration of an alkyne<sup>38, 39</sup>. The reactions noted are very effective, and the alkyne hydration and the isomerization occur 1000 to 3000 times faster than with a ligand that does not contain a pendant base.





### Scheme 1.5.2 Monoisomerization using a bifunctional ligand on ruthenium

There has also been work involving the oxidative addition of water to a platinum center that was enabled by the use of an N-H containing imidazolyl ligand<sup>40</sup>. The N-H was capable of stabilizing an anionic oxygenated ligand through hydrogen bonding, making the oxidative addition of water to the platinum center more favorable.

## 1.6 Electron-poor ligands

### 1.6.1 Definition and methods to determine donation strength

The electron donating ability of a phosphine ligand has long been used as a measure of how it will impact the catalytic cycle of a given metal complex. More electron-rich phosphines have been shown to increase the rate of oxidative addition of a substrate to a metal center, as shown later in this work the rate of reductive elimination can be improved using electron-poor ligands. Using hydroxyl groups in the ligand we envision assisting formation of metal-hydroxyl bonds through hydrogen bonding of the ligand hydroxyl to the metal bound oxygen.

### 1.6.2 Determination of electron donating strength of phosphine ligands

Several methods have been developed in order to more thoroughly characterize the electronics of phosphine ligands. One of the most common initial methods was to react the phosphine with  $\text{Ni}(\text{CO})_4$  to make the  $\text{LNi}(\text{CO})_3$  complex, followed by measuring the IR stretch of the A1 carbonyl<sup>41</sup>. The higher the wavenumber the CO stretching frequency is shifted the more electron poor the phosphine ligand is considered. Due to the toxicity of the Ni carbonyl compounds, a different method involving  $\text{L}_2\text{Rh}(\text{CO})\text{Cl}$  complexes was developed that gave similar information. Changing the complex used led to the discovery that the geometry of the metal center had some effect on the nature of the donation from the phosphine to form the metal phosphine bond<sup>42</sup>. Other methods include the electrochemical oxidation of phosphine ligands in order to determine the ionization energy of an electron from the lone pair on the phosphorus atom. This method was developed to hopefully determine a more metal center independent measurement of the donation capacity of the phosphine ligand, though a comprehensive study has yet to be done. As a measure of what types of ligands the compounds synthesized here, however, determining the CO stretching frequency in Rh complexes as a comparison is still a relevant measure and was used here.

The ligands examined below showed considerable electron-withdrawing character, comparable to phosphites as shown by using Rh carbonyl stretches (Table 1). This gives us more freedom in the selection of the pendant base containing substituent, as even a fairly electron rich and therefore more basic base would still give the desired electronic environment for the metal center. Moreover, the acidity or basicity of the attached pendant group through modification of the substituent that contains the pendant group.

### 1.6.3 Phosphites and phosphonates in catalysis

Alkyl and aryl phosphites and phosphonates are electron-poor ligands with a long and storied usage in transition metal catalysis<sup>43,44</sup> and have been used in a wide variety of different catalytic systems with applications ranging from fine chemical synthesis to industrial scale production. A major drawback is their susceptibility to hydrolysis<sup>45,46</sup> which may be incompatible with addition of water to an alkene. Another drawback would be that while phosphites can be sterically tuned<sup>47</sup>, the closest point at which a phosphite can be modified is separated from the phosphine by an oxygen atom. Our hypothesis is that using a ligand with modifications closer to the metal center would give more control over the steric environment, allowing for fine tuning should it be necessary.

### 1.6.4 Changing a catalytic cycle

Metal complexes containing electron-poor ligands have been shown to have different and sometimes dramatic effects on a catalytic cycle. One feature is that the electron-poor ligand performs the same reaction as any other ligand would, only less efficiently or more slowly due to their lowered electron donation to the metal center, which in turn slows oxidative addition of a substrate. More useful is when an electron-poor ligand is capable of performing a reaction other ligands cannot such as reductive elimination of a product that is otherwise difficult to form<sup>48</sup>, or changing the relative rates of different steps in the catalytic cycle to give a different products, such as polymerization of a substrate rather than  $\beta$ -hydride elimination<sup>49</sup>.

#### 1.6.5.1 Increased rate of reductive elimination

On palladium(II), it has long been known that using a chelating ligand (such as a diphosphine) with wide bite angle, somewhere between the ideal  $90^\circ$  angle for square planar Pd(II) and the ideal  $109^\circ$  for Pd(0), will enable faster reductive elimination.<sup>50,51</sup> Using electron-

withdrawing groups such as aryls with F or CF<sub>3</sub> groups can increase the rate of reductive elimination >1000 times<sup>52</sup>.

#### **1.6.5.2 Lower rate of oxidative addition**

As these electron-poor ligands will increase the rate of reductive elimination, they would also decrease the rate of oxidative addition, but Pd(0) ligated with phosphines such as [3,5-(CF<sub>3</sub>)C<sub>6</sub>H<sub>3</sub>]<sub>3</sub>P are fully capable of C-X oxidative additions and catalyzing alkoxyacylation, Suzuki, and Heck reactions<sup>53, 54</sup>.

### **1.7 Summary of electron-poor and bifunctional ligand properties and potential uses**

Our hypothesis was that the increased rate of reductive elimination of electron-poor ligands combined with the rate enhancement effects of ligands containing a pendant base would be useful in the addition of a nucleophile to an alkene in an anti-Markovnikov fashion.

## Chapter 2 Bidentate hybrid electron-poor phosphonate

As a first starter project, a bidentate hybrid electron-poor phosphonate was proposed as a ligand, as chelation would help to alleviate a possible issue related to electron-poor ligands. The first would be the fact that electron-poor ligands could be so electron deficient as to be easily displaced on a metal center. At that point the ligand would not be useful in a catalyst due to it not being present on the metal center during the catalytic cycle. Using a bidentate ligand with one phosphonate and one electron-poor phosphine would give the ligand the ability to chelate to the metal center increasing its ability to bind to the metal. Phosphonates such as this, though without the electron-poor substituents have been used to good effect in several reactions involving alkenes<sup>55,56</sup>. Hybrid phosphonate ligands have been used as ligands for polymerization catalysts<sup>57</sup>, a precedent that suggests modifying the ligand to be more electron-poor may change the catalytic cycle to give an addition product rather than the polymeric product. Studies by other groups<sup>58,59</sup> have shown that linear polymers can be more readily obtained by avoiding  $\beta$ -hydride elimination from a bound alkyl group. As electron-poor ligands have been shown to be capable of this exact function, it was hoped that using one would allow for different reactivity involving alkenes.

Our first target (Figure 2.1) was relatively simple, using commercially available \

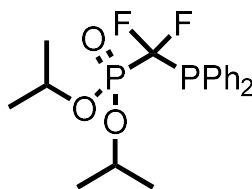


**Figure 2.1 Target bidentate hybrid electron-poor phosphonate**

chlorophosphines in order to determine if ligands of this type could be synthesized and isolated and to work out any issues with the planned strategy. The synthesis of these compounds seemed

relatively straightforward, and while the ligands themselves could be seen through the use of NMR spectroscopy, purification was complicated by the stability of both difluoromethyl and diphenylphosphine radicals. Column chromatography and distillation were attempted but led only to decomposition of the product. Attempts to remove the isopropyl groups using either  $\text{Me}_3\text{SiBr}$ ,  $\text{KOH}$  or  $\text{NaOH}$  only lead to decomposition. This project was set aside in favor of other, more promising projects. It was revisited several years later after finding a method of selectively removing only one of the isopropyl groups using  $\text{LiBr}$  in acetonitrile. This method was successful, and a  $\text{Cp}^*\text{IrLCl}$  complex was isolated. When tested, however, the complex was only capable of non-selectively and slowly isomerizing alkenes.



# Synthesis and crystal structure of an iridium complex containing the novel electron-poor hybrid monoanionic ligand $\text{Ph}_2\text{PCF}_2\text{PO}_2(\text{OiPr})^{\star}$

Daniel J. Sattler<sup>a</sup>, Jake B. Bailey<sup>b</sup>, Douglas B. Grotjahn<sup>a,\*</sup>

<sup>a</sup> Department of Chemistry, San Diego State University, San Diego, CA 92182, United States

<sup>b</sup> Department of Chemistry and Biochemistry, University of California San Diego, La Jolla, CA 92093, United States

## ARTICLE INFO

### Keywords:

Electron poor  
Iridium  
Bidentate ligand  
Bifunctional ligand  
Phosphonate

## ABSTRACT

Phosphines have long been used in catalysis, and a wide variety of ligands with almost any substituent are available. However, the vast majority of these phosphines have been relatively electron-rich. Monooxides of bisphosphines have been shown to form complexes that catalyze alkene polymerizations and hydroformylations. However, electron-poor versions of such ligands have not yet been explored. In this report, the hybrid ligand  $\text{Ph}_2\text{PCF}_2\text{PO}_2(\text{OiPr})$  with both phosphine and phosphonate ester moieties, linked with an electron deficient  $\text{CF}_2$  group was synthesized. A  $\text{Cp}^*\text{Ir}$  complex of the ligand was synthesized and characterized.

## 1. Introduction

Phosphines have long been used in catalysis, and a wide variety of ligands with almost any substituent are available. However, the vast majority of these phosphines are relatively electron-rich. A significant amount of research has also been devoted to the organic transformation of alkenes into other functional groups. Monooxides of bisphosphines (BPMO, **A** in [Chart 1](#)) have been shown to form complexes that catalyze alkene polymerizations [1–3] and hydroformylations [4]. However, more electron-poor ligands of type **A** have been unexplored so far. The goal of this project was to synthesize a hybrid P,O-ligand of type **D** in [Chart 1](#) which is electron-poor, and then modify the electronic and steric properties of this class of ligand further and to include pendant base or acid functionality as part of the ligand.

Electron-poor ligands have been underexplored in the literature. Several studies have shown how they can affect the reductive elimination step of a catalytic cycle, even to the point of outcompeting  $\beta$ -hydride elimination [5]. They have also been used to examine how effective they are in previously studied chemistry such as cross-coupling, hydroformylation [6] and carbonylation [7]. Several studies describe the properties and suitability of electron-poor ligands for catalysis [8,9], and several more discuss their use in stoichiometric reactions [10–12]. Reviews that focus on electron-poor phosphines discuss synthesis of the ligands and related metal complexes, but reactivity studies were limited to polymerization and hydrogenation [13].

The Grotjahn group has focused on the usage of ligands containing a

pendant base, finding them to have a significant impact on the rate [14] and selectivity [15] of a reaction. Combining electron-poor and bifunctional ligands would give a new type of ligand with unexplored properties. Another attractive feature of a bifunctional ligand is its ability to coordinate in a chelating manner, which utilizes the chelate effect to help the ligand stay coordinated [16], a concern when using electron-poor ligands.

In this work, a bifunctional, electron-poor ligand of type **D** and an associated Ir complex were synthesized and characterized. While no new reactivity was discovered from the complex, the ligand and complex by themselves and their syntheses are novel and hence are reported here.

## 2. Materials and methods

Nuclear magnetic spectra were recorded on a Varian VNMRs 400 MHz spectrometer with AutoX probe. Deuterated methanol and deuterated chloroform were stored over 3 and 4 Å molecular sieves, respectively. Signals were referenced to  $\text{SiMe}_4$  through the residual solvent resonance. Diethyl ether was distilled from sodium and benzophenone. Dichloromethane was distilled from calcium hydride. Toluene was degassed, and all organic solvents were stored in a glove box under nitrogen over 4 Å molecular sieves. Water was degassed and stored under nitrogen in a glove box. Chlorodiphenylphosphine and *t*-butyl lithium (1.9 M in pentane) were purchased from Sigma Aldrich and used without further purification. Diisopropyl (difluoromethyl)phosphonate (**1**) was synthesized according to literature procedure. Elemental

\* This paper is dedicated to Professor Arnie Rheingold for his devotion to x-ray crystallography and his peerless friendship over the years.

\* Corresponding author.

<https://doi.org/10.1016/j.poly.2022.116162>

Received 5 May 2022; Accepted 1 October 2022

Available online 6 October 2022

0277-5387/© 2022 Elsevier Ltd. All rights reserved.

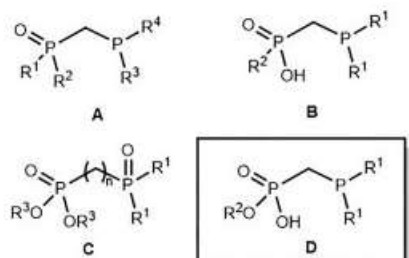
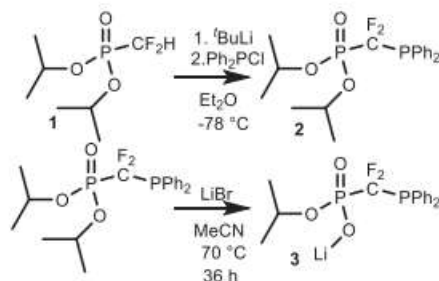


Chart 1. Comparison of similar bisphosphines ligands and this work.



Scheme 1. Synthesis of 3.

analysis was performed by NuMega Resonance labs in San Diego, CA. Coupling constants are reported in Hz.

Synthesis of **2**: Diisopropyl (difluoromethyl)phosphonate (**1**) (2.699 g, 12.5 mmol) and THF (120 mL) were added to a Schlenk flask, which was cooled to  $-78\text{ }^{\circ}\text{C}$ . *tert*-butyl lithium (6.8 mL, 1.9 M/L in pentane) was added dropwise over 5 min, and the reaction was stirred for 1 h. Chlorodiphenylphosphine (2.756 g, 12.5 mmol) was added dropwise, and the reaction was allowed to warm to ambient temperature over 4 h. The volatiles were then removed under vacuum. The residue was dissolved in DCM (25 mL) and washed with water ( $3 \times 50\text{ mL}$ ). The organic

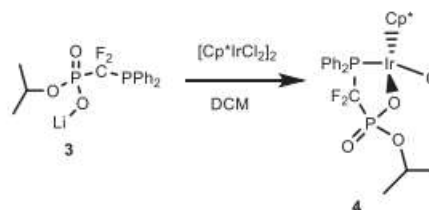
layer was collected and the volatiles removed under vacuum to give 3.333 g (66 %) of the crude product. This was used without further purification.

$^{31}\text{P}\{^1\text{H}\}$  ( $\text{CDCl}_3$ ):  $\delta$  26.1 (p,  $J_{\text{P-F}}$  26.3).  $^{19}\text{F}$  ( $\text{CDCl}_3$ ):  $\delta$   $-109.0$  (dd,  $J_{\text{P-F}}$  70, 95).  $^1\text{H}$  ( $\text{CDCl}_3$ ): 7.70 (t,  $J_{\text{H-H}}$  8, 4H), 7.40 (m, 6H), 4.75 (h,  $J_{\text{H-H}}$  6, 2H), 1.25 (dd,  $J_{\text{P-H}}$  22,  $J_{\text{H-H}}$  6, 12H).

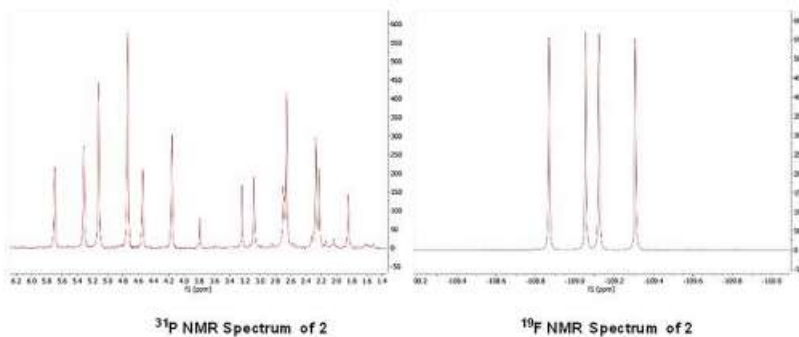
Synthesis of **3**: **2** (1.00 g, 2.5 mmol), acetonitrile (0.50 mL), and LiBr (0.217 g, 2.5 mmol) were added to a scintillation vial equipped with a stir bar. The reaction was heated at  $70\text{ }^{\circ}\text{C}$  for 18 h, removed from the heat and shaken, and then heated for another 18 h. The mixture was then cooled to room temperature, filtered, and the precipitate was washed with acetonitrile ( $1 \times 5\text{ mL}$ ), DCM ( $1 \times 5\text{ mL}$ ), and diethyl ether ( $1 \times 5\text{ mL}$ ). The white powder was then dried overnight under vacuum giving 0.910 g (58 %) of product.

$^{31}\text{P}\{^1\text{H}\}$  (MeOD):  $\delta$  3.2 (td,  $J_{\text{P-F}}$  82), 1.1 (q,  $J_{\text{P-F}} = J_{\text{P-P}}$  60).  $^1\text{H}$  (MeOD):  $\delta$  7.65 (td,  $J_{\text{H-H}}$  7.5, 2, 4H), 7.45–7.35 (m, 6H), 4.52 (h,  $J_{\text{H-H}}$  6, 1H), 1.12 (d,  $J_{\text{H-H}}$  6, 6H).  $^{13}\text{C}$  (MeOD):  $\delta$  135.0 (d,  $J_{\text{P-C}}$  20), 132.8 (dd,  $J_{\text{P-C}}$  13.2,  $J_{\text{P-S}}$  4.5),  $J_{\text{P-C}}$  2.2, assigned to ipso carbon of Ph), 128.9 (s), 127.6 (d,  $J_{\text{P-C}}$  7.6), 69.8 (dd,  $J_{\text{P-C}}$  6.8, 6.4), 23.5 (d,  $J_{\text{P-C}}$  4.1); signal for  $\text{CF}_2$  carbon is expected to be a dtd, and some of the signal resonances are seen but others are obscured by much more intense signals. Negative ion mode QTOF-MS  $m/z$  for  $\text{C}_{16}\text{H}_{17}\text{F}_2\text{O}_3\text{P}_2$ : Calculated 357.06211; Obtained 357.0675.

Synthesis of **4**: ligand **3** (0.100 g, 0.274 mmol) was added to a scintillation vial equipped with a stir bar.  $[\text{IrCp}^*\text{Cl}_2]_2$  (0.1093 g, 0.137 mmol) was then added, and 1.3 mL of  $\text{CH}_2\text{Cl}_2$  was added. The reaction was stirred overnight, and the solvent was removed to give 0.1989 g of residue. To the mixture was added 5 mL of  $\text{CH}_2\text{Cl}_2$ , which was filtered and the filtrate concentrated to give **4** (0.098 g, 45 % yield). X-ray quality crystals were grown by the slow evaporation of  $\text{CH}_2\text{Cl}_2$  from a



Scheme 2. Synthesis of 4.

Fig. 1. Left and right, respectively,  $^{31}\text{P}$  and  $^{19}\text{F}$  NMR spectra of **2** in  $\text{CDCl}_3$  at 161 and 376 MHz.



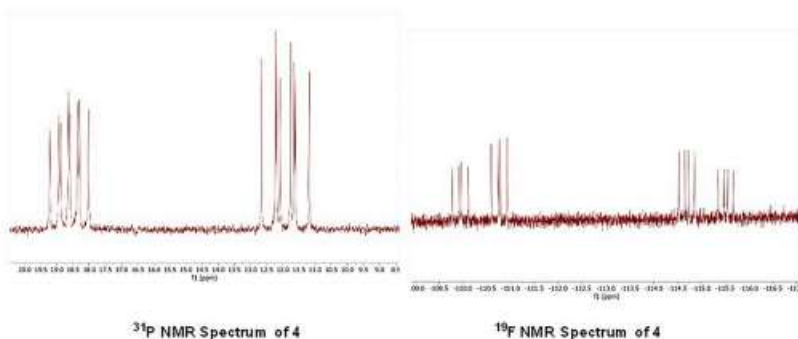


Fig. 2. Left and right, respectively,  $^{31}\text{P}$  and  $^{19}\text{F}$  NMR spectra of **2** in  $\text{CDCl}_3$  at 161 and 376 MHz respectively.

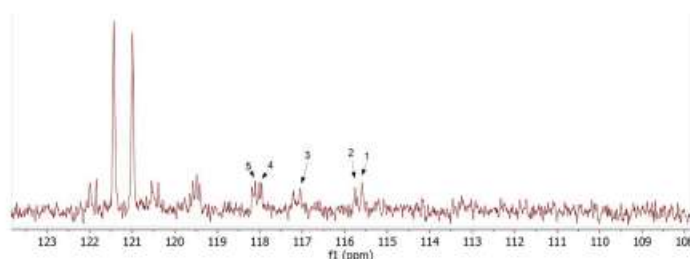


Fig. 3. Inset of  $^{13}\text{C}$  NMR spectrum of **4** highlighting the 16-peak dddd for the  $\text{CF}_2$  carbon. Frequencies for the peaks 1 to 5 are: 14531.0, 14552.0, 14715.0, 14828.4, 14847.6 Hz, respectively, giving  $J$  values of 21.0, 184.0, 297.3, and 316.6 Hz.

saturated solution of **4**.  $^{31}\text{P}\{^1\text{H}\}$  ( $\text{CDCl}_3$ ):  $\delta$  19.6 (td,  $J_{\text{P-F}}$  92,  $J_{\text{P-F}}$  44, 54), 11.5 (dt,  $J_{\text{P-F}}$  92,  $J_{\text{P-F}}$  74).  $^{13}\text{C}$  ( $\text{CDCl}_3$ ):  $\delta$  136.2 (d,  $J_{\text{P-C}}$  11.0), 134.3 (d,  $J_{\text{P-C}}$  10.0), 132.3, 131.9, 128.6 (d,  $J_{\text{P-C}}$  11.3), 128.5 (sl br d,  $J_{\text{P-C}}$  11.0), 127.5 (d,  $J_{\text{P-C}}$  58.4), 121.2 (d,  $J_{\text{P-C}}$  53.3), 118.8 (dddd,  $J_{\text{P-C}}$  316.6, 297.3,  $J_{\text{P-C}}$  184.0, 21.0), 93.1 (d,  $J_{\text{P-C}}$  2.8), 73.23 (d,  $J_{\text{P-C}}$  5.7), 73.18 (d,  $J_{\text{P-C}}$  5.7), 24.4 (d,  $J_{\text{P-C}}$  3.0), 24.0 (d,  $J_{\text{P-C}}$  5.0), 8.6.  $^1\text{H}$  ( $\text{CDCl}_3$ ): 7.75 (t, 11.3, 2H), 7.58 (t, 9.2, 1H), 7.50 (t, 6.0, 1.5H), 7.45 (s, 2H), 4.76 (h, 4.9, 1H), 1.48 (s, 15H), 1.28 (d,  $J_{\text{H-H}}$  5.6, 6H). Elem. anal. calcd for  $\text{C}_{28}\text{H}_{32}\text{ClF}_2\text{IrO}_3\text{P}_2$  (720.14): C, 43.36; H, 4.48. Found: C, 39.84; H, 4.54. Elem. anal. calcd for  $\text{C}_{28}\text{H}_{32}\text{ClF}_2\text{IrO}_3\text{P}_2 + 3.5 \text{H}_2\text{O}$  (783.20): C, 39.87; H, 5.02.

### 3. Results and discussion

The present investigation began with the design of a model compound that could be used to determine the most efficient method of synthesizing hybrid ligands of type **D** (see Chart 1) using **A** as a starting point. A diphenylphosphino substituent was chosen for the initial synthesis, but the substituents on the phosphine portion of the ligand could readily be changed to make it more electron-poor once the initial synthesis was optimized. The anion of **1** (Scheme 1) has been used in a variety of syntheses [17–20], and **1** was readily available in one step [21].

The synthesis of **2** initially seemed quite straightforward (Scheme 1), with the addition of *t*-butyl lithium to **1** at  $-78^\circ\text{C}$ , followed by addition of chlorodiphenylphosphine. The initial purification with a water wash to remove lithium followed by removal of volatile compounds *in vacuo*

gave a crude clear, viscous liquid. The crude yield was 80 %, and NMR spectroscopy showed mostly (ca. 90 %) one compound. Due to the number of NMR active nuclei in compound **2**, the spectra were complicated (Fig. 1), but this also allowed a more certain identification. In the  $^{31}\text{P}$  NMR spectrum shown below, two partly overlapping signals were seen at 4.90 and 2.59 ppm, with  $^2J_{\text{P-F}} = 62.1$  Hz, as well as coupling to the two fluorine atoms  $^2J_{\text{P-F}} = 93.1$  and 69.0 Hz, respectively. The  $^{19}\text{F}$  NMR spectrum showed a corresponding doublet of doublets,  $^2J_{\text{F-P}} = 93.1$  Hz,  $^2J_{\text{F-P}} = 69.0$  Hz.

Although the identity of **2** is assured, purification was much less straightforward. Compound **2** was found to be quite capable of coordinating Li ions formed from the *t*-butyl lithium used in the initial synthesis, verified by  $^7\text{Li}$  NMR spectroscopy. While the lithium was easily removed using a water wash, **2** decomposed upon attempted distillation even under reduced pressure, and column chromatography led to very poor mass recovery (less than 5%). It was suspected that **2** decomposed through a radical pathway, in part because both  $\text{Ph}_2\text{P}^\cdot$  [22] and fluoroalkyl radicals are known species [23–25].

To move past these issues, impure **2** was used in subsequent reactions. Several methods of phosphonate diester hydrolysis were attempted. Refluxing **1** with NaOH in water or  $\text{Me}_3\text{SiBr}$  in dichloromethane led to a mixture of several products. Gratifyingly, refluxing **1** with LiBr in dry acetonitrile [26] led to crystalline product **3** in 58 % yield, pure enough for metallations (Scheme 2).

The initial target was an  $\text{IrCp}^+$  complex, which was synthesized by stirring  $[\text{IrCp}^+\text{Cl}_2]_2$  and **3** in dichloromethane overnight to give the metal complex in 95 % yield (Scheme 2). The  $^{31}\text{P}$  NMR spectrum (Fig. 2)

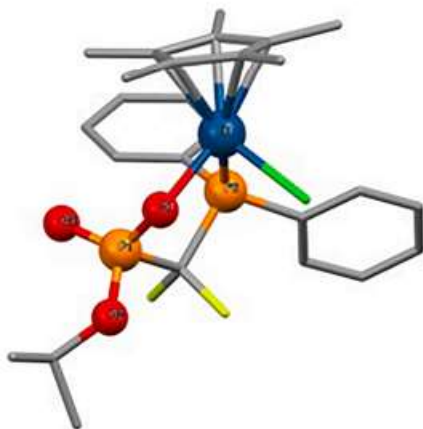


Fig. 4. Ball and stick representation of the molecular structure of **4** as determined by X-ray diffraction. The Ir, P, and O atoms are highlighted by representing them as spheres, whereas all other nonhydrogen atoms are represented using sticks. Key bond distances (Å): Ir–P 2.295, Ir–O 2.149, Ir–Cl 2.385. Key angles: O–Ir–P 87.06°, O–Ir–Cl 83.05°, and Cl–Ir–P 91.36°.

showed two signals, each a ddd, with  $J$  values matching those for the two signals in the  $^{19}\text{F}$  NMR spectrum, consistent with mutual coupling. Combined, these data indicate the presence of only one diastereomer.

Interestingly, the  $^{13}\text{C}$  NMR spectrum of **4** indicated that all carbons of the ligand were unique, consistent with the two phenyls being diastereotopic, and also the two isopropyl methyls. Moreover, the  $\text{CF}_2$  carbon appeared as a remarkable 16-line dddd pattern, barely resolved even after overnight acquisition (Fig. 3). The two largest splittings (316.6 and 297.3 Hz) were similar and were assigned to  $^1J_{\text{F-C}}$ , where the 21.0 Hz splitting was ascribed to  $^1J_{\text{P(=O)-C}}$  and the 184.0 Hz one to  $^1J_{\text{P(O)(O-)-C}}$  [27]. While no water was seen in the proton NMR spectrum for **4**, the elemental analysis was consistent with the presence of 3.5 water molecules per complex. As the complex is air stable, no precautions were taken in the lab or the lab of the company that performed the analysis to exclude water from the sample.

X-ray quality crystals of **4** were grown by slow evaporation of

dichloromethane (Fig. 4). The Ir–O3 bond distance in **4** was 2.149 Å, compared to 2.150 Å for the similar complex  $\kappa\text{-O,P-(Ph}_2\text{PC}_6\text{H}_4\text{PO}_3\text{H)Cp}^*\text{ClIr}$ ) [28]. The Ir–Cl bond length of 2.408 Å is also similar to the Ir–Cl bond in **4** of 2.385 Å [28].

In order to understand why only one isomer was seen in the NMR spectra and crystal structure, DFT calculations were performed to determine if there were structural differences preventing the formation of more than one isomer. Gas phase calculations were carried out using b3lyp/SDD as the functional and basis set, respectively. The observed diastereomer with isopropyl *cis* to chloride was found to be more stable than the *trans* diastereomer by 1.1 kcal/mol, and when dispersion was included in the calculations this difference increased to 3.4 kcal/mol between the two isomers, giving a  $K_{\text{eq}}$  of 295 at room temperature, corresponding to less than 0.1 % of the less stable *trans* isomer, which explained why both the NMR spectra and the isolated crystal showed evidence of only one species, that is also the complex calculated to be more stable. Both diastereomers are shown for comparison (Fig. 5).

However, examination of the structural features of the two different isomers did not give a clear reason why the observed isomer is preferred; a combination of subtle electronic and structural factors might contribute to this energy difference [29].

In order to test the metal complex for catalytic activity, **3** was ionized using silver hexafluorophosphate, and the resulting mixture was filtered through a silica plug into a J. Young NMR tube, and then hexene and either acetic acid or water was added. Tetrakis(trimethylsilyl)methane was used as an internal standard. The solution was monitored for changes over several days and then heated to 70 °C for 12 h but no changes were seen. No addition to the alkene was seen with either acetic acid or with water. A small amount of isomerization was seen, but  $\text{Cp}^*\text{Ir}$  complexes are known to isomerize alkenes and there are already several good methods to isomerize alkenes [30].

#### 4. Conclusions

A new chelating electron-poor ligand was synthesized, and its ability to coordinate to a metal was demonstrated. The resulting complex formed as a single diastereomer, and DFT calculations support a significant free energy difference between diastereomers. While the resulting complex was inactive as an alkene isomerization catalyst, the fact that no hybrid ligand containing both a phosphine moiety as well as a phosphonate moiety is known and the fact that there appears to be only one  $\text{Cp}^*\text{Ir-BPMO}$  complex known all motivate this report.

#### Declaration of Competing Interest

The authors declare that they have no known competing financial

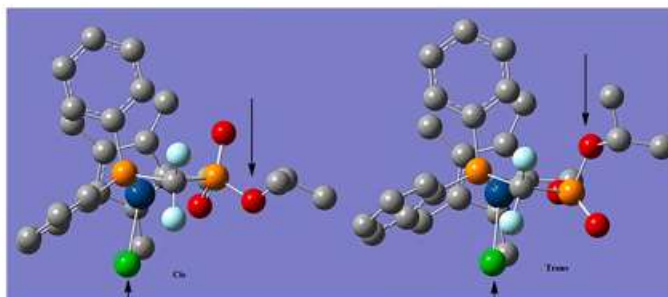


Fig. 5. Ball and stick representations of the calculated molecular structures showing *cis* and *trans* isomers, *trans* being lower energy. The arrows point to the green Cl atom and the O of the O-*i*Pr group.

interests or personal relationships that could have appeared to influence the work reported in this paper.

#### Data availability

Data will be made available on request.

#### Acknowledgements

This work is financially supported by the NSF, grant CHE-2102623. We would like to thank Dr. Gregory Elliott for high-accuracy mass spectrometry services, and Dr. David Onofrei for NMR spectroscopy assistance.

#### Appendix A. Supplementary data

Supplementary data to this article can be found online at <https://doi.org/10.1016/j.poly.2022.116162>.

#### References

- [1] E. Li, J. Ye, Z. Wang, H. Mu, Z. Jian, Indole-bridged highphosphine-manganese palladium catalysts for ethylene polymerization and copolymerization with polar monomers, *Polymer Chemistry* 11 (2020) 2740–2748.
- [2] J. Jung, H. Yamada, K. Mizaki, Copolymerization of Nonpolar Olefins and Allyl Acrylate Using Nickel Catalysts Bearing a Methylene-Bridged Bisphosphine Monoxide Ligand, *Macromolecules* 53 (2020) 2547–2556.
- [3] A. Hamada, P. Braunstein, Lithium–Palladium Complex Supported by Phosphonatephosphine and Chloride Ligands, *Inorg. Chem.* 47 (2008) 3934–3936.
- [4] I. Le Gall, P. Laurent, E. Soutier, J.-Y. Saladin, H. des Abbayes, Complexation on rhodium of bidentate and potentially hemilabile phosphorus ligands, *J. Organomet. Chem.* 567 (1998) 13–20.
- [5] B. Wunnicke, T. Debaendemaeker, M. Klöppel, B. Rieger, Electron-Poor Olefin Polymerization Catalysts Based on Semi-Fluorinated Bis(phosphine)s, *Eur. J. Inorg. Chem.* 2000 (2000) 2063–2070.
- [6] M.L. Clarke, D. Ellis, K.L. Mason, A.G. Orpen, P.G. Pringle, R.L. Wiggall, D. A. Zales, R.T. Baker, The electron-poor phosphines  $F(C_6H_4)(CF_2)_2-3,5)_2$  and  $F(C_6F_5)_2$  do not mimic phosphines as ligands for hydroformylation. A comparison of the coordination chemistry of  $F(C_6H_4)(CF_2)_2-3,5)_2$  and  $P(C_6F_5)_3$  and the unexpectedly low hydroformylation activity of their rhodium complexes, *Dalton Trans* (2005) 1294–1300.
- [7] A.M. Tórcio, H. Bartosz-Berchowski, Z. Cmilik, K. Nieszyty, J.J. Ziółkowski, Structural studies of  $PF_6^-$  complexes with fluorinated phosphines, phosphites, and phosphinites as precursors of benzyl benzoate carbonylation catalysis, and X-ray crystal structure of *cis*- $PF_6^- [PPh_2(OEt)_2]$ , *Can. J. Chem.* 79 (2001) 752–759.
- [8] S. Brunetti, D. Priester, P. Beel, J. Corrom, S.J. Hart, T. James, B.J. Thwaiter, A. C. Whitwood, J.M. Slatery, Filling a Niche in “Ligand Space” with Bulky, Electron-Poor Phosphorus(III) Alkoxides, *Chem. Eur. J.* 25 (2019) 2262–2271.
- [9] B.G. Anderson, J.L. Spencer, The Coordination Chemistry of Pentafluorophenylphosphino Phosne Ligands to Platinum and Palladium, *Chem. Eur. J.* 20 (2014) 6421–6432.
- [10] V. Alessi, G. Bonamandelli, C. Giamlithorou, U. Frey, E.P. Kündig, A.E. Merbach, C. M. Sauton, F. Vitau, J. Weber,  $[Cp^*Pt(R)_2Scop-F(OEt)_2][SiF_6]^-$ , a New Fluorinated Chiral Lewis Acid Catalyst: Synthesis, Dynamic NMR, Asymmetric Catalysis, and Theoretical Studies, *J. Am. Chem. Soc.* 126 (2004) 4843–4853.
- [11] M.E. Bruis, E. Peter Kündig, A new chiral ligand for the Fe–Lewis acid catalyzed asymmetric Diels-Alder reaction, *Chem. Commun.* (1998) 2835–2836.
- [12] S. Thanasipol, B. Lohweg, C. Bernard, C. Sauton, E.P. Kündig, Ruthenium Lewis Acid-Catalyzed Asymmetric Diels-Alder Reactions: Reverse-Face Selectivity for  $\alpha, \beta$ -Unsaturated Aldehydes and Ketones, *Helv. Chim. Acta* 99 (2016) 774–789.
- [13] A.E. Bridon, C.J. Hebert, Fluoroalkyl-containing phosphites, *Coord. Chem. Rev.* 257 (2013) 880–901.
- [14] D.B. Grotzahn, D.A. Lev, A General Bifunctional Catalyst for the Anti-Markovnikov Hydration of Terminal Alkynes to Aldehydes Gives Enzyme-Like Rate and Selectivity Enhancement, *J. Am. Chem. Soc.* 126 (2004) 12232–12233.
- [15] C.R. Larsen, O. Erkögen, D.B. Grotzahn, General catalytic control of the monoisomerization of 1-alkenes to *trans*-2-alkenes, *J. Am. Chem. Soc.* 136 (2014) 1226–1229.
- [16] 7 - Enthalpy-Driven Reactions I: Acid-Base Reactions, in: W.W. Porterfield (Ed.) *Inorganic Chemistry (Second Edition)*, Academic Press, San Diego, 1993, pp. 361–406.
- [17] Y. Yamamoto, Y. Ishida, T. Kurohara, M. Shibuya, T. Yasui, Synthesis of  $\gamma$ -Difluoromethylated Terminate Derivatives from Squarates Using Difluoromethylphosphonate, *Heterocycles* 99 (1) (2019) 363.
- [18] C. Alter, E. Hoge, Synthesis and characterization of a novel difluoromethylene phosphonic acid functionalized polymer, *J. Appl. Polym. Sci.* 135 (42) (2018) 46765.
- [19] C. Cocaud, C. Nicolas, T. Poisson, X. Fanececker, C.Y. Legault, O.R. Martin, Tunable Approach for the Stereoselective Synthesis of 1-C-Dienylphosphono (difluoroethyl) Iminosugars as Glycosyl Phosphate Mimics, *J. Org. Chem.* 82 (2017) 2753–2763.
- [20] Z. Feng, F. Chen, X. Zhang, Copper Catalyzed Cross-Coupling of Iodobenzines with Bromo- $\gamma$ -difluoro-phosphonate, *Org. Lett.* 14 (2012) 1936–1941.
- [21] G.M. Blackburn, U. Hägerle, A. Horngardt, A.J. Incey, D.L. Jakeman, R. Spinks, Automated lineshape analysis of complex NMR spectra for a novel synthetic tetrafluoroethylphosphonate, a potential ligand for phosphoglycerate kinase, *Phosphorus, Sulfur, Silicon Rel. Elem.* 191 (3) (2016) 367–372.
- [22] T. Lequeux, F. Lehouc, C. Lapin, H. Yang, G. Gouhier, S.R. Fiette, Sulfonyl- and Tetraaryldifluoroethylphosphonates as a Source of Phosphooxidofluoromethyl Radicals and Their Addition onto Alkenes, *Org. Lett.* 3 (2) (2001) 185–188.
- [23] V. Chernykh, P. Beier, Development of (2-bromo-1,1,2,2-tetrafluoroethyl)(phenyl) sulfone as tetrafluoroethyl-radical and tetrafluoroethyl-ene-radical synthons for sulfonates to alkenes, *J. Fluorine Chem.* 156 (2013) 307–313.
- [24] S. Barata-Valdejo, M.V. Goske, A.L. Postigo, Radical Fluoroalkylation Reactions, *ACS Catal.* 8 (8) (2018) 7287–7307.
- [25] C.P. Zhang, Q.Y. Chen, Y. Guo, J.C. Xiao, Y.C. Gu, Progress in fluoralkylation of organic compounds via sulfonate/halogenation initiation system, *Chem. Soc. Rev.* 41 (2012) 4536–4559.
- [26] J.M. Smith, R.J. Vierling, C.F. Meyers, Selective inhibition of E. coli d-deoxy-*S*-phosphate synthase by acetylphosphonates, *MedChemComm* 3 (2012) 65–67.
- [27] H.-D. Köhnseckel, S. Berger, S. Brunst,  $^{13}C$ -NMR-Spektroskopie, Georg Thieme Verlag, Stuttgart, 1984, pp. 530–534.
- [28] A. Labed, F. Jiang, I. Labed, A. Latse, M. Peters, M. Arhard, A. Kaliniche, Z. Kabotche, G.V.M. Sharma, C. Brunneau, Iridium-Catalyzed Sustainable Access to Functionalized Imidolides through Hydrogen Autotransfer, *ChemCatChem* 7 (7) (2015) 1090–1096.
- [29] We thank a reviewer for discussing the possibility of a second order asymmetric induction that may have occurred during the crystallization of **4**. We do not believe that the initially observed solution diastereomer is different than the crystallized diastereomer, in large part because the solvents used are not that polar, and ionization of a metal-oxygen bond seems unlikely.
- [30] T.C. Cao, A.L. Cooksy, D.B. Grotzahn, Origins of High Kinetic (E)-Selectivity in Alkene Isomerization by a Cp\*Pt(PN) Catalyst: a Combined Experimental and Computational Approach, *ACS Catal.* 10 (2020) 15250–15258, and references therein.

Due to the lack of desired reactivity of the ligand synthesized, as well as the instability found in ligands of this type we chose to shift focus to different ligands that will be discussed in the next chapter.

Chapter 2, contains a reprint of the material as it appears in *Polyhedron*. Sattler, Daniel J., Bailey, Jake, Grotjahn, Douglas B., vol. 228, December 2022. The dissertation author was the primary investigator and author of this paper.

## Chapter 3 Imidazole based electron-poor ligands

### 3.1 Background and goals

As previously discussed in Chapter 1, bifunctional ligands may have considerable beneficial effects on a catalytic cycle. There are a variety of different functional groups that can act as a pendant functional group in a bifunctional ligand, but with the extensive successful use of imidazoles in the Grotjahn group as a pendant base for reactions with alkenes and alkynes previously discussed, imidazoles were the first choice for my initial studies.

The benefits of electron-poor ligands have already been discussed in Chapter 1, so for this work the identity of the electron-poor substituents to be used had to be determined. Phosphites have already been extensively studied, and as noted before can be vulnerable to nucleophilic substitution or transformation in the presence of an acidic proton to form the phosphonate<sup>60</sup>. In order to investigate the steric environment of the ligand as well as the electronic properties, trifluoromethyl and pentafluorophenyl were chosen for their significant electron withdrawing capabilities as well as the large difference in bulk that they would provide. Addition of pentafluorophenyl substituents to P-Cl units is accomplished using Grignard reagents, and formation of the bis(pentafluorophenyl)bromo- and chlorophosphines has been accomplished on large scale allowing for Grignard reagents to be converted to the corresponding aryl- or alkylbis(pentafluorophenyl)phosphine. Investigations involving other perfluoroalkyl substituents were also planned should greater steric modifications be required.

Before beginning the synthesis, several strategies were considered for the addition of the electron-poor containing substituents to the phosphine. While perfluoro lithium reagents have been used in the past<sup>61</sup>, their thermal instability, caused by facile decomposition into LiF and perfluoroalkenes<sup>62</sup> and their tendency to explode<sup>63</sup> motivated a search to find another route to add

trifluoromethyl substituents to a phosphine.

One possibility was the usage of Togni reagents, (Figure 3.1.1). Togni reagents have been used as trifluoromethylation reagents for a variety of different substituents<sup>64</sup> including on alkenes and alkynes<sup>65</sup> and are also relatively simple to make or commercially available. While they were a viable option, the planned synthetic strategy included the use of bisphosphines, in particular on a ferrocene backbone in order to take advantage of its wide bite angle to even further increase the rate of reductive elimination. Togni reagents have been reported to oxidize ferrocene<sup>66</sup> which would preclude their use in our synthetic strategy as they would require the addition of the desired pendant-base containing substituent at the beginning of the synthesis rather than at the end as was desired.

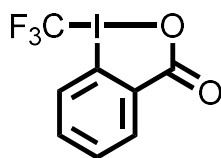


**Figure 3.1.1 Representative Togni reagent for use in trifluoromethylation**

Radical addition of fluoroalkyls has also been used to make fluoroalkylphosphines. An example uses trimethylsilylphosphines and iodoperfluoroalkanes though the reaction is sensitive to the steric bulk around the phosphine. Radical addition is known (Scheme 3.1.1) in the literature<sup>67</sup> and was examined in some initial preliminary work using (CF<sub>3</sub>)<sub>2</sub>CHI but the results were inconclusive.



**Scheme 3.1.1 Alternate route to formation of perfluoro- alkyl and aryl phosphines**

The commercially available Ruppert-Prakash reagent,  $\text{Me}_3\text{SiCF}_3$ , was chosen because it readily displaces alkoxy or phenoxy groups from a phosphonite and adds trifluoromethyl under relatively mild conditions (Scheme 3.1.2).



**Scheme 3.1.2 General reaction for Ruppert Prakash reagent and a phosphite or phosphonite**

### 3.2 Strategy and reasoning

The chosen route was to synthesize the dichlorophosphines, and then use an alcohol or phenol and an amine base to form the phosphonite and a protonated base. Using a nonpolar solvent such as pentane or hexane would allow for removal of the salt through filtration. As phosphonites are generally stable towards water in an extraction at room temperature, removal of any remaining protonated base with a water wash should be available as needed.

The use of trifluoroethoxy instead of the more usual phenoxy was chosen because it was believed that it would be a better leaving group, leading to faster reactions when adding the trifluoromethyl groups, moreover the lower boiling point of  $\text{CF}_3\text{CH}_2\text{OH}$  was also seen as a benefit as many of the phosphonites would be oily liquids and so the removal of excess trifluoroethanol from the synthesis of said phosphonites would be simpler and more efficient.

The starting pendant-base containing substituent was 4-*t*-butyl *N*-methyl imidazole, (abbreviated **Im'H**) which was synthesized using methods previously developed in unpublished work in the Grotjahn lab. The synthesis of  $\text{Im}'\text{PCl}_2$  was known in the Grotjahn group<sup>68</sup>. Dichlorophenyl phosphine was also used, both as an eventual control compound and to investigate

the synthetic strategy using a relatively inexpensive starting material that was commercially available.

This strategy worked well with the initial substrate, Im'H (Figure 3.2.1)

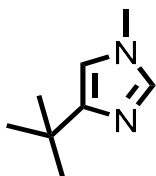
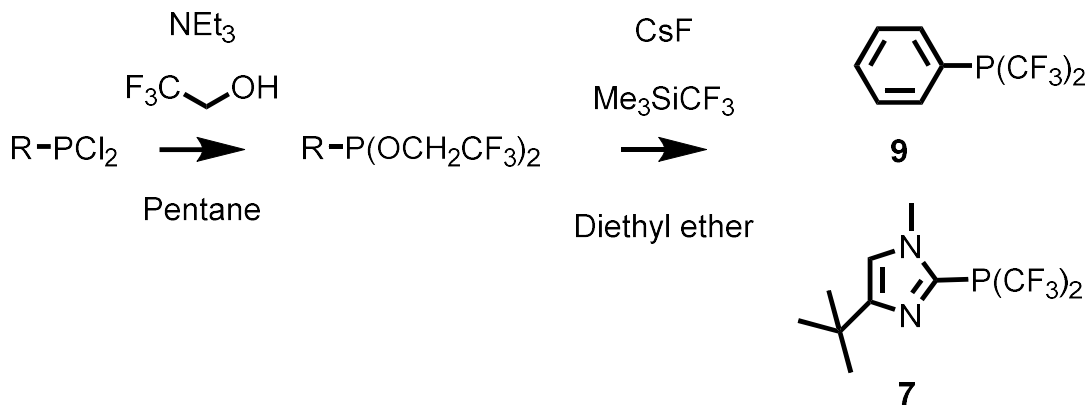


**Figure 3.2.1 4-*t*-butyl N-methyl imidazole (Im'H)**

and phenyl, though triethylammonium salts were still present in small amounts even after filtration through a fine, fritted glass filter. Using sodium hydride to deprotonate the trifluoroethanol was effective, and the sodium salts produced in reaction with the dichlorophosphine were readily removed by filtration. It was believed that we could safely store the sodium trifluoroethoxide, however when drying approximately 30 grams in a vacuum desiccator, a small fire and explosion was noted destroying the product. Thankfully, while it cannot be stored long term it can be isolated and weighed so long as it is used shortly after synthesis.

Incorporation of the trifluoromethyl groups using Ruppert-Prakash reagent proceeded well, though purification became an issue. The final components of the reaction mixture were the product bis(trifluoromethyl)phosphine, trifluoroethoxy containing silanes, and cesium salts. Removal of the cesium salts was readily accomplished using filtration, and vacuum distillation gave the desired products (Scheme 3.2.1).

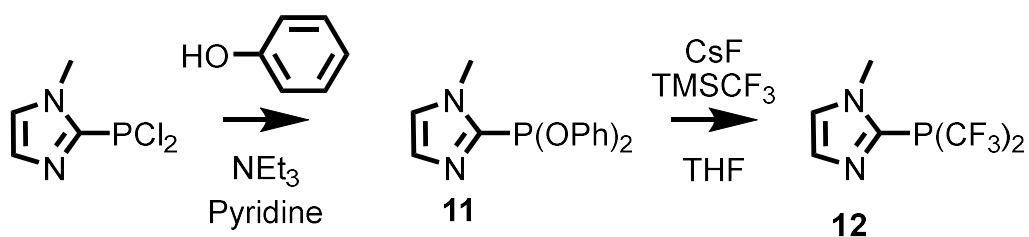




**Scheme 3.2.1. Synthetic route to bis(trifluoromethyl)phosphines**

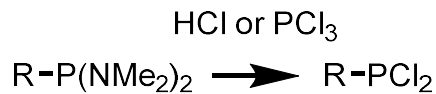
Several changes were made, and new information was found during the work on this synthesis. One of the first was that while the synthesis itself worked relatively well, the method used to synthesize the imidazole dichlorophosphines was not useful for the synthesis of other dichlorophosphines such as from anisoles or phenols as discussed in chapter 4. The simplest strategy would be to add the desired substituent through either a Grignard or lithium reagent acting on  $\text{PCl}_3$ , giving a mixture of the mono-, di-, and trisubstituted phosphine followed by purification. Hence, bis(dimethylamino)chlorophosphine was used to prevent more than one substitution on the phosphine. The dimethylamino groups could then be substituted for chlorides using  $\text{PCl}_3$  or  $\text{HCl}$  allowing for trifluoroethoxy substitution.

In the course of developing the synthetic strategy, several issues arose that required modification as well as revealing issues with the strategy in general. Synthesis of the unsubstituted imidazolyl phosphines was only achieved in a much lower yield (Scheme 3.2.2). The final product was seen by NMR spectroscopy, but in very low yield that was not able to be isolated in pure form using this strategy.



### Scheme 3.2.2 Synthesis of bis(trifluoromethyl) N-methyl imidazolyl phosphine

One change made led to both a beneficial advancement and a good reason to move away from imidazoles as the pendant base containing substituent. Literature investigation into a way to more precisely control formation of the dichlorophosphines showed that dialkyl amino substituents on a phosphine are resistant to nucleophilic substitution. They are also readily removed by treatment with either protic acid or  $\text{PCl}_3$  to give the dichlorophosphines. (Scheme 3.2.2).



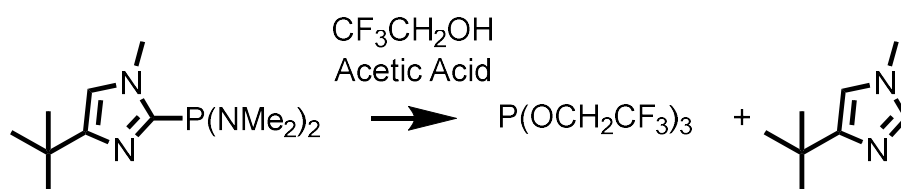
### Scheme 3.2.3 Methods for substitution of a dimethylamide for a chloride on a phosphine

Using aminophosphine intermediates would allow for a more controlled and atom-economical addition of a substituent containing a pendant group to a phosphine. Experimentally it was found that it is possible to bypass the dichlorophosphine step altogether using acid-catalyzed removal of the  $\text{NMe}_2$  in the presence of the desired alcohol to form the phosphonite (Scheme 3.2.3).



**Scheme 3.2.4 Formation of phosphonites directly from dimethylamino-substituted phosphines**

Surprisingly, the P-C bond of imidazolyl phosphines are also capable of acidic cleavage, even when catalytic acetic acid is the acidic proton source (Scheme 3.2.5).

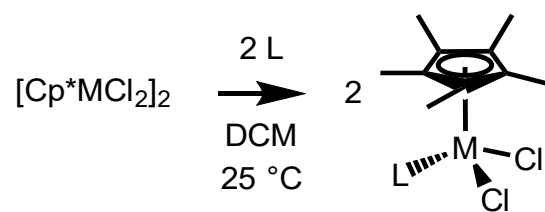


**Scheme 3.2.5 Cleavage of P-N and P-C bonds under mild acidic conditions**

### 3.3 Initial testing for catalytic activity

The new ligand Im<sup>\*</sup>P(CF<sub>3</sub>)<sub>2</sub> (7), combined with bis(trifluoromethyl)phenyl phosphine still gave an excellent starting point including a control ligand without pendant base for initial studies into the reactivity of electron-poor phosphines containing a pendant base, such as testing to determine if they would be useable as ligands or if their electron-poor nature prevented their coordination to metal complexes.

Initially the ligands were coordinated to [Cp<sup>\*</sup>RhCl<sub>2</sub>]<sub>2</sub> and [Cp<sup>\*</sup>IrCl<sub>2</sub>]<sub>2</sub> (Scheme 3.3.1) which are known to generally give stable complexes.



**Scheme 3.3.1** Coordination of Im'P(CF<sub>3</sub>)<sub>2</sub> and PhP(CF<sub>3</sub>)<sub>2</sub> to Rh and Ir

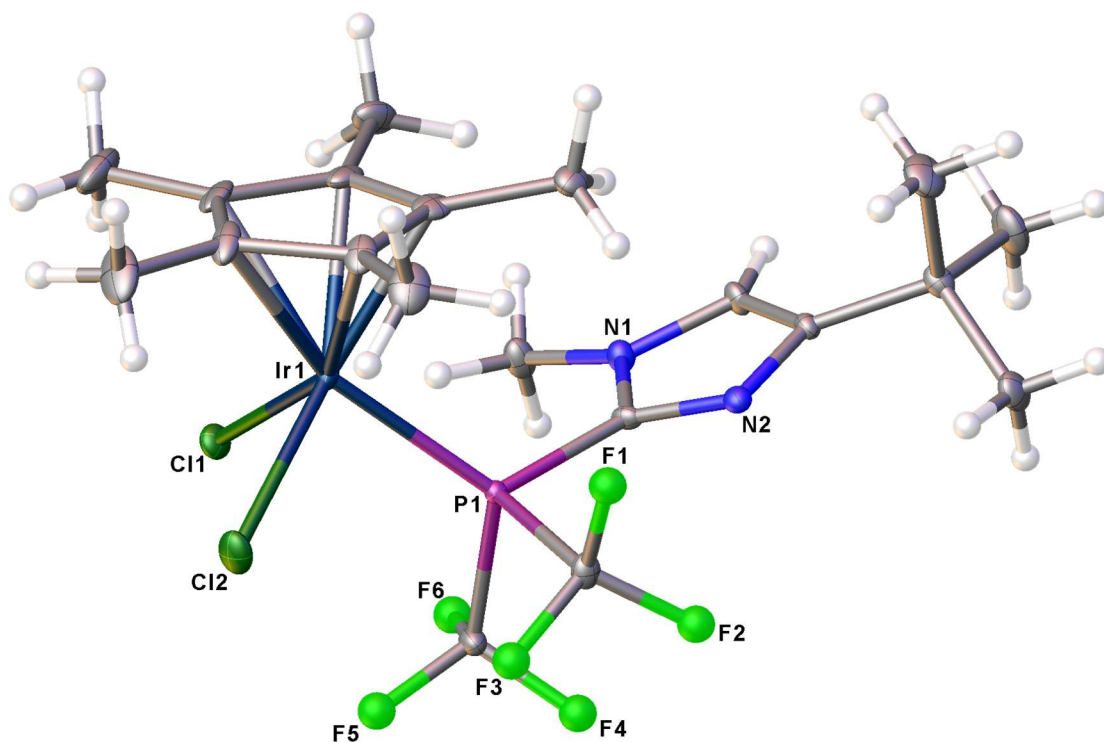


**Figure 3.3.1** X-Ray diffractometry structure of Cp\*IrCl<sub>2</sub>(Im'P(CF<sub>3</sub>)<sub>2</sub>)

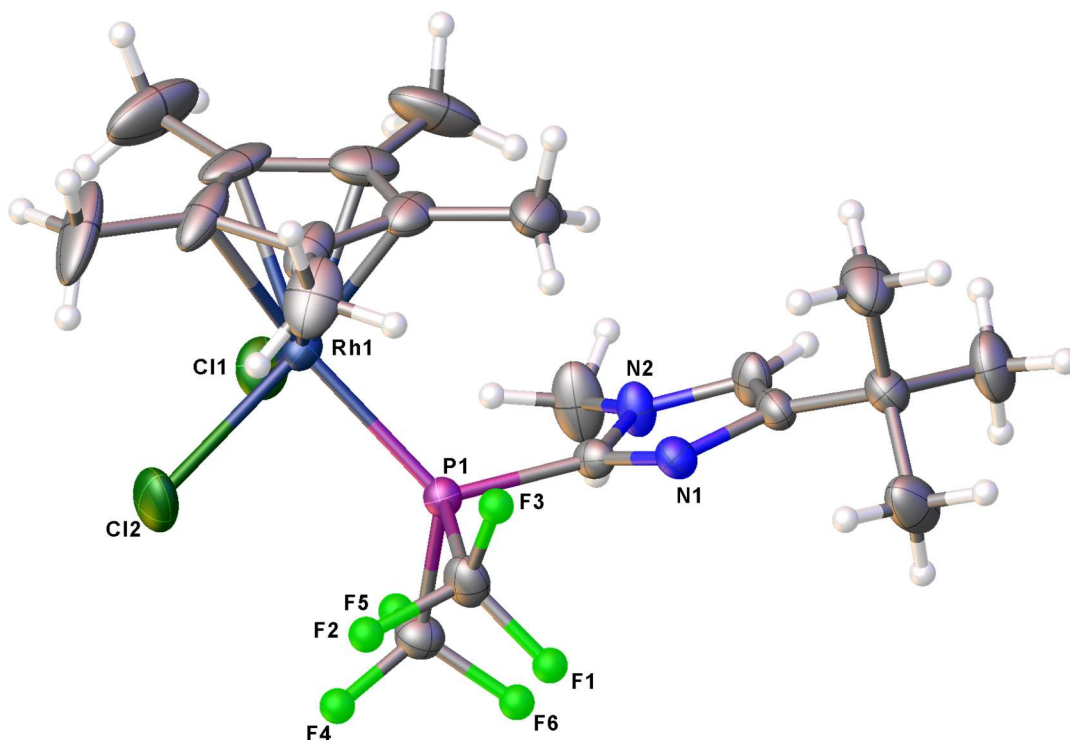


**Figure 3.3.2 X-Ray diffractometry structure of Cp\*RhCl<sub>2</sub>(Im'P(CF<sub>3</sub>)<sub>2</sub>)**

Gratifyingly the ligands were capable of coordinating to the metal center and X-ray crystal structures of the compounds were obtained (Figures 3.3.1 and 3.3.2). Before ionization of the metal center to remove the chloride ion the complexes were air stable. After ionization they were very reactive to air and moisture in an unknown fashion. These complexes did show evidence of interactions with an alkene by NMR spectroscopy, though only a mixture of isomers was formed when they were reacted. Addition of a nucleophile, both acetic acid and water were used, but gave no reaction with the alkene.

The bis(pentafluorophenyl) derivatives could be synthesized by first making the bromo(bispentafluorophenyl)phosphine using literature procedures<sup>69</sup>, followed by addition of the pendant group containing substituent. The N-methyl imidazolyl compound (**31**) (Figure 3.3.1) was

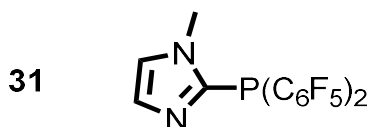
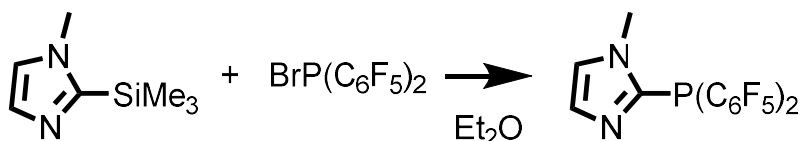


**Figure 3.3.3 Compound 31**

synthesized using 2-trimethylsilyl N-methyl imidazole (Scheme 3.3.2) in a previously reported method<sup>70</sup>.



**Scheme 3.3.2 Synthesis of N-methylimidazolyl bis(pentafluorophenyl)phosphine**

Addition using aryl lithium reagents gave a mixture of products, suggesting that the pentafluorophenyl substituent is susceptible to nucleophilic substitution similar to trifluoromethyl substituents<sup>71</sup> or through  $S_NAr$ . The route to compound **31** is relatively atom economical because of the lower number of steps.

The vulnerability of the C2-imidazole phosphorus bond<sup>72</sup> to acid and to oxidative addition to a metal (Braden Silva, unpublished results), combined with some calculations performed by Dr. Grotjahn caused a review of what pendant group containing substituent should be used in this work, and is discussed in chapter 4.

### **3.4 Catalytic investigation involving high-throughput experimentation in collaboration with the University of Pennsylvania**

#### **3.4.1 Hypothesis and design of experiments**

High-throughput experimentation (HTE) has become a valuable tool in a chemist's arsenal

for optimization of reaction conditions and screening compounds for activity. The main benefit of high-throughput experimentation is that many reactions can be run in parallel, then analyzed quickly to give the desired information. Another major benefit of high-throughput experimentation is that the scale of a reaction is very small, with reactions run in the course of this work requiring less than 10 mg of a ligand to run multiple reactions, and even lower amounts are possible. The small scale and speed of reaction and analysis can save a chemist considerable time and material during an investigation. The small amount of compound required for high-throughput experimentation also allows for screening of a new ligand or catalyst for currently unsolved problems or other useful and impactful chemistry with minimal effort.

The Grotjahn lab has a long-standing collaboration with the HTE facility at the University of Pennsylvania, to which I traveled for one week to learn how to set up and run high-throughput experiments, as well as test some of the ligands created in this work for their catalytic activity related to addition of a hydroxyl group to an alkene. If any of the ligands showed positive or potentially positive results, further investigations would have been performed at SDSU on a larger scale and with continued optimization.

The substrate chosen for this testing was 10-phenyl-1-decene, (Figure 3.4.1.1). 10-Phenyl-1-decene was chosen as it was large enough to be easily detected in the mass spectrometer after gas chromatography, it had a UV-vis chromophore, and it also gave two potential outcomes for reaction with a catalyst, namely potential isomerization of an alkene from its terminal position as well as addition of a hydroxyl group to an alkene. Isomerization was not the desired outcome for these ligands but it would inform us if there were an interaction between the catalyst and alkene. Moreover, if the double bond moved 8 positions into conjugation with the phenyl ring, that would be a sign of a new alkene isomerization catalyst possibly worth exploring at SDSU.

### 3.4.2 Results

The two ligands screened were the bis(trifluoromethyl)phenyl phosphine and  $\text{Im}^*\text{P}(\text{CF}_3)_2$  (Figure 3.4.2.1). These ligands, along with other commercially available ligands were mixed in a glove box with a metal precursor in a reaction vial with a stir bar and allowed to mix for 10 min. The relevant alkene and hydroxyl containing compound were then added in the glove box, the reaction was heated to 100 °C and stirred for 12 h. The solutions were quenched with methanol that contained mesitylene as a standard and analyzed by GC-MS. Twenty four reactions were run at a time and a representative example gas chromatographic trace is shown (Figure 3.4.2.1). No addition to the alkene was shown, the only other peak identifiable was starting material, and that was not always present.

Given the equivocal results just discussed, and given various examples of imidazole-phosphorus bond instability, the research was switched to synthesis and evaluation of phenolic phosphines, in Chapter 4.

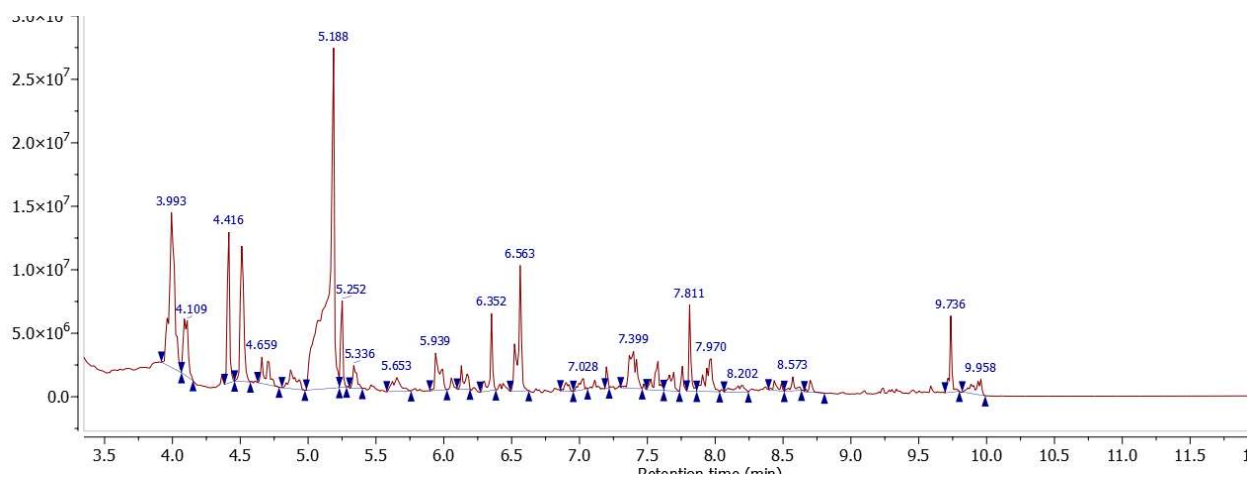


**Figure 3.4.2.1** An example of one gas chromatographic trace showing the complexity of one reaction



## Chapter 4 Phenol- and anisole-based ligands

While imidazole was believed to be a good starting point as a pendant base containing substituent, the difficulties that arose during the synthesis of **7** as well as the possible degradation of the ligand during the catalytic cycle led us to choose a different source of pendant functionality. The carbon-phosphorus bonds in imidazole species could not only be acid sensitive, but in some cases was cleaved by the metal center in a complex (Braden Silva, unpublished results).

Calculations by Dr. Grotjahn suggested that phenylphosphines with an ortho OH or OCH<sub>3</sub> group could enter into stronger hydrogen-bonding interactions with a OR group coordinated to Pt(II) (Figure 4.1)

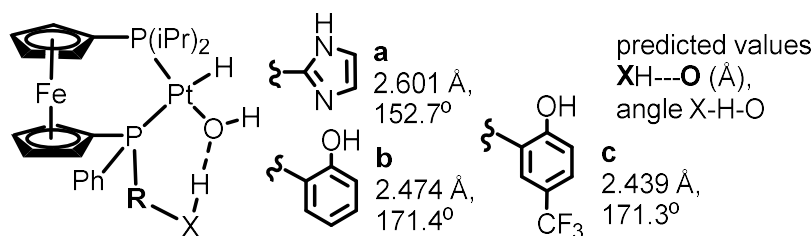


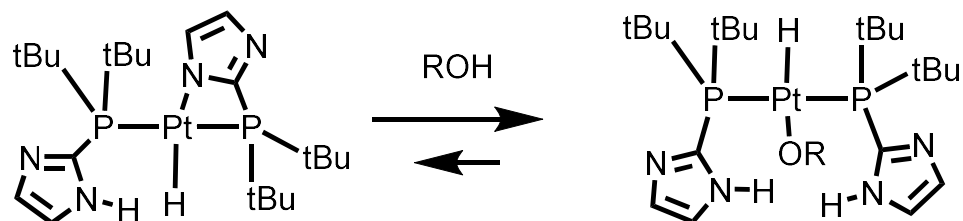
**Figure 4.1** More favorable hydrogen-bonding with phenols than with the NH imidazole

Moreover, we were unable to find literature precedent for the breaking of the carbon-phosphorus bond in hydroxyl- and methoxy-substituted phosphines.

### 4.1 Oxidative addition of water to platinum complexes

Previous work in the Grotjahn lab has shown that bifunctional ligands containing imidazolyl substituents are capable of activating a water molecule through oxidative addition in platinum complexes<sup>40</sup> (Scheme 4.1.1), though they did not catalyze the desired alkene hydration reaction, possibly because reductive elimination of any OH and alkyl ligands on a putative

intermediate was prevented by trans disposition of the two phosphines.



#### Scheme 4.1.1. Addition of hydroxyl containing molecules to a Pt center

Our hypothesis was that using phenol as a substituent would enable similar or superior reactivity of the metal center in analogy to Fig. 4.1. Colleague Guja Gojiashvili in the Grotjahn lab made parent compound **32** (Figure 4.1.1), however, surprisingly, the free OH interacted strongly with the platinum, even showing Pt-H coupling in NMR spectroscopy, and possibly preventing the desired reactions with a variety of O-H reagents.

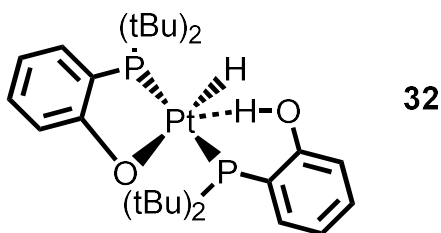
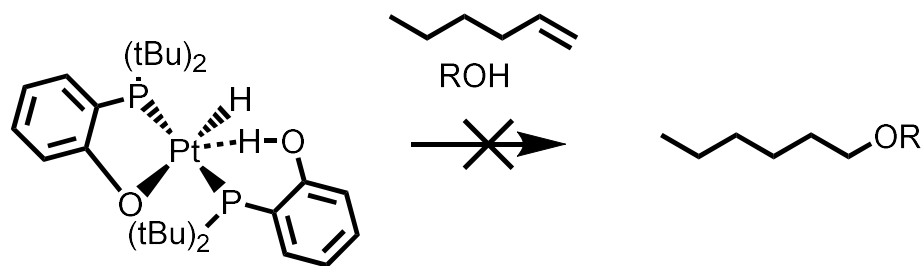


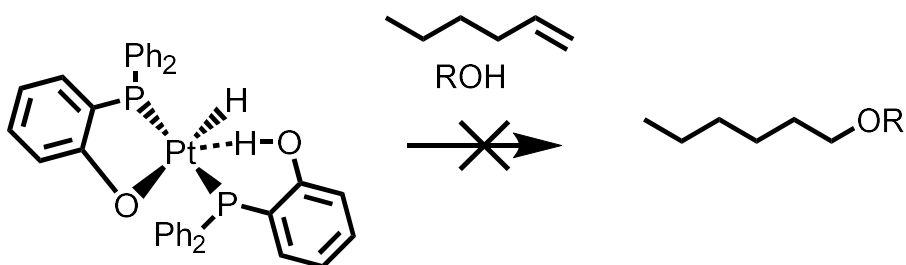
**Figure 4.1.1. Pt complex with hydrogen bonding from pendant hydroxyl group on a phosphine ligand**

Pt coupling seen with H-O hydrogen



R = CH<sub>3</sub>SO<sub>2</sub>, H, CH<sub>3</sub>CO,

No Pt coupling seen with H-O hydrogen



R = CH<sub>3</sub>SO<sub>2</sub>, H, CH<sub>3</sub>CO,

#### Scheme 4.1.2 Investigations into alkene addition using Pt-H complexes

Calculations verified that there was some interaction between a pendant hydroxyl hydrogen and the platinum, and so further calculations were performed in order to determine how a substituent on the phenolic ring could be modified in order to change the electronic and steric properties of a bifunctional ligand. Gas phase calculations were carried out by Guja on changing the ligand tBu for other groups, and by me on substitutions on the aromatic ring of the phenolic group, using b3lyp/SDD as the functional and basis set, respectively, with different functional groups placed at each of the carbon atoms not bound to an oxygen or phosphorus atom to determine what effect on the Pt-H distance modification of the electron density of the aryl ring would have. A secondary benefit of these calculations was the determination of which compounds could be placed ortho to the hydroxyl group on the phenol to determine if the coordination of the pendant

hydroxyl hydrogen could be prevented through steric means. Calculations performed by the author showed that the interaction could be weakened to a small extent by addition of an electron withdrawing group, whereas using other electron-poor substituents on the phosphine had a greater overall impact on the Pt-H interaction (see Fig. 4.1.4), lengthening the distance by ca. 0.1 Å, motivating the synthesis of several electron-poor phosphines in the next section. Ligands that had steric interactions preventing synthesis of stable complexes were discovered, but overall the Pt-H interaction was most changed by changing -PtBu<sub>2</sub> to P(CF<sub>3</sub>)<sub>2</sub> rather than by changing any substituent on the phenol ring . (Unfortunately the ligand synthesis took so much time that in the end, testing of the resulting complexes has not yet occurred.)

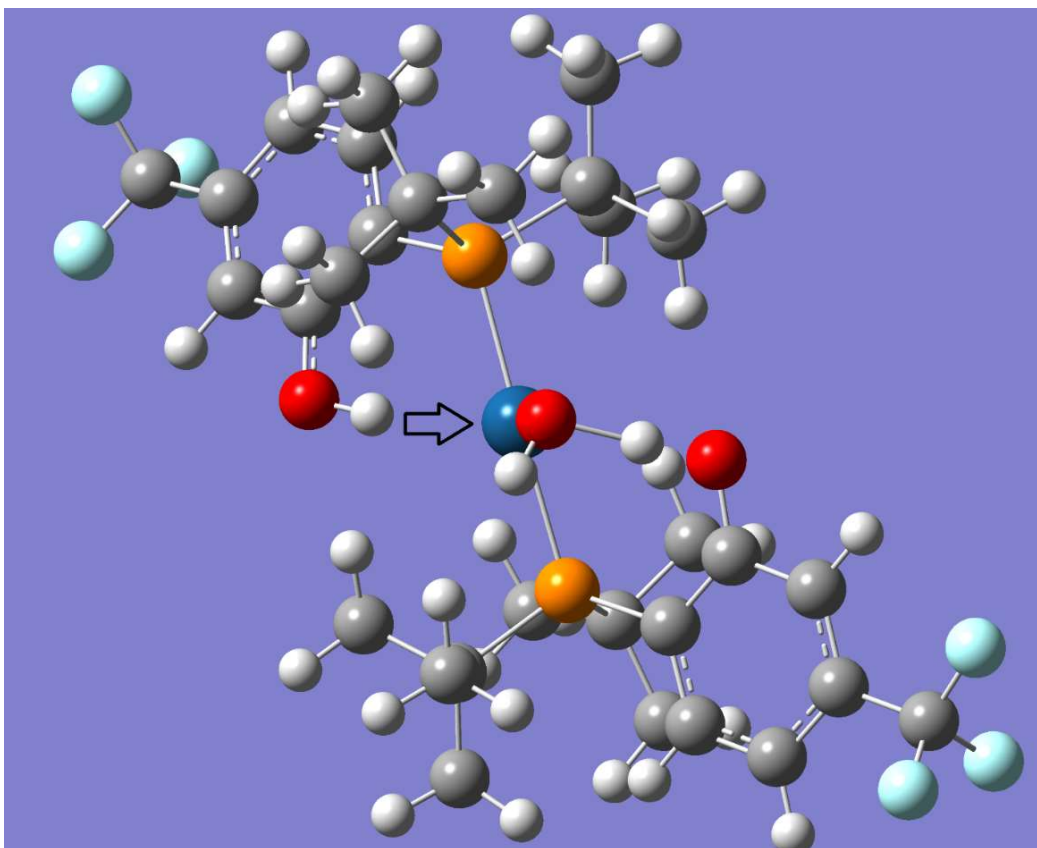


**Figure 4.1.2** Calculated structure using two phenolic phosphines with an electron withdrawing CF3 para to OH, showing bond geometry and H-Pt distance (2.175 Å) of OH---Pt interaction.

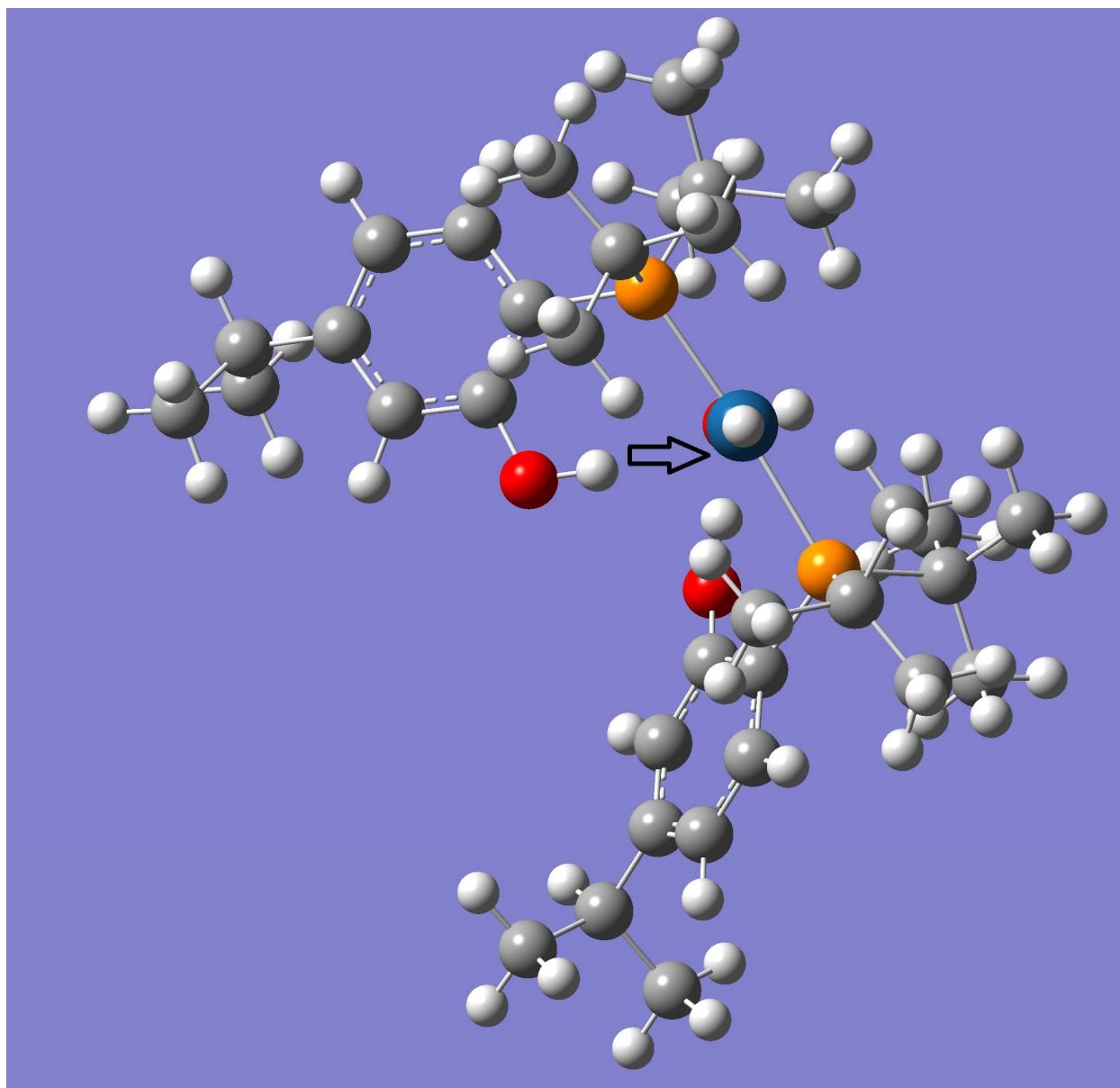


**Figure 4.1.3** Calculated structure using two phenolic phosphines with an electron donating *i*-Pr para to P, showing bond geometry and H-Pt distance (2.156 Å) of OH---Pt interaction.

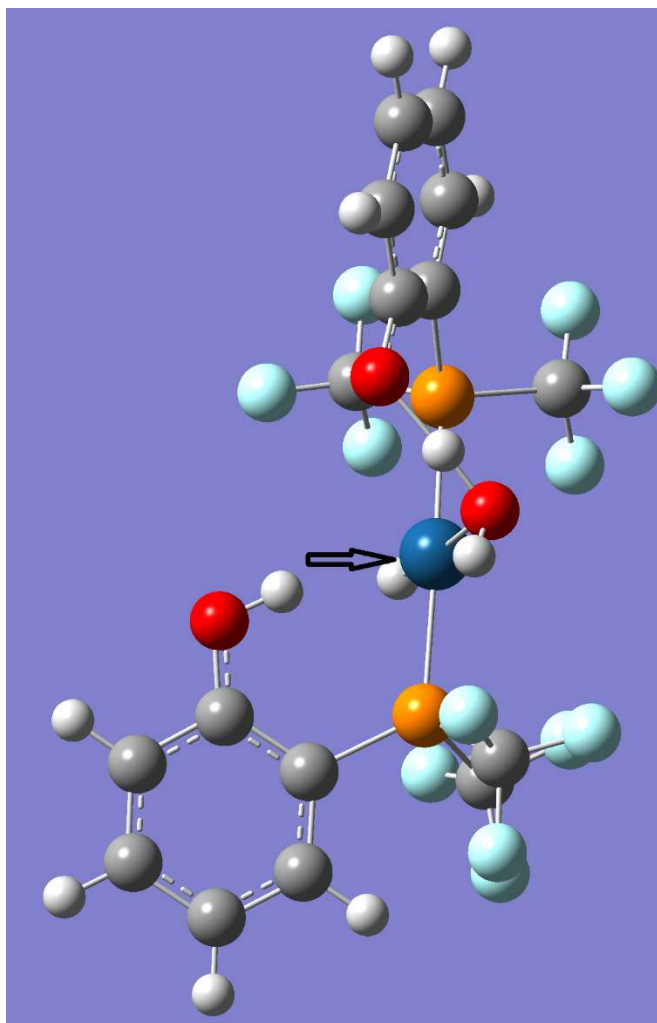
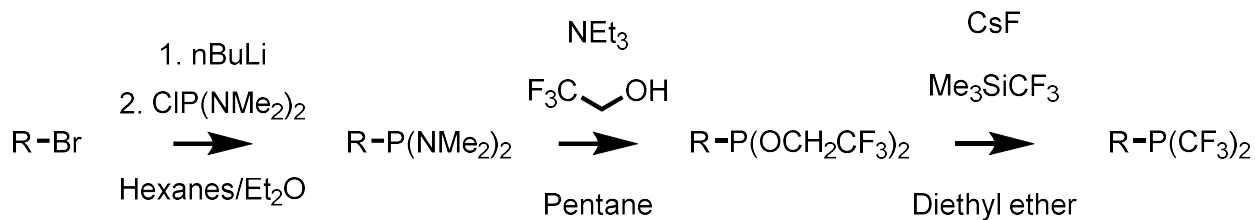


**Figure 4.1.4** Calculated structure using two phenolic phosphines with two electron withdrawing CF<sub>3</sub> on P, showing bond geometry and H-Pt distance (2.255 Å) of OH----Pt interaction.

## 4.2 Synthesis of monodentate electron-poor bifunctional ligands

The synthetic procedure was similar, however, which made the synthesis of new ligands relatively straightforward (Scheme 4.2.1), giving the products in Figure 4.2.1.



**Scheme 4.2.1. Synthetic route to bis(trifluoromethyl) aryl phosphines before demethylation with BBr<sub>3</sub>**

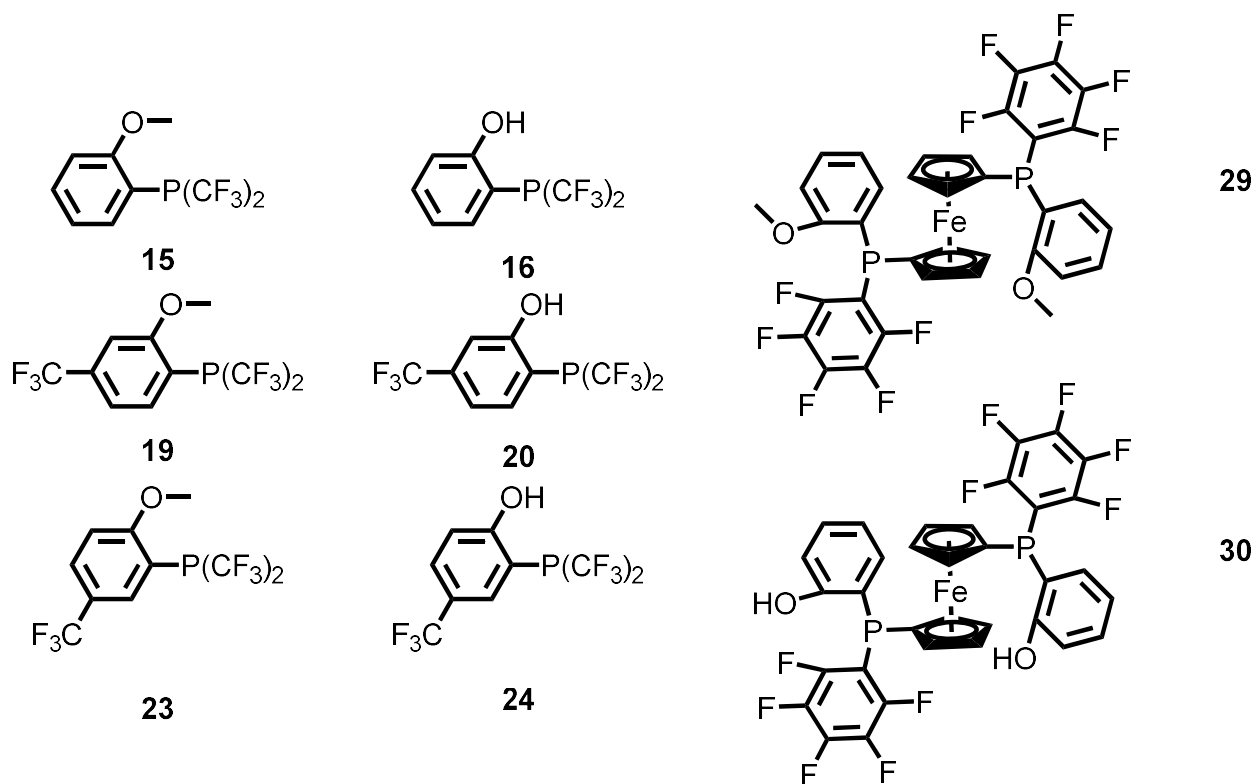
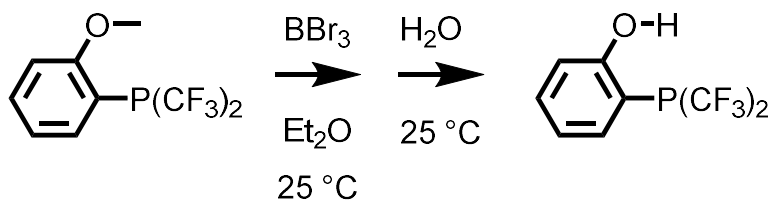


**Figure 4.2.1. Mono- and bidentate ligands synthesized**



**Scheme 4.2.2. Demethylation of anisoles using BBr<sub>3</sub>**

The main difference would be that the hydroxyl group on the phenol needed to be protected in



some fashion in order to not interfere with synthesis. This was not seen as a major downside, as the methoxy group would still be able to function in a pendant fashion allowing for its additional use as a potential ligand. Demethylation using  $\text{BBr}_3$  was also a relatively straightforward and effective method of obtaining the phenolic ligand (Scheme 4.2.2). From Chapter 3, the discovery that trifluoroethanol and acetic acid form the phosphonate from the amino phosphine would simplify the overall procedure and allowing one to avoid a complicated and very air- and moisture-sensitive reaction and purification. Once the phosphonite was formed, addition of the Ruppert-Prakash reagent gave the desired bis(trifluoromethyl)phosphine in good overall yield. Demethylation was accomplished at  $25\text{ }^\circ\text{C}$ , and purification was simplified as the bis(trifluoromethyl)phosphines are very difficult to protonate, even with a strong acid such as  $\text{HBr}$  that is formed during the demethylation and work up. Yields were very low during the first text experiments, and this is believed to be in part due to the slight solubility of the phosphine due to the trifluoromethyl substituents and the hydroxyl group.

Purification was also greatly simplified using anisole-based substituents. The main side product from the synthesis of the phosphonite is any of the starting lithiated anisole that was protonated by advantageous water. These anisoles have much lower boiling points than phosphonites and can be readily removed through low pressure distillation, while the phosphonite can be readily distilled using vacuum distillation.

Ligands containing methoxy groups also gave us another option as a pendant acceptor of a hydrogen bond. Functionally this gave us two ligands with only one additional step needed to make the second ligand.

Ligands such as those shown in Figure 4.2.1 should promote the conversion of an aryl

halide to an ester when using carbon monoxide, alcohol, and a base through several possible effects. A pendant substituent should be capable of hydrogen bonding to an incoming alkoxide, favoring approach to the acyl carbon, or would accept a hydrogen bond from the alcohol, increasing its nucleophilicity; either possibility would increase the rate of reaction at the acyl group, as shown in Figure 4.2.2.

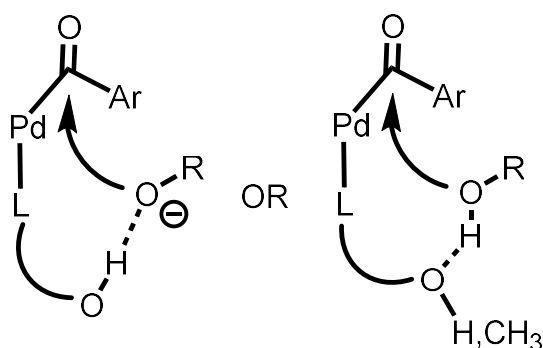
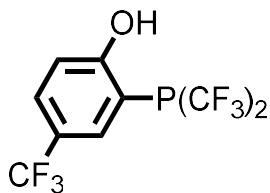
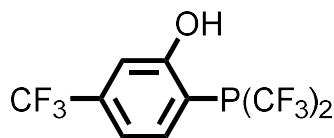


**Figure 4.2.2. Two possible ways a pendant group could increase rate of acyl attack**

An additional benefit of using phenyl rings that have varied substituents is that we can tune the properties of both the pendant substituent and the phosphorus atom that is bound to the metal by changing the position or identity of additional groups on the aromatic ring. In this way we can cause a pendant hydroxyl group to be more or less acidic, or cause the phosphine to bind more or less strongly (Figure 4.2.3)



More strongly impacts  
pKa of pendant hydroxyl

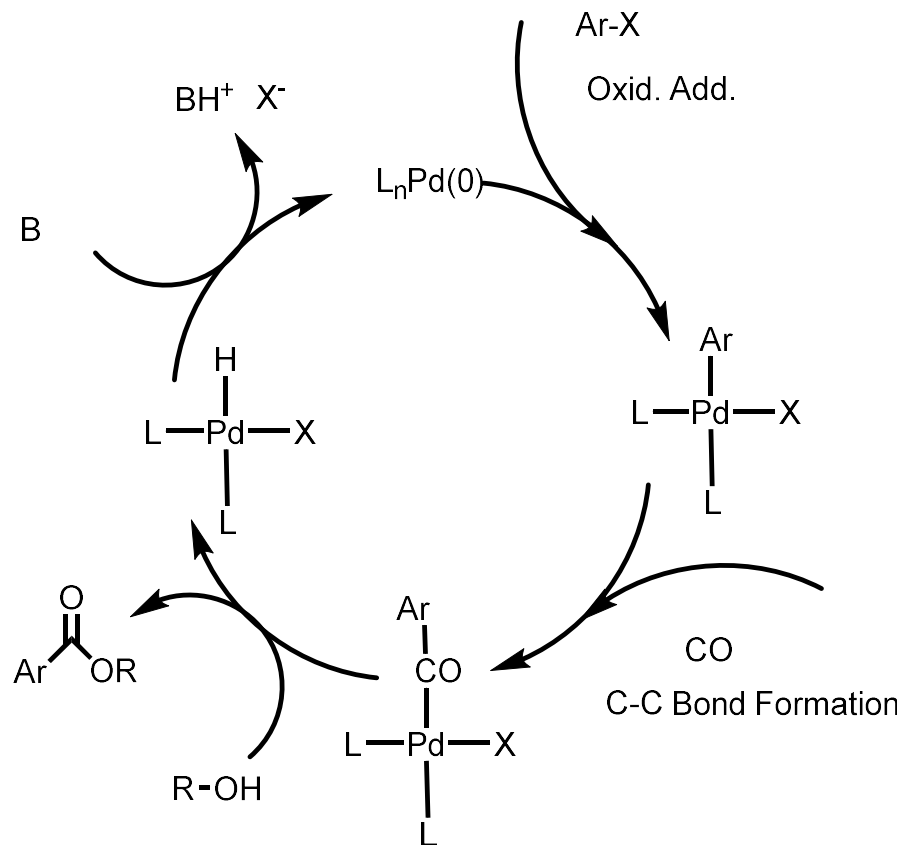


More strongly impacts properties of phosphine ligand

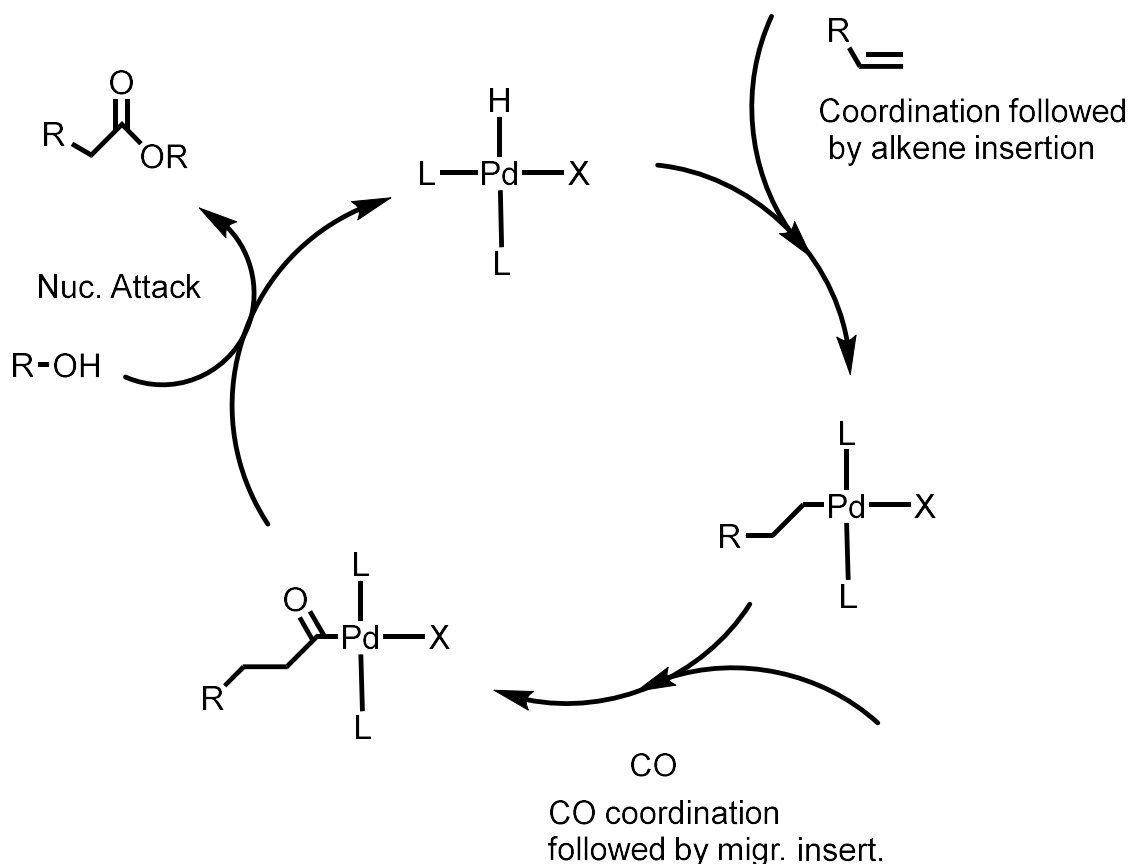
Figure 4.2.3. Impact of aryl substituents on properties of ligands We chose to explore carbonylative cross-coupling of aryl halides if alkene addition chemistry was not realized for electron-poor ligands; a brief review of carbonylation comes in the next section.

#### 4.2: Addition of carbon monoxide and either H<sub>2</sub>, H<sub>2</sub>O, or ROH

The following section briefly introduces processes that reaction CO and either hydrogen, water, or alcohols with either alkenes / alkynes or aryl halides such as alkoxy carbonylation, Reppe carbonylation, hydroformylation, the Monsanto and Cativa processes, the Lucite-Alpha process, oxidative carbonylation, and hydrocarboxylation and hydroesterification. The different processes all differ in their uses, reaction conditions, and reagents involved, the currently accepted mechanisms are shown below (Schemes 4.2.1 and 4.2.2).



**Scheme 4.2.1. General mechanism for carbonylative cross-coupling of aryl halides**



**Scheme 4.2.2. General mechanism for alkoxy carbonylation of an alkene**

#### 4.2.1 Hydroformylation/Reduction

Hydroformylation of an alkene to form an aldehyde or ketone was first discovered in the 1930's<sup>73</sup> and is used extensively in industry<sup>74</sup>. Transforming an aldehyde to the corresponding alcohol using molecular hydrogen is a common strategy. Other methods that combine the two steps using one catalyst have been developed<sup>75-77</sup>. Internal alkenes have also been effectively transformed into the corresponding alcohols by utilizing the ability of a metal catalyst to isomerize alkenes<sup>78</sup>, though this method gives both the primary and secondary alcohol and is limited in the functional groups the alkene can contain. Hydroformylation and reduction to the alcohol is effective, but reaction conditions that are not amenable to functionalized alkenes due to the

reduction step limits its usefulness.

#### **4.2.2 Hydroesterification/Alkoxy carbonylation**

Alkoxy carbonylation has also been in use since its initial discovery in 1938<sup>79</sup> by Reppe at BASF. The initial work involved considerable pressure (700-900 atm) of carbon monoxide and elevated temperatures (approximately 300 °C) and toxic Ni(CO)<sub>4</sub> as the metal precursor but was a useful organic synthesis for the formation of esters. The first major improvement to the reaction using palladium was reported in 1968<sup>80</sup> and lowered the pressure to only 300 atm and the temperature to 60-100 °C. The alkoxy carbonylation of alkynes has also been improved with the reaction taking place at 45 °C and only 60 atm<sup>81</sup> using a bifunctional ligand, 2-PyridylPPh<sub>2</sub>.

#### **4.2.3 Alcohol carbonylation**

Addition of carbon monoxide to an alcohol has also been developed, with several processes having been developed to do so. Two currently used related methods are the Monsanto process first developed in 1968<sup>82</sup> which uses a rhodium iodide based catalyst and the Cativa process<sup>83</sup> which is similar enough to the Monsanto process that it can be performed in the same plant. While the production of acetic acid is a form of carbonylation, it is not a focus of this work.

#### **4.2.4 Lucite Alpha process**

The Lucite Alpha process<sup>84</sup> is a two-step process used primarily for the production of methyl methacrylate. The first step, a palladium-catalyzed carbonylation of an alkene in the presence of methanol in order to form methyl propionate, is of relevance to this work and is followed by reaction with formaldehyde in the presence of cesium oxide to form methyl methacrylate and water.

#### **4.2.5 Oxidative carbonylation**

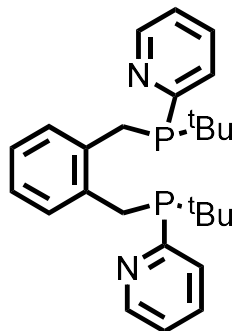
Oxidative carbonylation has considerable use in the production of dimethyl oxalate<sup>85</sup>. Oxidative carbonylation uses two different catalysts in industry depending on the substrate to be carbonylated. Methanol is reacted with carbon monoxide and an oxidant to form dimethyl carbonate and dimethyl oxalate using a copper catalyst, while the oxidative carbonylation of alkenes uses a palladium catalyst.

#### **4.2.6 Addition of a new functional group using carbonylative cross-coupling of aryl halides**

Carbonylative cross-coupling of aryl halides is also of value as functionalization of aromatic rings through the addition of a carbonyl group is useful synthetically. Previous work in this area has shown reaction conditions that require either increased pressure, elevated temperature or extended time. Investigations by other groups have focused on milder conditions for this reaction as well as increased yields. There is still room for improvement however, and electron-poor bifunctional ligands have yet to be widely investigated in this manner.

#### **4.3 Electron-poor bifunctional ligands and their use in carbonylative cross-coupling of aryl halides**

Bifunctional ligands such as those in Figure 4.3.1 have been used in carbonylative cross-coupling reactions<sup>86</sup> to good effect, giving up to 95% yield of a methyl ester from 4-iodomethylbenzene<sup>87</sup>. This high yield did require elevated temperatures (80 °C), elevated pressure (up to two Atm CO), and extended reaction times (6-8 h).



#### 4.3.1. Structure of 1,2-bis(di-*tert*-butylphosphinomethyl)benzene, a ligand commonly used in carbonylation reactions

Using a bifunctional ligand in carbonylation chemistry also provides additional options during the catalytic cycle to help stabilize or even regenerate<sup>88</sup> the active palladium-hydride species when Pd(0) is formed, as the protonated ligand can oxidatively add to Pd(0) to form the Pd-H species, the resting state of the catalyst. Protonation of the ligand can occur either by reductive elimination from the Pd-H species (Scheme 4.3.1) or by reaction with a protic solvent<sup>89</sup>.

The use of electron-poor ligands other than phosphites or phosphonates has yet to be discussed in the literature. Our hypothesis was that combining the known effectiveness of bifunctional ligands and electron-poor ligands in carbonylation reactions could improve the reactivity of a metal complex and allow for milder reaction conditions in a carbonylation reaction.

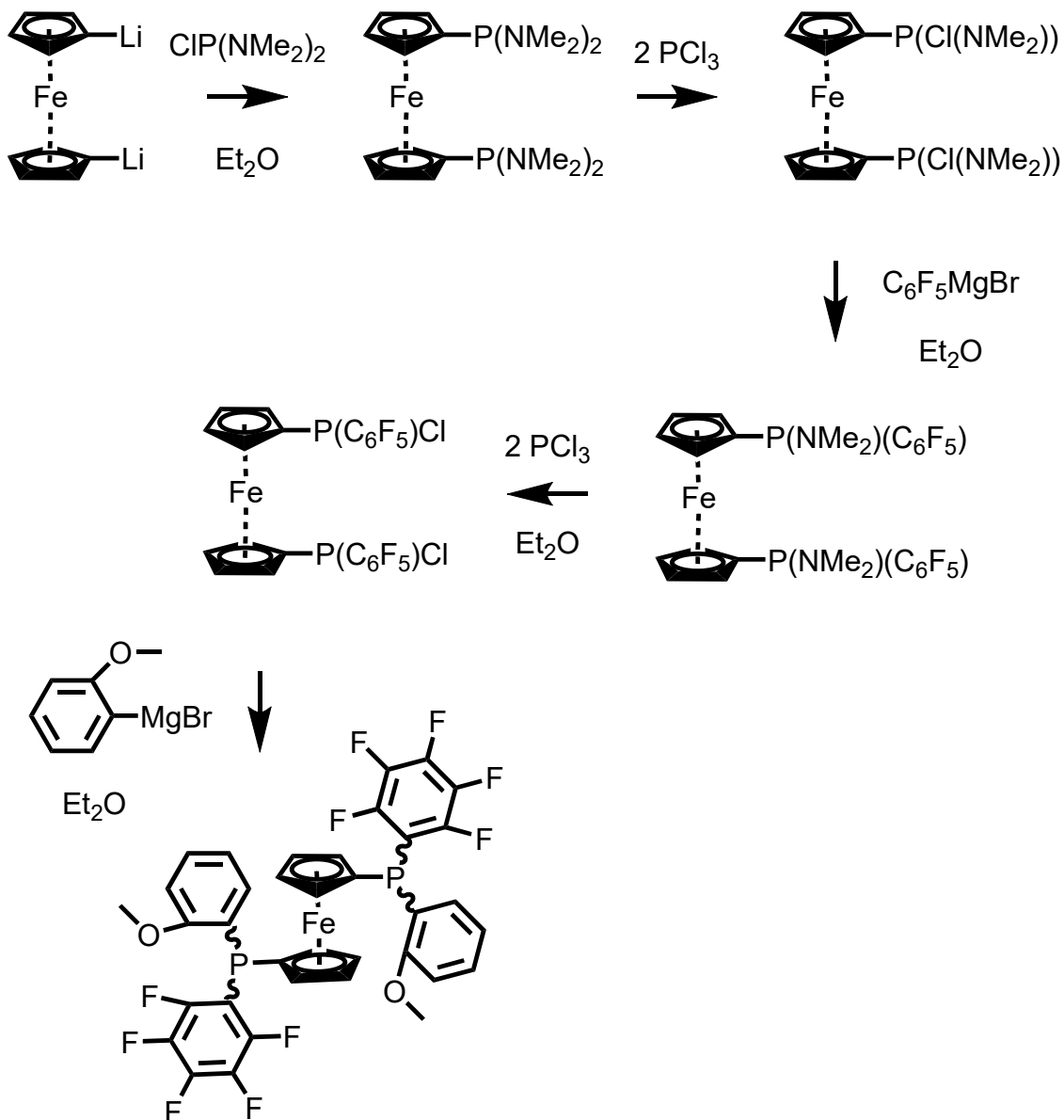
#### 4.3.1. Preliminary results of carbonylative cross coupling using electron-poor bifunctional ligands

Preliminary results showed promise. Conversion was seen to a greater amount than a control experiment with only palladium metal precursor present and no ligand. A black precipitate, which is believed to be Pd(0) or Pd(CO)<sub>n</sub>, common degradation products of a catalyst in carbonylation reactions was seen almost immediately. One method to increase the stability of the catalyst and prevent formation of Pd(CO)<sub>n</sub> was to synthesize a bidentate electron-poor bifunctional



ligand. Ferrocene was chosen as the backbone of the ligand due to the wide bite angle of ferrocene and wider bite angles increasing the rate of reductive elimination.

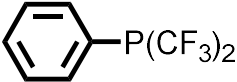
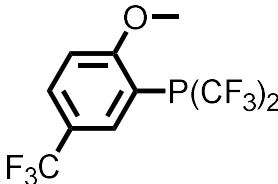
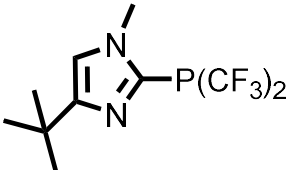
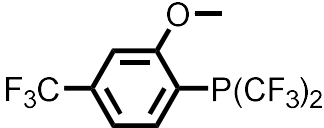
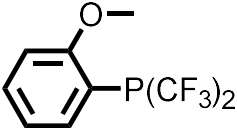
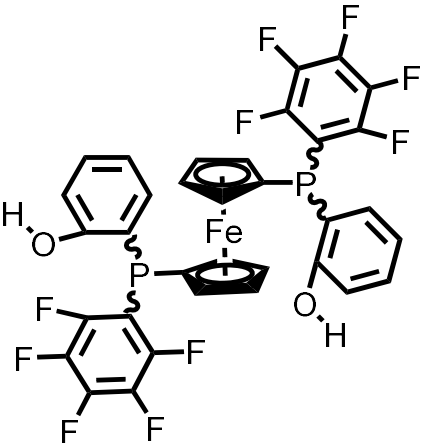
A similar strategy to the synthesis of the monodentate phosphines was utilized, with some changes to accommodate the backbone (Scheme 4.3.1).



**Scheme 4.3.1. Synthesis of bidentate electron-poor bifunctional phosphines with a ferrocene backbone**

#### 4.4 Initial results from carbonylative cross-coupling using electron-poor ligands

Experiments were performed at room temperature at 1 Atm of pressure. Each run was setup in the same fashion. The ligand to be investigated,  $(\text{CH}_3\text{CN})\text{PdCl}_2$ , degassed methanol that had been dried over 3 Å molecular sieves for 24 hours, 4-iodotoluene and a stir bar were added to a 500 mL Schlenk flask inside of a glove box. The flask was then purged with carbon monoxide gas for 5 minutes to replace the nitrogen. Triethylamine was added and after 20 min of reaction time an aliquot was taken and the conversion was determined by comparing the integration of the aromatic proton signals in the  $^1\text{H}$  NMR spectrum of the starting material, 4-iodotoluene, with the aromatic proton signals of methyl para-toluate. Conversion percentages are shown below in **Table 4.4.1**.

	% Conver.		% Conver.
	23		21%
	5%		3%
	60%*		16%

**Table 4.4.1 Initial results from carbonylative cross-coupling experiments**

Results were above the control conversion percentage (10%) for anisole containing phosphines. Conversion was still low for most, however optimization had yet to be performed to determine the best conditions for the reaction. The full range of phenols from this work have not yet been made and tested. Co-solvents have yet to be explored, as well as the concentration of the ligand and catalyst.

One other concern that arose is that the reactions with highest conversion rate also showed several other products containing aromatic peaks. It is possible the starting material is reacting to give unknown side products, though the other products were not identified as yet. Further investigations are needed once optimization of the reaction conditions has been completed.

Other carbonylation reactions that were previously discussed in Chapter 4.2 like the Monsanto or Cativa process require harsher conditions. Carbonylative cross-couplings in particular can give yields up to 95%<sup>87</sup>, but require elevated pressures (up to two Atm), elevated temperatures (80 °C) and longer reaction times (6-8 h). The conditions used in these experiments are considerably milder, and much more amenable to use on a laboratory scale or with more sensitive substrates.

## Chapter 5

### Coordinating-ion-spray mass spectroscopy as a method for the analysis of poorly ionizable or highly air- and acid-sensitive phosphines

#### 5.1 CIS-MS spectroscopy as an analytical method

##### 5.1.1 Original development, usage, and transition away from elemental analysis

###### 5.1.1.1 Development and usage

Coordinating-ion-spray mass spectroscopy (CIS-MS) was developed to more reliably and accurately detect organic molecules that were less capable of being ionized or gave very poor sensitivity<sup>90</sup>. The first reports of this techniques use were with fatty acids<sup>91</sup> or peroxides that showed potential biological activity<sup>92</sup> but were difficult to detect, because when ionized using other methods they would decompose, preventing detection of the molecular ion. The use of CIS-MS has become more widespread since its development, being used recently for the detection of performance-enhancing drugs in professional sports<sup>93</sup>, and pesticides<sup>94</sup>, both using  $\text{Ag}^+$  ion. Addition of an ion in combination with fast atom bombardment has also been reported<sup>95</sup>, though none of these cases have been used with air- and moisture-sensitive phosphines.

###### 5.1.1.2 Transitions away from elemental analysis

Elemental analysis has historically been used as a measure of the purity of a compound, though recently discussions have arisen<sup>96,97</sup> about its use. One of the main points of discussion is that results generally come as percentage values, with no discussion of the test environment, techniques, or access to raw data to examine. If a compound fails elemental analysis, the scientist is left wondering whether the sample was impure or if there was an issue that arose during testing. Smaller institutions that do not have an in-house or nearby facility are left to ship their compounds. If the compound had to be shipped, then the question of the sample surviving shipping arises. The cost associated with shipping and testing is also an issue, with no control or explanation as to why

a compound failed the analysis the scientist is left to continue sending samples for testing until the correct values are obtained which can become burdensome. Purchasing and maintaining an analyzer for in-house analyses can also be difficult for smaller institutions. Despite the above considerations, elemental analysis of new compounds is still a requirement for publication of new compounds in some scientific journals, though not all<sup>98</sup>.

Usage of elemental analysis is also of concern to chemists working with extremely sensitive compounds such as air- and/or moisture-sensitive organometallic compounds with metal-carbon bonds or phosphines. The company providing the analysis may not have the proper equipment or training to properly handle compounds of this type and considerable effort, time, and money can be spent attempting to obtain an elemental analysis through a method not under the reporting chemist's control. The ACS journals *Organometallics* and *Journal of Organic Chemistry* do allow use of NMR spectroscopy to demonstrate >95% purity along with high-resolution mass spectrometry (HRMS) taking the place of elemental analysis on a case by case basis<sup>99</sup>.

## **5.2 Use of CIS-MS for analysis of compounds synthesized in this work**

### **5.2.1 High-resolution mass spectrometry without the use of a coordinating ion**

With the reactivity of many of the intermediates synthesized in this work, we felt that elemental analyses would be difficult if not impossible to obtain. We chose to use HRMS and NMR to verify the identity and purity of our target molecules. The initial attempt to analyze 1,1'-bis(dimethylamino pentafluorophenyl phosphino)ferrocene unfortunately showed no peaks consistent with either the product  $m/z$  for  $C_{26}H_{20}F_{10}FeN_2P_2$  (calculated = 668.0291) or identifiable fragments (Figure 5.2.1).

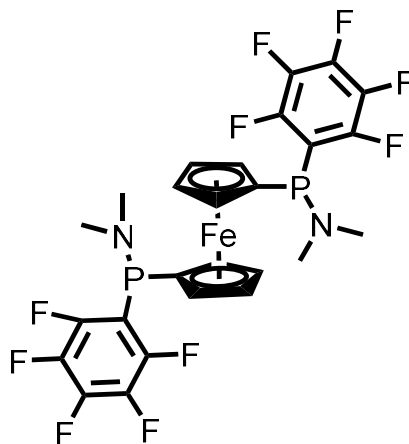


**Figure 5.2.2.1 1,1'-bis(dimethylamino pentafluorophenyl phosphino)ferrocene**

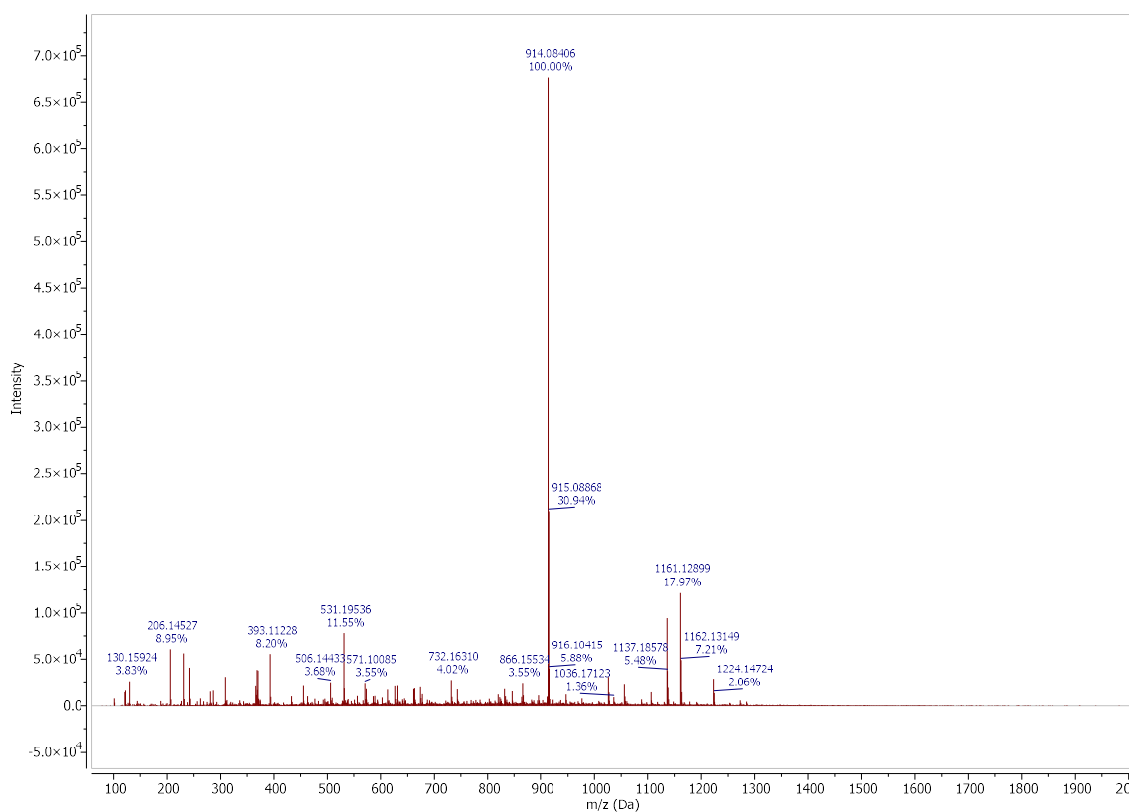


**Figure 5.2.1 Mass spectrum of 1,1'-bis(dimethylamino pentafluorophenyl phosphino)ferrocene without Ag<sup>+</sup> ion**

Compounds containing dimethylamino substituents or trifluoroethyl phosphonites gave similar results. The ionization source, in this case acetic acid in acetonitrile, was believed to either react with the dimethylamino moiety, or in the case of the phosphonite and phosphine to not be acidic enough to protonate the molecule so that it could be detected. Gratifyingly, addition of  $\text{Ag}^+$  ions to 1,1'-bis(dimethylamino pentafluorophenyl phosphino)ferrocene in the form of  $\text{AgPF}_6$  or  $\text{AgNO}_3$  did give us the relevant  $\text{M}+\text{Ag}$  peak in the spectrum with the corresponding isotopic pattern of  $\text{Ag}^+$  (Figure 5.2.2)  $m/z$  for  $\text{C}_{26}\text{H}_{20}\text{F}_{10}\text{FeN}_2\text{P}_2\text{Ag}$  (calculated = 774.93424, experimental = 774.93033).

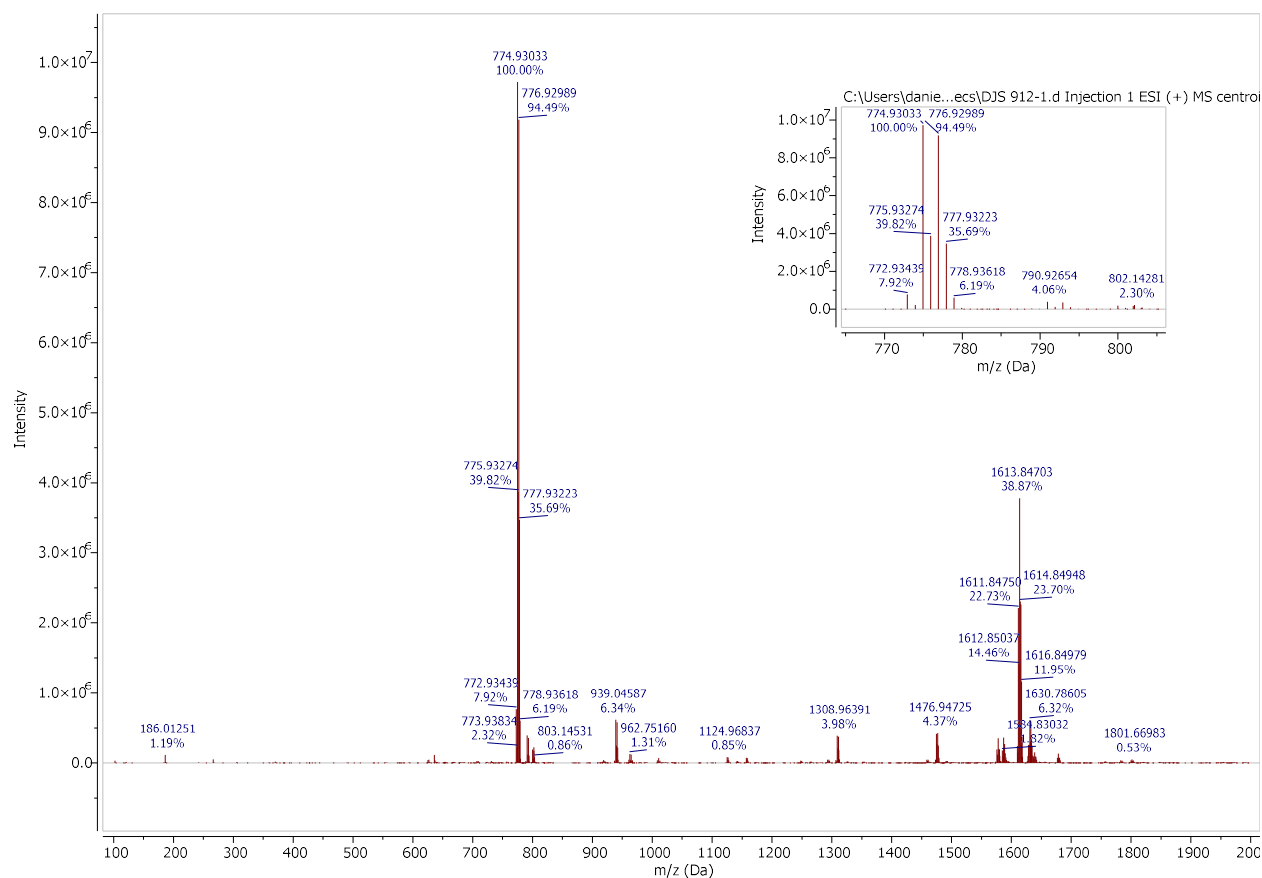


**Figure 5.2.2 Mass spectrum of 1,1'-bis(dimethylamino pentafluorophenyl phosphino)ferrocene with  $\text{Ag}^+$  ion added**

The phenyl bis(trifluoromethyl) phosphine spectra only gave us a peak corresponding to



Ag+CH<sub>3</sub>CN, with no molecular ion present (Figure 5.2.3). We hypothesized that the phosphine was too electron-poor to coordinate to the Ag<sup>+</sup> in the presence of CH<sub>3</sub>CN and therefore a softer Lewis acid was

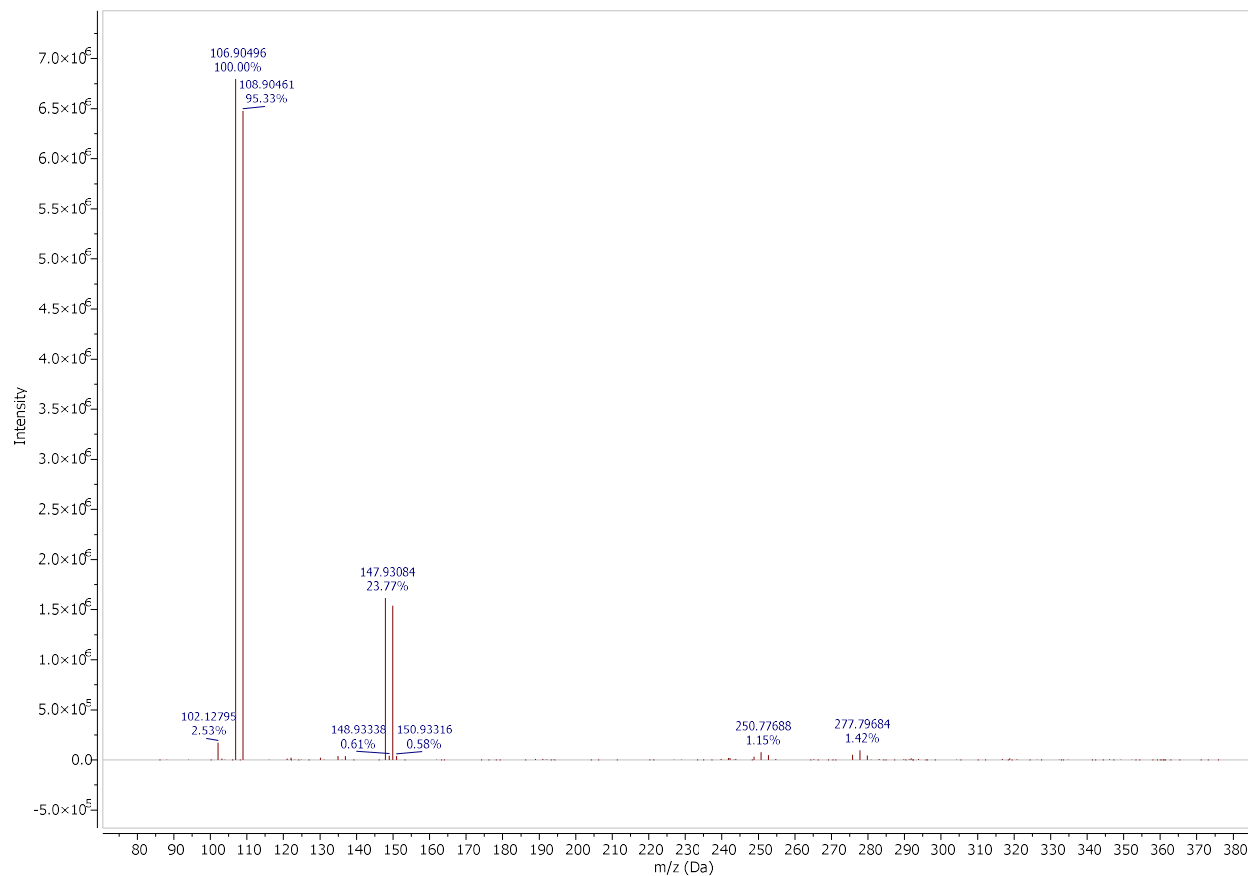


**Figure 5.2.3 Phenylbis(trifluoromethyl)phosphine with AgNO<sub>3</sub> addition**

required to coordinate the phosphine. We first tested phenylbis(trifluoromethyl)phosphine with Me<sub>2</sub>SAuCl as our Lewis acid source which gratifyingly gave us the relevant peak of M+AuCH<sub>3</sub>CN in the spectrum C<sub>8</sub>H<sub>5</sub>F<sub>6</sub>PAuCH<sub>3</sub>CN m/z (calculated = 483.9964, experimental 483.9967) (Figure 5.2.3).

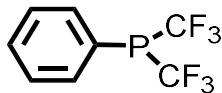


Figure 5.2.4 Phenylbis(trifluoromethyl)phosphine

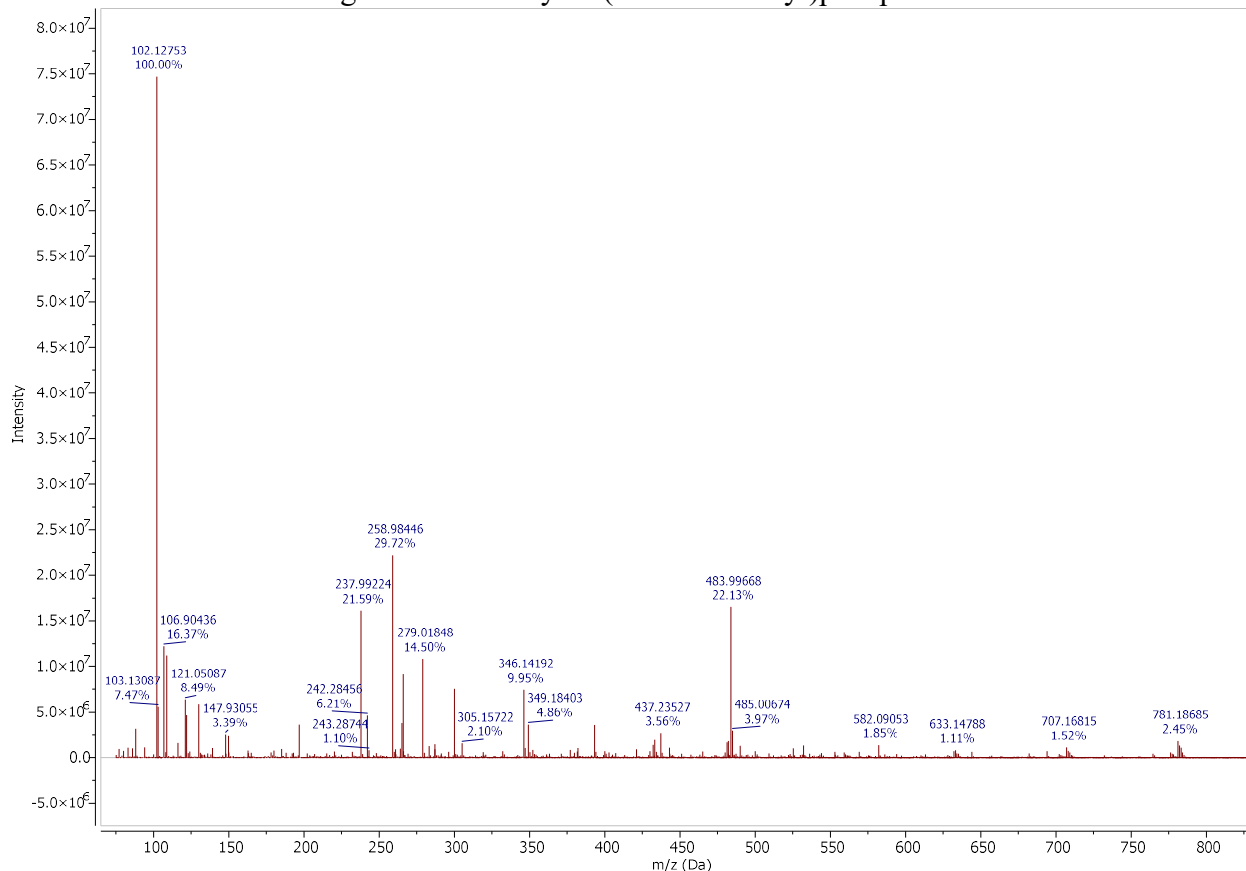


Figure 5.2.5 Mass spectrum of phenylbis(trifluoromethyl)phosphine ( $C_8H_5F_6PAuCH_3CN$ ) with addition of  $Me_2SAuCl$

The photosensitivity of the  $Me_2SAuCl$  and the complex produced on coordination of the ligand was shown by the production of an elemental gold mirror on the sample vial after approximately 2 h, leading us to examine the solvent used in sample preparation. When using acetonitrile as the solvent for the phosphine and the gold complex, approximately 20 min are needed before the appearance of  $L+AuCH_3CN$  in the spectrum. We hypothesized that this was because the acetonitrile was competing with the binding of the ligand to the gold, and so to avoid this delay in preparation of the sample the coordination chemistry was performed in THF as it

binds less strongly to metal centers. Immediately after mixing the ligand and  $\text{Me}_2\text{SAuCl}$  the solution was injected into the spectrometer, the expected  $\text{M}^+\text{AuCH}_3\text{CN}$  peak was seen. The speed at which the ligand binds to gold in THF allowed us to make a sample of appropriate concentration in THF and then separately make a solution of  $\text{Me}_2\text{SAuCl}$  in THF when the spectrometer was available for use and then mix directly before injection. Sample preparation in this manner avoided photochemical decomposition of the gold complex and streamlined sample preparation. Coordination of  $\text{CH}_3\text{CN}$  still occurs inside the spectrometer during analysis as the carrier solvent is  $\text{CH}_3\text{CN}$ , but once bound the ligand is not noticeably displaced by the acetonitrile.

Chapter five, in part contains work that is currently being prepared for submission for publication of the material. Sattler, Daniel J., Elliott, Gregory, Grotjahn, Douglas B. The dissertation author was the primary investigator and author of the material.

## **Chapter 6. Future directions**

Future directions include finishing syntheses of phenolic phosphines from their anisole precursors, optimization of the carbonylative cross coupling reaction, as well as further testing of the electron-poor phenolic ligands with precursors of platinum and other metals, such as nickel, to determine if they are capable of catalyzing the addition of hydroxyl groups to an alkene.

## References

1. Chemists Seek Greater Recognition for Catalysis. *Chemical & Engineering News Archive* **1993**, 71 (22), 23-27.
2. Dong, G.; Teo, P.; Wickens, Z. K.; Grubbs, R. H., Primary Alcohols from Terminal Olefins: Formal Anti-Markovnikov Hydration via Triple Relay Catalysis. *Science* **2011**, 333 (6049), 1609-1612.
3. Perkowski, A. J.; Nicewicz, D. A., Direct Catalytic Anti-Markovnikov Addition of Carboxylic Acids to Alkenes. *Journal of the American Chemical Society* **2013**, 135 (28), 10334-10337.
4. Hamilton, D. S.; Nicewicz, D. A., Direct Catalytic Anti-Markovnikov Hydroetherification of Alkenols. *Journal of the American Chemical Society* **2012**, 134 (45), 18577-18580.
5. Tsui, E.; Metrano, A. J.; Tsuchiya, Y.; Knowles, R. R., Catalytic Hydroetherification of Unactivated Alkenes Enabled by Proton-Coupled Electron Transfer. *Angewandte Chemie International Edition* **2020**, 59 (29), 11845-11849.
6. Zhang, K.; Cai, L., Enantioselective hydroamination of arylalkenes with secondary amines via cobalt catalysis. *Chem Catalysis* **2023**, 3 (3), 100553.
7. Liu, H.; Saha, S.; Eisen, M. S., Recent advances in organo- lanthanides and actinides mediated hydroaminations. *Coordination Chemistry Reviews* **2023**, 493, 215284.
8. Notz, S.; Scharf, S.; Lang, H. Jumping in the Chiral Pool: Asymmetric Hydroaminations with Early Metals *Molecules* [Online], 2023.
9. Huang, L.; Arndt, M.; Gooßen, K.; Heydt, H.; Gooßen, L. J., Late Transition Metal-Catalyzed Hydroamination and Hydroamidation. *Chemical Reviews* **2015**, 115 (7), 2596-2697.
10. Patel, M.; Saunthwal, R. K.; Verma, A. K., Base-Mediated Hydroamination of Alkynes. *Accounts of Chemical Research* **2017**, 50 (2), 240-254.
11. Wen, W.; Guo, Q.-X., Recent Advances in Chiral Aldehyde Catalysis for Asymmetric Functionalization of Amines. *Synthesis* **2022**, 55 (05), 719-732.
12. Miller, D. C.; Ganley, J. M.; Musacchio, A. J.; Sherwood, T. C.; Ewing, W. R.; Knowles, R. R., Anti-Markovnikov Hydroamination of Unactivated Alkenes with Primary Alkyl Amines. *Journal of the American Chemical Society* **2019**, 141 (42), 16590-16594.
13. Musacchio, A. J.; Lainhart, B. C.; Zhang, X.; Naguib, S. G.; Sherwood, T. C.; Knowles, R. R., Catalytic intermolecular hydroaminations of unactivated olefins with secondary alkyl amines. *Science* **2017**, 355 (6326), 727-730.

14. Miller, D. C.; Choi, G. J.; Orbe, H. S.; Knowles, R. R., Catalytic Olefin Hydroamidation Enabled by Proton-Coupled Electron Transfer. *Journal of the American Chemical Society* **2015**, *137* (42), 13492-13495.
15. Brown, H. C.; Zweifel, G., A STEREOSPECIFIC CIS HYDRATION OF THE DOUBLE BOND IN CYCLIC DERIVATIVES. *Journal of the American Chemical Society* **1959**, *81* (1), 247-247.
16. Wilczynski, R.; Sneddon, L. G., Transition metal catalyzed reactions of alkynes and boron hydrides: synthesis of 2-(cis-2-butenyl)pentaborane(9) and its conversion into monocarbon carboranes. *Journal of the American Chemical Society* **1980**, *102* (8), 2857-2858.
17. Männig, D.; Nöth, H., Catalytic Hydroboration with Rhodium Complexes. *Angewandte Chemie International Edition in English* **1985**, *24* (10), 878-879.
18. Zhang, Y.-D.; Li, X.-Y.; Mo, Q.-K.; Shi, W.-B.; Zhao, J.-B.; Zhu, S.-F., Highly Regioselective Cobalt-Catalyzed Hydroboration of Internal Alkynes. *Angewandte Chemie International Edition* **2022**, *61* (36), e202208473.
19. Parsutkar, M. M.; Bhunia, S.; Majumder, M.; Lalisse, R. F.; Hadad, C. M.; RajanBabu, T. V., Ligand Control in Co-Catalyzed Regio- and Enantioselective Hydroboration: Homoallyl Secondary Boronates via Uncommon 4,3-Hydroboration of 1,3-Dienes. *Journal of the American Chemical Society* **2023**, *145* (13), 7462-7481.
20. Hu, M.; Tan, B. B.; Ge, S., Enantioselective Cobalt-Catalyzed Hydroboration of Fluoroalkyl-Substituted Alkenes to Access Chiral Fluoroalkylboronates. *Journal of the American Chemical Society* **2022**, *144* (33), 15333-15338.
21. Company, T. C. Silanes. <https://thechemco.com/chemical/silanes/> (accessed 7/31/23).
22. Mechtler, C.; Baumgartner, J.; Marschner, C., Alkynylsilyl Anions — Versatile Building Blocks for Silicon-Containing Polymers. In *Organosilicon Chemistry V*, 2003; pp 171-174.
23. Franz, A. K.; Wilson, S. O., Organosilicon Molecules with Medicinal Applications. *Journal of Medicinal Chemistry* **2013**, *56* (2), 388-405.
24. Chabaud, L.; James, P.; Landais, Y., Allylsilanes in Organic Synthesis – Recent Developments. *European Journal of Organic Chemistry* **2004**, *2004* (15), 3173-3199.
25. Karstedt, B. D. PLATINUM COMPLEXES OF UNSATURATED SILOXANES AND PLATINUM CONTAINING ORGANOPOLYSILOXANES. US3775452A, 1971.
26. Liu, T.; Mao, X.-R.; Song, S.; Chen, Z.-Y.; Wu, Y.; Xu, L.-P.; Wang, P., Enantioselective Nickel-Catalyzed Hydrosilylation of 1,1-Disubstituted Allenes. *Angewandte Chemie International Edition* **2023**, *62* (11), e202216878.

27. Zhang, W.-R.; Zhang, W.-W.; Li, H.; Li, B.-J., Amide-Directed, Rhodium-Catalyzed Enantioselective Hydrosilylation of Unactivated Internal Alkenes. *Organic Letters* **2023**, *25* (10), 1667-1672.
28. Díez, V.; Espino, G.; Jalón, F. A.; Manzano, B. R.; Pérez-Manrique, M., Synthesis and structure of new palladium complexes with the ligand 2-(diphenylphosphino)-1-methylimidazole: Evidence of hemilability. *Journal of Organometallic Chemistry* **2007**, *692* (7), 1482-1495.
29. Weng, Z.; Teo, S.; Hor, T. S. A., Metal Unsaturation and Ligand Hemilability in Suzuki Coupling. *Accounts of Chemical Research* **2007**, *40* (8), 676-684.
30. Noyori, R.; Yamakawa, M.; Hashiguchi, S., Metal–Ligand Bifunctional Catalysis: A Nonclassical Mechanism for Asymmetric Hydrogen Transfer between Alcohols and Carbonyl Compounds. *The Journal of Organic Chemistry* **2001**, *66* (24), 7931-7944.
31. Shvo, Y.; Czarkie, D.; Rahamim, Y.; Chodosh, D. F., A new group of ruthenium complexes: structure and catalysis. *Journal of the American Chemical Society* **1986**, *108* (23), 7400-7402.
32. Casey, C. P.; Singer, S. W.; Powell, D. R.; Hayashi, R. K.; Kavana, M., Hydrogen Transfer to Carbonyls and Imines from a Hydroxycyclopentadienyl Ruthenium Hydride: Evidence for Concerted Hydride and Proton Transfer. *Journal of the American Chemical Society* **2001**, *123* (6), 1090-1100.
33. Jensen, D. R.; Pugsley, J. S.; Sigman, M. S., Palladium-Catalyzed Enantioselective Oxidations of Alcohols Using Molecular Oxygen. *Journal of the American Chemical Society* **2001**, *123* (30), 7475-7476.
34. Ferreira, E. M.; Stoltz, B. M., The Palladium-Catalyzed Oxidative Kinetic Resolution of Secondary Alcohols with Molecular Oxygen. *Journal of the American Chemical Society* **2001**, *123* (31), 7725-7726.
35. Grotjahn, D. B.; Larsen, C. R.; Gustafson, J. L.; Nair, R.; Sharma, A., Extensive Isomerization of Alkenes Using a Bifunctional Catalyst: An Alkene Zipper. *Journal of the American Chemical Society* **2007**, *129* (31), 9592-9593.
36. Paulson, E. R.; Moore, C. E.; Rheingold, A. L.; Pullman, D. P.; Sindewald, R. W.; Cooksy, A. L.; Grotjahn, D. B., Dynamic  $\pi$ -Bonding of Imidazolyl Substituent in a Formally 16-Electron  $\text{Cp}^*\text{Ru}(\kappa^2\text{-P,N})^+$  Catalyst Allows Dramatic Rate Increases in (E)-Selective Monoisomerization of Alkenes. *ACS Catalysis* **2019**, *9* (8), 7217-7231.
37. Cao, T. C.; Cooksy, A. L.; Grotjahn, D. B., Origins of High Kinetic (E)-Selectivity in Alkene Isomerization by a  $\text{CpRu(PN)}$  Catalyst: a Combined Experimental and Computational Approach. *ACS Catalysis* **2020**, *10* (24), 15250-15258.
38. Grotjahn, D. B.; Incarvito, C. D.; Rheingold, A. L., Combined Effects of Metal and Ligand Capable of Accepting a Proton or Hydrogen Bond Catalyze Anti-Markovnikov Hydration of Terminal Alkynes. *Angewandte Chemie International Edition* **2001**, *40* (20), 3884-3887.

39. Grotjahn, D. B.; Lev, D. A., A General Bifunctional Catalyst for the Anti-Markovnikov Hydration of Terminal Alkynes to Aldehydes Gives Enzyme-Like Rate and Selectivity Enhancements. *Journal of the American Chemical Society* **2004**, *126* (39), 12232-12233.
40. Grotjahn, D. B.; Gong, Y.; DiPasquale, A. G.; Zakharov, L. N.; Rheingold, A. L., Bifunctional Imidazolylphosphine Ligands as Hydrogen Bond Donors Promote N–H and O–H Activation on Platinum. *Organometallics* **2006**, *25* (24), 5693-5695.
41. Tolman, C. A., Steric effects of phosphorus ligands in organometallic chemistry and homogeneous catalysis. *Chemical Reviews* **1977**, *77* (3), 313-348.
42. Kendall, A. J.; Zakharov, L. N.; Tyler, D. R., Steric and Electronic Influences of Buchwald-Type Alkyl-JohnPhos Ligands. *Inorganic Chemistry* **2016**, *55* (6), 3079-3090.
43. Front Matter. In *The Organometallic Chemistry of the Transition Metals*, 2014; pp i-xvi.
44. Franke, R.; Selent, D.; Borner, A., Applied hydroformylation. *Chem Rev* **2012**, *112* (11), 5675-732.
45. Christiansen, A.; Selent, D.; Spannenberg, A.; Kockerling, M.; Reinke, H.; Baumann, W.; Jiao, H.; Franke, R.; Borner, A., Heteroatom-substituted secondary phosphine oxides (HASPOs) as decomposition products and preligands in rhodium-catalysed hydroformylation. *Chemistry* **2011**, *17* (7), 2120-9.
46. Hegg, E. L.; Deal, K. A.; Kiessling, L. L.; Burstyn, J. N., Hydrolysis of Double-Stranded and Single-Stranded RNA in Hairpin Structures by the Copper(II) Macrocycle Cu([9]aneN<sub>3</sub>)Cl<sub>2</sub>. *Inorg. Chem.* **1997**, *37*, 1715-1718.
47. Modak, A. S.; Gard, J. K.; Merriman, M. C.; Winkeler, K. A.; Bashkin, J. K.; Stern, M. K., Toward Chemical Ribonucleases. 2. Synthesis and Characterization of Nucleoside-Bipyridine Conjugates. Hydrolytic Cleavage of RNA by Their Copper(II) Complexes. *J. Am. Chem. Soc.* **1991**, *113*, 283-291.
48. Nielsen, M. C.; Bonney, K. J.; Schoenebeck, F., Computational Ligand Design for the Reductive Elimination of ArCF<sub>3</sub> from a Small Bite Angle PdII Complex: Remarkable Effect of a Perfluoroalkyl Phosphine. *Angewandte Chemie International Edition* **2014**, *53* (23), 5903-5906.
49. Wursche, R.; Debaerdemaeker, T.; Klinga, M.; Rieger, B., Electron-Poor Olefin Polymerization Catalysts Based on Semi-Fluorinated Bis(phosphane)s. *European Journal of Inorganic Chemistry* **2000**, *2000* (9), 2063-2070.
50. Marcone, J. E.; Moloy, K. G., Kinetic Study of Reductive Elimination from the Complexes (Diphosphine)Pd(R)(CN). *Journal of the American Chemical Society* **1998**, *120* (33), 8527-8528.
51. Grushin, V. V.; Marshall, W. J., Facile Ar–CF<sub>3</sub> Bond Formation at Pd. Strikingly Different Outcomes of Reductive Elimination from [(Ph<sub>3</sub>P)<sub>2</sub>Pd(CF<sub>3</sub>)Ph] and [(Xantphos)Pd(CF<sub>3</sub>)Ph]. *Journal of the American Chemical Society* **2006**, *128* (39), 12644-12645.



52. Korenaga, T.; Abe, K.; Ko, A.; Maenishi, R.; Sakai, T., Ligand Electronic Effect on Reductive Elimination of Biphenyl from cis-[Pt(Ph)<sub>2</sub>(diphosphine)] Complexes Bearing Electron-Poor Diphosphine: Correlation Study between Experimental and Theoretical Results. *Organometallics* **2010**, *29* (18), 4025-4035.
53. Trzeciak, A. M.; Bartosz-Bechowski, H.; Ciunik, Z.; Niesyty, K.; Ziólkowski, J. J., Structural studies of PdCl<sub>2</sub>L<sub>2</sub> complexes with fluorinated phosphines, phosphites, and phosphinites as precursors of benzyl bromide carbonylation catalysts, and and X-ray crystal structure of cis-PdCl<sub>2</sub>[PPh<sub>2</sub>(OEt)]<sub>2</sub>. *Canadian Journal of Chemistry* **2001**, *79* (5-6), 752-759.
54. Zoltán Daliczek, T. S., Zoltán Finta, Géza Timári, Gábor Vlád Palladium catalyst, method for its preparation and its use.
55. Li, K.; Ye, J.; Wang, Z.; Mu, H.; Jian, Z., Indole-bridged bisphosphine-monoxide palladium catalysts for ethylene polymerization and copolymerization with polar monomers. *Polymer Chemistry* **2020**, *11* (15), 2740-2748.
56. Jung, J.; Yasuda, H.; Nozaki, K., Copolymerization of Nonpolar Olefins and Allyl Acetate Using Nickel Catalysts Bearing a Methylene-Bridged Bisphosphine Monoxide Ligand. *Macromolecules* **2020**, *53* (7), 2547-2556.
57. Wilders, A. M.; Contrella, N. D.; Sampson, J. R.; Zheng, M.; Jordan, R. F., Allosteric Effects in Ethylene Polymerization Catalysis. Enhancement of Performance of Phosphine-Phosphinate and Phosphine-Phosphonate Palladium Alkyl Catalysts by Remote Binding of B(C<sub>6</sub>F<sub>5</sub>)<sub>3</sub>. *Organometallics* **2017**, *36* (24), 4990-5002.
58. Nakano, R.; Chung, L. W.; Watanabe, Y.; Okuno, Y.; Okumura, Y.; Ito, S.; Morokuma, K.; Nozaki, K., Elucidating the Key Role of Phosphine–Sulfonate Ligands in Palladium-Catalyzed Ethylene Polymerization: Effect of Ligand Structure on the Molecular Weight and Linearity of Polyethylene. *ACS Catalysis* **2016**, *6* (9), 6101-6113.
59. Weiss, E.; Hencken, G., Über Metall-Alkyl-Verbindungen XII. Verfeinerung der Kristallstruktur des Methylolithiums. *J. Organomet. Chem.* **1970**, *21*, 265-268.
60. Walsh, E. N., Conversion of Tertiary Phosphites to Secondary Phosphonates. Diphenyl Phosphonate<sup>1</sup>. *Journal of the American Chemical Society* **1959**, *81* (12), 3023-3026.
61. Ernst, M. F.; Roddick, D. M., Synthesis and coordination properties of bis(bis(pentafluoroethyl)phosphino)ethane. *Inorg. Chem.* **1989**, *28* (9), 1624-1627.
62. Burton, D. J.; Yang, Z.-Y., Fluorinated organometallics: Perfluoroalkyl and functionalized perfluoroalkyl organometallic reagents in organic synthesis. *Tetrahedron* **1992**, *48* (2), 189-275.
63. Chambers, R. D., Organometallic Compounds. In *Fluorine in Organic Chemistry*, 2004; pp 365-398.
64. Charpentier, J.; Fruh, N.; Togni, A., Electrophilic trifluoromethylation by use of hypervalent iodine reagents. *Chem Rev* **2015**, *115* (2), 650-82.

65. Janson, P. G.; Ghoneim, I.; Ilchenko, N. O.; Szabó, K. J., Electrophilic Trifluoromethylation by Copper-Catalyzed Addition of CF<sub>3</sub>-Transfer Reagents to Alkenes and Alkynes. *Org. Lett.* **2012**, *14* (11), 2882-2885.
66. Armanino, N.; Koller, R.; Togni, A., Electrophilic Trifluoromethylation of Primary Phosphines: Synthesis of aP-Bis(trifluoromethyl) Derivative of BINAP. *Organometallics* **2010**, *29* (7), 1771-1777.
67. Brisdon, A. K.; Herbert, C. J., A generic route to fluoroalkyl-containing phosphanes. *Chemical Communications* **2009**, (43), 6658-6660.
68. Zeng, X. Studies of rhodium(I) complexes containing imidazolylphosphines : structure and reactivity relevant to catalysis. San Diego State University, 2006.
69. Magnelli, D. D.; Tesi, G.; Lowe, J. U., Jr.; McQuiston, W. E., Synthesis and Characterization of Some Perfluorophenylphosphine Derivatives. *Inorganic Chemistry* **1966**, *5* (3), 457-461.
70. Moore, S. S.; Whitesides, G. M., Synthesis and coordinating properties of heterocyclic-substituted tertiary phosphines. *The Journal of Organic Chemistry* **1982**, *47* (8), 1489-1493.
71. Schwenk, R.; Togni, A., P-Trifluoromethyl ligands derived from Josiphos in the Ir-catalysed hydrogenation of 3,4-dihydroisoquinoline hydrochlorides. *Dalton Transactions* **2015**, *44* (45), 19566-19575.
72. Karthik, V.; Gupta, V.; Anantharaman, G., Synthesis, Structure, and Coordination Chemistry of Phosphine-Functionalized Imidazole/Imidazolium Salts and Cleavage of a C–P Bond in an NHC–Phosphenium Salt using a Pd(0) Precursor. *Organometallics* **2015**, *34* (15), 3713-3720.
73. Adkins, H.; Krsek, G., Hydroformylation of Unsaturated Compounds with a Cobalt Carbonyl Catalyst. *Journal of the American Chemical Society* **1949**, *71* (9), 3051-3055.
74. Franke, R.; Selent, D.; Börner, A., Applied Hydroformylation. *Chemical Reviews* **2012**, *112* (11), 5675-5732.
75. Baya, M.; Houghton, J.; Konya, D.; Champouret, Y.; Daran, J.-C.; Almeida Leñero, K. Q.; Schoon, L.; Mul, W. P.; Oort, A. B. v.; Meijboom, N.; Drent, E.; Orpen, A. G.; Poli, R., Pd(I) Phosphine Carbonyl and Hydride Complexes Implicated in the Palladium-Catalyzed Oxo Process. *Journal of the American Chemical Society* **2008**, *130* (32), 10612-10624.
76. Frediani, P.; Mariani, P.; Rosi, L.; Frediani, M.; Comucci, A., One-pot syntheses of alcohols from olefins through Co/Ru tandem catalysis. *Journal of Molecular Catalysis A: Chemical* **2007**, *271* (1), 80-85.
77. MacDougall, J. K.; Cole-Hamilton, D. J., Direct formation of alcohols in homogeneous hydroformylation catalysed by rhodium complexes. *Journal of the Chemical Society, Chemical Communications* **1990**, (2), 165-167.

78. Wu, L.; Fleischer, I.; Jackstell, R.; Profir, I.; Franke, R.; Beller, M., Ruthenium-Catalyzed Hydroformylation/Reduction of Olefins to Alcohols: Extending the Scope to Internal Alkenes. *Journal of the American Chemical Society* **2013**, *135* (38), 14306-14312.
79. Masthead. *Justus Liebigs Annalen der Chemie* **1953**, 582 (1), fmi-fmi.
80. Bittler, K.; Kutepow, N. V.; Neubauer, D.; Reis, H., Carbonylation of Olefins under Mild Temperature Conditions in the Presence of Palladium Complexes. *Angewandte Chemie International Edition in English* **1968**, *7* (5), 329-335.
81. Drent, E.; Arnoldy, P.; Budzelaar, P. H. M., Efficient palladium catalysts for the carbonylation of alkynes. *Journal of Organometallic Chemistry* **1993**, *455* (1), 247-253.
82. Paulik, F. E.; Roth, J. F., Novel catalysts for the low-pressure carbonylation of methanol to acetic acid. *Chemical Communications (London)* **1968**, (24), 1578a-1578a.
83. Sunley, G. J.; Watson, D. J., High productivity methanol carbonylation catalysis using iridium: The Cativa™ process for the manufacture of acetic acid. *Catalysis Today* **2000**, *58* (4), 293-307.
84. Kent, J. A., *Handbook of Industrial Chemistry and Biotechnology*. 2012; p 1562.
85. Wahlgren, C.; Addison, A. W., Synthesis of Some Benzimidazole-, Pyridine-, and Imidazole-Derived Chelating Agents. *J. Heterocycl. Chem.* **1989**, *26*, 541-543.
86. Sang, R.; Hu, Y.; Razzaq, R.; Jackstell, R.; Franke, R.; Beller, M., State-of-the-art palladium-catalyzed alkoxy-carbonylations. *Organic Chemistry Frontiers* **2021**, *8* (4), 799-811.
87. McNulty, J.; Nair, J. J.; Sliwinski, M.; Robertson, A. J., Efficient palladium-catalysed carbonylative and Suzuki–Miyaura cross-coupling reactions with bis(di-tert-butylphosphino)-o-xylene. *Tetrahedron Letters* **2009**, *50* (20), 2342-2346.
88. Goldbach, V.; Falivene, L.; Caporaso, L.; Cavallo, L.; Mecking, S., Single-Step Access to Long-Chain  $\alpha,\omega$ -Dicarboxylic Acids by Isomerizing Hydroxycarbonylation of Unsaturated Fatty Acids. *ACS Catalysis* **2016**, *6* (12), 8229-8238.
89. Goldbach, V.; Krumova, M.; Mecking, S., Full-Range Interconversion of Nanocrystals and Bulk Metal with a Highly Selective Molecular Catalyst. *ACS Catalysis* **2018**, *8* (6), 5515-5525.
90. Bayer, E.; Gfrörer, P.; Rentel, C., Coordination-Ionspray-MS (CIS-MS), a Universal Detection and Characterization Method for Direct Coupling with Separation Techniques. *Angewandte Chemie International Edition* **1999**, *38* (7), 992-995.
91. Rentel, C.; Gfrörer, P.; Bayer, E., Coupling of capillary electrochromatography to coordination ion spray mass spectrometry, a novel detection method. *ELECTROPHORESIS* **1999**, *20* (12), 2329-2336.

92. Havrilla, C. M.; Hachey, D. L.; Porter, N. A., Coordination (Ag<sup>+</sup>) Ion Spray–Mass Spectrometry of Peroxidation Products of Cholesterol Linoleate and Cholesterol Arachidonate: High-Performance Liquid Chromatography–Mass Spectrometry Analysis of Peroxide Products from Polyunsaturated Lipid Autoxidation. *Journal of the American Chemical Society* **2000**, *122* (33), 8042-8055.
93. Kim, S.-H.; Cha, E.-J.; Lee, K. M.; Kim, H. J.; Kwon, O.-S.; Lee, J., Simultaneous ionization and analysis of 84 anabolic androgenic steroids in human urine using liquid chromatography-silver ion coordination ionspray/triple-quadrupole mass spectrometry. *Drug Testing and Analysis* **2014**, *6* (11-12), 1174-1185.
94. Mustapha, A. M.; Pasilis, S. P., Gas-phase copper and silver complexes with phosphorothioate and phosphorodithioate pesticides investigated using electrospray ionization mass spectrometry. *Journal of Mass Spectrometry* **2015**, *50* (1), 145-152.
95. Musselman, B. D.; Allison, J.; Watson, J. T., Utility of silver ion attachment in fast atom bombardment mass spectrometry. *Analytical Chemistry* **1985**, *57* (12), 2425-2427.
96. Katsnelson, A., Chemists Debate the Value of Elemental Analysis. *ACS Central Science* **2022**, *8* (12), 1569-1572.
97. Kuveke, R. E. H.; Barwise, L.; van Ingen, Y.; Vashisth, K.; Roberts, N.; Chitnis, S. S.; Dutton, J. L.; Martin, C. D.; Melen, R. L., An International Study Evaluating Elemental Analysis. *ACS Central Science* **2022**, *8* (7), 855-863.
98. [https://publish.acs.org/publish/author\\_guidelines?coden=joceah](https://publish.acs.org/publish/author_guidelines?coden=joceah) (accessed July 18).
99. An Editorial About Elemental Analysis. *Organometallics* **2016**, *35* (19), 3255-3256.

## Appendices

Experimental .....	70
Compound 1 .....	70
Synthesis of 2 .....	71
Synthesis of 3 .....	71
Synthesis of 4 .....	71
Synthesis of 5 .....	71
Synthesis of 6 .....	71
Synthesis of 7 .....	72
Synthesis of 8 .....	72
Synthesis of 9 .....	73
Synthesis of 10: .....	73
Synthesis of 11 .....	74
Synthesis of 12 .....	74
Synthesis of 13 .....	92
Synthesis of 14 .....	92
Synthesis of 15 .....	92
Synthesis of 16 .....	93
Synthesis of 17 .....	93
Synthesis of 18 .....	93
Synthesis of 19 .....	94
Synthesis of 20 .....	94
Synthesis of 21 .....	94
Synthesis of 22 .....	94

Synthesis of 23:.....	95
Synthesis of 24.....	95
Synthesis of 25.....	95
Synthesis of 26.....	95
Synthesis of 27.....	95
Synthesis of 28.....	95
Synthesis of 29.....	95
Synthesis of 30.....	96
Compound 6.....	75
Compound 7.....	77
Compound 8.....	79
Compound 9.....	83
Compound 10.....	87
Compound 11.....	88
Compound 12.....	90
Compound 13.....	96
Compound 14.....	100
Compound 15.....	105
Compound 16.....	109
Compound 17.....	113
Compound 18.....	115
Compound 19.....	119
Compound 20.....	123
Compound 21.....	124

Compound 22.....	125
Compound 23.....	128
Compound 24.....	133
Compound 25.....	133
Compound 26.....	139
Compound 27.....	141
Compound 28.....	141
Compound 29.....	142
Compound 30.....	143
Compound 31.....	144

## Experimental

Critical safety note: If using sodium trifluoroethoxide salt for addition of trifluoroethoxide to a chlorophosphine, do not fully dry the salt. A simple filtration, followed by transfer of the wet salt to the reaction flask is sufficient. Fully drying the salt under vacuum can cause violent decomposition.

NMR spectra were obtained on either a Varian 400 MHz or Varian 500MHz NMR spectrometer. Tetrakis(trimethylsilyl)methane was used as an internal standard for  $^1\text{H}$  and  $^{13}\text{C}$  spectra, with the lock solvent being used for the  $^{19}\text{F}$  and  $^{31}\text{P}$  spectra. QTOF-MS was obtained on an Agilent Technologies 6530 Accurate Mass Q-TOF LC/MC. Samples were either run through an Agilent 1200 HPLC coupled to the mass spectrometer or directly infused, with the technician deciding which was appropriate. The addition of  $\text{Ag}^+$  as an ionizing agent for some compounds that utilized Coordination Ion Spray Mass Spectrometry (CSI-MS) with  $\text{Ag}^+$  as a counterion was accomplished with the addition of a 1 mg/1 mL acetonitrile solution of  $\text{AgPF}_6$  or  $\text{AgNO}_3$  to the dissolved compound. Spectrometry (CSI-MS) with  $\text{Au}^+$  was accomplished by the addition of a 1 mg/1 mL solution of  $(\text{Me}_2\text{S})\text{AuCl}$  in THF to a THF solution of the analyte.  $[(\text{COE})_2\text{RhCl}]_2$  was synthesized according to literature procedures<sup>1</sup>.

**Compound 1:** Diisopropyl(difluoromethyl)phosphonate was synthesized according to literature procedures.

**Synthesis of 2:** Diisopropyl (difluoromethyl)phosphonate (**1**) (2.699 g, 12.5 mmol) and THF (120 mL) were added to a Schlenk flask, which was cooled to -78 °C. Tert-butyl lithium (6.8 mL, 1.9 M/L in pentane) was added dropwise over 5 min, and the reaction was stirred for 1 h. Chlorodiphenylphosphine (2.756 g, 12.5 mmol) was added dropwise, and the reaction was allowed to warm to ambient temperature over 4 h. The volatiles were then removed under vacuum. The residue was dissolved in DCM (25 mL) and washed with water (3 x 50 mL). The organic layer was collected and the volatiles removed under vacuum to give 3.333 g (66%) of the crude product as a clear colorless oil. This was used without further purification.

$^{31}\text{P}$ ( $^1\text{H}$ ) ( $\text{CDCl}_3$ ):  $\delta$  26.1 (p,  $J_{\text{P-F}}$  26.3).  $^{19}\text{F}$  ( $\text{CDCl}_3$ )  $\delta$  -109.0 (dd,  $J_{\text{P-F}}$  70, 95).  $^1\text{H}$  ( $\text{CDCl}_3$ ): 7.70 (t,  $J_{\text{H-H}}$  8, 4H), 7.40 (m, 6H), 4.75 (h,  $J_{\text{H-H}}$  6, 2H), 1.25 (dd,  $J_{\text{P-H}}$  22,  $J_{\text{H-H}}$  6, 12H).

**Synthesis of 3:** **2** (1.00 g, 2.5 mmol), acetonitrile (0.50 mL), and LiBr (0.217 g, 2.5 mmol) were added to a scintillation vial equipped with a stir bar. The reaction was heated at 70 °C for 18 h, removed from the heat and shaken, and then heated for another 18 h. The mixture was then cooled to room temperature, filtered, and the precipitate was washed with acetonitrile (1 x 5 mL), DCM (1 x 5 mL), and diethyl ether (1 x 5 mL). The white powder was then dried overnight under vacuum giving 0.910 g (58%) of an off white solid.

$^{31}\text{P}$ ( $^1\text{H}$ ) (MeOD):  $\delta$  3.2 (td,  $J_{\text{P-F}}$  82), 1.1 (q,  $J_{\text{P-F}} = J_{\text{P-P}}$  60).  $^1\text{H}$  (MeOD):  $\delta$  7.65 (td,  $J_{\text{H-H}}$  7.5, 2, 4H), 7.45-7.35 (m, 6H), 4.52 (h,  $J_{\text{H-H}}$  6, 1H), 1.12 (d,  $J_{\text{H-H}}$  6, 6H).  $^{13}\text{C}$ ( $^1\text{H}$ ) (MeOD):  $\delta$  135.0 (d,  $J_{\text{P-C}}$  20), 132.8 (dtd,  $^1J_{\text{P-C}}$  13.2,  $^3J_{\text{P-F}}$  4.5,  $^3J_{\text{P-C}}$  2.2, assigned to ipso carbon of Ph), 128.9 (s), 127.6 (d,  $J_{\text{P-C}}$  7.6), 69.8 (dd,  $J_{\text{P-C}}$  6.8, 6.4), 23.5 (d,  $J_{\text{P-C}}$  4.1); signal for  $\text{CF}_2$  carbon is expected to be a dtd, and some of the signal resonances are seen but others are obscured by much more intense signals. Negative ion mode QTOF-MS  $m/z$  for  $\text{C}_{16}\text{H}_{17}\text{F}_2\text{O}_3\text{P}_2$ : Calculated 357.06211; Obtained 357.0675.

**Synthesis of 4:** Ligand **3** (0.100 g, 0.274 mmol) was added to a scintillation vial equipped with a stir bar.  $[\text{IrCp}^*\text{Cl}_2]_2$  (0.1093 g, 0.137 mmol) was then added, and  $\text{CH}_2\text{Cl}_2$  (1.3 mL) was added. The reaction was stirred overnight, and the solvent was removed to give 0.098 g of **3** as a light yellow solid (95% yield). X-ray quality crystals were grown by the slow evaporation of  $\text{CH}_2\text{Cl}_2$  from a saturated solution of **3**.  $^{31}\text{P}$ ( $^1\text{H}$ ) ( $\text{CDCl}_3$ ):  $\delta$  19.6 (td,  $J_{\text{P-P}}$  92,  $J_{\text{P-F}}$  44, 54), 11.5 (dt,  $J_{\text{P-P}}$  92,  $J_{\text{P-F}}$  74).  $^{13}\text{C}$ ( $^1\text{H}$ ) ( $\text{CDCl}_3$ ):  $\delta$  136.2 (d,  $J_{\text{P-C}}$  11.0), 134.3 (d,  $J_{\text{P-C}}$  10.0), 132.3, 131.9, 128.6 (d,  $J_{\text{P-C}}$  11.3), 128.5 (sl br d,  $J_{\text{P-C}}$  11.0), 127.5 (d,  $J_{\text{P-C}}$  58.4), 121.2 (d,  $J_{\text{P-C}}$  53.3), 118.8 (dddd,  $J_{\text{F-C}}$  316.6, 297.3,  $J_{\text{P-C}}$  184.0, 21.0), 93.1 (d,  $J_{\text{P-C}}$  2.8), 73.23 (d,  $J_{\text{P-C}}$  5.7), 73.18 (d,  $J_{\text{P-C}}$  5.7), 24.4 (d,  $J_{\text{P-C}}$  3.0), 24.0 (d,  $J_{\text{P-C}}$  5.0), 8.6.  $^1\text{H}$  ( $\text{CDCl}_3$ ) 7.75 (t, 11.3 2H), 7.6 (t, 9.2 1H), 7.5 (t, 6.0 1.5H), 7.4 (s, 2H), 4.7 (h, 4.9, 1H), 1.5 (s, 15H), 1.3 (d,  $J_{\text{H-H}}$  5.6, 6H).

**Synthesis of 5:** Compound **5** was synthesized following literature procedures.

**Synthesis of 6:** To compound **5** (5.9575 g, 32.5 mmol) was added tetrahydrofuran (50 mL) and the resulting solution was cooled to -40 °C, and triethylamine (6.9185 g, 68.3 mmol) was added dropwise. To this was then added 2,2,2-trifluoroethanol (6.8399 g 68.3 mmol). The reaction was stirred at -40 °C for 1 h, then allowed to warm to room temperature overnight. The volatiles were removed under vacuum. Hexanes (200 mL) were then added, and the slurry stirred for 10 min.



This was then filtered through a fine glass frit, washed with hexane (1 x 50 mL), and the volatiles were removed under vacuum to give **6** (8.0324 g) in 67% yield as a clear light yellow oil.

$^{31}\text{P}$  ( $^1\text{H}$ ) ( $\text{C}_6\text{D}_6$ ):  $\delta$  155.5(broad s).  $^{19}\text{F}$  ( $\text{C}_6\text{D}_6$ ):  $\delta$  -75.3 (td,  $J_{\text{P-F}}$  4.7,  $J_{\text{H-F}}$  8.7).  $^1\text{H}$  ( $\text{C}_6\text{D}_6$ ):  $\delta$  6.09(s, 1H), 4.10-3.78 (m, 4H), 3.05 (s, 3H), 1.34(s, 9H).  $^{13}\text{C}$  ( $^1\text{H}$ ) ( $\text{C}_6\text{D}_6$ ):

**Synthesis of 7:** Compound **6** (8.0324 g, 21.9 mmol) was added to a 300 mL pressure vessel with stir bar. To this was added hexanes (100 mL) and trimethyltrifluoromethylsilane (9.7184 g, 68.3 mmol). Cesium fluoride (1.2359 g, 8.1 mmol) was then added, and the reaction was stirred overnight. The volatiles were removed by bulb to bulb distillation under static vacuum. The oily liquid remaining was then distilled under reduced pressure (xxxx torr) and the fraction collected at xxxx °C was **7**, a clear, light yellow oil, (xxxx g xxxx mmol) in xxx % yield.

$^{31}\text{P}$  ( $^1\text{H}$ ) ( $\text{CDCl}_3$ ):  $\delta$  -24.6 (h,  $J_{\text{P-F}}$  87.3).  $^{19}\text{F}$  ( $\text{CDCl}_3$ ):  $\delta$  -53.7(d,  $J_{\text{P-F}}$  87.3).  $^1\text{H}$  ( $\text{CDCl}_3$ ):  $\delta$  7.70 (t,  $J_{\text{H-H}}$  8, 4H), 7.40 (m, 6H), 4.75 (h,  $J_{\text{H-H}}$  6, 2H), 1.25 (dd,  $J_{\text{P-H}}$  22,  $J_{\text{H-H}}$  6, 12H).

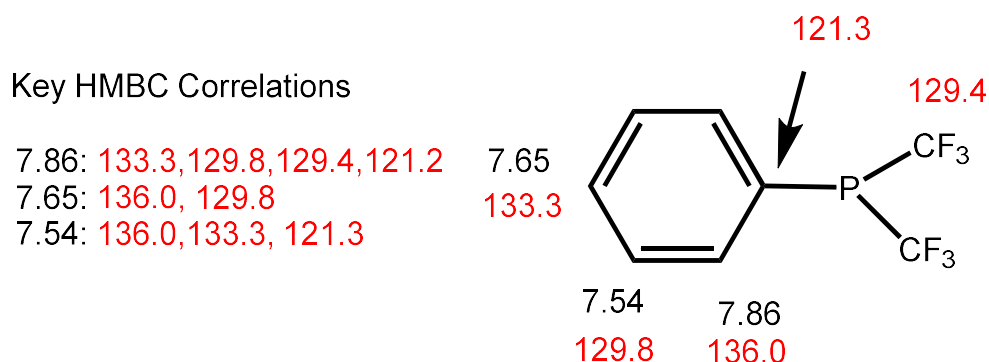
**Synthesis of 8:** Dichlorophenylphosphine (Fisher, used as received; 3.00 g 16.7 mmol) was added to a Schlenk flask with stir bar. Hexane (30 mL) was added, and the solution was cooled to 0 °C. Triethylamine (5.14 mL, 36.8 mmol) was added. Trifluoroethanol (2.57 mL, 35.2 mmol) was added dropwise, and the reaction was allowed to warm to room temperature overnight. The mixture was then filtered through a fine glass fritted funnel. The organic layer was washed with  $\text{Na}_2\text{CO}_3$  (1 M/L x 20 mL), then  $\text{H}_2\text{O}$  (2 x 30 mL). The organic layer was collected, dried with  $\text{Na}_2\text{SO}_4$ , the  $\text{Na}_2\text{SO}_4$  was removed and the volatiles were removed under vacuum to give **9** (4.6170 g, 15.1 mmol) in 87 % yield as a clear oil.

$^{31}\text{P}$  ( $^1\text{H}$ ) ( $\text{CDCl}_3$ ):  $\delta$  166.7 (h,  $J_{\text{P-F}}$  3.7).  $^{19}\text{F}$  ( $\text{CDCl}_3$ ):  $\delta$  -75.3(td,  $J_{\text{P-F}}$  3.7,  $J_{\text{H-F}}$  8.8).  $^1\text{H}$  ( $\text{CDCl}_3$ ):  $\delta$  7.65-7.60 (m, 2H), 7.52(m, 2H), 7.50, (m, 1H), 4.27-4.00 (m, 4H).  $^{13}\text{C}$  ( $^1\text{H}$ ) ( $\text{CDCl}_3$ ):  $\delta$  137.9, (d  $J_{\text{P-C}}$  19.8), 131.4, (s) 129.8, (d,  $J_{\text{P-C}}$  20.8), 129.0,(d,  $J_{\text{P-C}}$  5.4), 123.7, (qd,  $J_{\text{C-F}}$  277.5,  $J_{\text{P-C}}$  6.1) 63.98, (qd  $J_{\text{C-F}}$  36.1,  $J_{\text{P-C}}$  9.2)

QTOF-MS m/z for  $\text{C}_{10}\text{H}_9\text{F}_6\text{O}_2\text{PAg}$ : Calculated 412.9295; Obtained 412.9301

**Synthesis of 9:** **8** (20.0 g, 65.0 mmol) was added to a Schlenk flask with stir bar. To this was added diethyl ether (200 mL) and trimethyltrifluoromethylsilane (19.5238 g, 137.2 mmol). Cesium fluoride (2.4812 g, 16.3 mmol) was then added, and the reaction was stirred for 12 h. The reaction mixture was then filtered through a fine glass fritted funnel, the volatiles were removed under vacuum. The oily liquid remaining was then distilled under reduced pressure (0.5 torr) and the fraction collected at 87-90 °C was a clear colorless liquid (4.3980 g, 17.8 mmol) in 27% yield. The carbon spectrum displayed complex 2<sup>nd</sup> order coupling beyond the initial C-F one bond coupling for the trifluoromethyl carbon peak, and further coupling constants were unable to be determined.\* <sup>31</sup>P(<sup>1</sup>H) (CDCl<sub>3</sub>): δ 0.0 (h, *J*<sub>P-F</sub> 79.7). <sup>19</sup>F (CDCl<sub>3</sub>): δ -53.9 (d, *J*<sub>P-F</sub> 79.7). <sup>1</sup>H (CDCl<sub>3</sub>): δ 7.88-7.80 (m, 2H), 7.67-7.61 (m, 1H), 7.56-7.49 (m, 2H). <sup>13</sup>P(<sup>1</sup>H) (CDCl<sub>3</sub>): δ 136.0 (d, *J*<sub>C-P</sub> 29.0), 133.3, (d, *J*<sub>C-P</sub> 1.5), 129.4 (d, *J*<sub>C-P</sub> 10), 128.3\* (qm, *J*<sub>C-F</sub> 319.7), 121.3, (dhept, *J*<sub>C-P</sub> 10.3, *J*<sub>C-F</sub> 2.5).

QTOF-MS m/z for C<sub>10</sub>H<sub>8</sub>F<sub>6</sub>NPAu: Calculated 483.9964; Obtained 483.9950



**Synthesis of 10:** N-methyl imidazole (2.000 g, 24.3 mmol, obtained from Fisher, degassed and stored over 4 Å molecular sieves) was added to a Schlenk flask with stir bar. To this was added tetrahydrofuran (25 mL). This solution was cooled to 0 °C, and n-butyl lithium (9.9 mL, 2.5 M/L) was added dropwise over 10 min. This was stirred for 30 min at 0 °C. Bis(dimethylamino)chlorophosphine (3.238 g, 20.8 mmol) was dissolved in THF (3 mL), and was

then added dropwise to the reaction mixture. This was allowed to warm to room temperature over 2 h, and then water (1.0 mL) was added to quench the reaction. Volatiles were removed under vacuum, the crude product was redissolved in dichloromethane (20 mL) and washed with NaHCO<sub>3</sub> (1 x 30 mL) and water (2 x 30 mL). The organic layer was collected, dried with Na<sub>2</sub>SO<sub>4</sub>, the Na<sub>2</sub>SO<sub>4</sub> was removed and the volatiles were removed under vacuum to give **11** (2.3965 g) in 57 % crude yield.

<sup>31</sup>P(<sup>1</sup>H) (C<sub>6</sub>D<sub>6</sub>): δ 78.1 (s). <sup>1</sup>H (C<sub>6</sub>D<sub>6</sub>): δ 7.25 (d, *J*<sub>H-H</sub> 1.8, 1H), 6.52 (d, 1.8, 1H), 3.10 (s, 3H), 3.25 2.78 (d, *J*<sub>P-H</sub> 9.4, 12H). <sup>13</sup>C(<sup>1</sup>H): δ 149.1, (s), 129.3 (s), 122.5 (s), 41.7, (P-N-CH<sub>3</sub>, d, *J*<sub>P-C</sub> 16.1), 32.9, (N<sub>Im</sub>-CH<sub>3</sub> d, *J*<sub>P-C</sub> 10.1).

QTOF-MS m/z for 2M+Ag C<sub>16</sub>H<sub>34</sub>N<sub>8</sub>P<sub>2</sub>Ag: Calculated 507.14326; Obtained 507.14331

**Synthesis of 11:** Compound **11** was synthesized according to literature procedures<sup>1</sup>, and was not fully purified. N-Methylimidazole (2.0027 g, 24.3 mmol, degassed and stored over 4 Å molecular sieves), triethylamine (5.09 mL, 36.5 mmol), and tetrahydrofuran were added to a Schlenk flask with stir bar. The solution was cooled to 0 °C, and trichlorophosphine (2.13 mL, 24.3 mmol) was added dropwise. The reaction was allowed to warm to room temperature overnight with stirring. Triethylamine (20.37 mL, 97.4 mmol) was added and the mixture was again cooled to 0 °C. Phenol (9.1702, g 97.4 mmol) was dissolved in tetrahydrofuran (30 mL) and added dropwise via syringe to the reaction mixture. This was then allowed to warm to room temperature overnight with stirring. The mixture was filtered through a fine frit. The filter cake was washed with hexanes (50 mL), and the solution was allowed to sit overnight. Solvents and other volatiles were removed *in vacuo*. Diethyl ether (150 mL) and hexanes (150 mL) were added to the crude oily product, and to this was added 0.1 M/L KOH solution (600 mL). This was vigorously stirred overnight, and then separated. The aqueous layer was washed with ether (3 x 100mL) and this was combined with the original organic layer. The combined organic layer was washed with water (3 x 100 mL), dried with Na<sub>2</sub>SO<sub>4</sub>. The Na<sub>2</sub>SO<sub>4</sub> was removed, and the volatiles were removed *in vacuo*.

<sup>31</sup>P(<sup>1</sup>H) (CDCl<sub>3</sub>): δ 144.4 (s), <sup>1</sup>H (CDCl<sub>3</sub>): δ 7.14-7.01, (m, 8H), 3.85, (s, 3H). <sup>13</sup>C(<sup>1</sup>H) (CDCl<sub>3</sub>): δ 149.1, (s), 129.3 (s), 122.5 (s) 41.7, (P-N-CH<sub>3</sub>, d, *J*<sub>P-C</sub> 16.1), 32.9, (N<sub>Im</sub>-CH<sub>3</sub> d, *J*<sub>P-C</sub> 10.1)

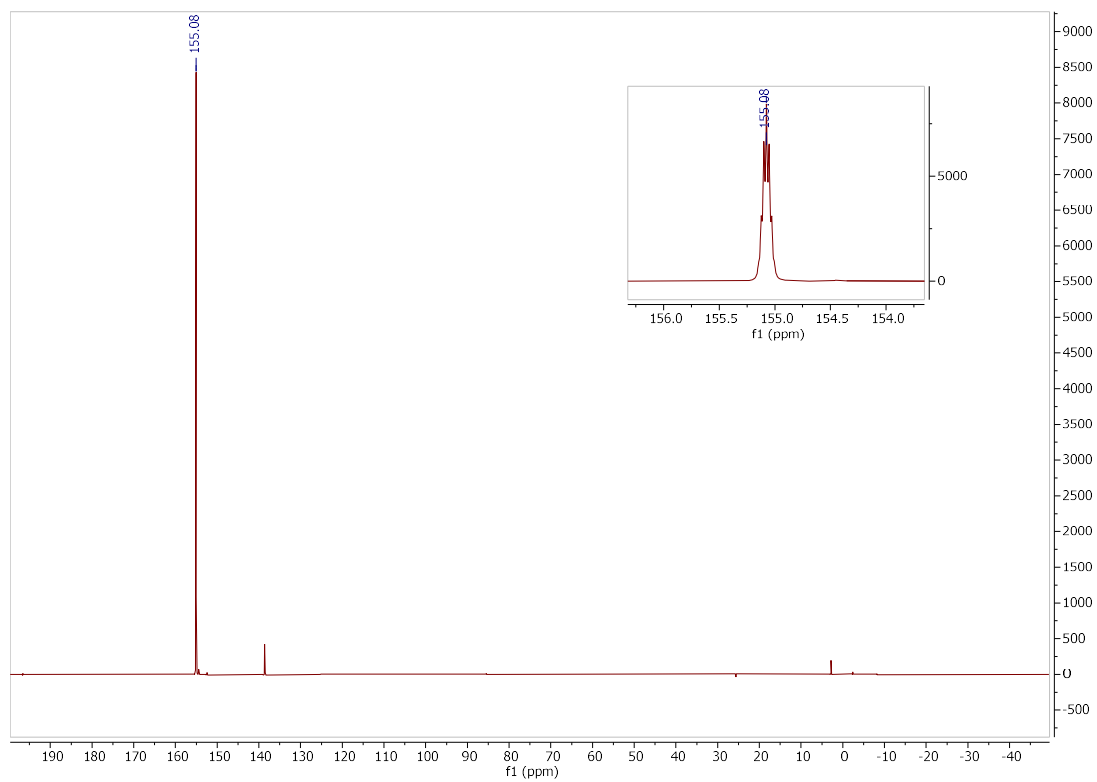
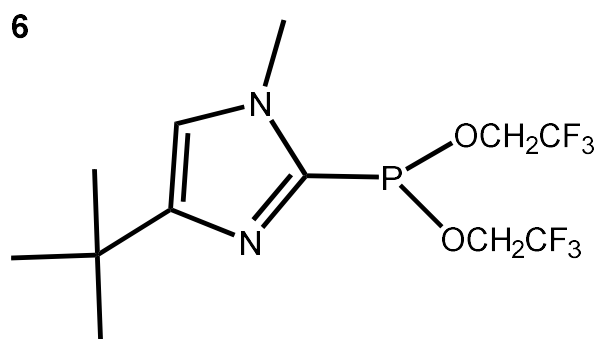
QTOF-MS m/z for 2M+Au C<sub>32</sub>H<sub>30</sub>N<sub>4</sub>O<sub>4</sub>P<sub>2</sub>Au: Calculated: 793.1408, obtained: 793.1354

**Synthesis of 12:** Compound **11** (1.9987 g, 6.7 mmol) was added to a Schlenk flask with a stir bar. Tetrahydrofuran (30 mL) was added, followed by trimethyltri(fluoromethyl)silane (3.0 mL, 20.3 mmol). Cesium fluoride (1.0034 g 6.7 mmol) was then added, and the reaction was stirred overnight. The reaction was then filtered through a fine glass fritted funnel and the volatiles removed under vacuum.

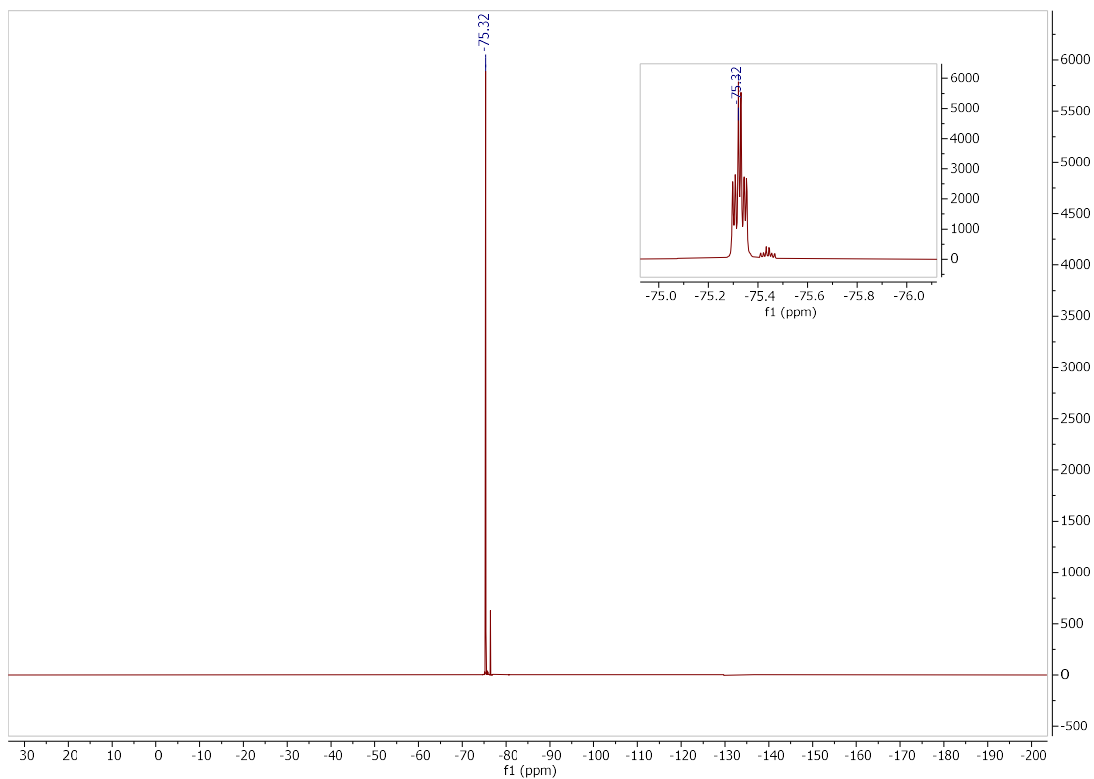
<sup>31</sup>P(<sup>1</sup>H) (CDCl<sub>3</sub>): δ -25.6 (h, *J*<sub>P-F</sub> 87.7). <sup>19</sup>F (CDCl<sub>3</sub>): δ -53.5, (d, *J*<sub>P-F</sub> 87.7) δ <sup>1</sup>H (CDCl<sub>3</sub>): δ 7.14-7.01, (m, 8H), 3.85, (s, 3H), 2.31, (s, 3H) <sup>13</sup>C(<sup>1</sup>H) (CDCl<sub>3</sub>): δ 149.1, (s), 129.3 (s), 122.5 (s) 41.7, (P-N-CH<sub>3</sub>, d, *J*<sub>P-C</sub> 16.1), 32.9, (N<sub>Im</sub>-CH<sub>3</sub> d, *J*<sub>P-C</sub> 10.1)

QTOF-MS m/z for M+AuCH<sub>3</sub>CN: C<sub>8</sub>H<sub>8</sub>F<sub>6</sub>N<sub>3</sub>PAu: Calculated 488.00255; Obtained 514.00127

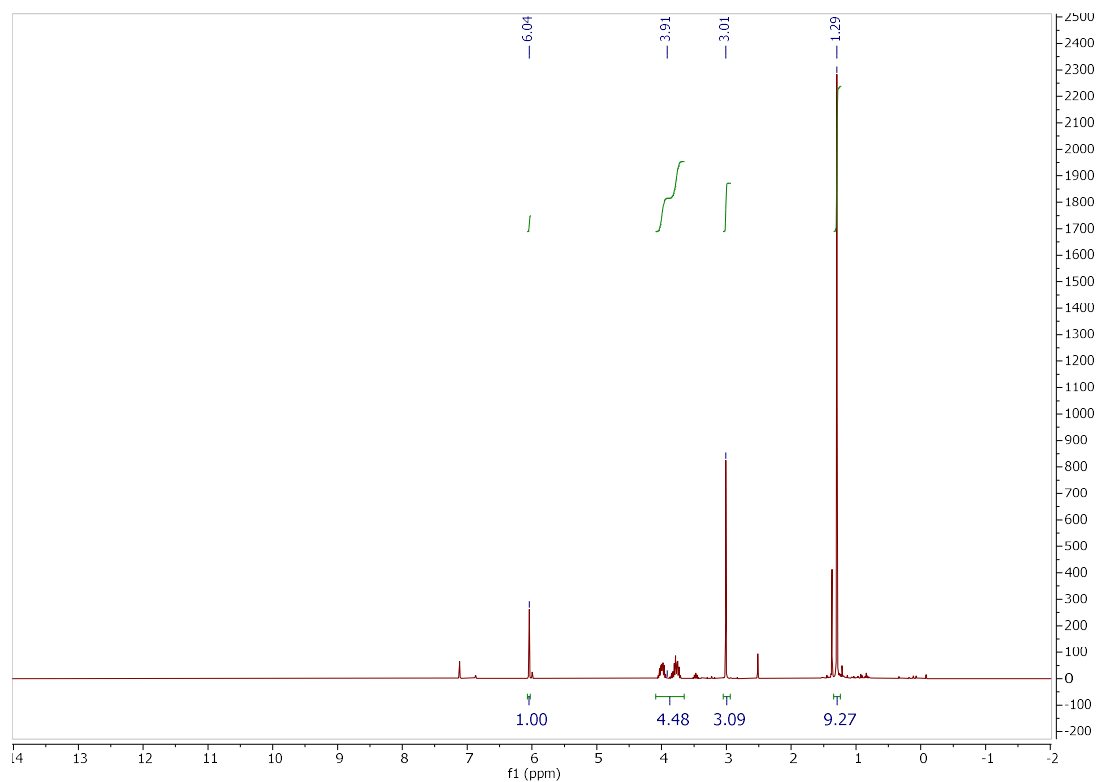
### Compound 6



### $^{31}\text{P}(^1\text{H})$ NMR spectrum of compound 6

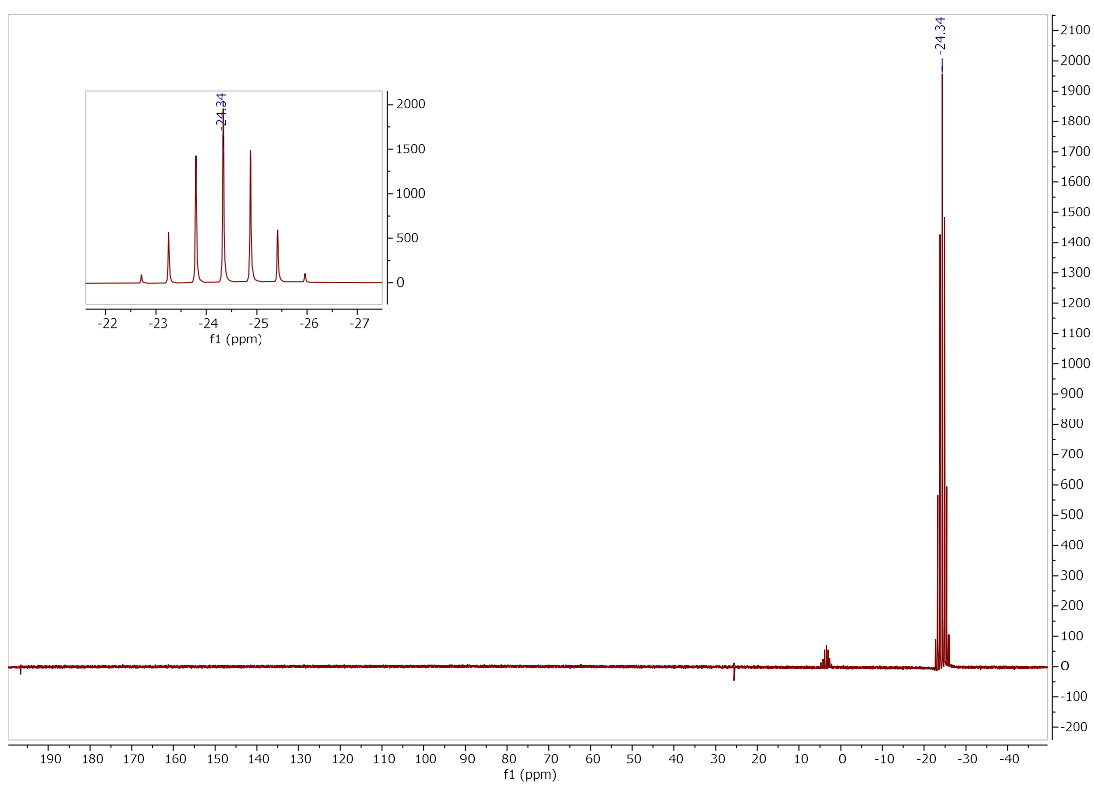
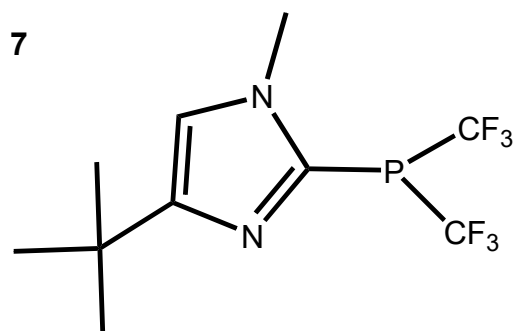


### $^{19}\text{F}$ NMR spectrum of compound 6

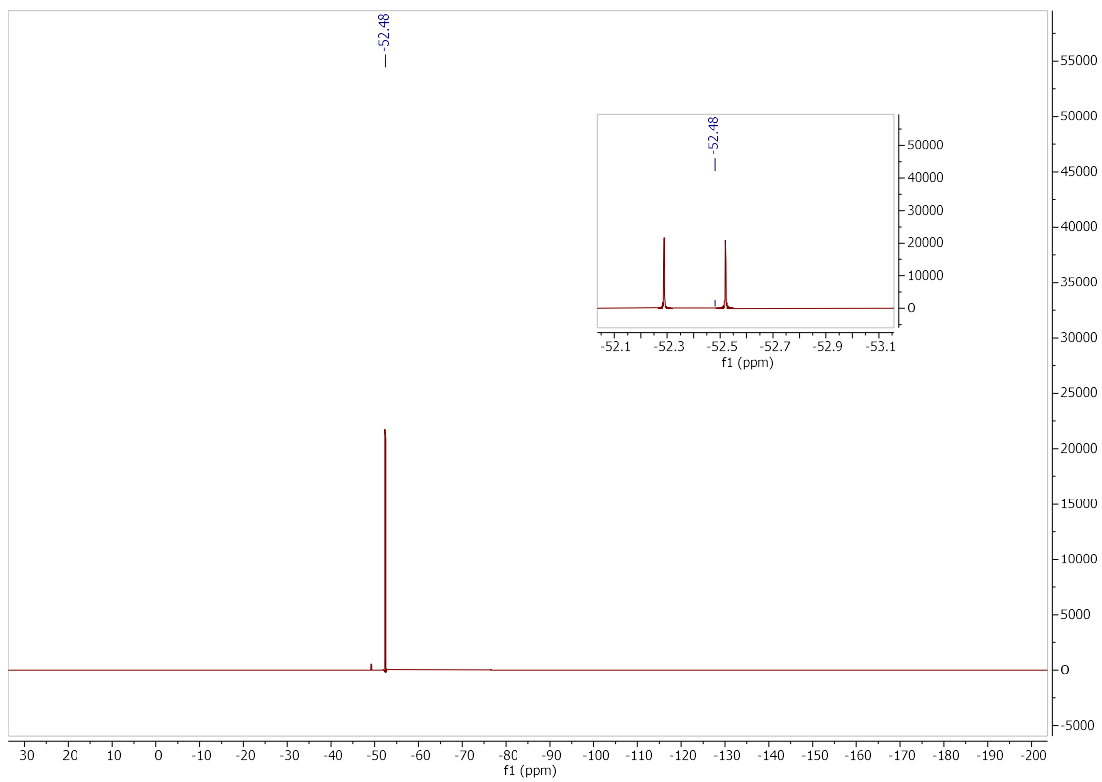


# <sup>1</sup>H NMR spectrum of compound 6

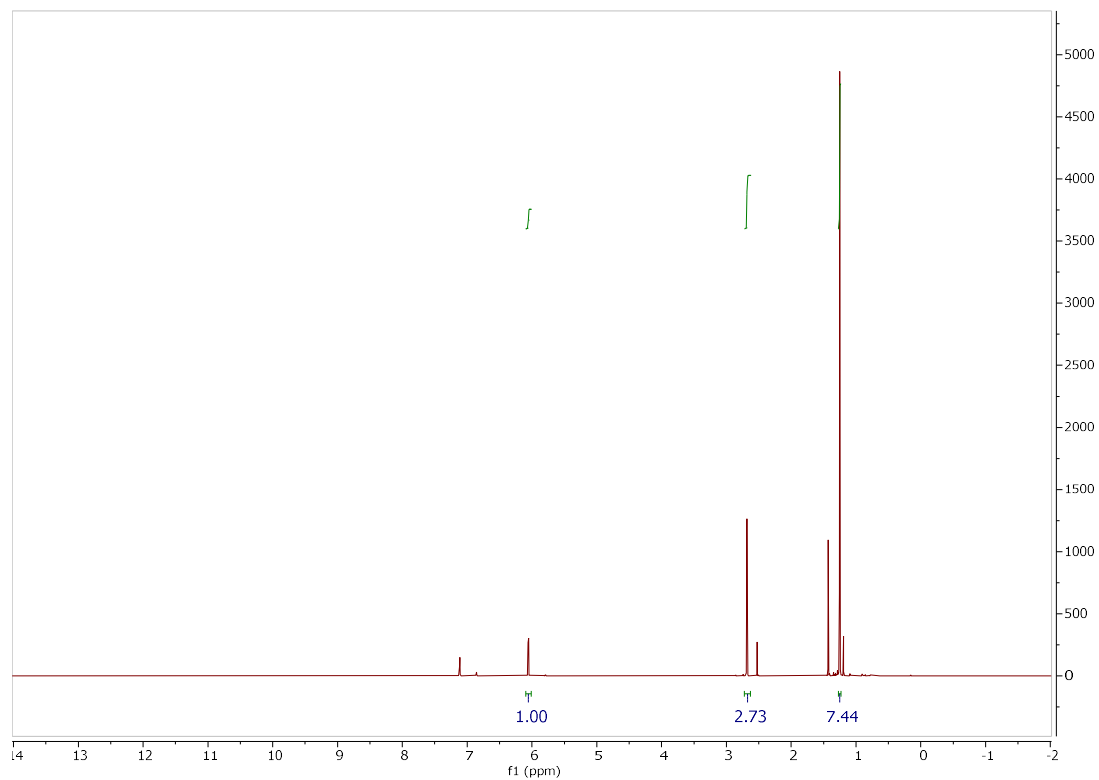
## Compound 7



## <sup>31</sup>P(<sup>1</sup>H) NMR spectrum of compound 7

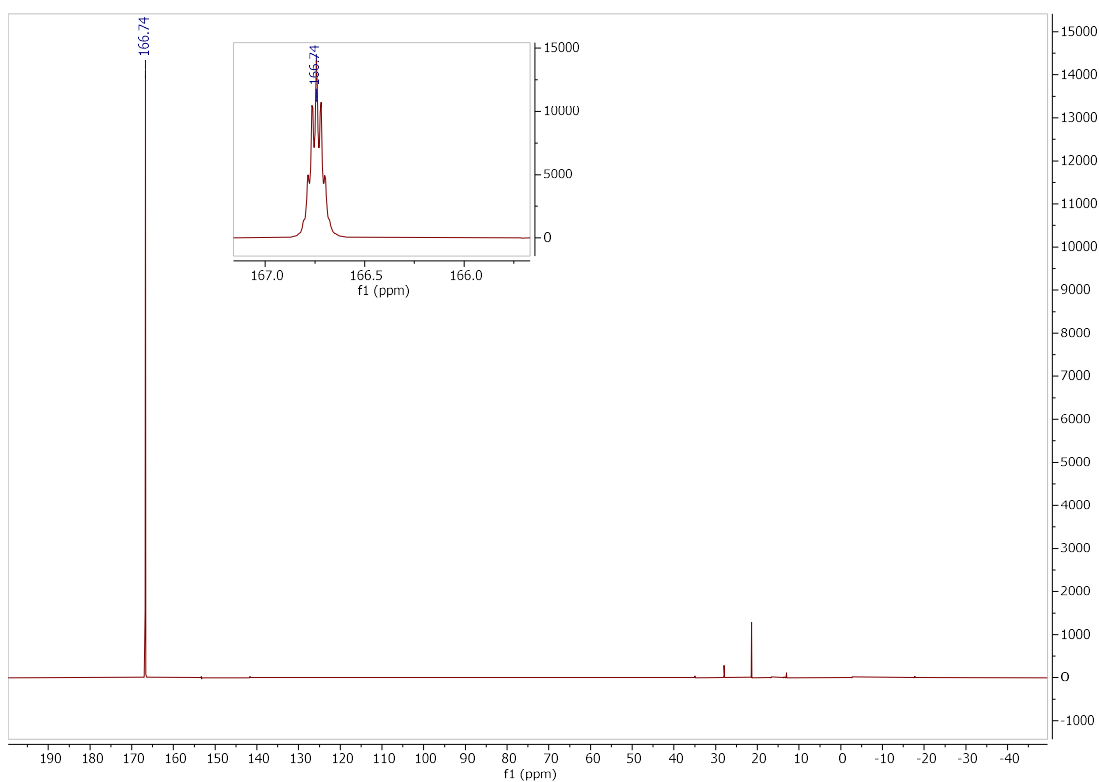
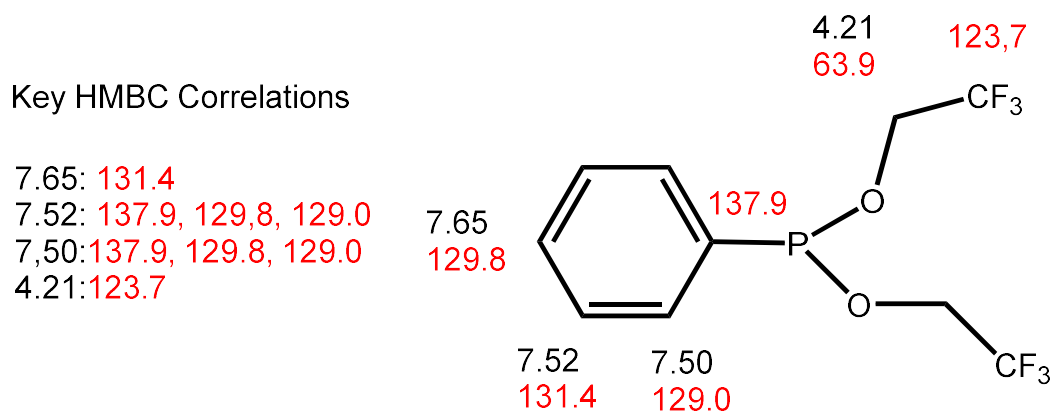


**$^{19}\text{F}$  NMR spectrum of compound 6**



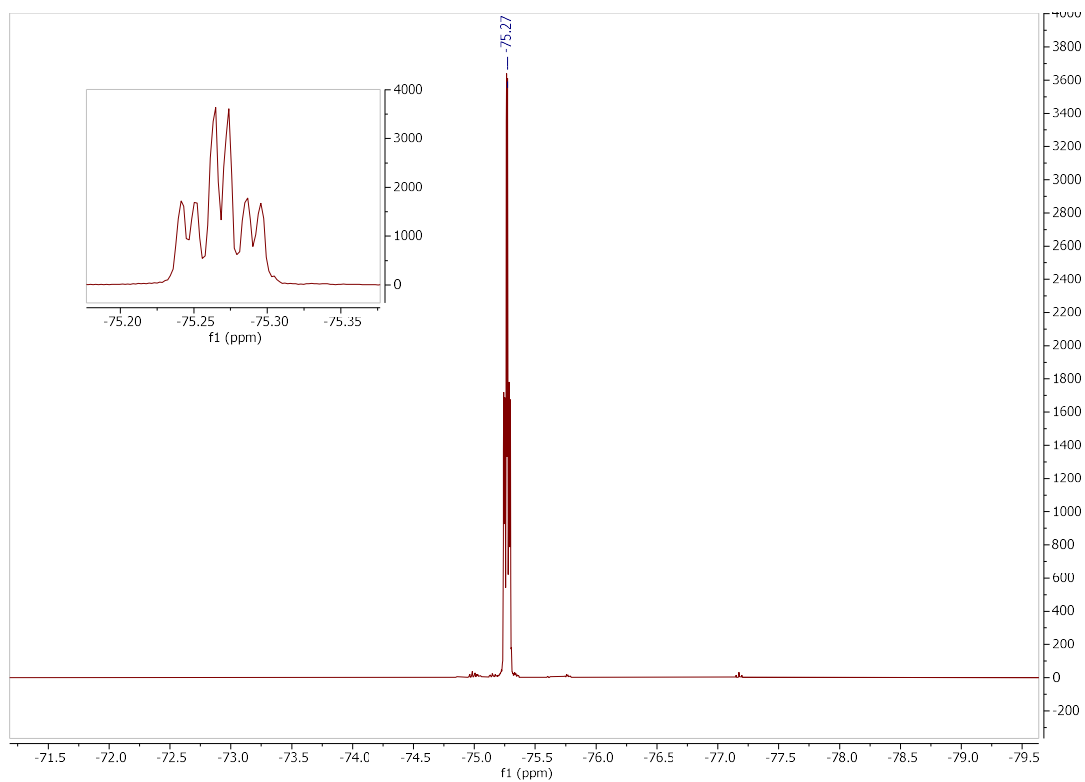
# <sup>1</sup>H NMR spectrum of compound 7

## Compound 8

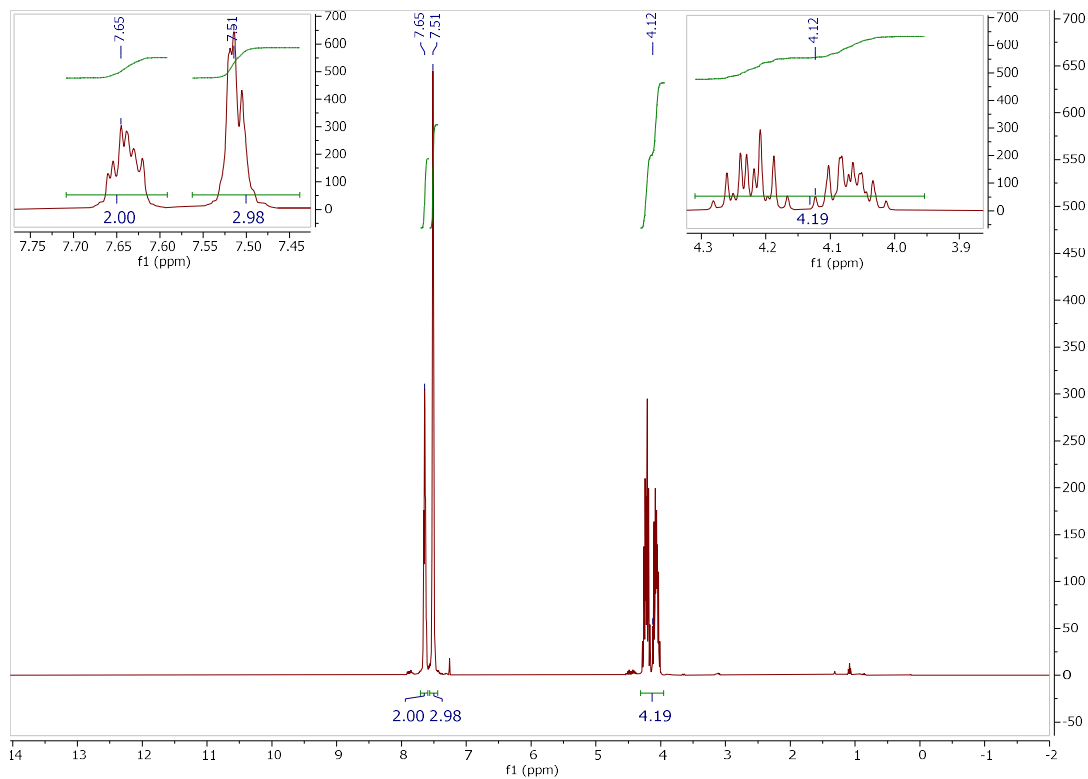


## <sup>31</sup>P(<sup>1</sup>H) NMR spectrum of compound 8

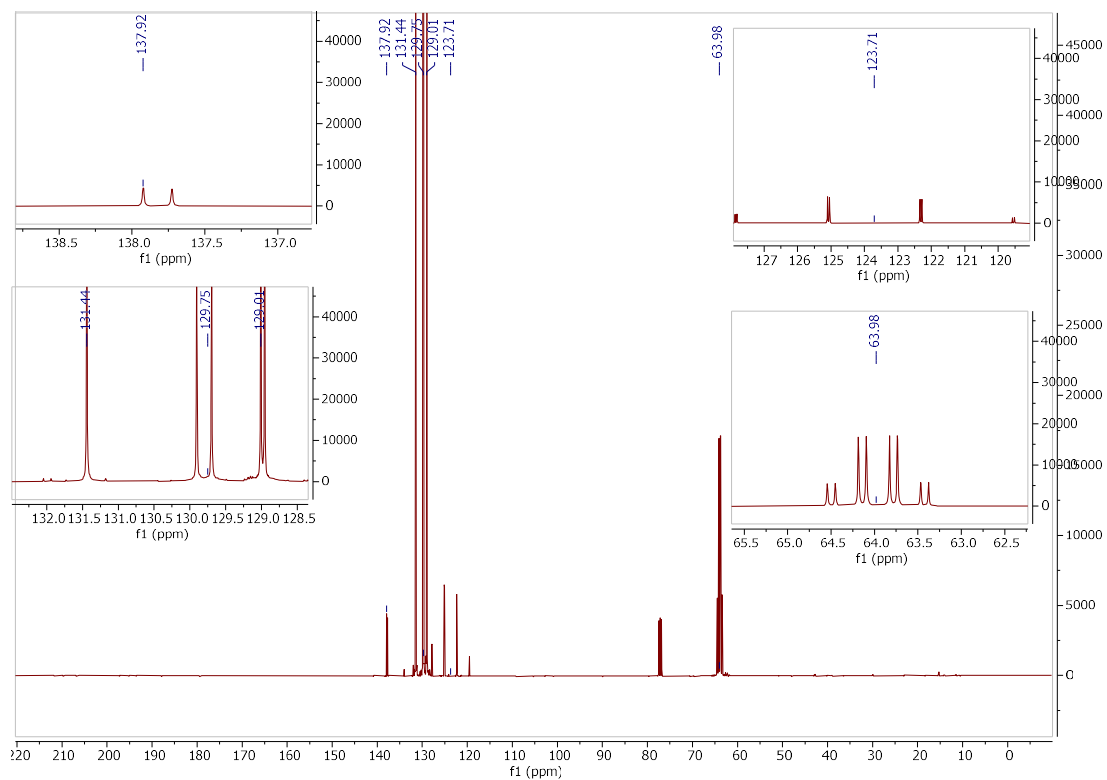




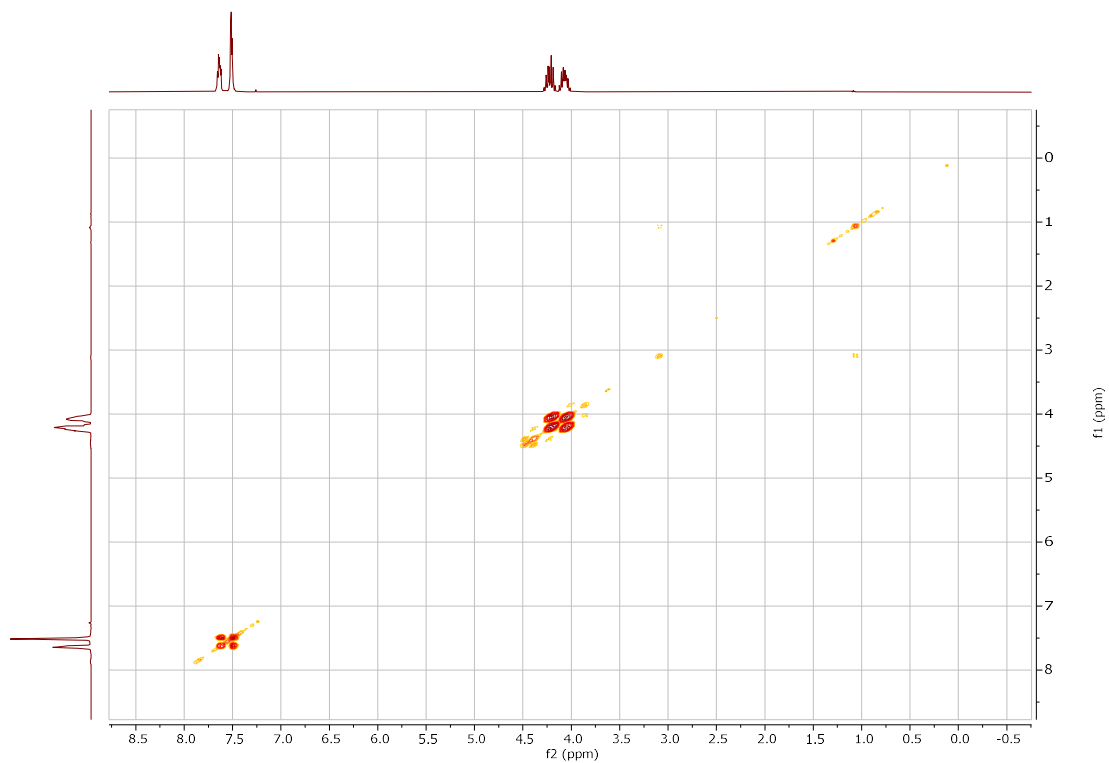
**<sup>19</sup>F NMR spectrum of compound 8**



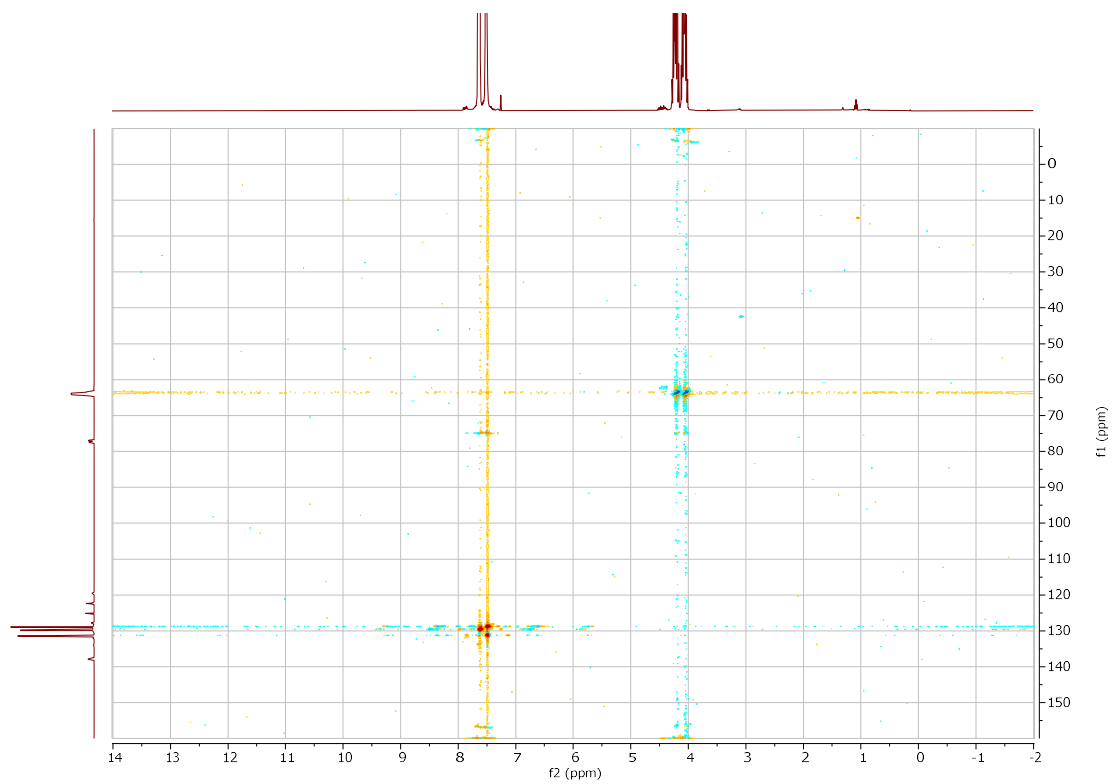
**<sup>1</sup>H NMR spectrum of compound 8**



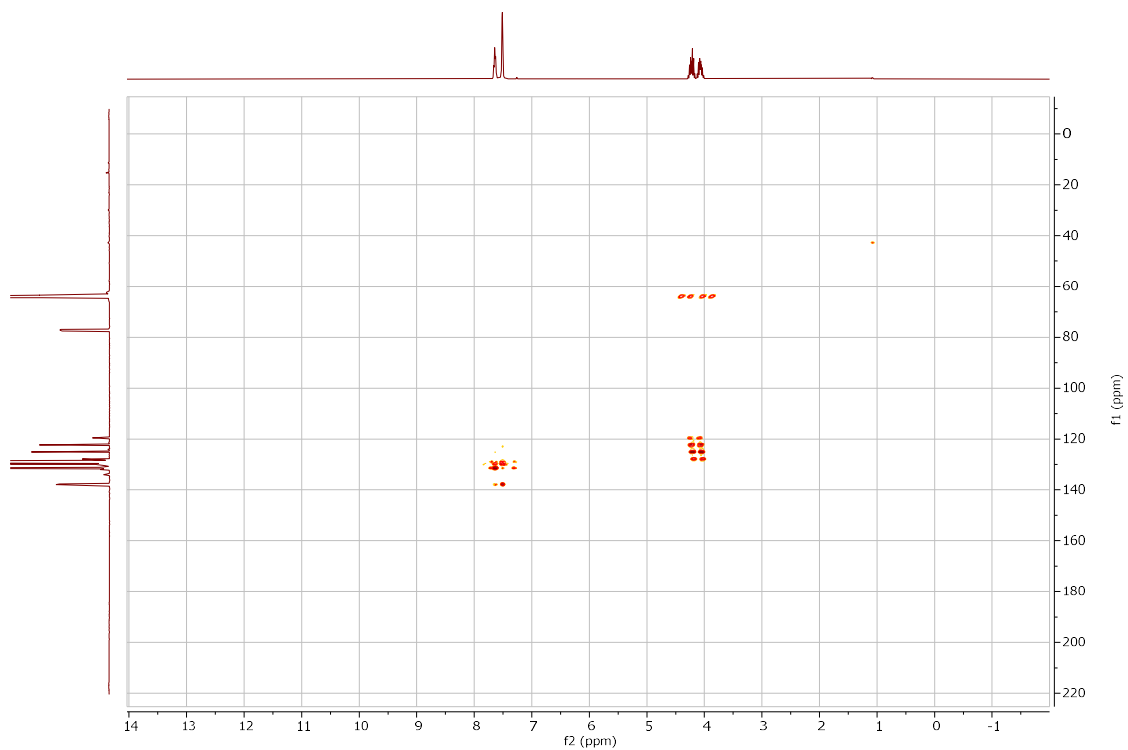
**$^{13}\text{C}(^1\text{H})$  NMR spectrum of compound 8**



**$^1\text{H}-^1\text{H}$  COSY NMR spectrum of compound 8**



**$^{13}\text{C}$ - $^1\text{H}$  HSQC NMR spectrum of compound 8**



**$^{13}\text{C}$ - $^1\text{H}$  HMBC NMR spectrum of compound 8**

## Compound 9

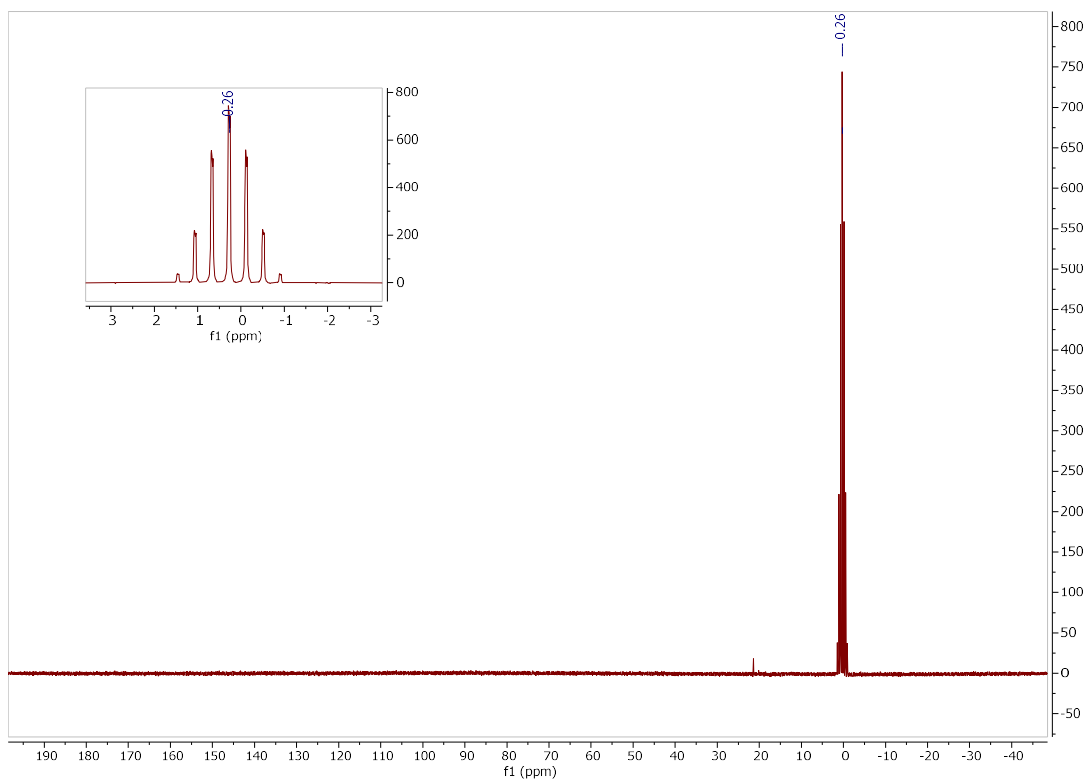
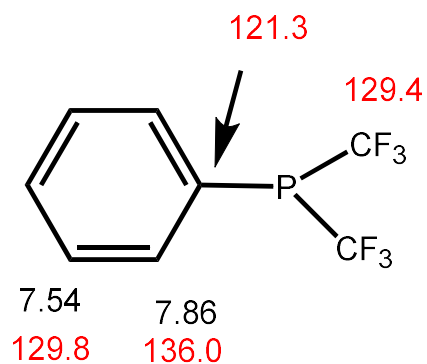
### Key HMBC Correlations

7.86: 133.3, 129.8, 129.4, 121.2

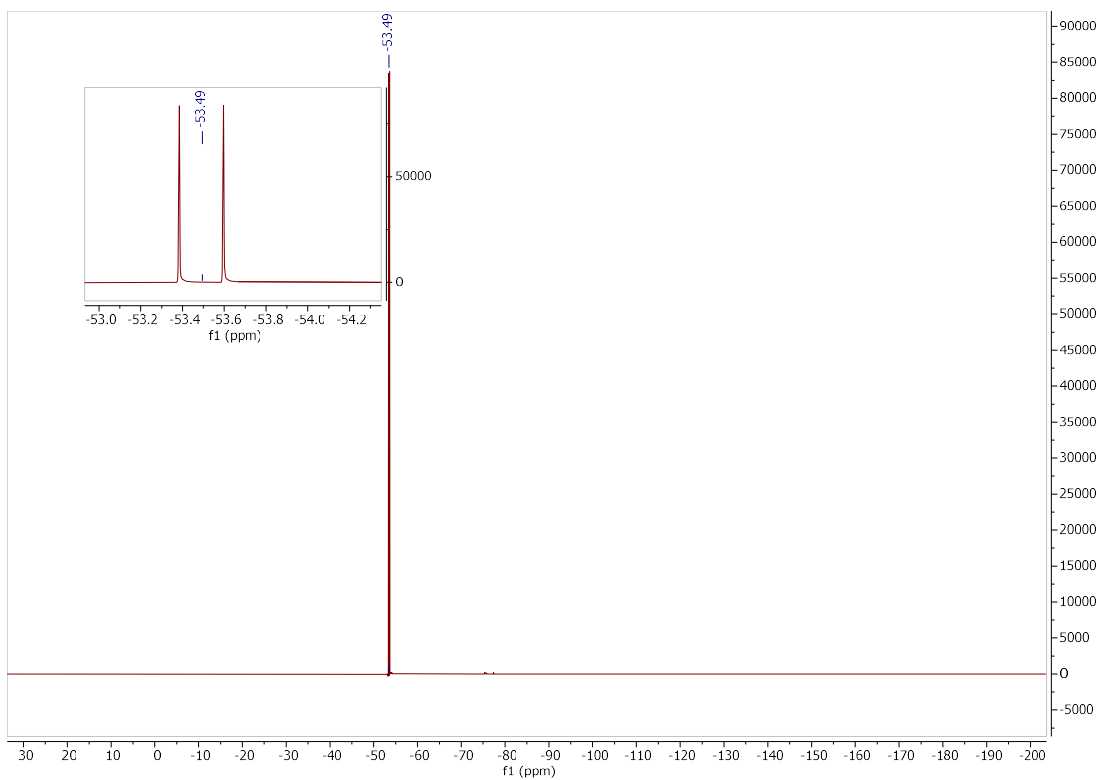
7.65: 136.0, 129.8

7.54: 136.0, 133.3, 121.3

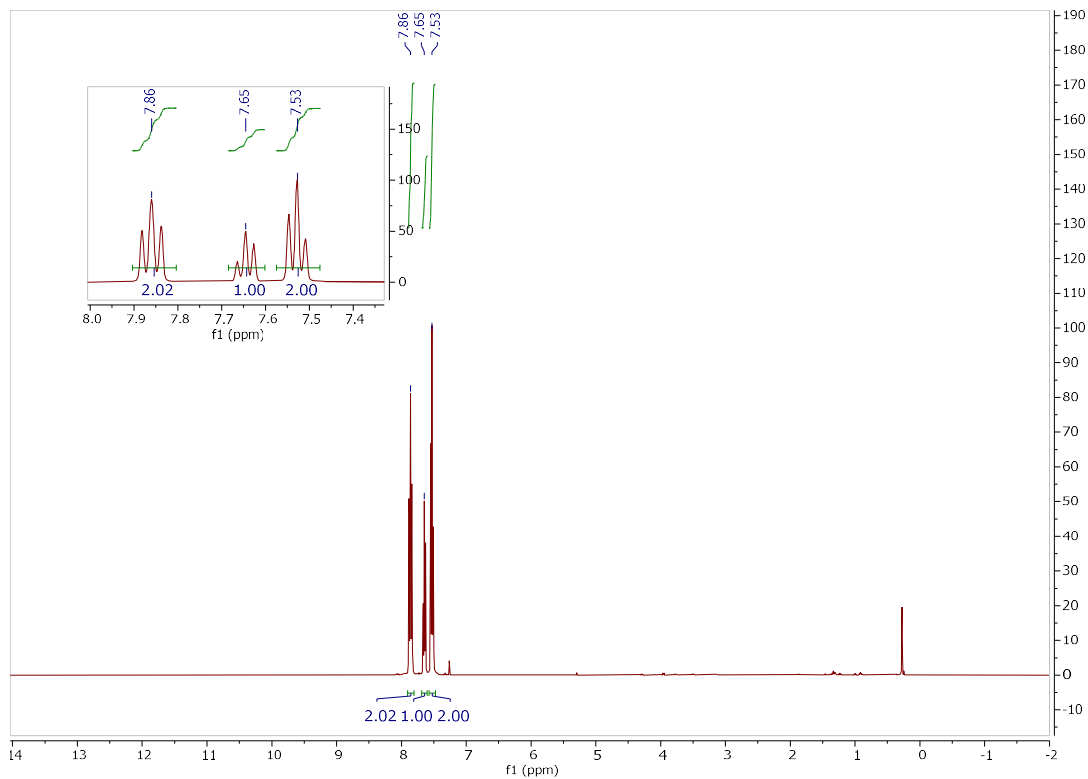
7.65  
133.3



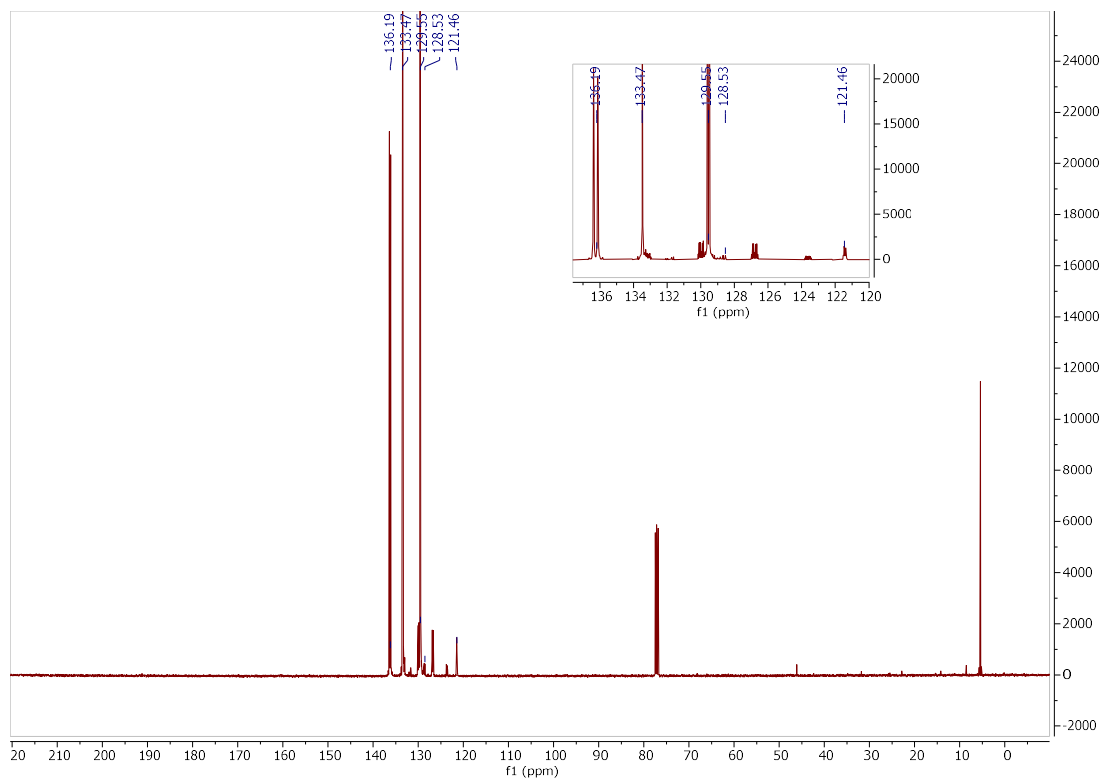
**$^{31}\text{P}(^1\text{H})$  NMR spectrum of compound 9**



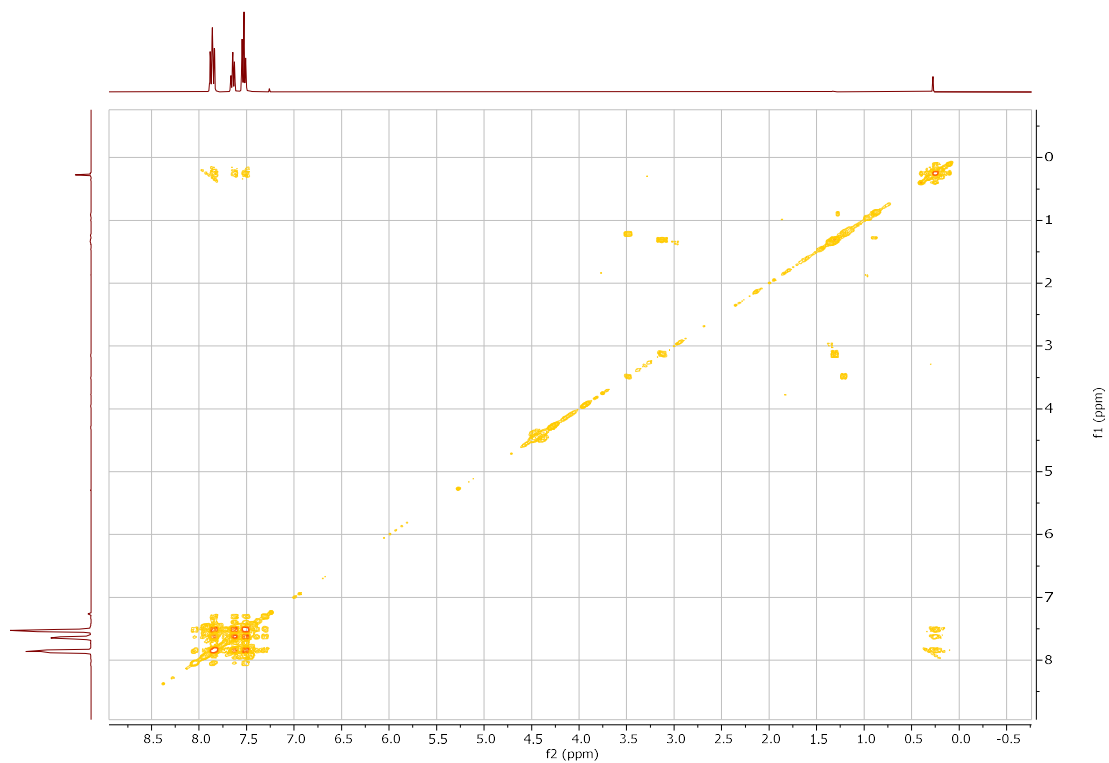
**<sup>19</sup>F NMR spectrum of compound 9**



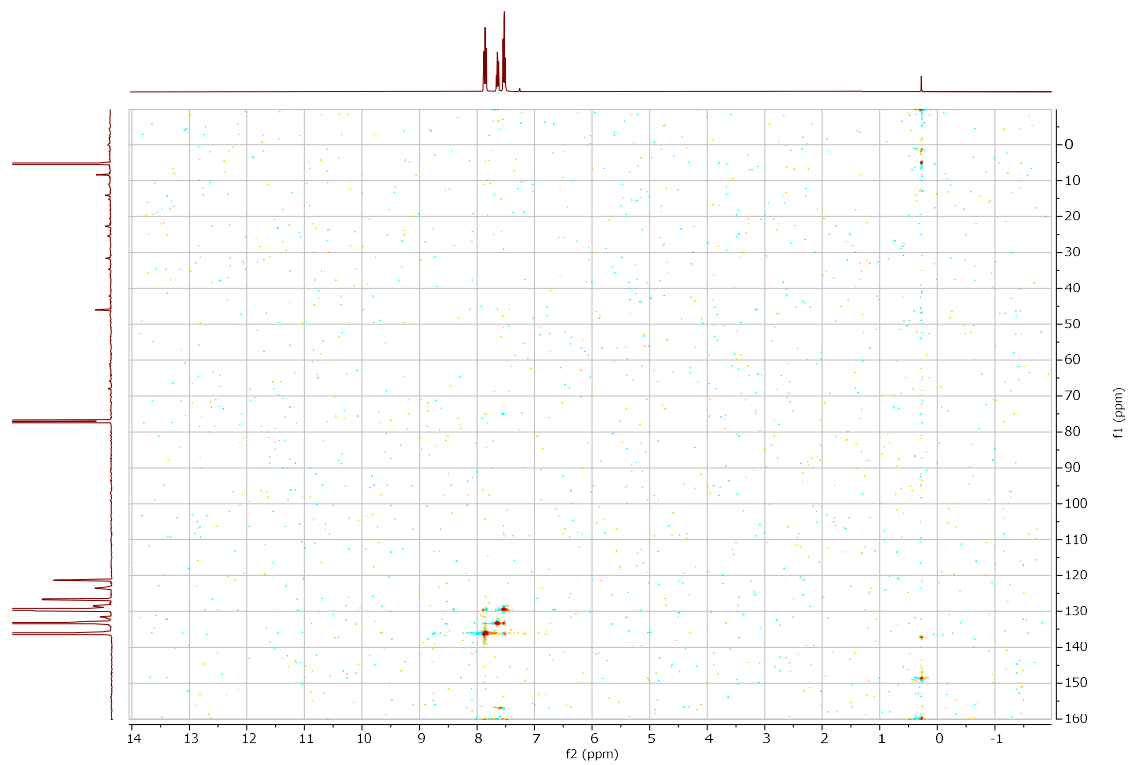
**<sup>1</sup>H NMR spectrum of compound 9**



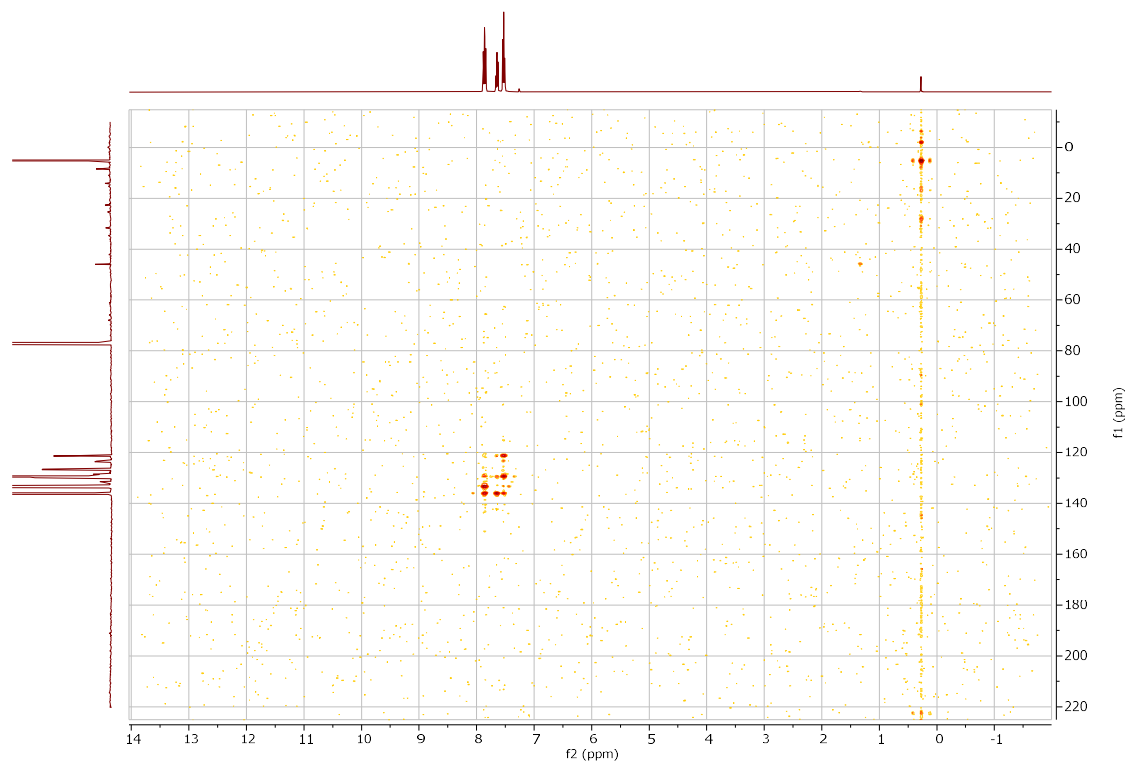
$^{13}\text{C}(^1\text{H})$  NMR spectrum of compound 9



$^1\text{H}-^1\text{H}$  COSY compound 9



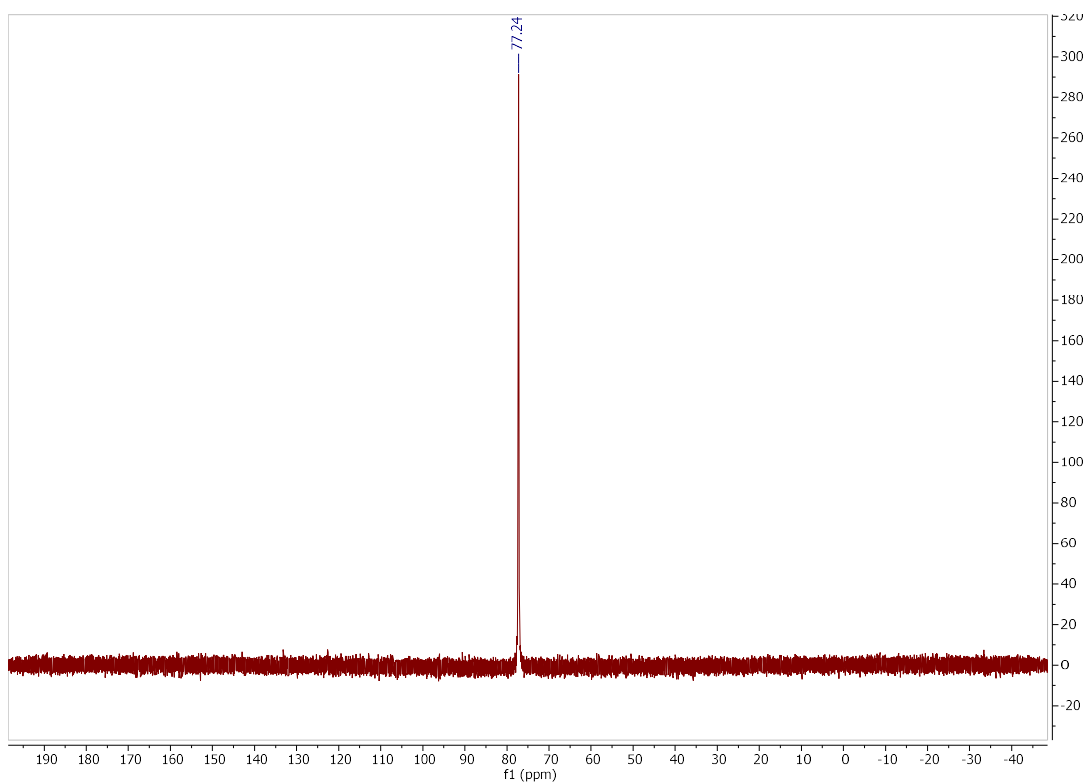
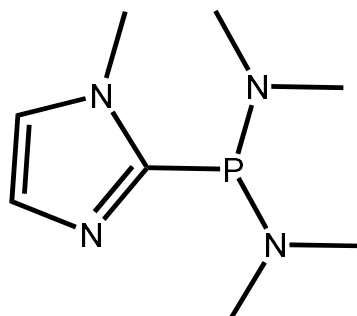
**$^{13}\text{C}$ - $^1\text{H}$  HSQC NMR spectrum of compound 9**



**$^{13}\text{C}$ - $^1\text{H}$  HMBC NMR spectrum of compound 9**

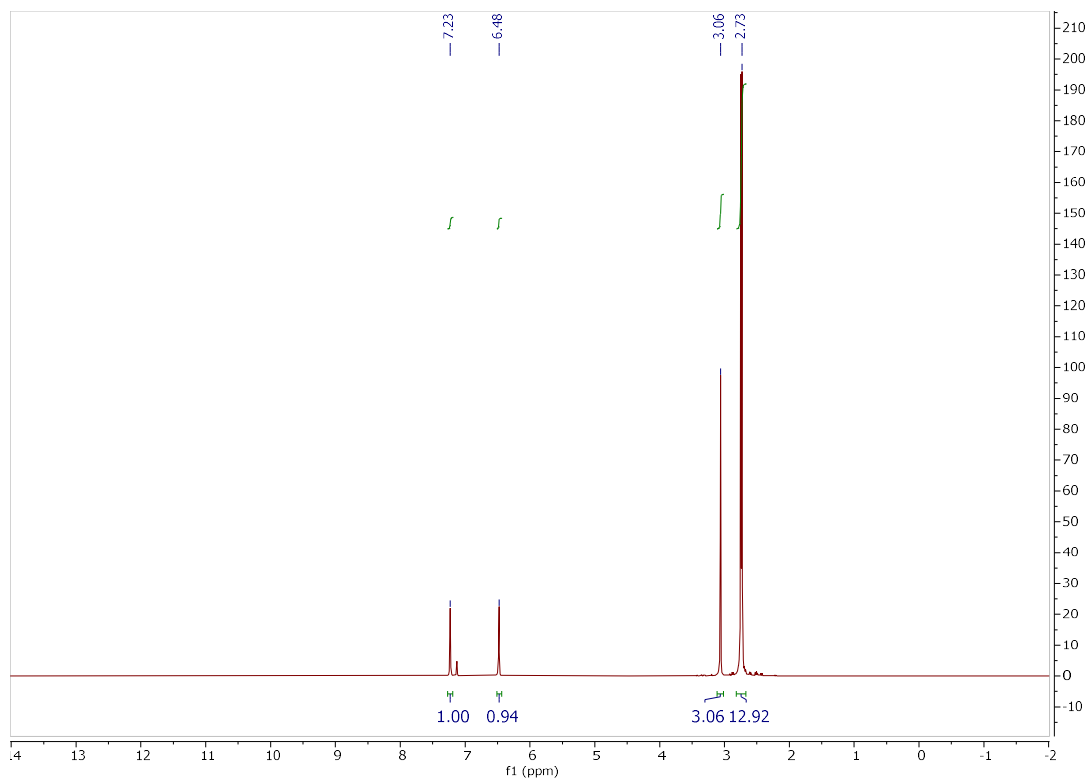
### Compound 10

10



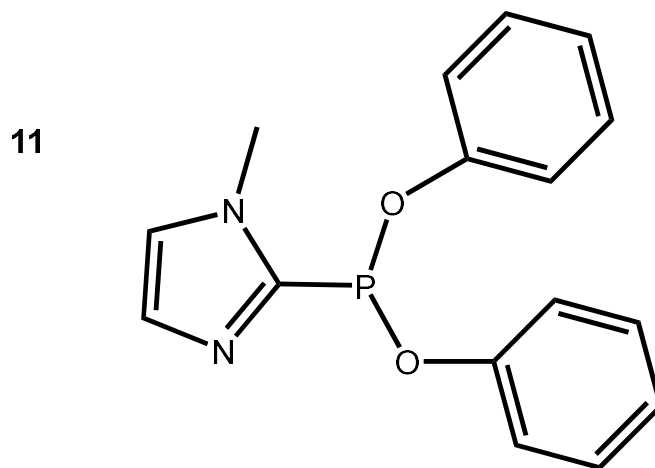
$^{31}\text{P}$ ( $^1\text{H}$ ) NMR spectrum of compound 10

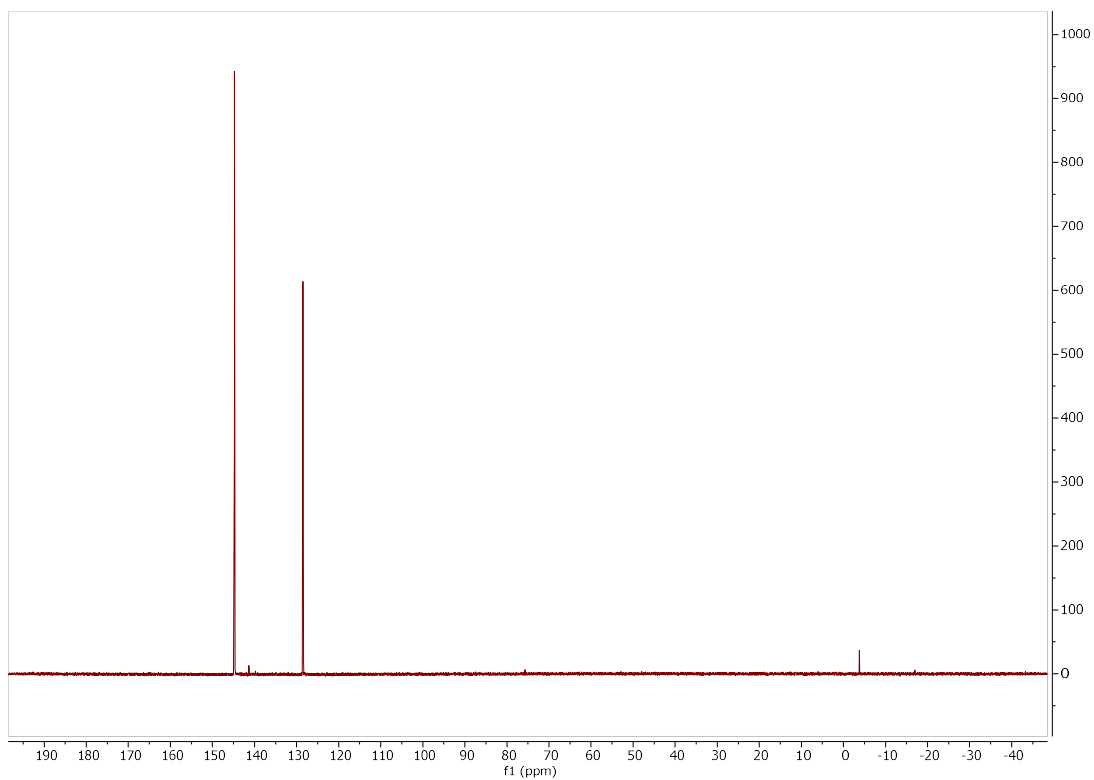




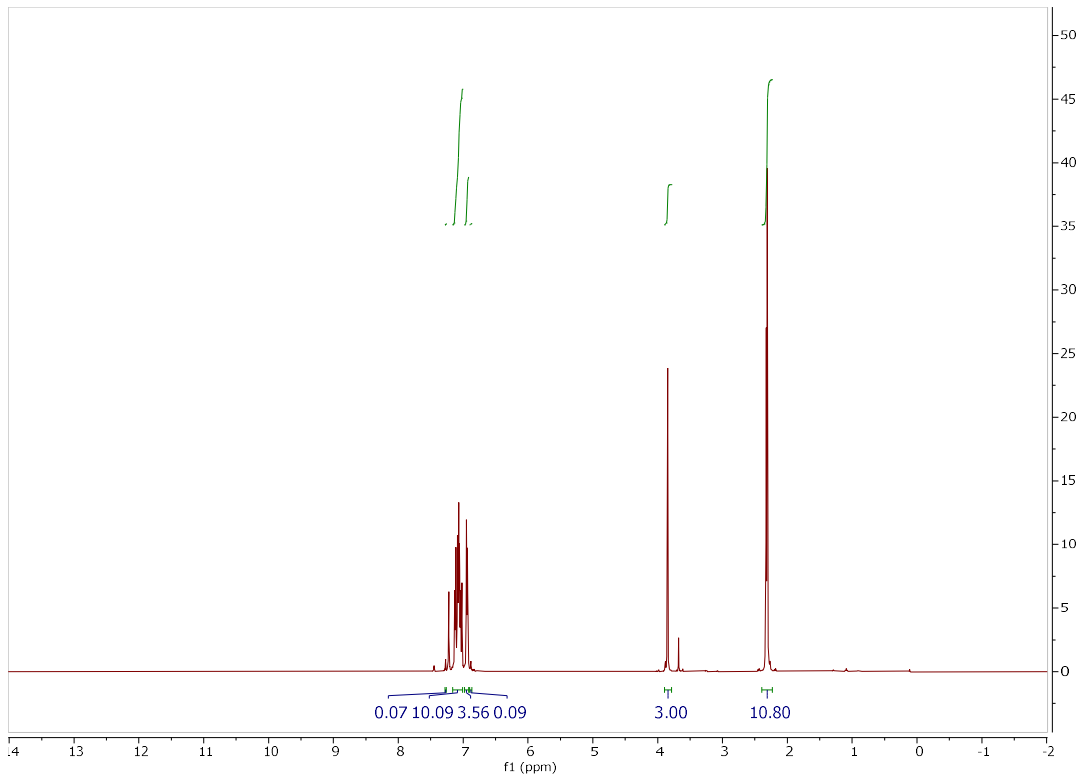
**<sup>1</sup>H NMR spectrum of compound 10**

**Compound 11**





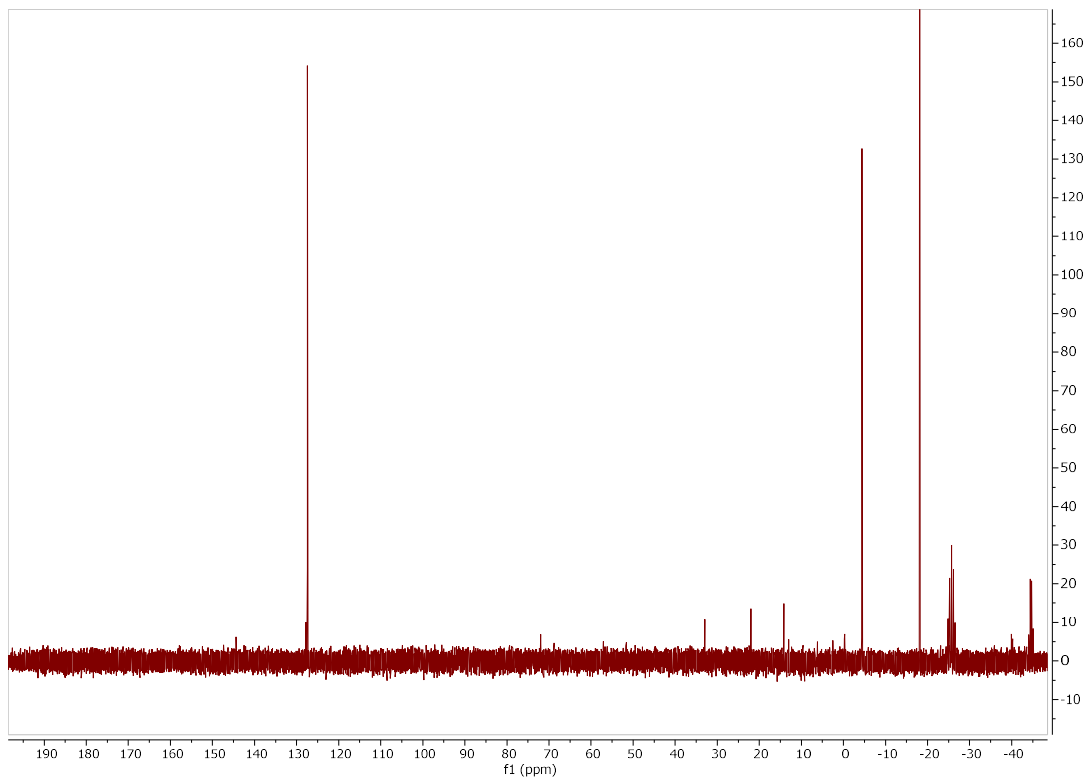
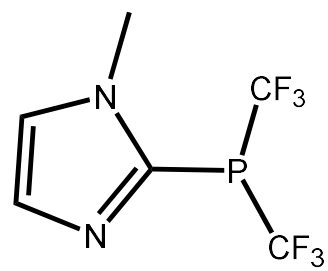
**$^{31}\text{P}$ ( $^1\text{H}$ ) NMR spectrum of compound 11**



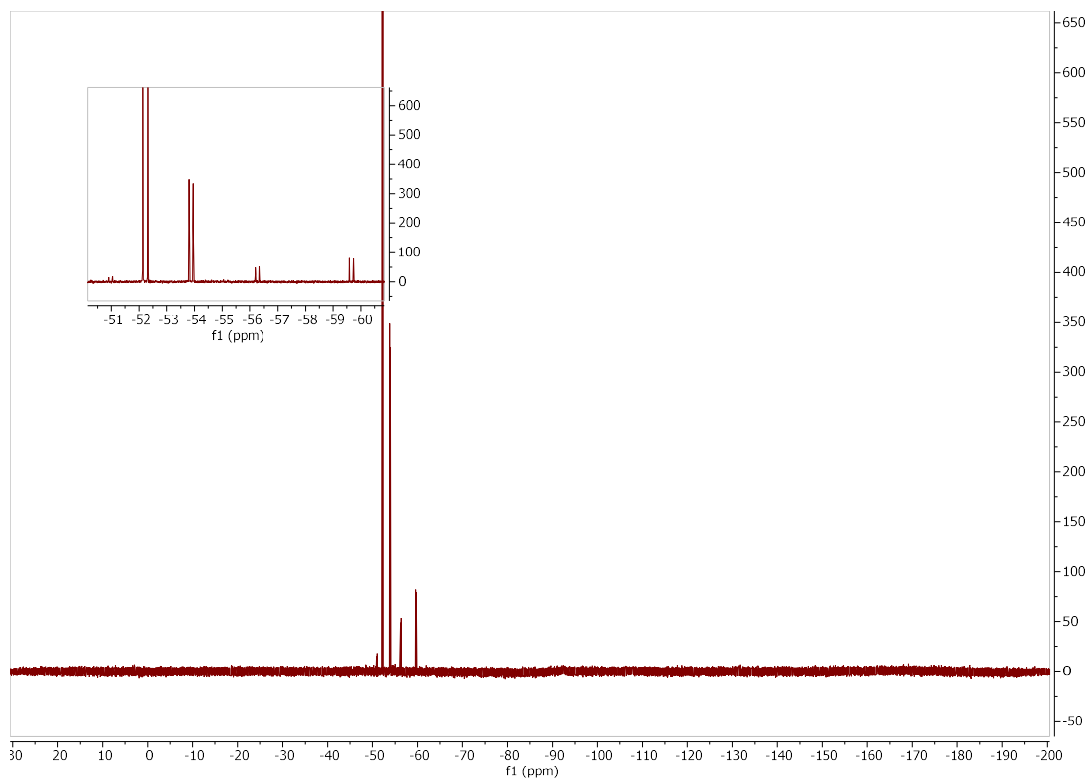
**$^1\text{H}$  NMR spectrum of compound 11**

**Compound 12**

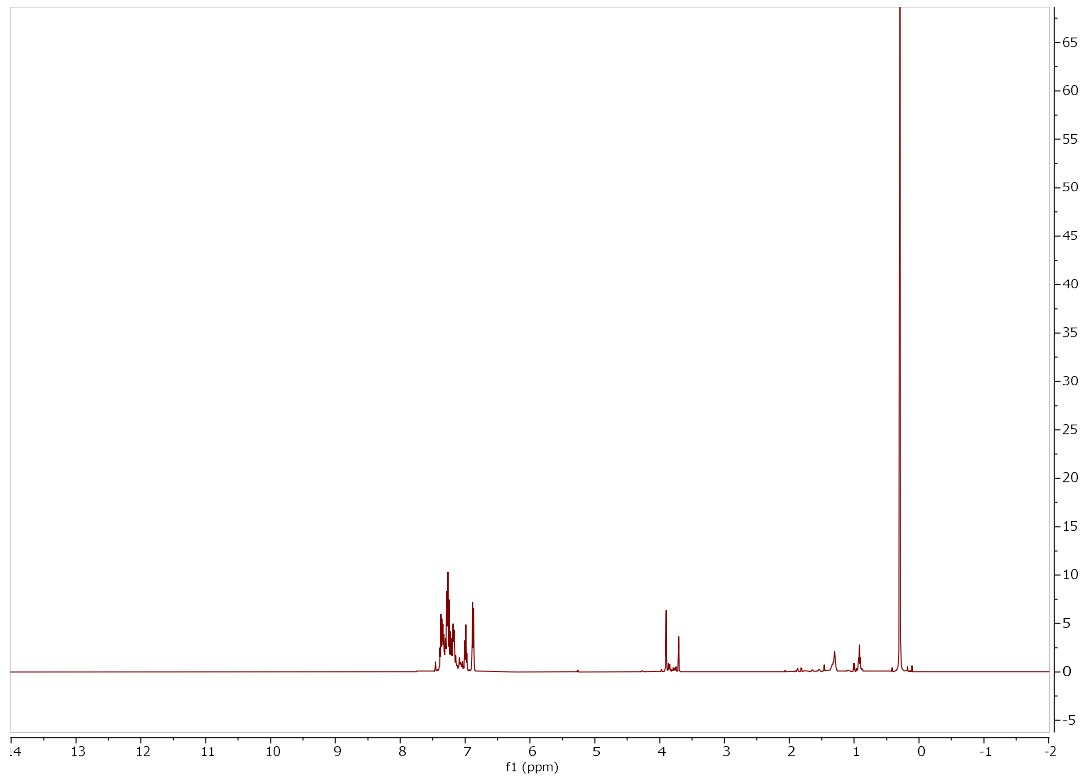
**12**



**$^{31}\text{P}(^1\text{H})$  NMR spectrum of compound 12**



**$^{19}\text{F}$  NMR spectrum of compound 12**



**$^1\text{H}$  NMR spectrum of compound 12**

## Chapter 4 Appendices

**Synthesis of 13:** 5.00 g of 2-bromoanisole was added to a Schlenk flask with stir bar. 50 mL of pentane was added, followed by 11.1 mL of nBuLi (2.5 M/L). The mixture was stirred for 4 hours, then filtered through a fine frit. The white precipitate was transferred to a new Schlenk flask with stir bar, and diethyl ether (50 mL) was added. Chloro bis(dimethylamino)phosphine (3.9997 g 25.8 mmol) was added dropwise, and the reaction was stirred for 2 hours. Hexanes (100 mL) were added, and the solution was washed with water (3 x 50mL), dried with Na<sub>2</sub>SO<sub>4</sub>, and the volatiles were removed in vacuo to give 5.0925 g (84%) of compound 13. <sup>31</sup>P(<sup>1</sup>H) (C<sub>6</sub>D<sub>6</sub>): δ 97.6 <sup>1</sup>H (C<sub>6</sub>D<sub>6</sub>): δ 7.55-7.51 (m, 1H), 7.14-7.07 (m, 1H), 6.96-6.91 (m, 1H), 6.55-6.49 (m, 1H), <sup>13</sup>C (<sup>1</sup>H) (C<sub>6</sub>D<sub>6</sub>): δ 161.1 (d, J<sub>C-P</sub> 15), 132.6, (d, J<sub>C-P</sub> 5.7), 129.6 (d, J<sub>C-P</sub> 1.6), 129.1, 120.9, 110.6, 55.3, 41.8 (d, J<sub>C-P</sub> 18.7),

QTOF-MS m/z for C<sub>11</sub>H<sub>19</sub>N<sub>2</sub>OPAg: Calculated 333.0285; Obtained 333.0257

**Synthesis of 14:** 13 (5.0925 g 22.5 mmol) was added to a Schlenk flask with stir bar. Hexanes (50 mL) were added. 2,2,2-Trifluoroethanol (13.665 g 135 mmol) was added to the mixture. Acetic acid (1.35 g 22.5 mmol) was added, and the reaction was stirred for 12 h. After verifying the reaction had gone to completion, K<sub>3</sub>PO<sub>4</sub> (42.9443 g 198 mmol) was added. Diethyl ether (100 mL) and hexanes (200 mL) were added, The mixture was filtered through a fine frit, and the filtrate was washed with water (3 x 50 mL), dried with Na<sub>2</sub>SO<sub>4</sub>, and the volatiles were removed *in vacuo* to give 5.4434 g (72%) of compound 14.

<sup>31</sup>P(<sup>1</sup>H) (CDCl<sub>3</sub>): δ 160.3 <sup>1</sup>H (CDCl<sub>3</sub>): δ 7.61-7.56 (m, 1H), 7.49-7.43 (m, 1H), 7.08-7.02 (m, 1H), 6.95-6.89 (m, 1H) <sup>13</sup>C (<sup>1</sup>H) (CDCl<sub>3</sub>): δ 161.8 (d, J<sub>C-P</sub> 18), 133.2, 130.6 (d, J<sub>C-P</sub> 4.7), 124.8, 123.4 (qd J<sub>C-F</sub> 278 J<sub>C-P</sub> 7.7) 121.2, 110.7, 64.3 (qd J<sub>C-F</sub> 35.2 J<sub>C-P</sub> 9.8), 55.8,

QTOF-MS m/z for C<sub>11</sub>H<sub>11</sub>F<sub>6</sub>O<sub>3</sub>PAg: Calculated 442.9400 Obtained 442.9410

**Synthesis of 15:** 14 (5.4434 g 16.2 mmol) was added to a Schlenk flask with stir bar. Diethyl ether (50 mL) was added. Trimethyl(trifluoromethyl)silane (6.907 g 48.5 mmol) was added. Cesium fluoride (2.459 g 16.1 mmol) was added, and the reaction was stirred for 12 h. The mixture was then filtered through a fine frit, and the filtrate was washed with water (3 x 40 mL) and dried with Na<sub>2</sub>SO<sub>4</sub>. The crude product was distilled under reduced pressure, with the compound 15 distilling at 85 °C at 6 Torr to give 2.7298 g (61%)

<sup>31</sup>P(<sup>1</sup>H) (CDCl<sub>3</sub>): δ -9.2, (h J<sub>P-F</sub> 80) <sup>19</sup>F (CDCl<sub>3</sub>): δ -52.6 (d, J<sub>P-F</sub> 78.9). <sup>1</sup>H (CDCl<sub>3</sub>): δ 7.75-7.69 (m, 1H), 7.58-7.52 (m, 1H), 7.11-7.05 (m, 1H), 7.02-6.96 (m, 1H) <sup>13</sup>C (<sup>1</sup>H) (CDCl<sub>3</sub>): δ 163.7 (d,

$J_{C-P}$  20), 134.7 (d,  $J_{C-P}$  1,5), 134.6, 128.9 (qdq  $J_{C-F}$  320  $J_{C-P}$  24.5  $J_{C-F}$  6) 121.9 (d  $J_{C-P}$  2) 111,5 (d,  $J_{C-P}$  3), 110.1 (m), 56,2 (d  $J_{C-P}$  1).

**Synthesis of 16:** **15** (.200 g 0.72 mmol) was added to a Schlenk flask with stir bar. Dichloromethane (3 mL) was added. The mixture was cooled to -78 °C, and BBr<sub>3</sub> (1.0887 g 4.3 mmol) was added. The reaction was stirred for 2 days. Water (5 mL) was added, and the mixture stirred for 20 minutes. The mixture was placed in a separatory funnel, and the dichloromethane layer was collected. The volatiles were removed *in vacuo* to give 0.0523 g (27%) **16**.

<sup>31</sup>P(<sup>1</sup>H)(CDCl<sub>3</sub>): δ -12.6, (h  $J_{P-F}$  80.3) <sup>19</sup>F (CDCl<sub>3</sub>): δ -52.5 (d,  $J_{P-F}$  80.3). <sup>1</sup>H (CDCl<sub>3</sub>): δ 7.74-7.65 (m, 1H), 7.48-7.40 (m, 1H), 7.08-7.02 (m, 1H), 6.93-6.86 (m, 1H), 5.86, (s, b, 1H) <sup>13</sup>C (<sup>1</sup>H) (CDCl<sub>3</sub>):

**Synthesis of 17:** 2-Bromo-5-(trifluoromethyl)anisole (5.00 g 19.6 mmol) was added to a Schlenk flask with stir bar. Hexanes (75 mL) was added. This mixture was cooled to 0 °C. nBuLi (8,15 mL 2.5 M/L) was added dropwise, and the reaction was stirred for 4 h. The mixture was filtered through a fine frit, and the precipitate was transferred to a new Schlenk flask with stir bar. Diethyl ether (75 mL) was added, and the mixture was cooled to 0 °C. Chloro bis(dimethylamino)phosphine (2.5476 g 16.4 mmol) was added dropwise, and the reaction was stirred for 12 hours. Pentane (100 mL) was added, and the solution was washed with water (3 x 50 mL), dried with Na<sub>2</sub>SO<sub>4</sub>, and the volatiles were removed *in vacuo* to give 4.2761 g (73%) of compound **17**.

<sup>31</sup>P(<sup>1</sup>H)(CDCl<sub>3</sub>): δ 95.7 <sup>19</sup>F (CDCl<sub>3</sub>): δ -63.1, <sup>1</sup>H (CDCl<sub>3</sub>): δ 7.48-7.44 (m, 1H), 7.24-7.20 (m, 1H), 7.05-7.00 (m, 1H), 3.89 (s, 3H), 2.69, (d  $J_{P-H}$  9.7 <sup>13</sup>C (<sup>1</sup>H) (CDCl<sub>3</sub>): δ

**Synthesis of 18:** **17** (4.2761 g 14.5 mmol) was added to a Schlenk flask with stir bar. Hexanes (75 mL) was added. 2,2,2-Trifluoroethanol (5.8818 g 58.1 mmol) was added.. Acetic acid (0.8917 g 14.5 mmol) was added. The reaction mixture was stirred for 12 h. K<sub>3</sub>PO<sub>4</sub> (21.5612 g 101 mmol) was added. Diethyl ether (100 mL) and hexanes (200 mL) were added, The mixture was filtered through a fine frit, and the filtrate was washed with water (3 x 50 mL), dried with Na<sub>2</sub>SO<sub>4</sub>, and the volatiles were removed *in vacuo* to give 4.2951 g (74%) of compound **18**.

<sup>31</sup>P(<sup>1</sup>H)(CDCl<sub>3</sub>): δ 160.9, <sup>19</sup>F (CDCl<sub>3</sub>): δ -63.17, -75.30 (td,  $J_{F-H}$  8.4  $J_{P-F}$  4.3). <sup>1</sup>H (CDCl<sub>3</sub>): δ 7.73-7.67 (m, 1H), 7.34-7.29 (m, 1H), 7.14-7.10 (m, 1H), 4.13 (m, 4H) 3.94 (s, 3H) <sup>13</sup>C (<sup>1</sup>H) (CDCl<sub>3</sub>): δ 161.9 (d,  $J_{C-P}$  17.5), 135.3 (q,  $J_{C-F}$  33.7), 131.3 (d,  $J_{C-P}$  4.9), 129.4 (d,  $J_{C-P}$  26.0), 123.8 (qd  $J_{C-F}$  277.9  $J_{C-P}$  6.3), 123.7 (q, 272.7), 117.9 (q  $J_{C-F}$  3.7), 107.7 (q  $J_{C-F}$  3.9), 64.6 (qd  $J_{C-F}$  36.6  $J_{C-P}$  12.0), 55.8,

**Synthesis of 19: 18** (4.2951 g 9.6 mmol) was added to a Schlenk flask with stir bar. Diethyl ether (50 mL) was added. Trimethyl(trifluoromethyl)silane (4.1192 g 28.9 mmol) was added. Cesium fluoride (1.4667 g 9.6 mmol) was added, and the reaction was stirred for 12 h. The mixture was filtered through a fine glass frit. The filtrate was distilled, with **19** distilling at 95 °C at 5 Torr to give 2.1521 g (64%).

$^{31}\text{P}$ ( $^1\text{H}$ )( $\text{CDCl}_3$ ):  $\delta$  -9.7, (h  $J_{\text{P-F}}$  78.6)  $^{19}\text{F}$ ( $\text{CDCl}_3$ ):  $\delta$  -52.1 (d,  $J_{\text{P-F}}$  78.6), -63.7.  $^1\text{H}$ ( $\text{CDCl}_3$ ):  $\delta$  7.85-7.79 (m, 1H), 7.36-7.31 (m, 1H), 7.21-7.17 (m, 1H), 3.98 (s 3H).  $^{13}\text{C}$ ( $^1\text{H}$ )( $\text{CDCl}_3$ ):  $\delta$  163.8 (d,  $J_{\text{C-P}}$  19.6), 136.5 (q,  $J_{\text{C-F}}$  31.9), 135.2, 128.5 (qdq  $J_{\text{C-F}}$  324.8  $J_{\text{C-P}}$  23.3  $J_{\text{C-F}}$  5.2), 123.3 (q  $J_{\text{C-F}}$  275.4), 118.6 (d,  $J_{\text{C-P}}$  3.8), 115.3 (d  $J_{\text{C-P}}$  12.8), 56.6.

### Synthesis of 20:

**Synthesis of 21:** 2-bromo-4(trifluoromethyl)anisole (10.0000g 39 mmol) was added to a Schlenk flask with stir bar. Hexanes (100 mL) was added, and the reaction was cooled to 0 °C. nBuLi (14.65 mL 2.5 M/L) was added dropwise, and the reaction was stirred for 4 hours. The mixture filtered through a fine glass frit, and the precipitate was transferred to a new Schlenk flask with stir bar. Diethyl ether (100 mL) was added, and the reaction was cooled to 0 °C. Chloro bis(dimethylamino)phosphine was added dropwise, and the reaction was stirred for 2 hours. Hexanes (100 mL) was added to the reaction mixture, and this was washed with water (3 x 100 mL), dried with  $\text{Na}_2\text{SO}_4$ , and the volatiles were removed *in vacuo* to give 8.3851 g (72%) of compound **21**.

$^{31}\text{P}$ ( $^1\text{H}$ )( $\text{CDCl}_3$ ):  $\delta$  93.7  $^{19}\text{F}$ ( $\text{CDCl}_3$ ):  $\delta$  -62.5,  $^1\text{H}$ ( $\text{CDCl}_3$ ):  $\delta$  7.32-7.29 (m, 1H), 7.24-7.19 (m, 1H), 6.63-6.58 (m, 1H), 3.57 (s, 3H), 2.37, (d  $J_{\text{P-H}}$  9.5)  $^{13}\text{C}$ ( $^1\text{H}$ )( $\text{CDCl}_3$ ):  $\delta$

**Synthesis of 22: 21** (8.3851 g 28 mmol) was added to a Schlenk flask with stir bar. Hexanes (100 mL) were added. 2,2,2-Trifluoroethanol (11.3718 g 113 mmol) was added. Acetic acid (1.68 g 28 mmol) was added, and the reaction was stirred for 12 h.  $\text{K}_3\text{PO}_4$  (42.2870 g 199 mmol) was added. Diethyl ether (200 mL) and hexanes (100 mL) were added, and the mixture was stirred for 1 h. The mixture was filtered through a fine frit, and the filtrate was washed with water (3 x 100 mL), dried with  $\text{Na}_2\text{SO}_4$ , and the volatiles were removed *in vacuo* to give 7.8259 g (67%) of compound **22**.

$^{31}\text{P}$ ( $^1\text{H}$ )( $\text{CDCl}_3$ ):  $\delta$  160.8  $^{19}\text{F}$ ( $\text{CDCl}_3$ ):  $\delta$  -61.8, -75.4 (td,  $J_{\text{F-H}}$  8.1  $J_{\text{P-F}}$  4.5).  $^1\text{H}$ ( $\text{CDCl}_3$ ):  $\delta$  7.87 (s, 1H), 7.75-7.71 (m, 1H), 7.03-6.98 (m, 1H), 4.14 (m, 4H), 3.95, (s 3H).  $^{13}\text{C}$ ( $^1\text{H}$ )( $\text{CDCl}_3$ ):  $\delta$

**Synthesis of 23:** 22 (7.8259 g 19.4 mmol) was added to a Schlenk flask with stir bar. Diethyl ether (100 mL) was added. Trimethyl(trifluoromethyl)silane (11.0132g 77.4 mmol) was added. Cesium fluoride (2.9435 g 19,3 mmol) was added, and the reaction was stirred for 12 h. The mixture was then filtered through a fine glass frit and the filtrate was washed with water (3 x 50 mL). The filtrate was distilled, with the fraction distilling at 100 °C at 5 Torr, giving 2.6339 g (40%) of **23**.

$^{31}\text{P}$ ( $^1\text{H}$ ) ( $\text{CDCl}_3$ ):  $\delta$  -10.1, (h  $J_{\text{P-F}}$  79.6)  $^{19}\text{F}$  ( $\text{CDCl}_3$ ):  $\delta$  -52.1 (d,  $J_{\text{P-F}}$  79.6), -62.1.  $^1\text{H}$  ( $\text{CDCl}_3$ ):  $\delta$  7.95 (s, 1H), 7.83-7.77 (m, 1H), 7.10-7.04 (m, 1H).  $^{13}\text{C}$  ( $^1\text{H}$ ) ( $\text{CDCl}_3$ ):  $\delta$  165.7 (d,  $J_{\text{C-P}}$  18.2), 131.9 (d,  $J_{\text{C-P}}$  3.0), 131.8 (d,  $J_{\text{C-P}}$  10.0), 128.4 (qdq  $J_{\text{C-F}}$  320.1  $J_{\text{C-P}}$  23.4  $J_{\text{C-F}}$  6.1) 124.6, 123.9, 111.8 (m), 111.5 (d  $J_{\text{C-P}}$  2.5), 56.7.

#### **Synthesis of 24:**

**Synthesis of 25:** **25** was synthesized using literature procedures<sup>2</sup>

**Synthesis of 26:** **25** (6,8419 g 16,2 mmol) was added to a Schlenk flask with stir bar. Tetrahydrofuran (50 mL) was added. Trichlorophosphine (4.4502 g 32.4 mmol) was added dropwise, and the mixture was stirred for 12 h. The volatiles were removed by heating the flask to 50 °C under vacuum for 6 hours to give 6.3523 g(94%) of **26**.

**Synthesis of 27:** Magnesium turnings (0.948 g 39.5 mmol) was added to a Schlenk flask with stir bar. Diethyl ether (60 mL) was added to the flask, and one crystal of  $\text{I}_2$  was added. This was stirred for 10 min. Bromopentafluorobenzene (4.8772 g 19.7 mmol) was added dropwise to the flask, and the mixture was allowed to stir for 12 h. **26** (2.0012 g 4.9 mmol) was dissolved in diethyl ether (20 mL). The pentafluorophenyl Grignard reagent was added dropwise to the solution of **26** and was then stirred for 4 hours. The mixture was filtered through a fine frit and the filter cake was washed with hexanes (40 mL). The volatiles were removed under vacuum to give 2.5445 g (79%) of **27**.

**Synthesis of 28:** **27** (2.5445 g 3.8 mmol) was added to a Schlenk flask with stir bar. Diethyl ether (50 mL) was added to the flask. Trichlorophosphine (2.0916 g 15.2 mmol) was added dropwise, and the reaction was stirred for 12 h. The volatiles were removed under vacuum at 50 °C to give 2.3465 g (95%) of **28**.

**Synthesis of 29:** Magnesium turnings (0.7310 g 30.4 mmol) were added to a Schlenk flask with stir bar. Diethyl ether (50 mL) was added. One crystal of  $\text{I}_2$  was added and the mixture was stirred for 10 minutes. 2-Bromoanisole (2.8486 g 15.2 mmol) was added dropwise, and the reaction stirred for 12 h. **28** (2.3465 g 3.8 mmol) was added to a Schlenk flask with stir bar. Diethyl ether (100 mL) was added and the solution cooled to 0 °C. The Grignard reagent was added dropwise to the solution of **28**, and stirred for 12 h. The solution was filtered through a medium frit with Celite to remove the majority of magnesium salts. The filtrate was washed with water (3 x 50 mL), dried with  $\text{Na}_2\text{SO}_4$ , and the volatiles were removed *in vacuo*. The crude product was

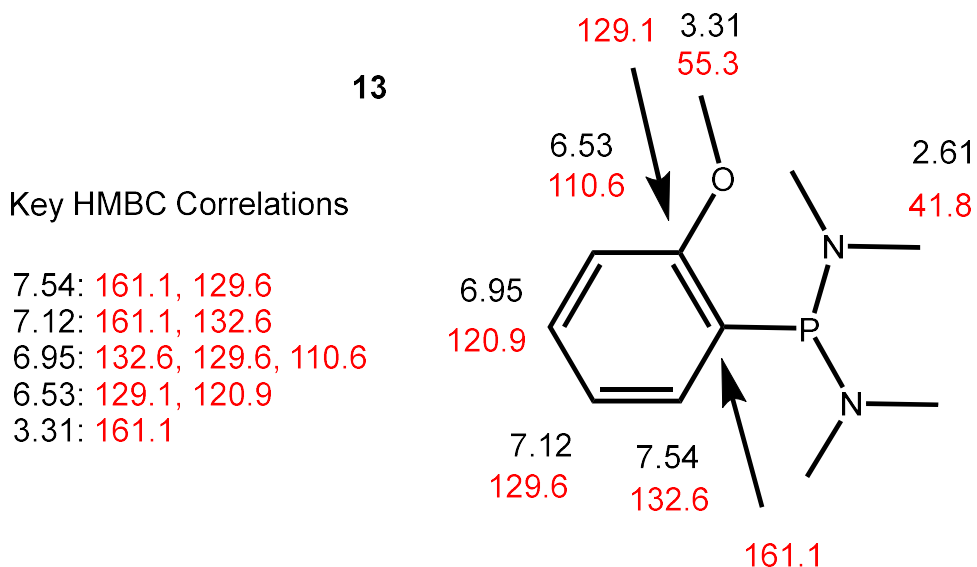


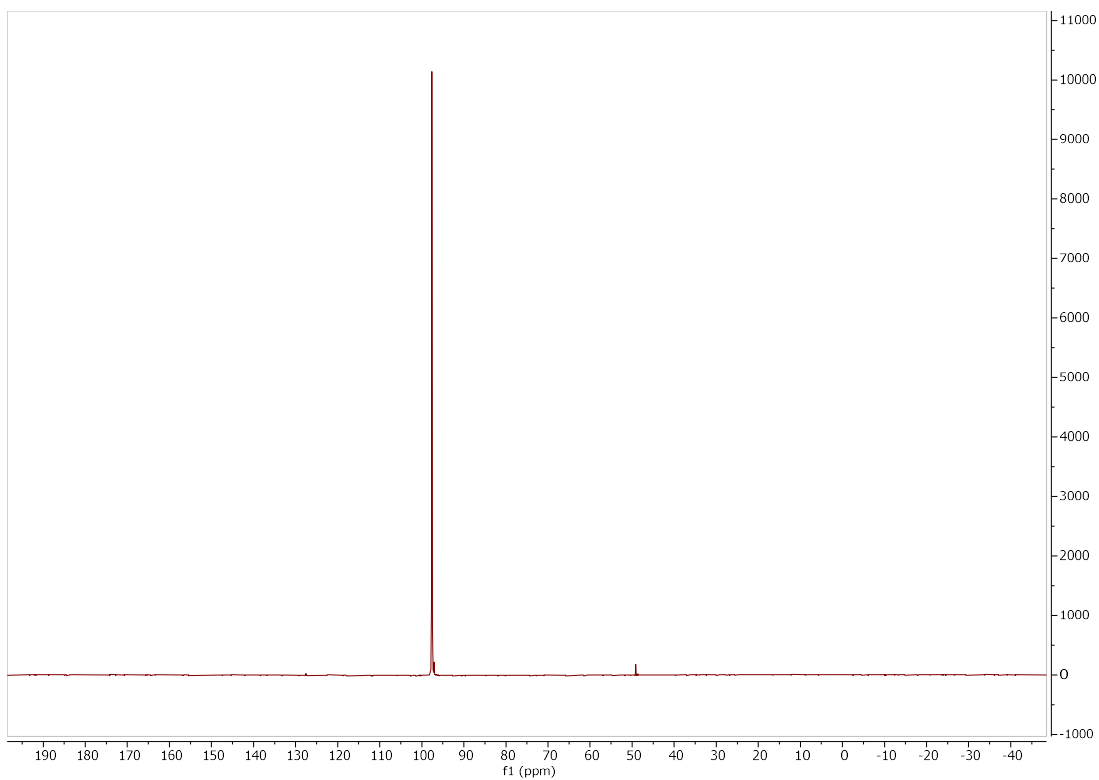
redissolved in diethyl ether and filtered through a silica plug to remove phosphine oxides. The crude product was then purified using flash column chromatography using 5% ethyl acetate 95% hexanes, with the pure product having an  $R_f$  of 0.3. The two diastereomers were visible on the TLC plate but were unable to be separated in the column.

**Synthesis of 30:** **29** (0.2000 g 0.2 mmol) was added to a Schlenk flask with stir bar. Dichloromethane (3 mL) was added. Boron tribromide (0.3784 g 1.5 mmol) was added dropwise, and the reaction was stirred for 2 days. Water (10 mL) was added, and the mixture transferred to a separatory funnel. The organic layer was collected, dried with  $\text{Na}_2\text{SO}_4$ , and the volatiles were removed to give **30** (0.1702 g 88%).

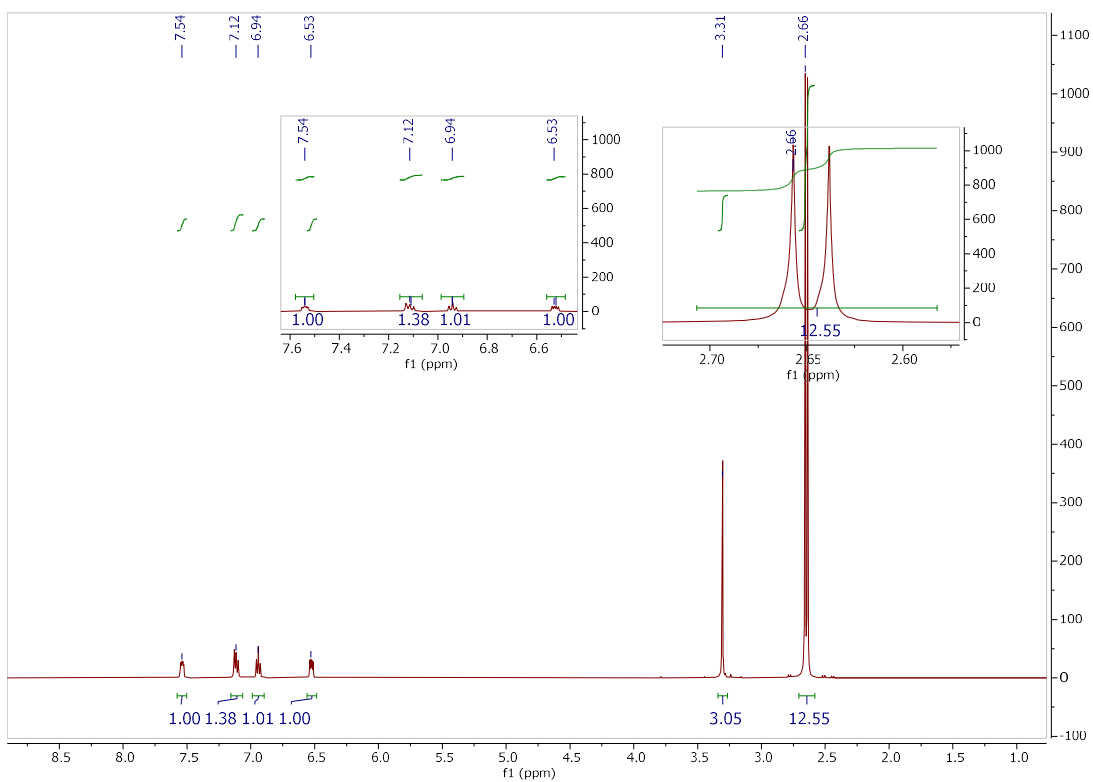
**Synthesis of 31:** 2-trimethylsilyl-N-Methyl Imidazole (0.52419 g 0.5 mmol) was added to a scintillation vial with stir bar. Pentane (2 mL) was added. Bis(pentafluorophenyl)bromophosphine (0.2000 g 0.6 mmol) was added dropwise with vigorous stirring, and the reaction was stirred for 12 h. Volatiles were removed under vacuum overnight to give **31** (0.5214 g) in 94% yield.

### Compound 13

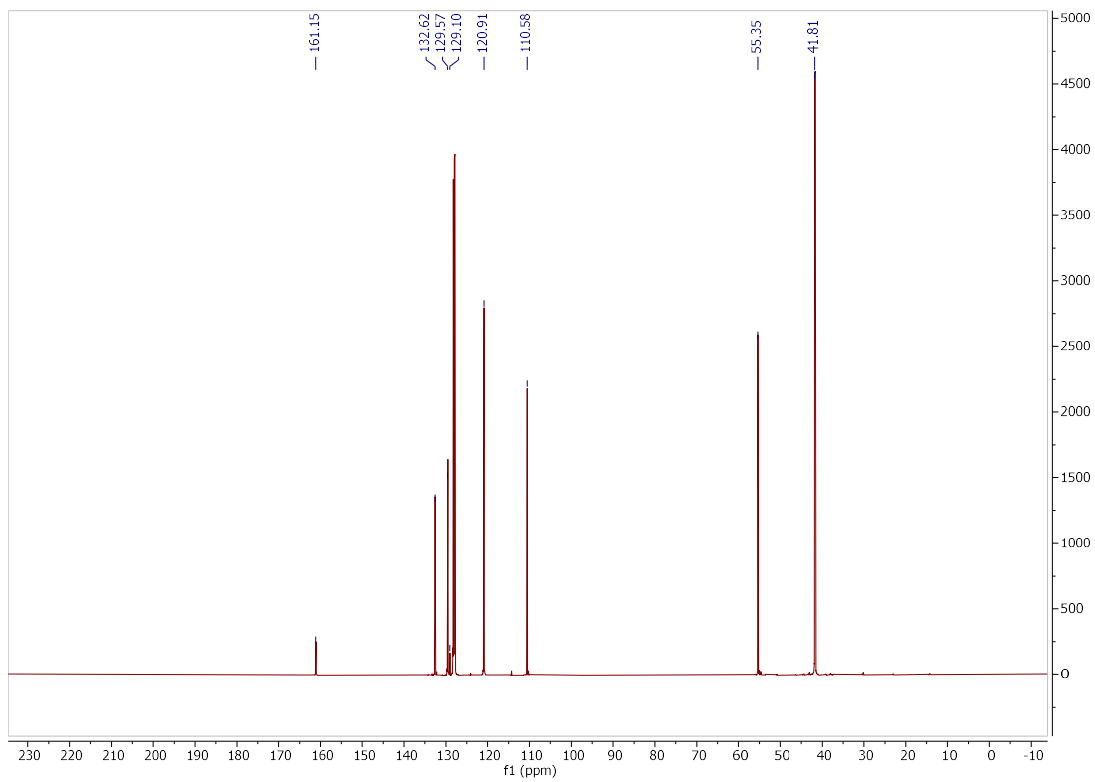




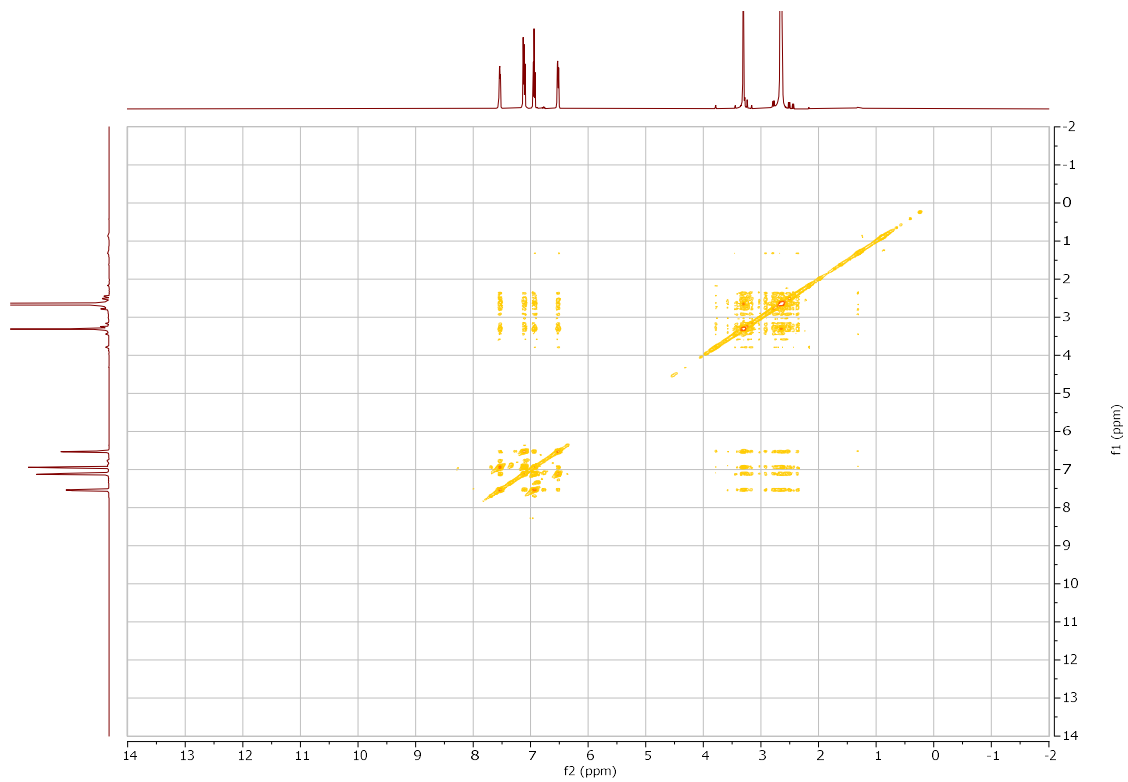
**$^{31}\text{P}$ ( $^1\text{H}$ ) NMR spectrum of compound 13**



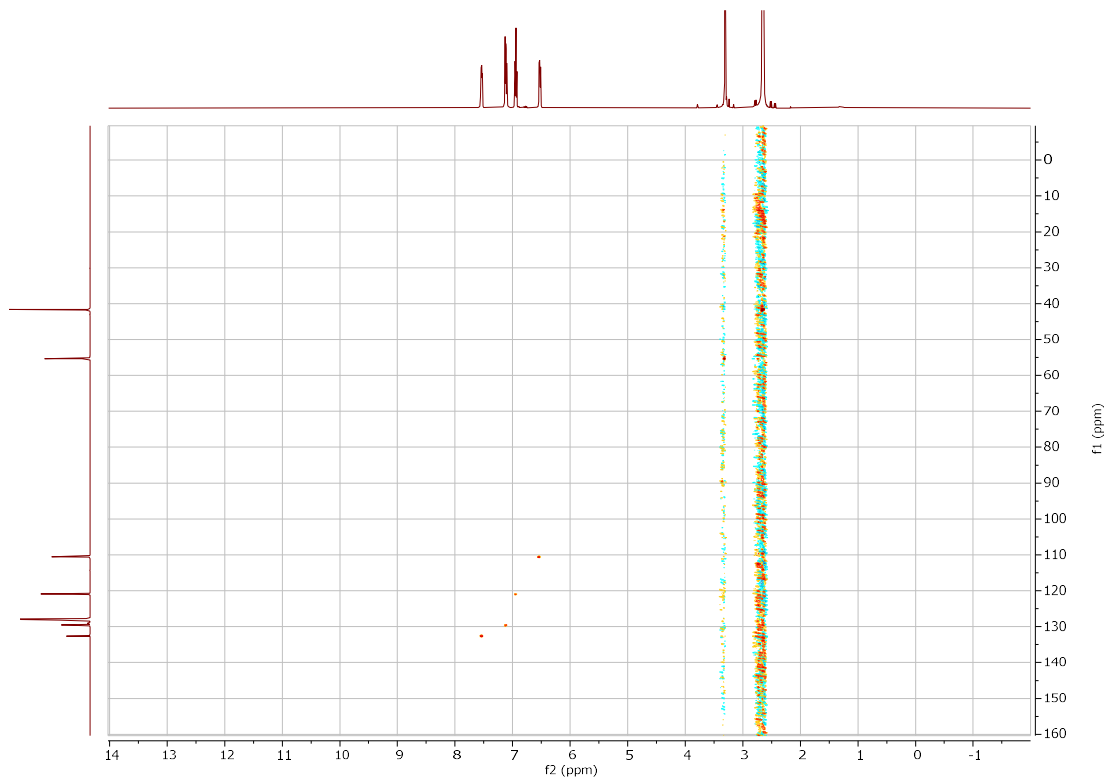
### $^1\text{H}$ NMR spectrum of compound 13



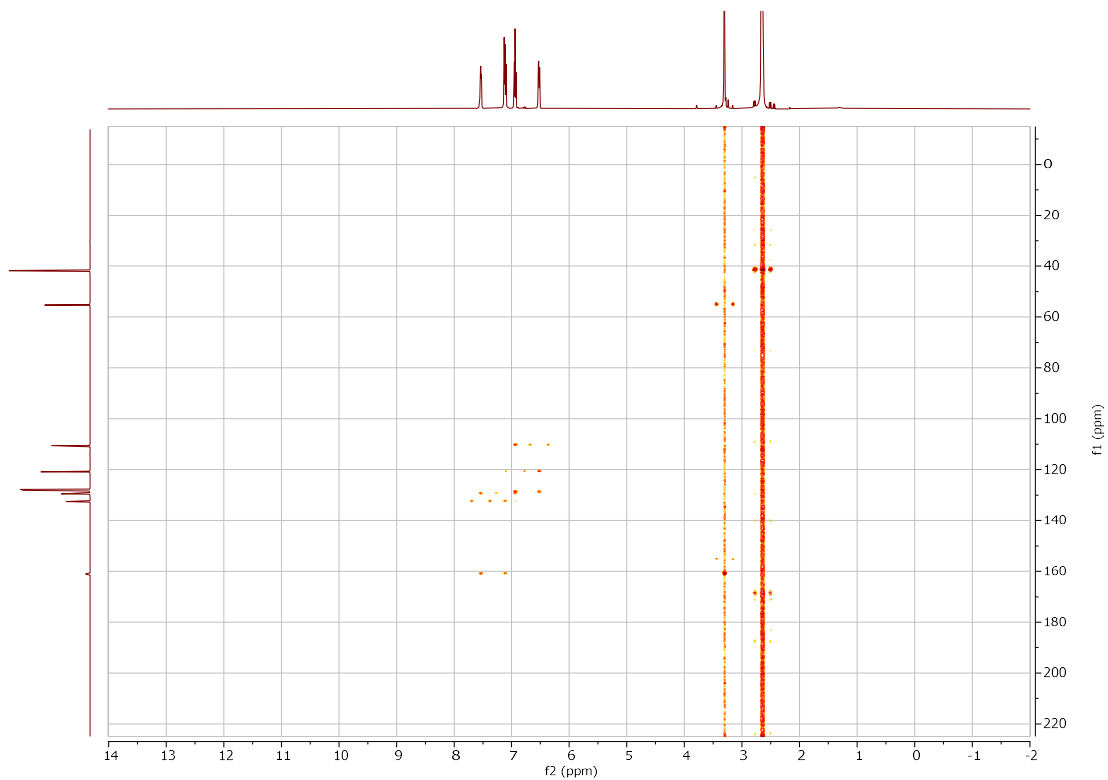
### $^{13}\text{C}(^1\text{H})$ NMR spectrum of compound 13



**$^1\text{H}$ - $^1\text{H}$  COSY NMR spectrum of compound 13**

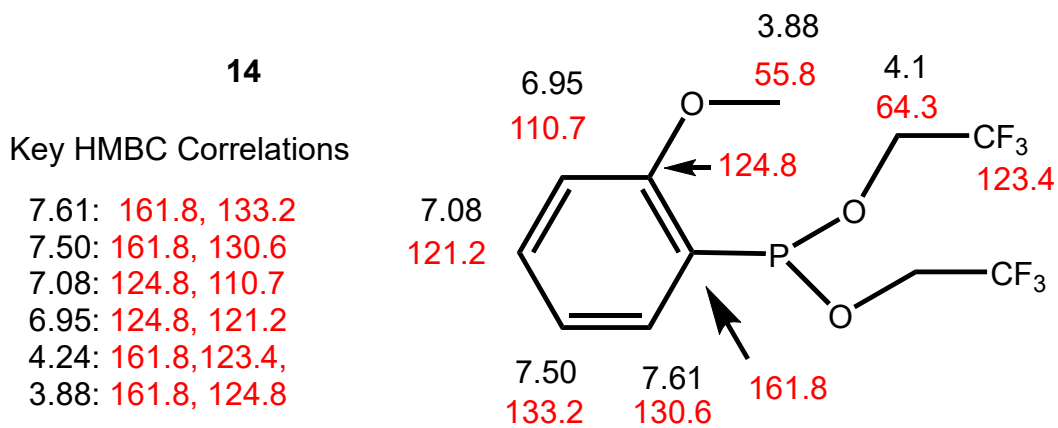


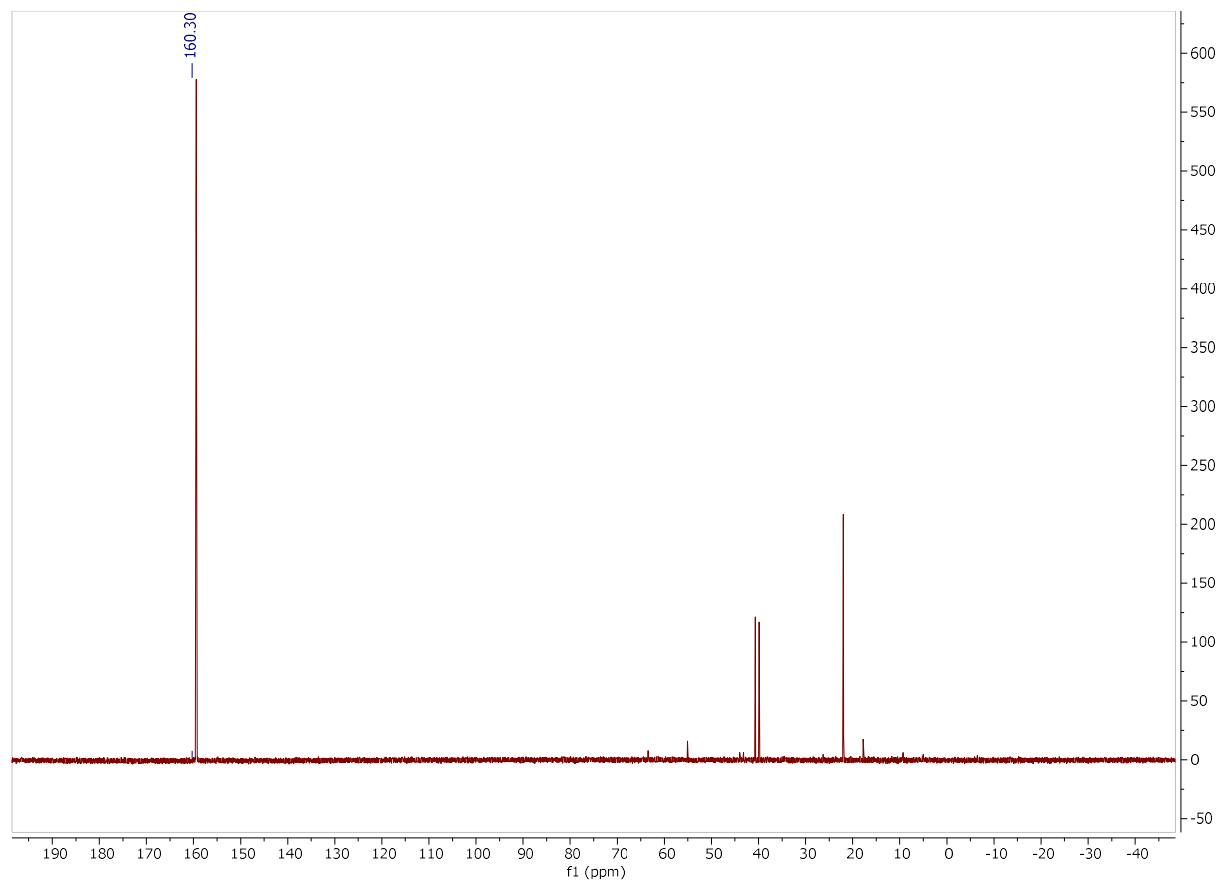
**$^{13}\text{C}$ - $^1\text{H}$  HSQC NMR spectrum of compound 13**



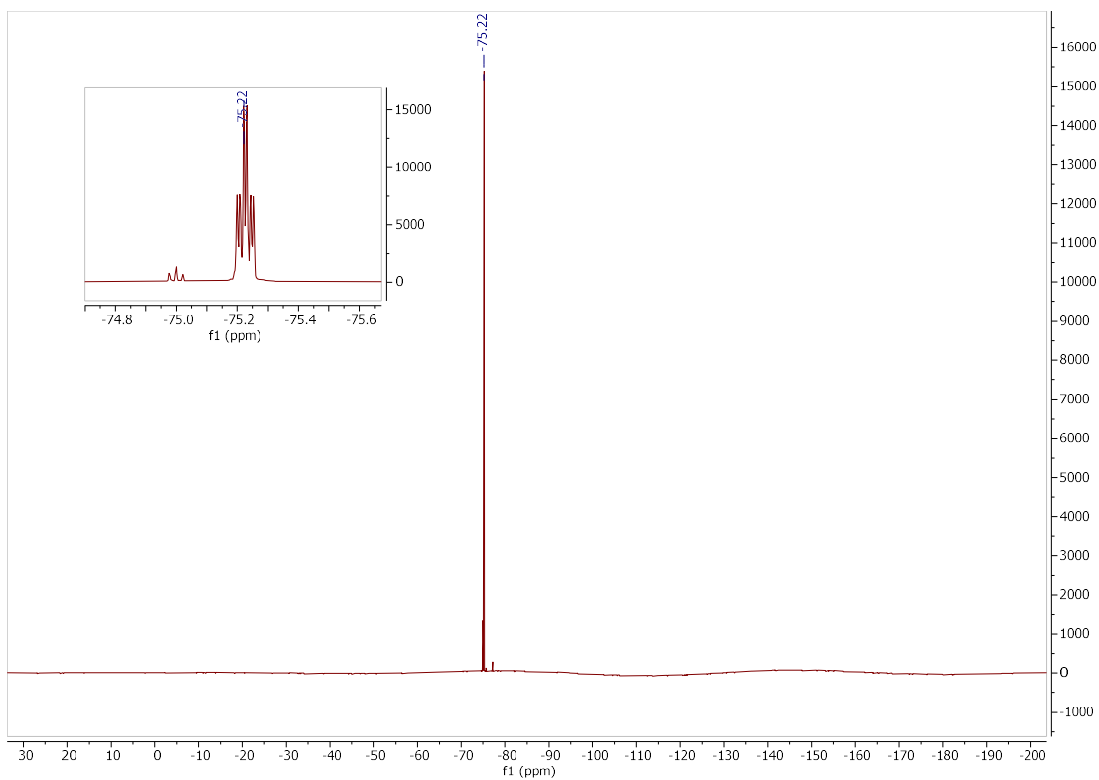
$^{13}\text{C}$ - $^1\text{H}$  HMBC NMR spectrum of compound 13

### Compound 14

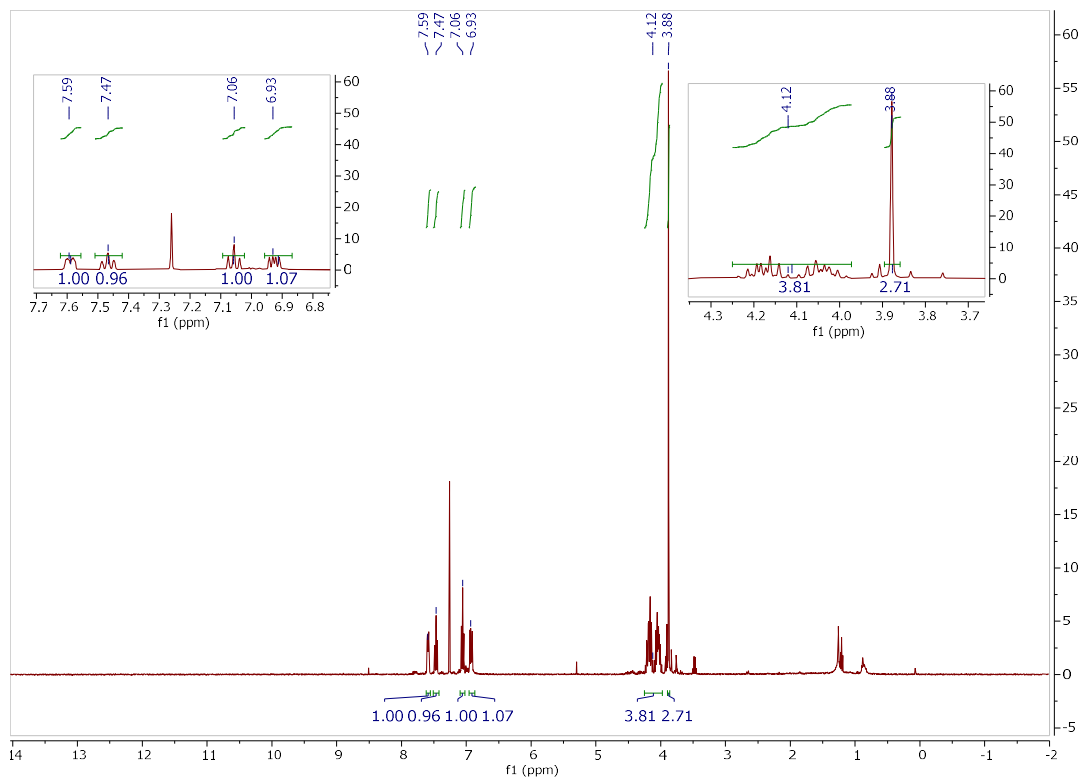




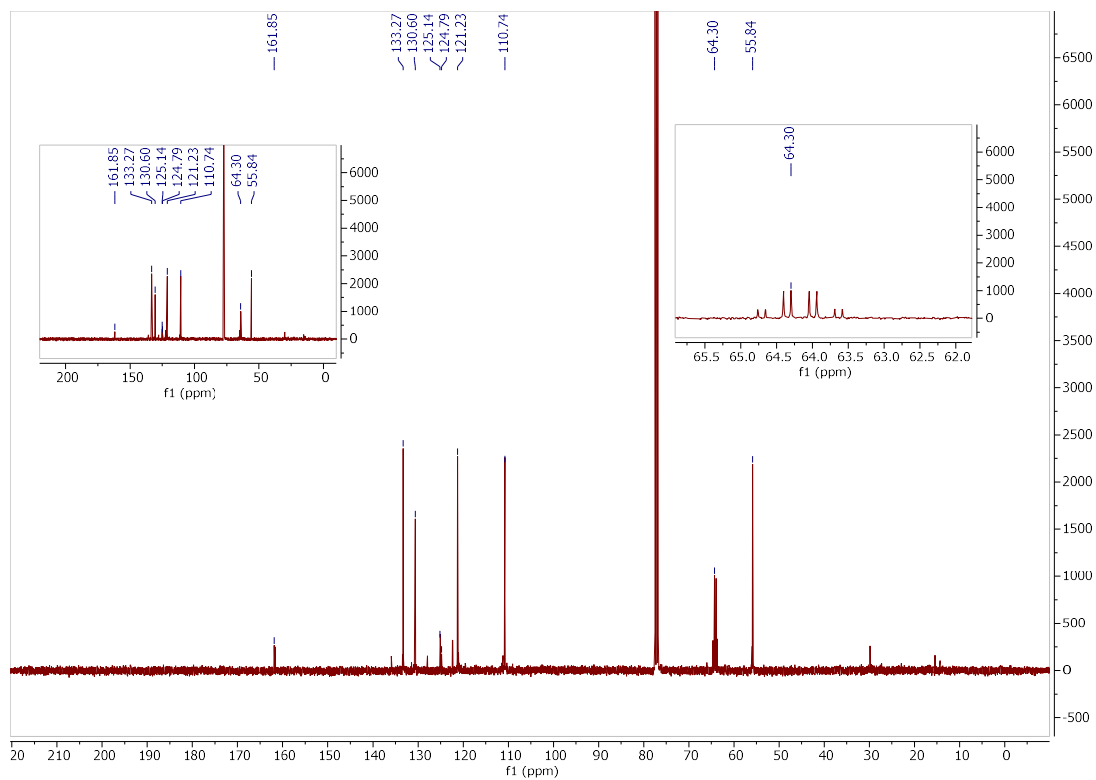
**$^{31}\text{P}(^1\text{H})$  NMR spectrum of compound 14**



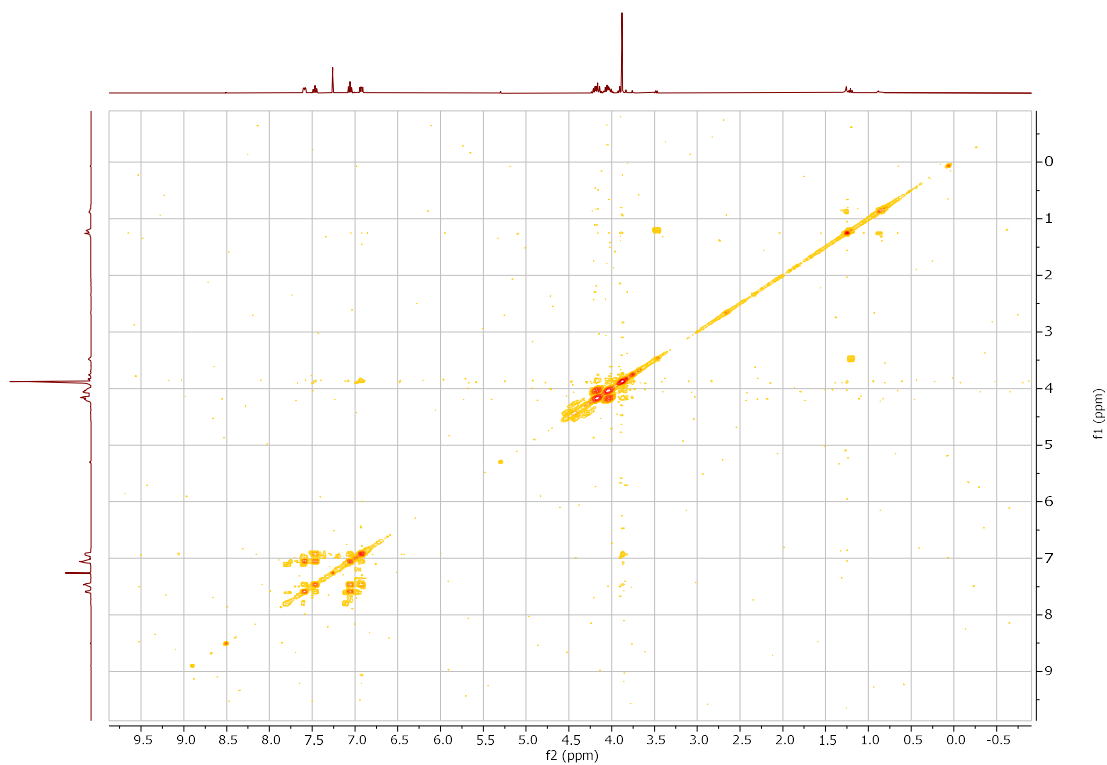
**<sup>19</sup>F NMR spectrum of compound 14**



**<sup>1</sup>H NMR spectrum of compound 14**

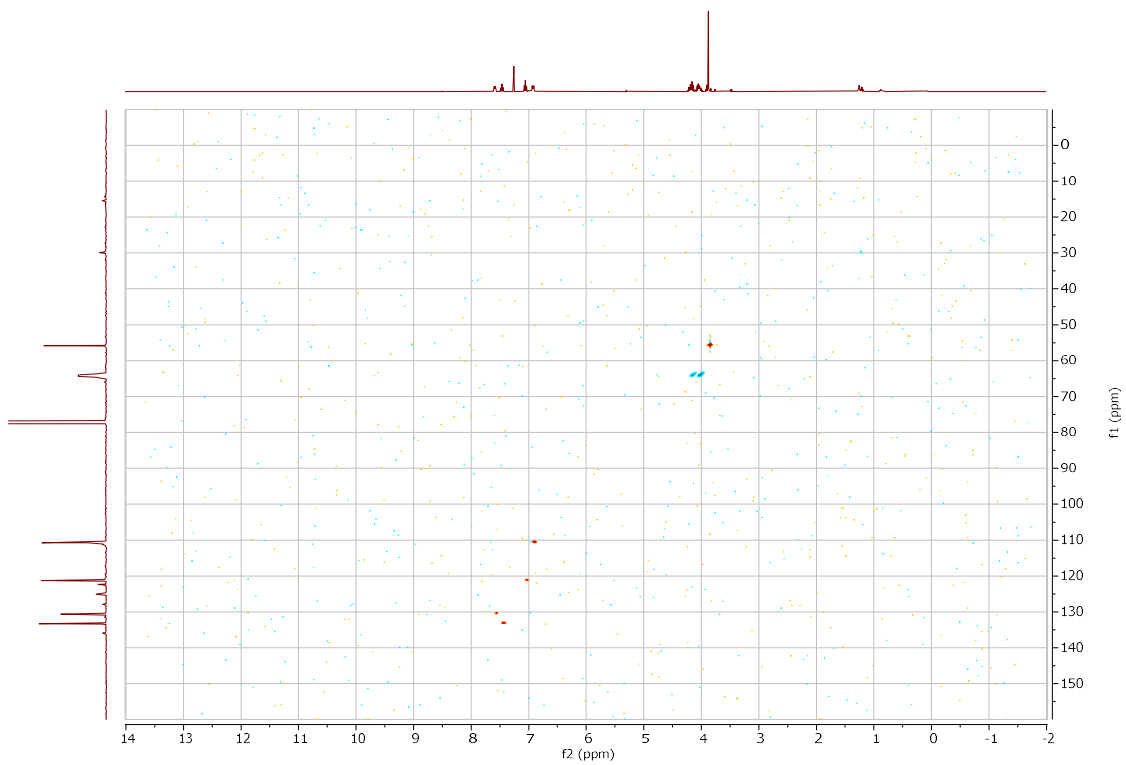


**$^{13}\text{C}(^1\text{H})$  NMR spectrum of compound 14**

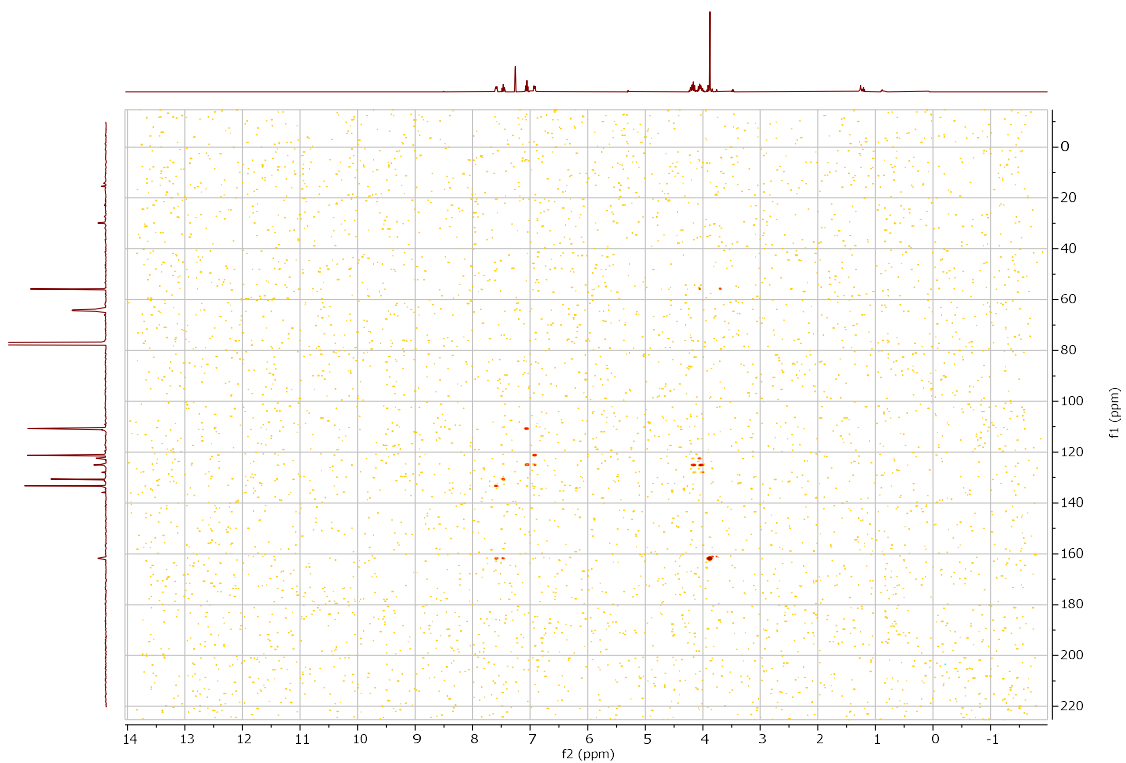


**$^1\text{H}$ - $^1\text{H}$  COSY NMR spectrum of compound 14**





**$^{13}\text{C}$ - $^1\text{H}$  HSQC NMR spectrum of compound 14**



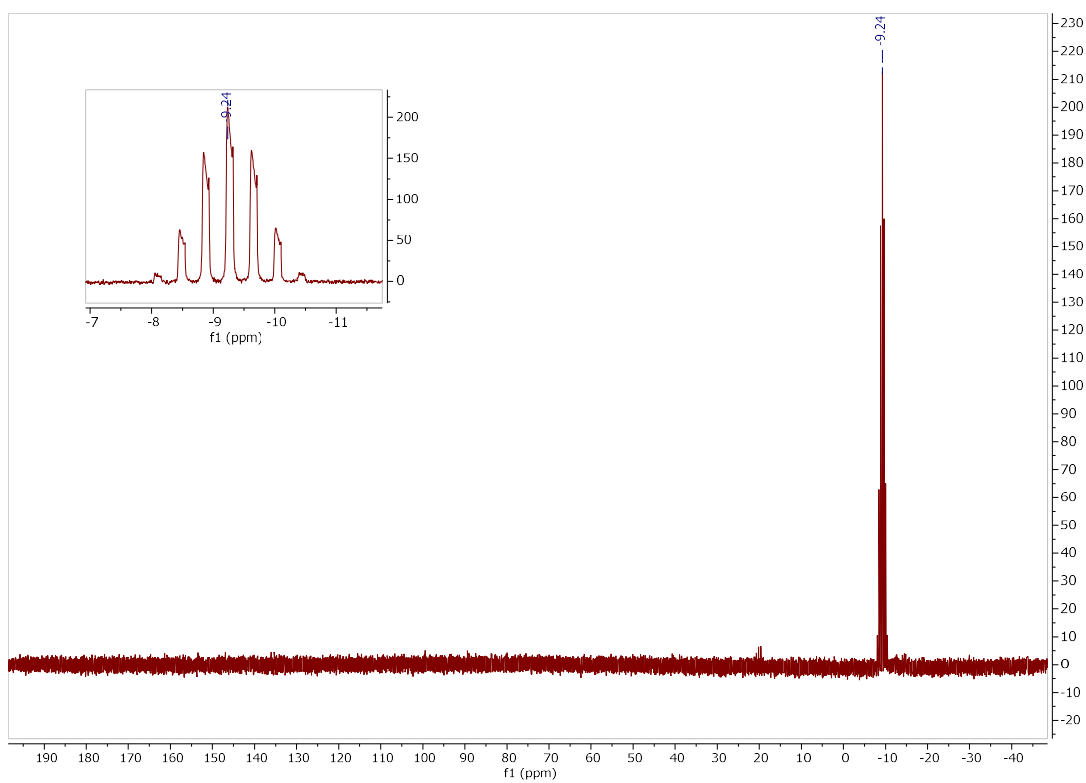
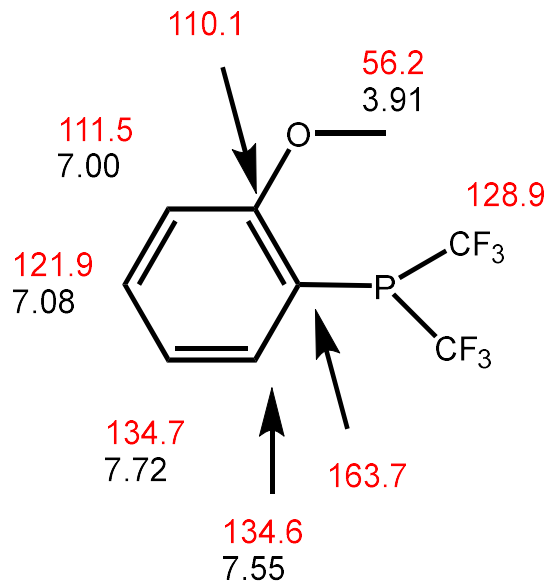
**$^{13}\text{C}$ - $^1\text{H}$  HMBC NMR spectrum of compound 14**

# Compound 15

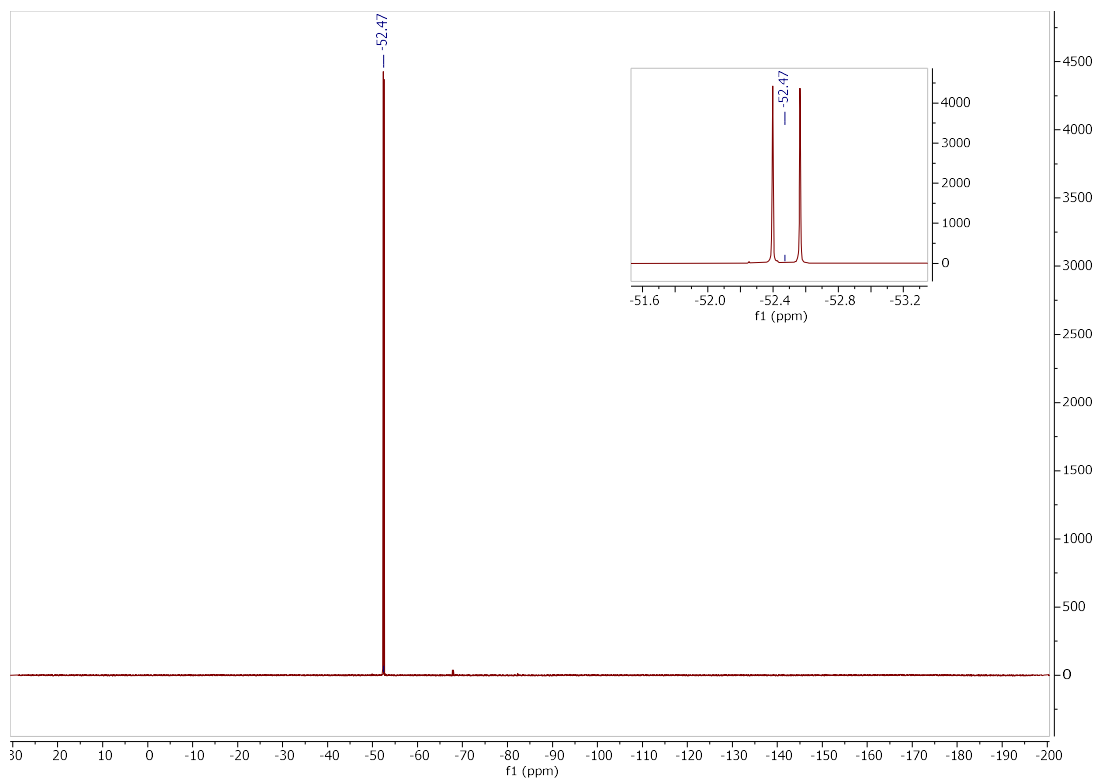
15

## Key HMBC Correlations

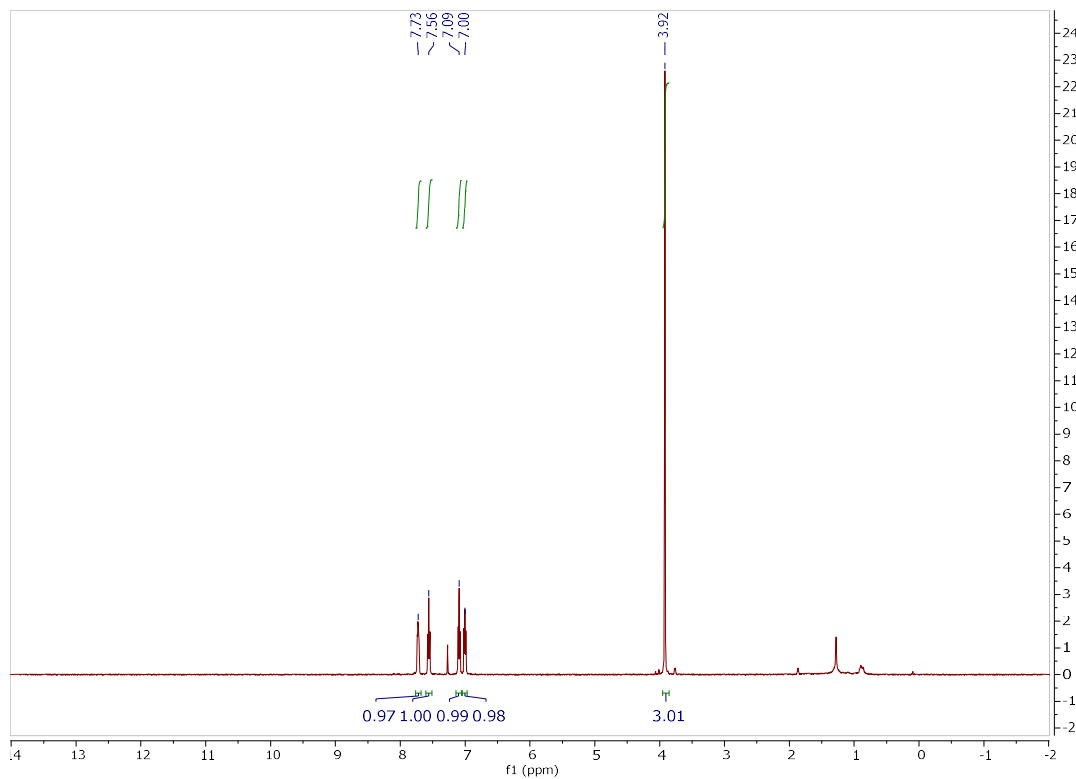
7.72: 163.7, 134.6, 111.5  
7.55: 163.7, 134.7  
7.08: 134.7, 111.5, 110.1  
7.00: 163.7, 121.9, 110.1  
3.91: 163.7, 111.5



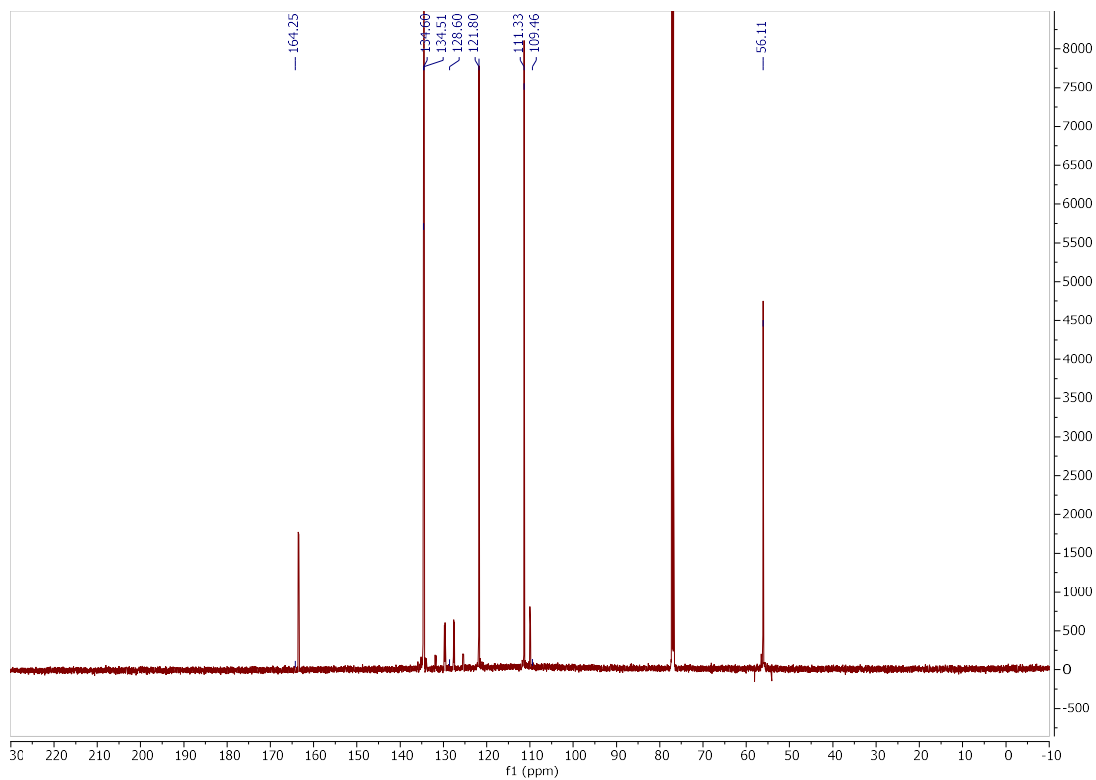
<sup>31</sup>P(<sup>1</sup>H) NMR spectrum of 15



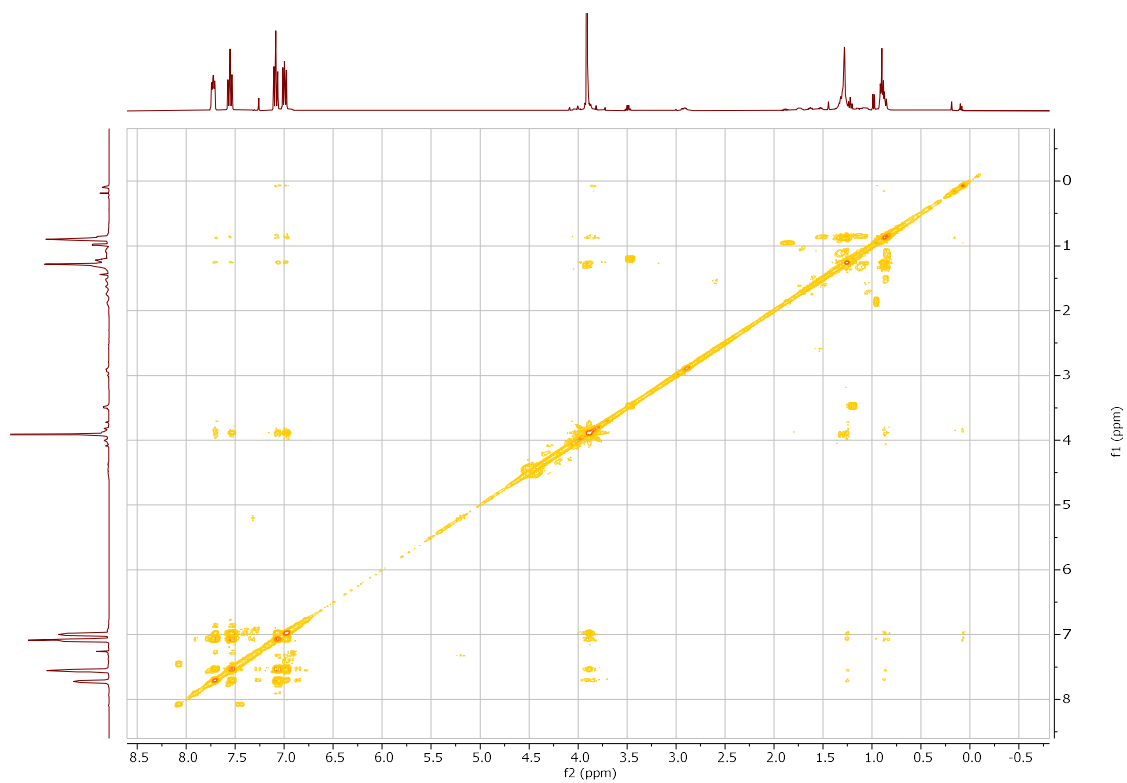
**$^{19}\text{F}$  NMR spectrum of compound 15**



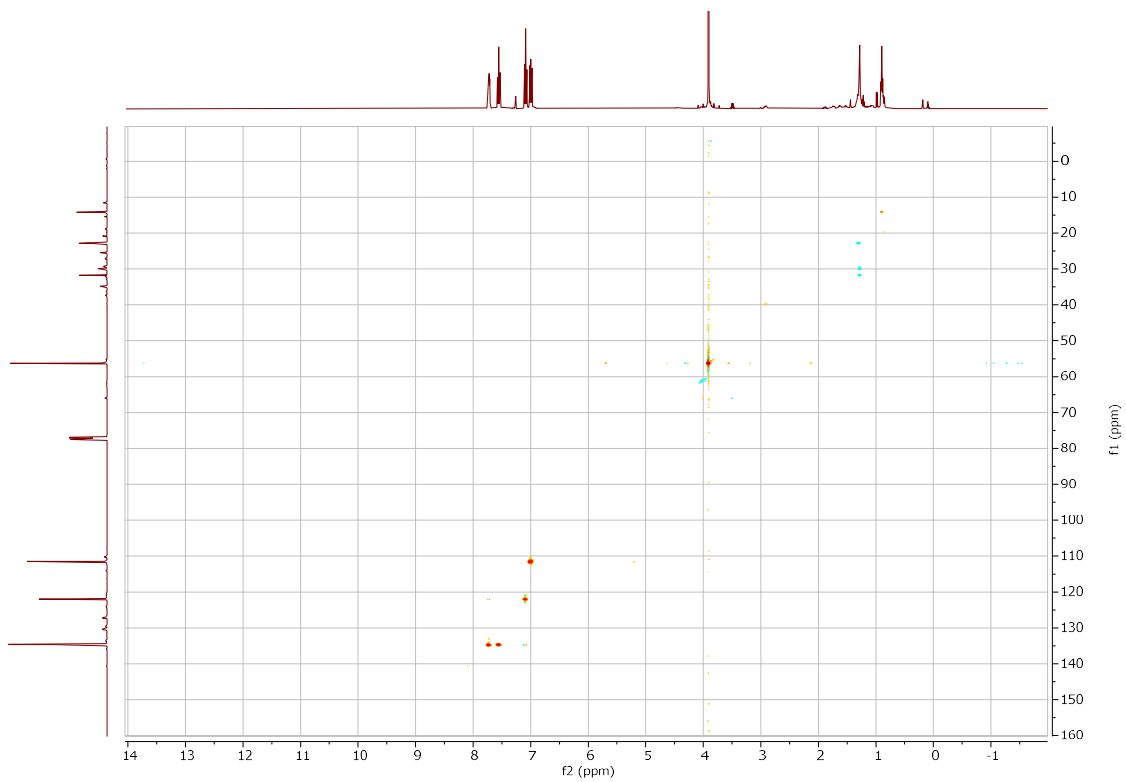
**$^1\text{H}$  NMR spectrum of compound 15**



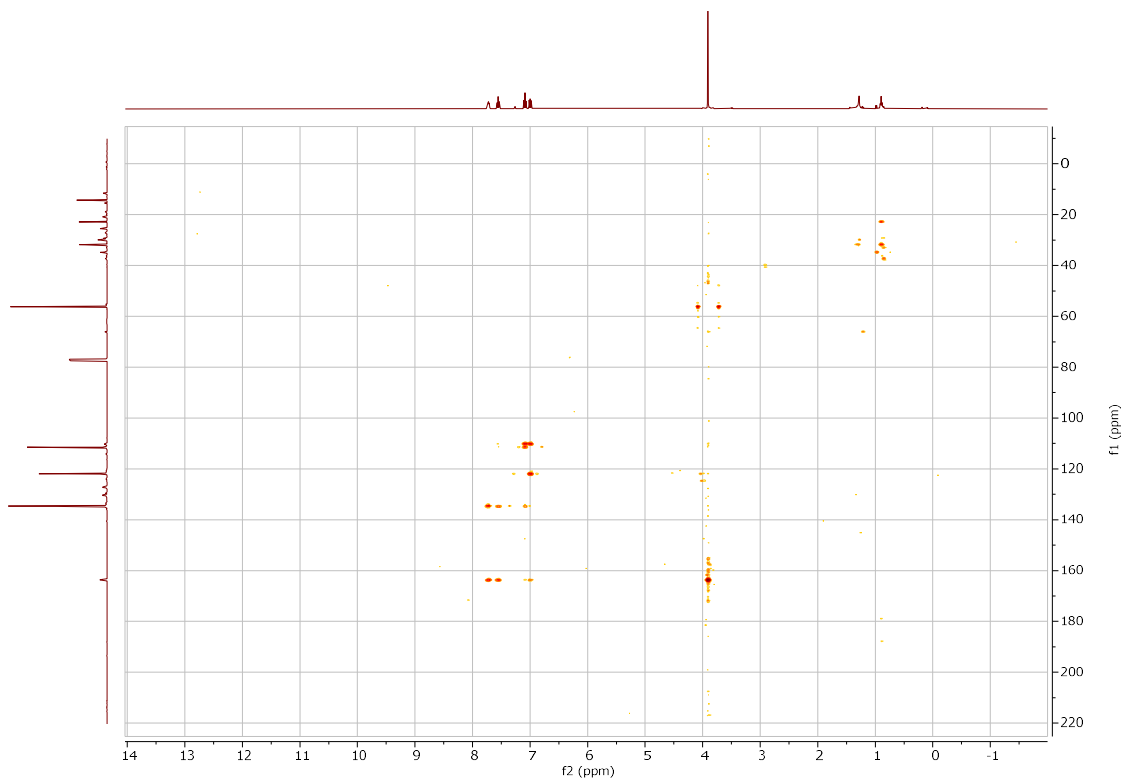
**<sup>13</sup>C(<sup>1</sup>H) NMR spectrum of compound 15**



**<sup>1</sup>H-<sup>1</sup>H COSY NMR spectrum of compound 15**

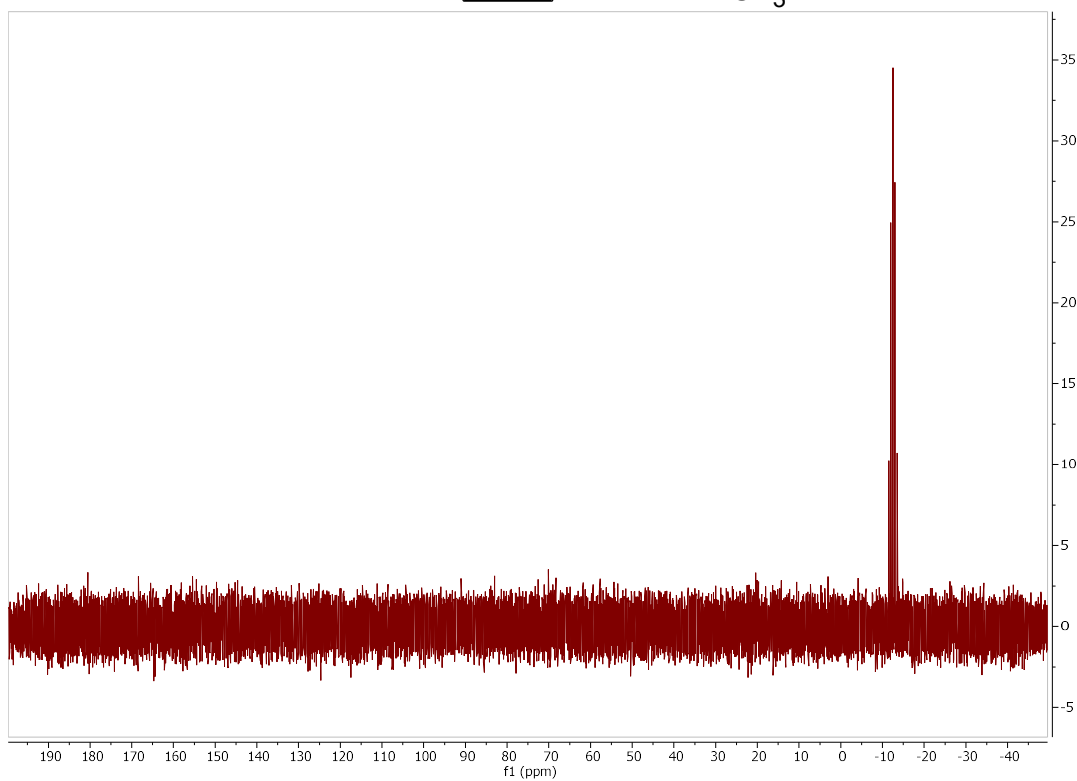
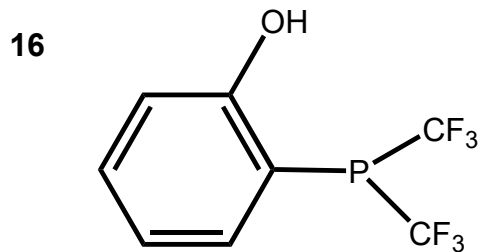


**$^{13}\text{C}$ - $^1\text{H}$  HSQC NMR spectrum of compound 15**

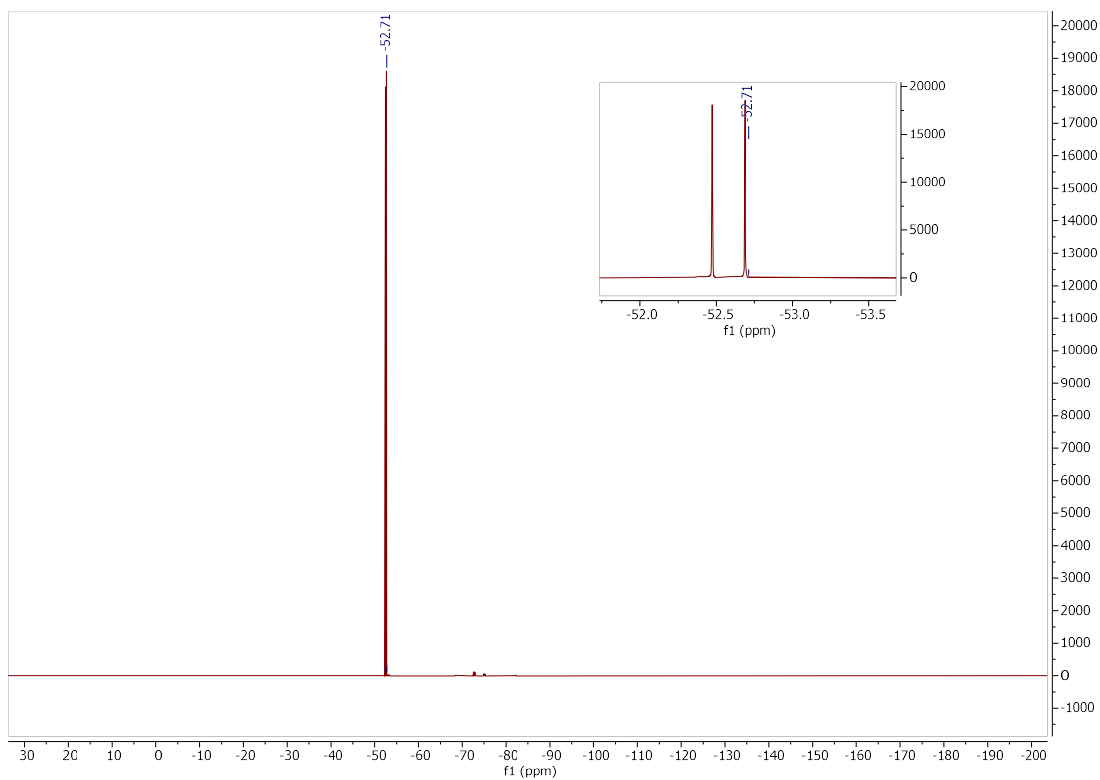


**$^{13}\text{C}$ - $^1\text{H}$  HMBC NMR spectrum of compound 15**

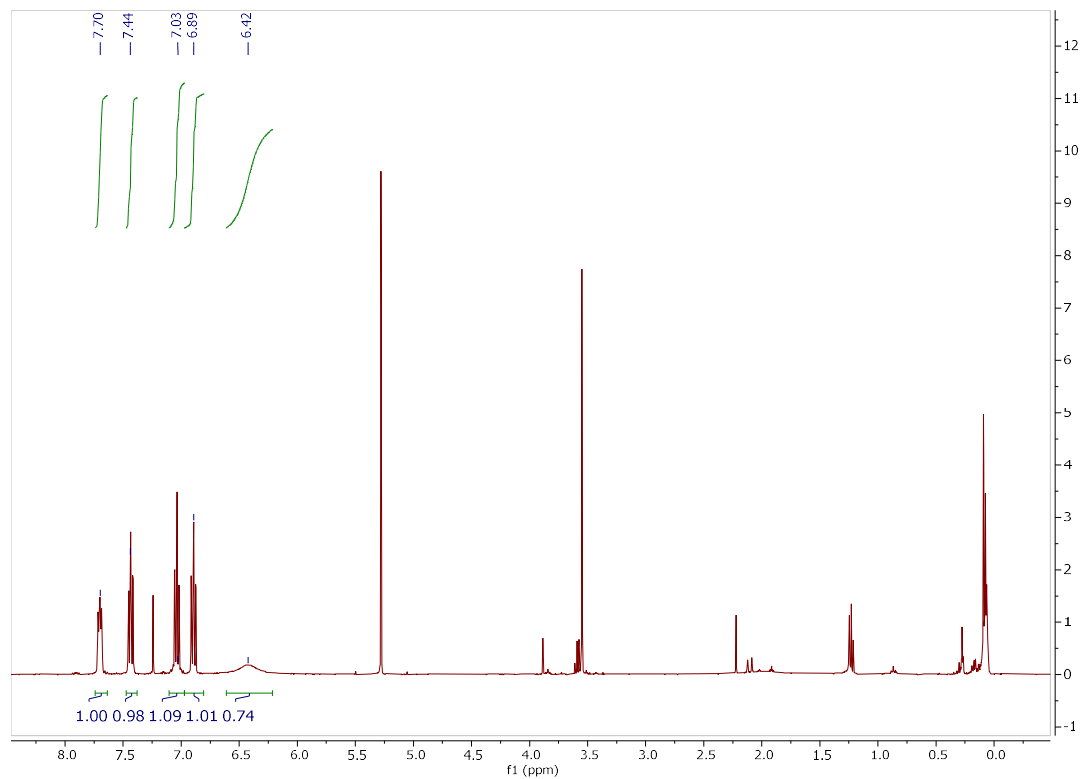
**Compound 16**



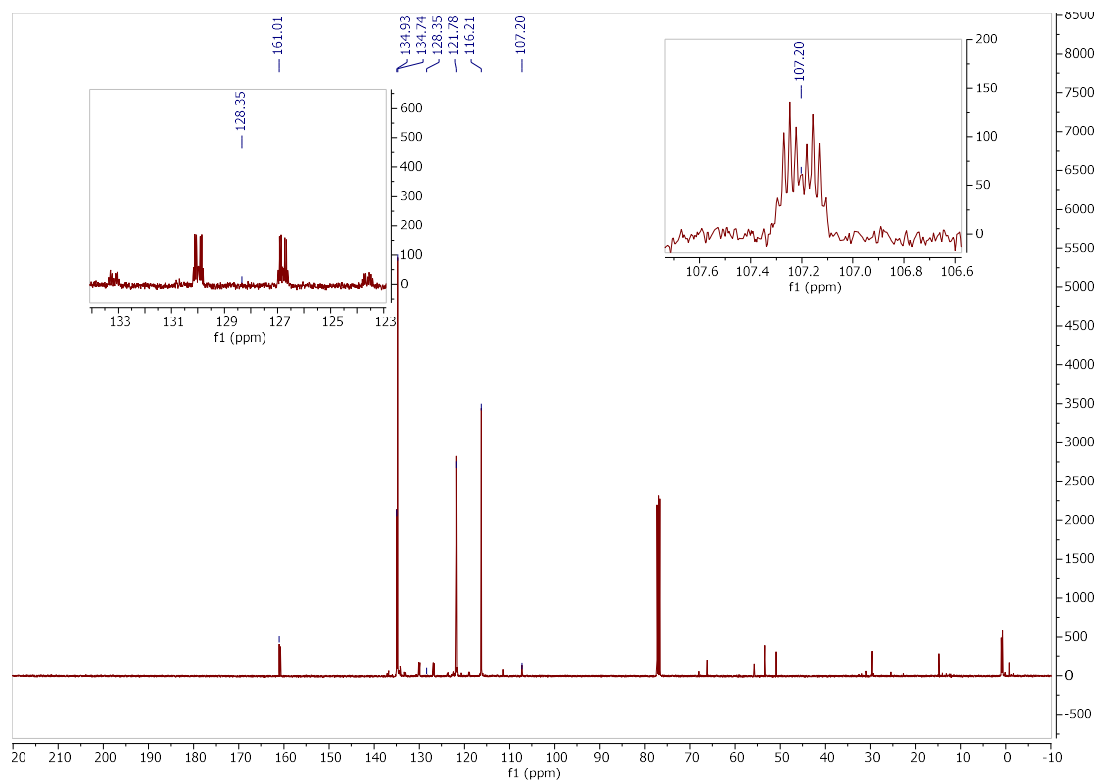
**$^{31}\text{P}(^1\text{H})$  NMR spectrum of compound 16**



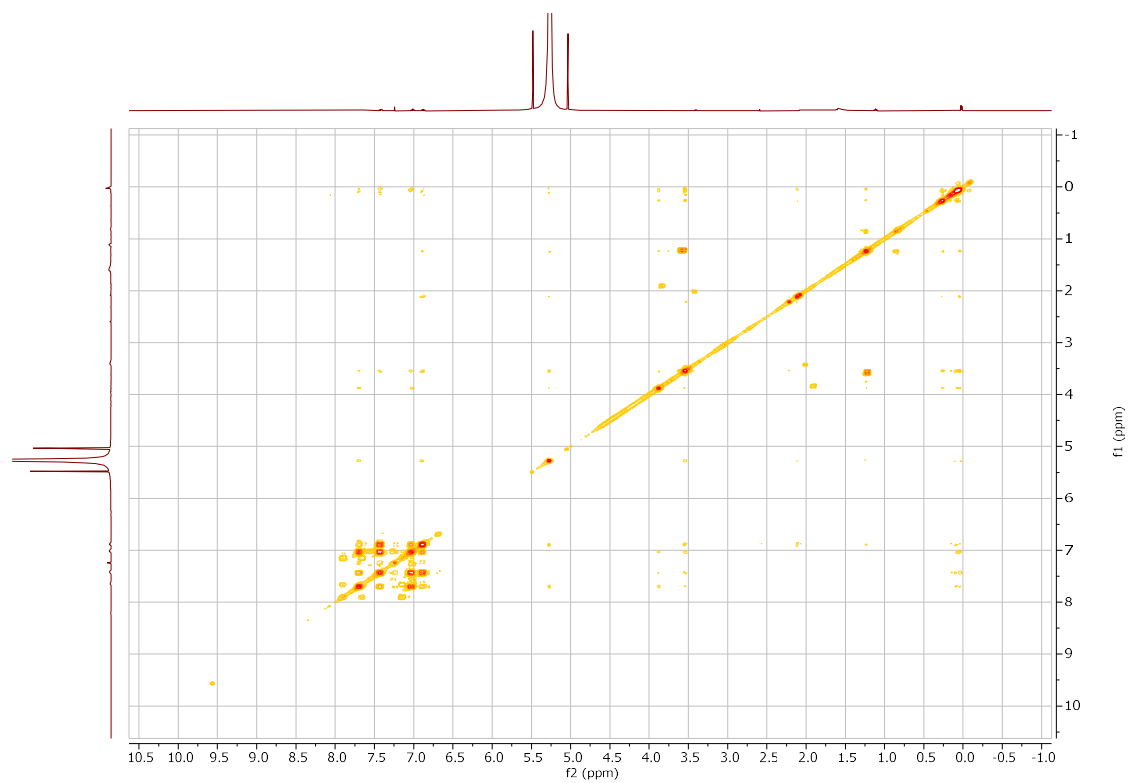
**$^{19}\text{F}$  NMR spectrum of compound 16**



**$^1\text{H}$  NMR spectrum of compound 16**

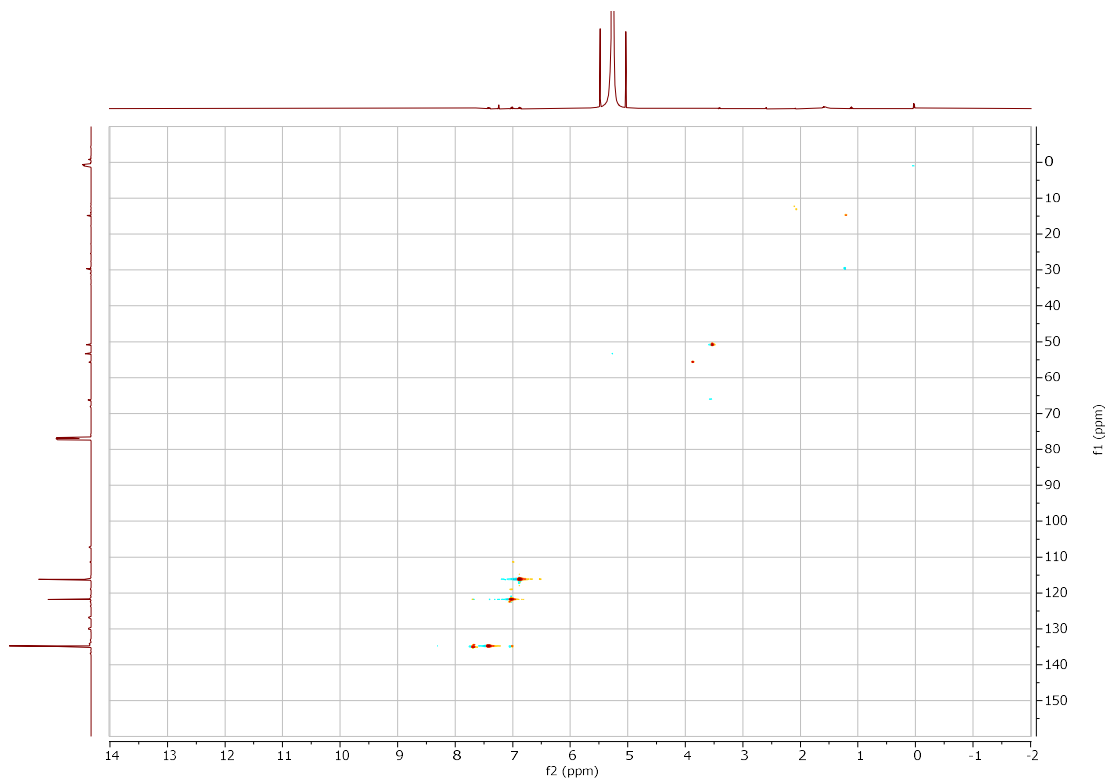


**$^{13}\text{C}(^1\text{H})$  NMR spectrum of compound 16**

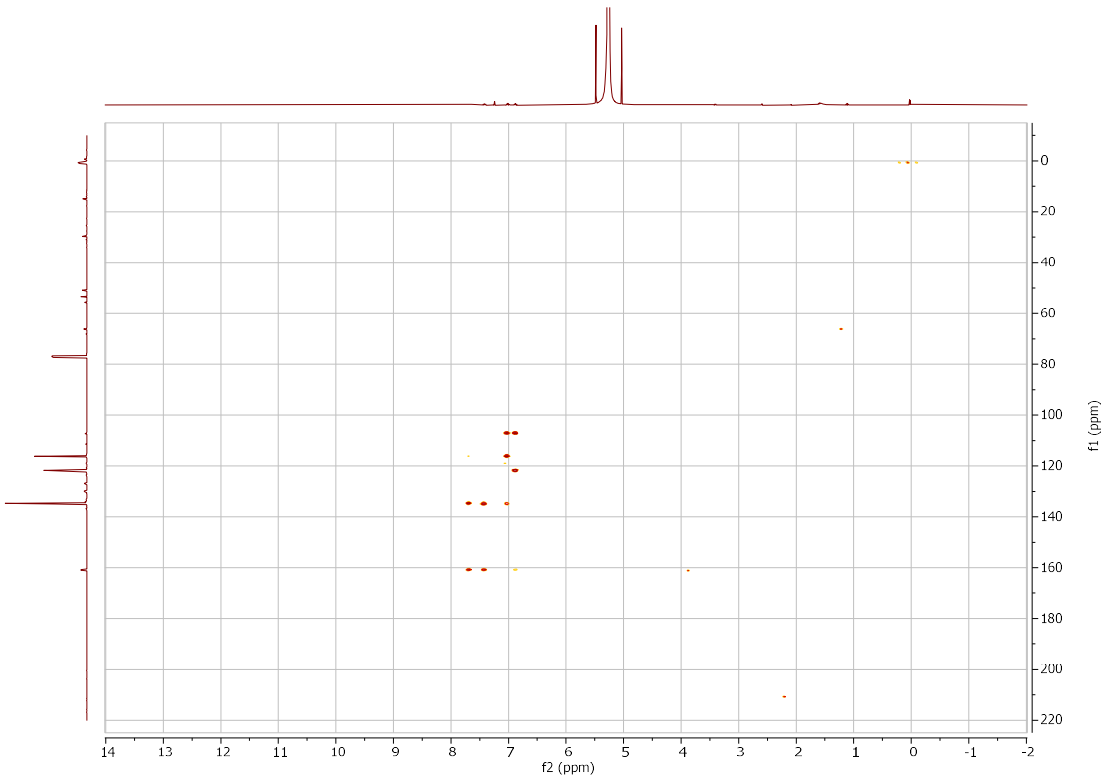


**$^1\text{H}-^1\text{H}$  COSY NMR spectrum of compound 16**



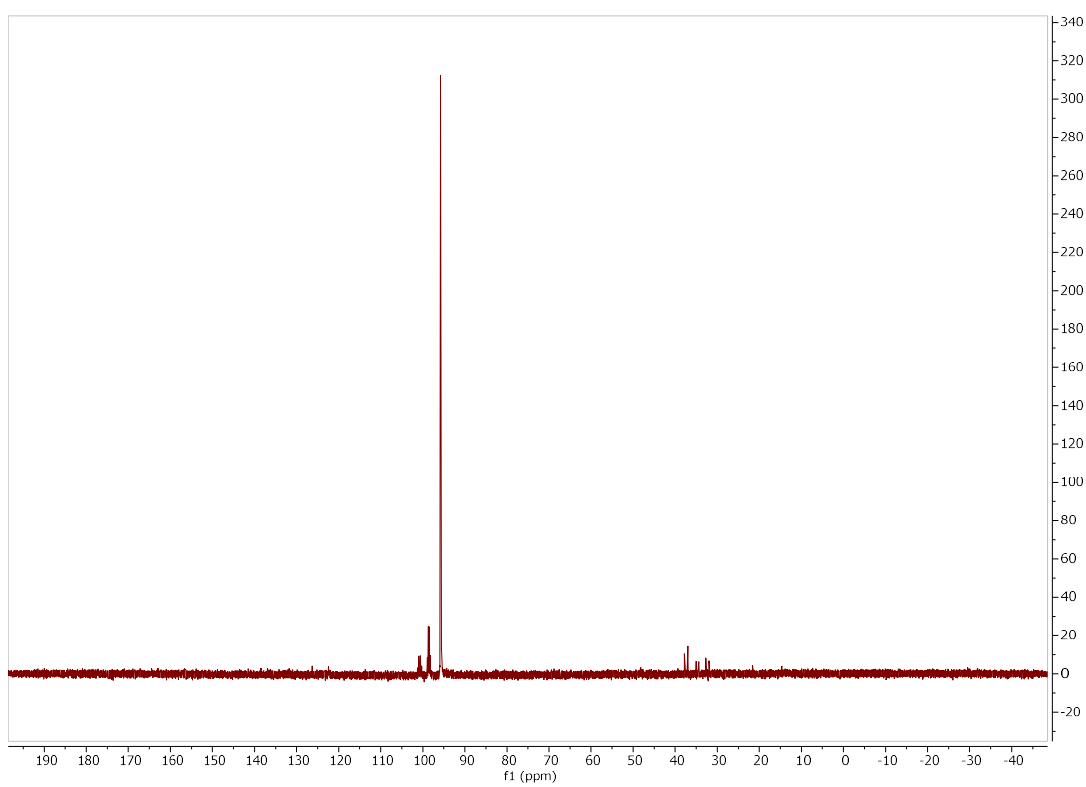
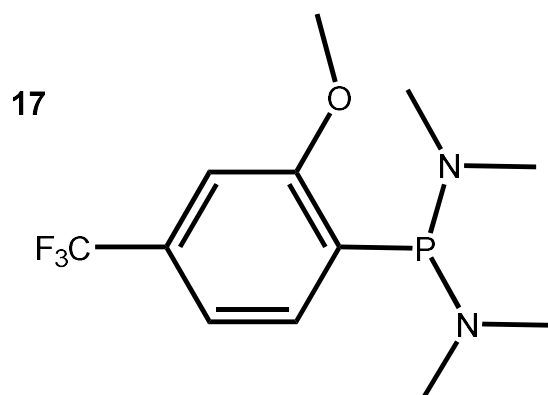


**$^{13}\text{C}$ - $^1\text{H}$  HSQC NMR spectrum of compound 16**

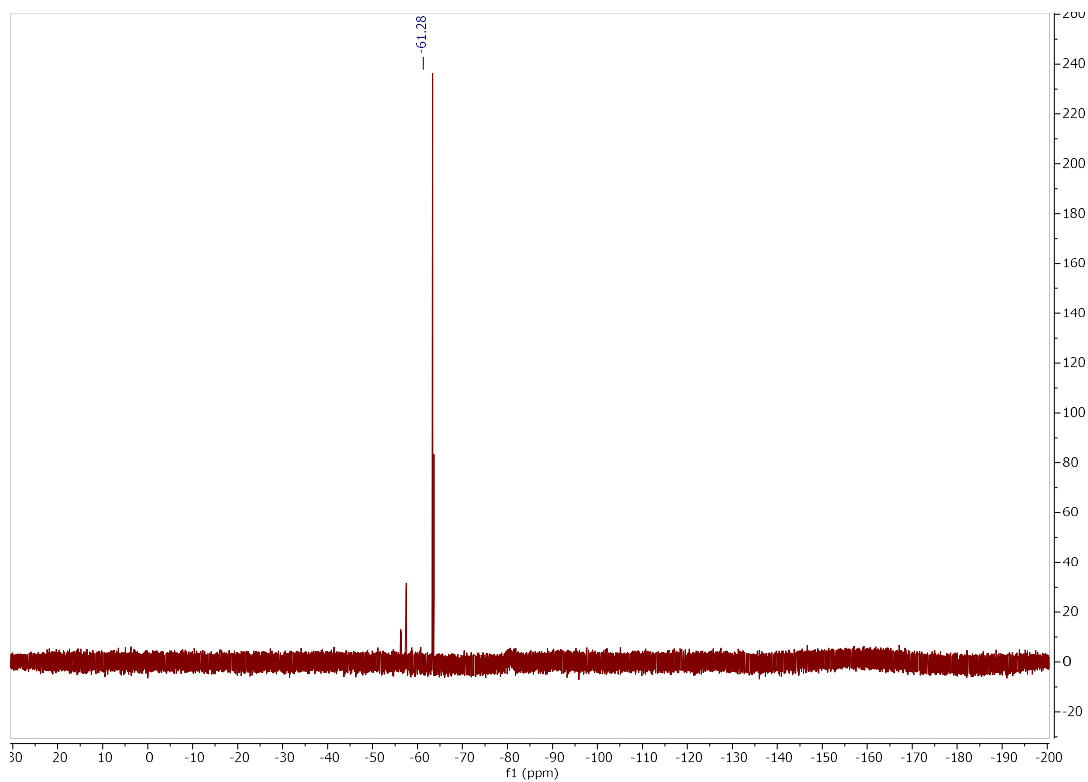


**$^{13}\text{C}$ - $^1\text{H}$  HMBC NMR spectrum of compound 16**

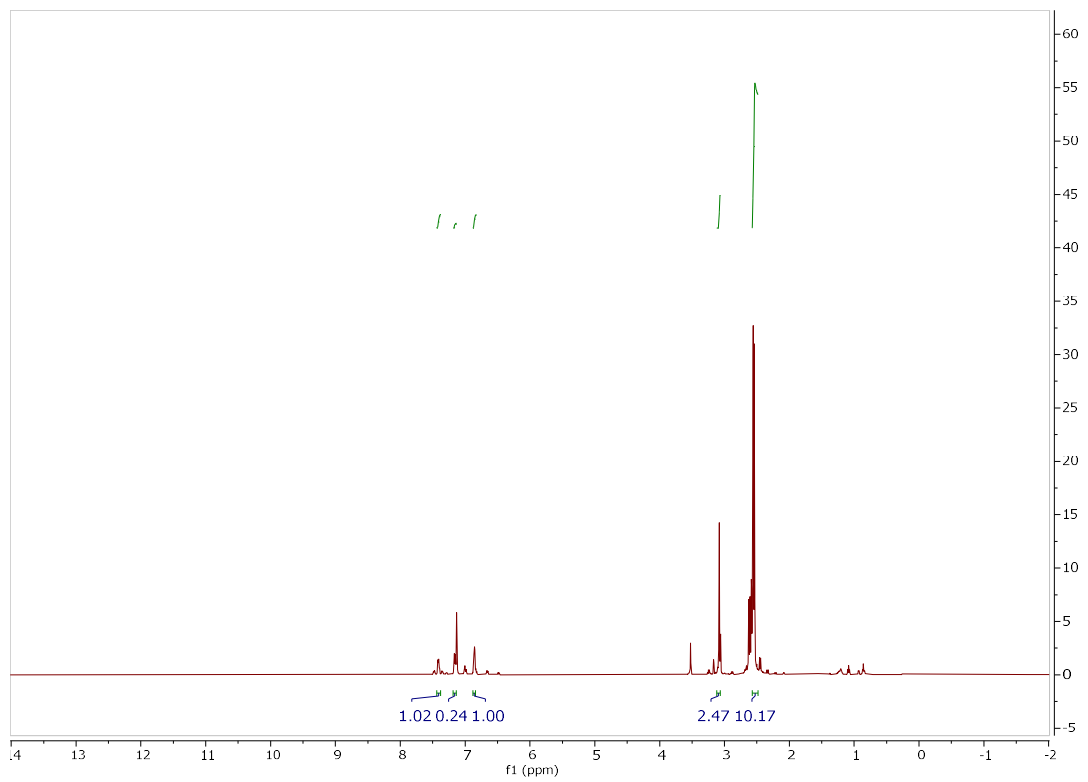
### Compound 17



$^{31}\text{P}(^1\text{H})$  NMR spectrum of compound 17



**$^{19}\text{F}$  NMR spectrum of compound 17**



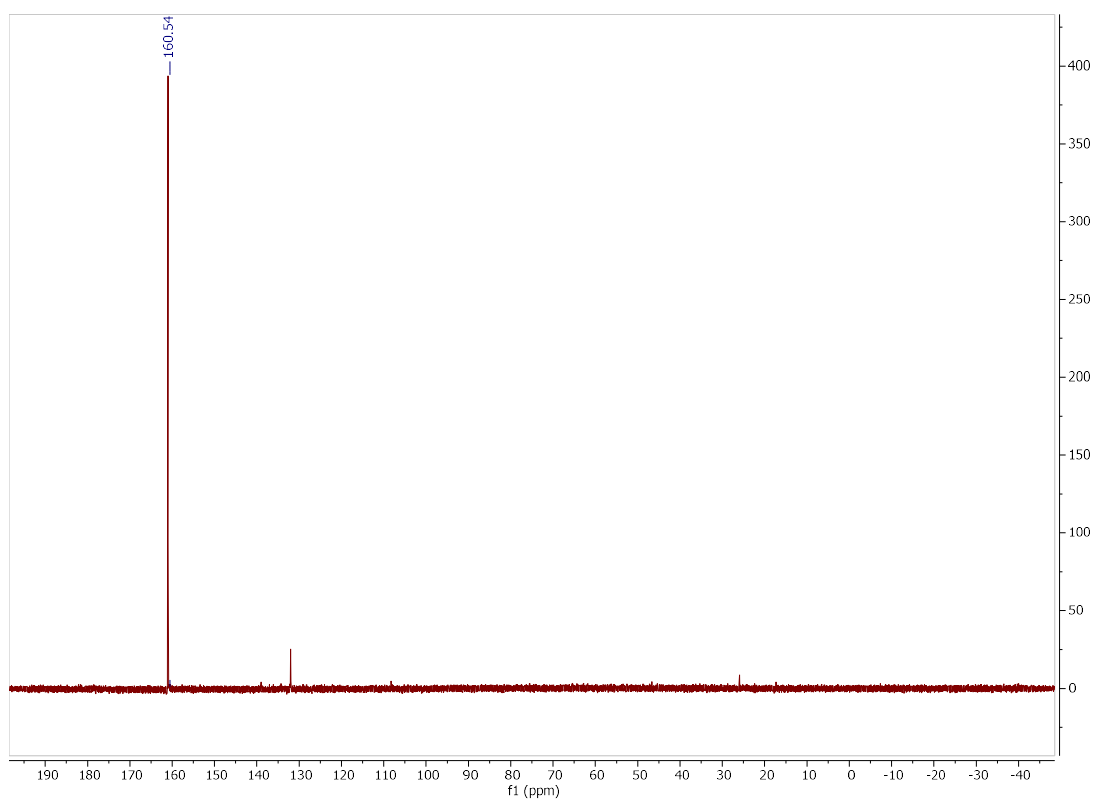
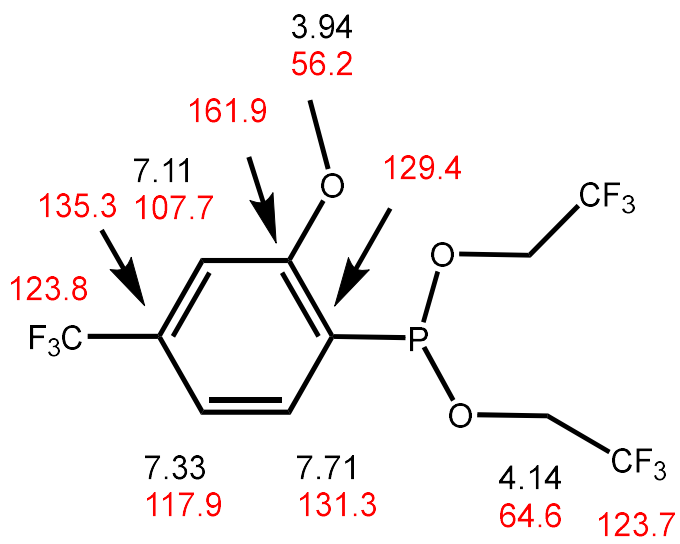
**$^1\text{H}$  NMR spectrum of compound 17**

# Compound 18

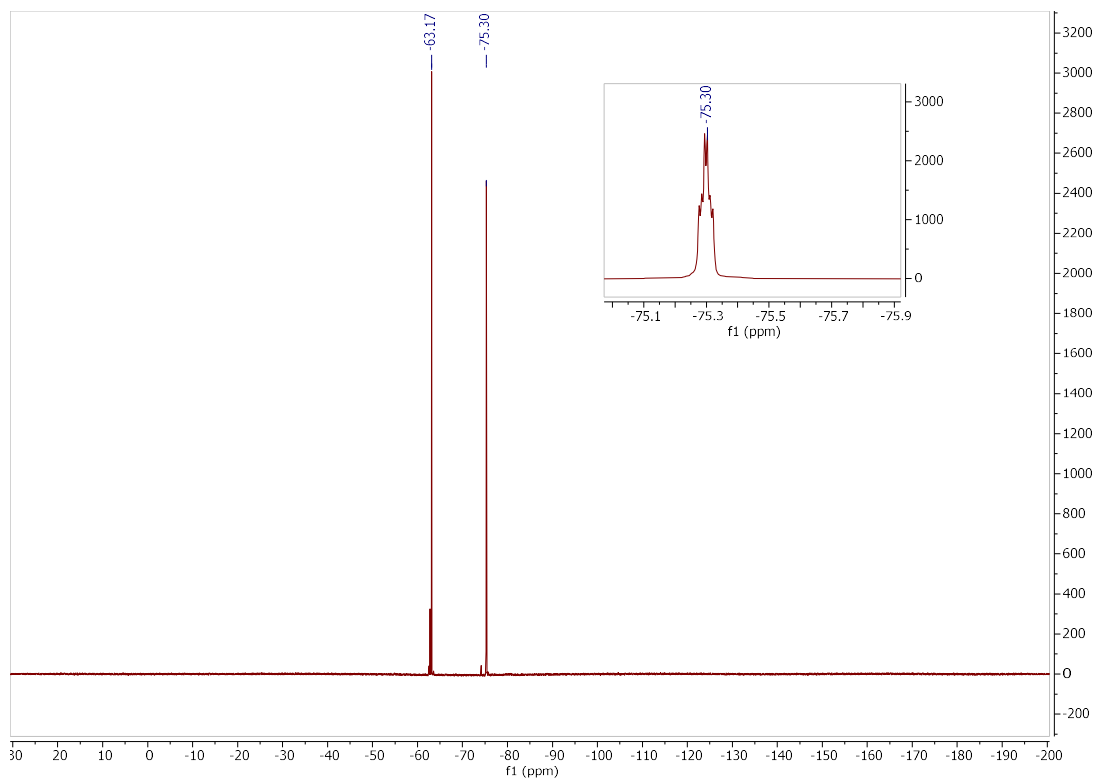
18

## Key HMBC Correlations

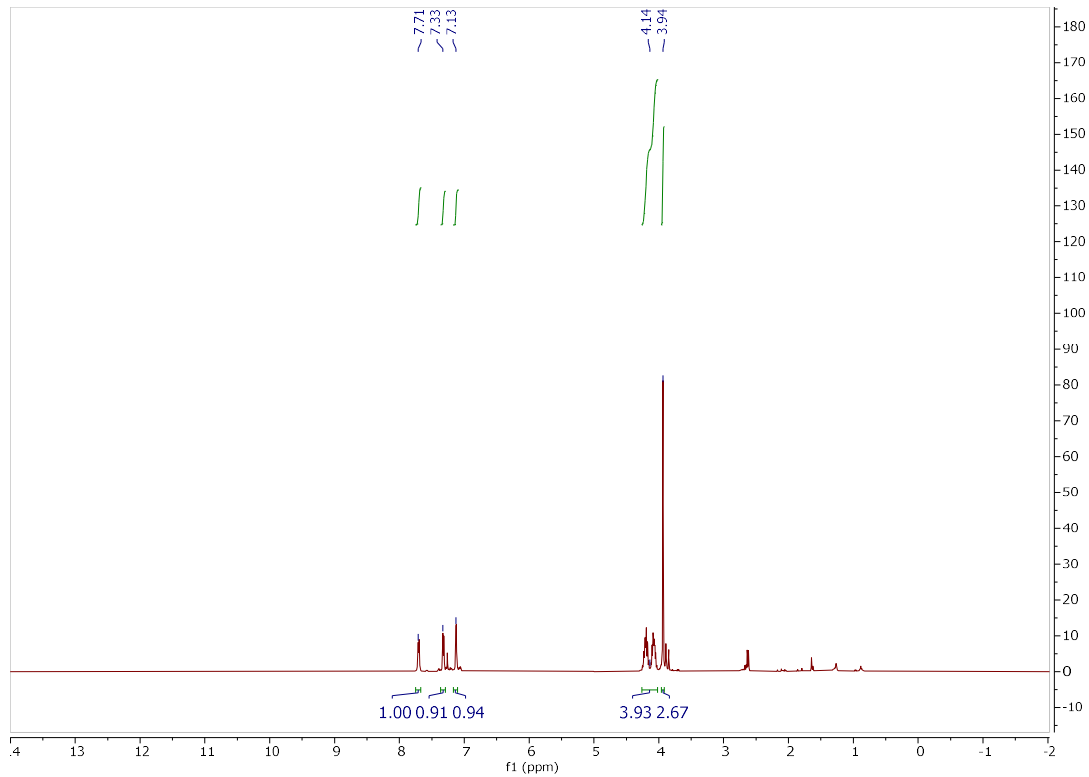
- 7.71: 161.9, 135.3, 117.9
- 7.33: 129.4, 107.7
- 7.11: 161.9, 129.4, 123.8, 117.9,
- 4.14: 123.7
- 3.94: 161.9



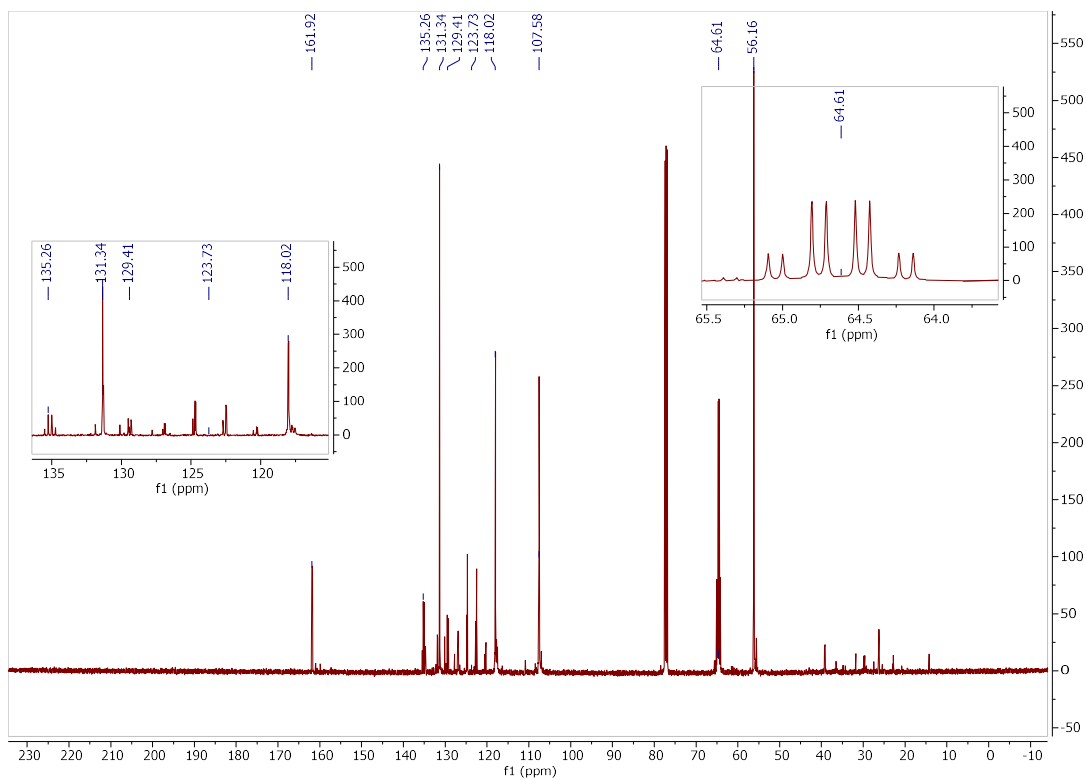
<sup>31</sup>P(<sup>1</sup>H) NMR spectrum of compound 18



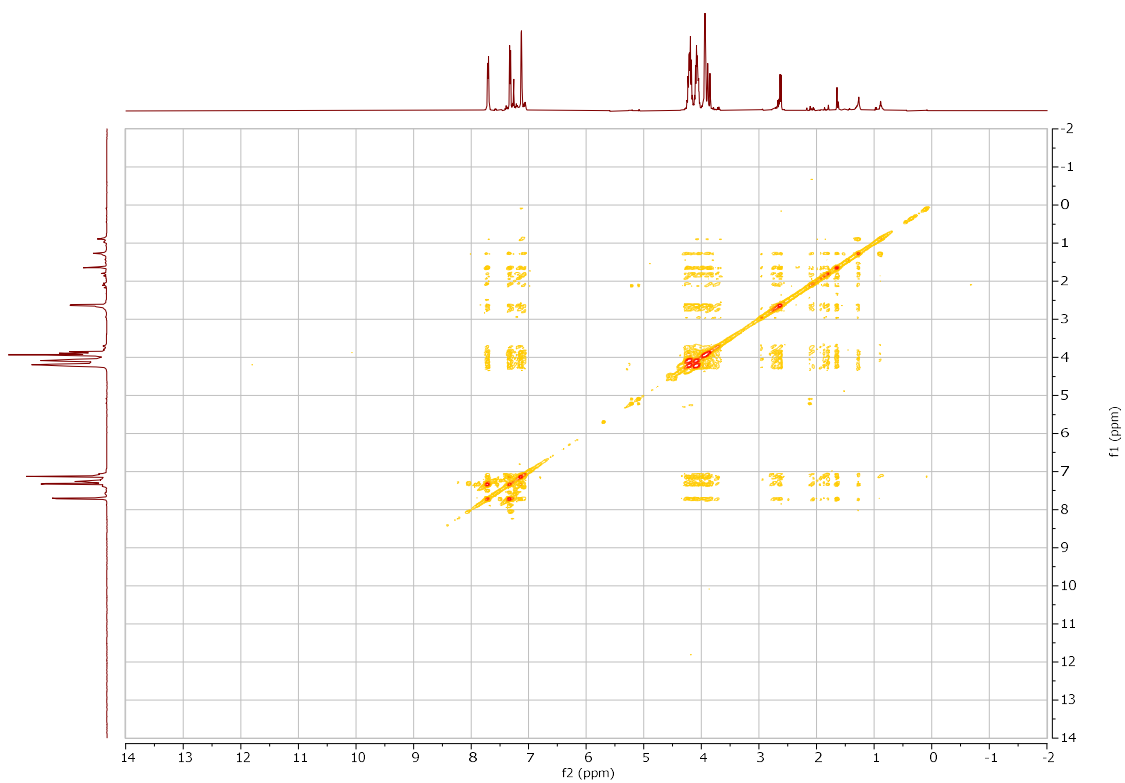
**$^{19}\text{F}$  NMR spectrum of compound 18**



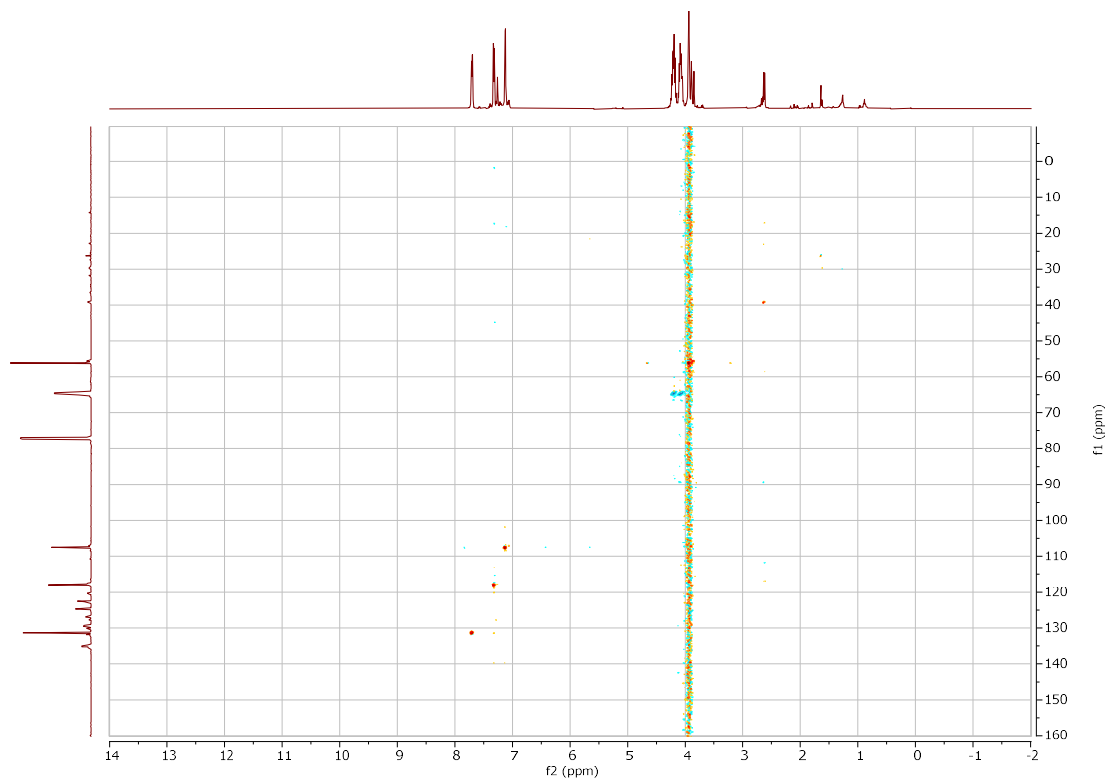
**$^1\text{H}$  NMR spectrum of compound 18**



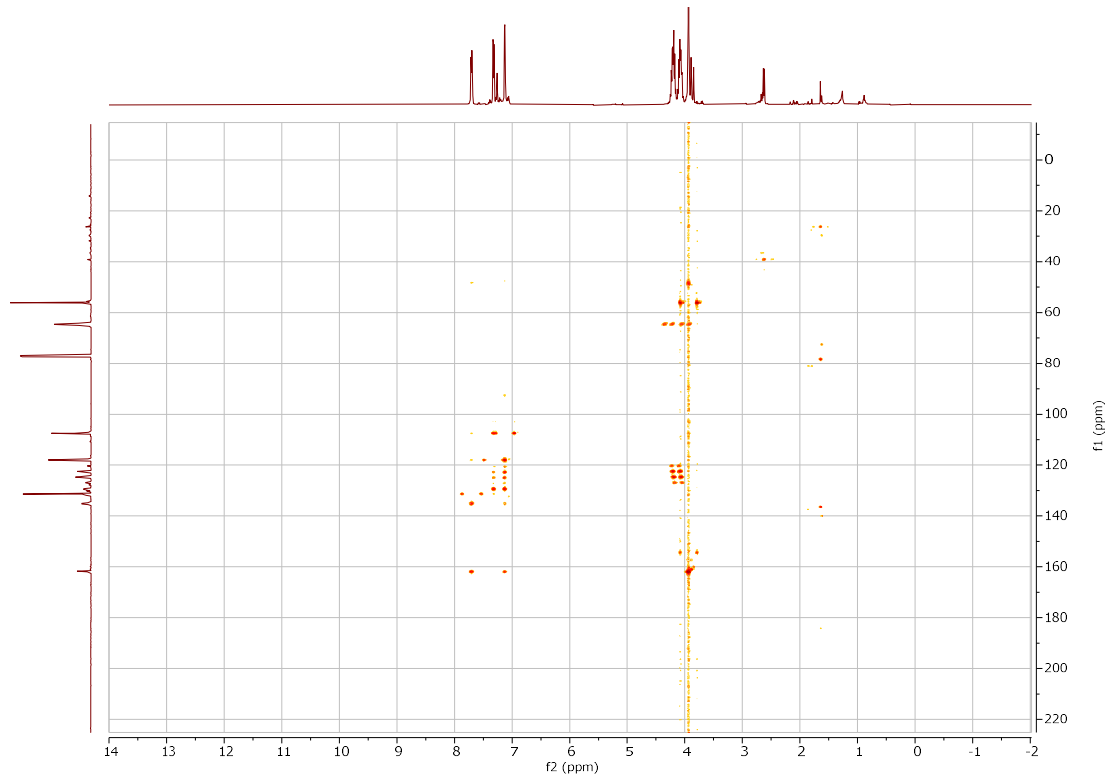
$^{13}\text{C}(^1\text{H})$  NMR spectrum of compound 18



$^1\text{H}-^1\text{H}$  COSY NMR spectrum of compound 18



**$^{13}\text{C}$ - $^1\text{H}$  HSQC NMR spectrum of compound 18**



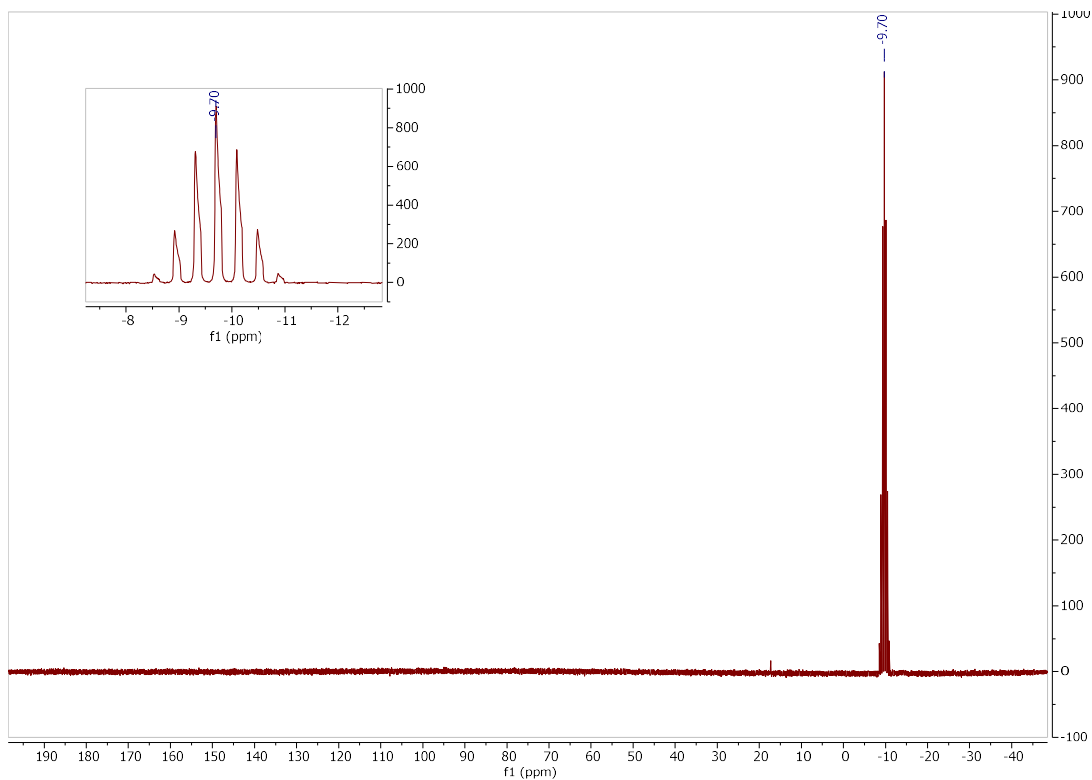
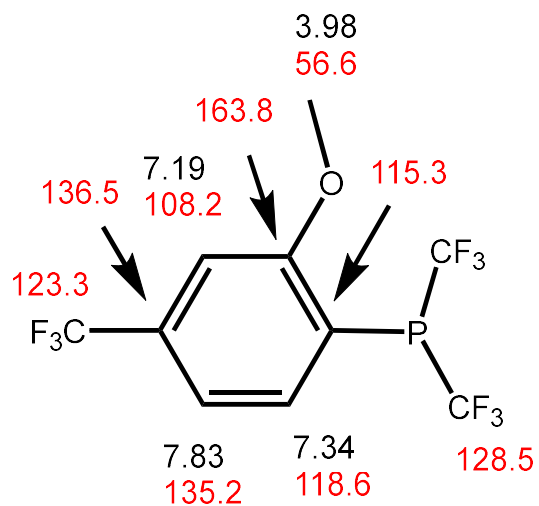
**$^{13}\text{C}$ - $^1\text{H}$  HMBC NMR spectrum of compound 18**

# Compound 19

19

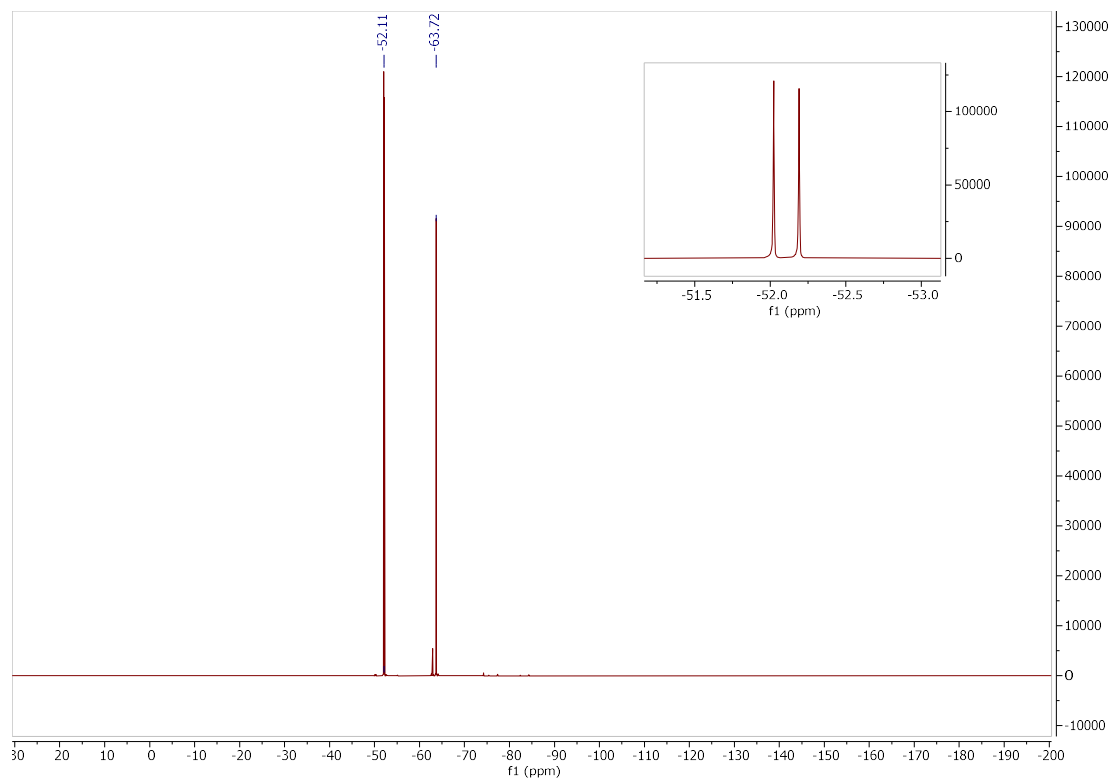
## Key HMBC Correlations

7.83: 163.8, 136.5, 123.3, 115.3, 108.2  
7.34: 135.2, 128.5, 123.3, 115.3,  
7.19: 163.8, 136.5, 128.5, 123.3, 118.6, 115.3  
3.94: 163.8

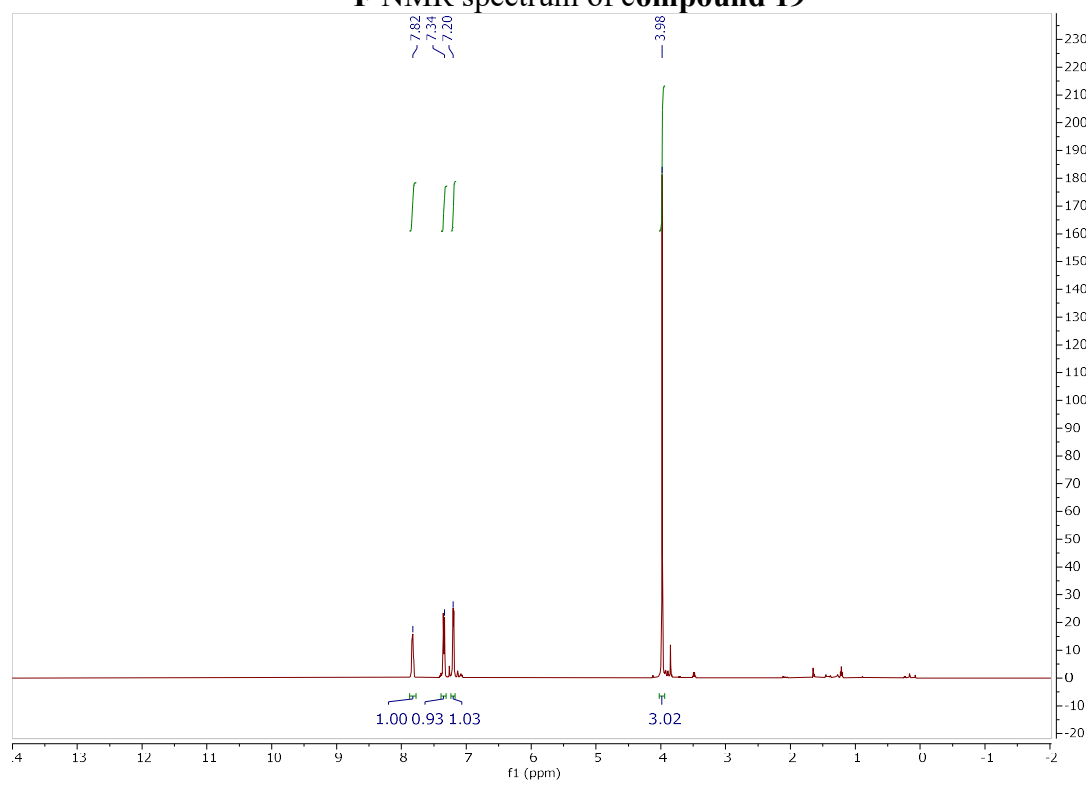


$^{31}\text{P}(^1\text{H})$  NMR spectrum of compound 19

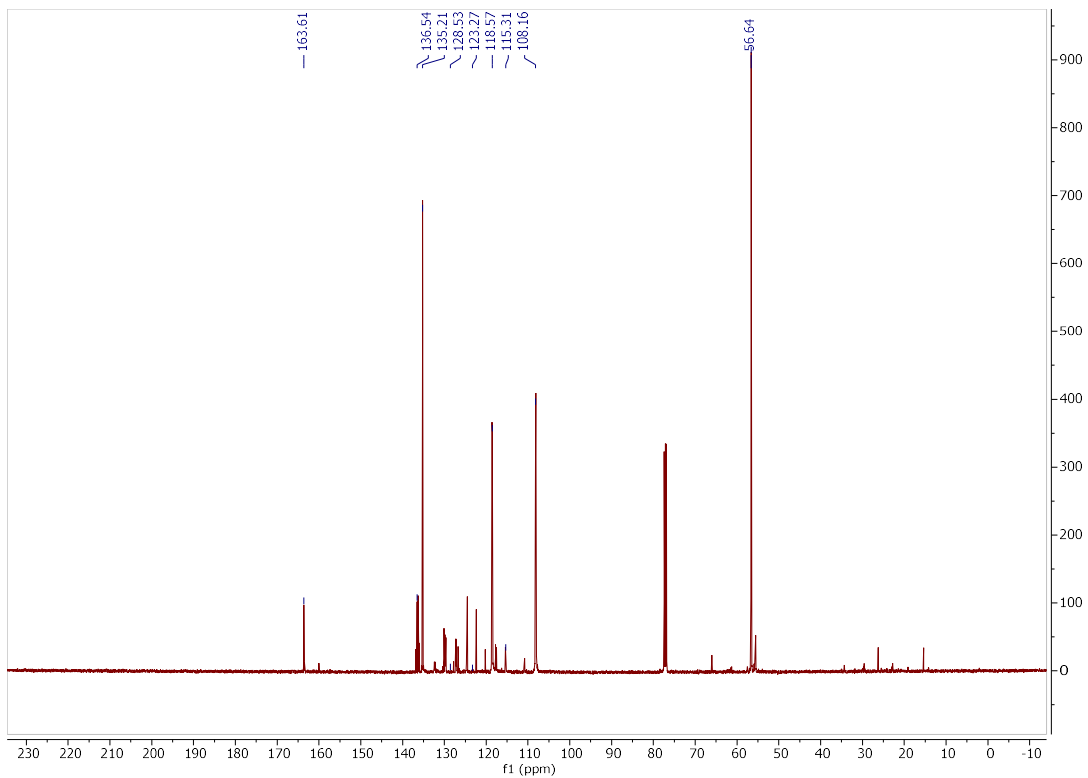




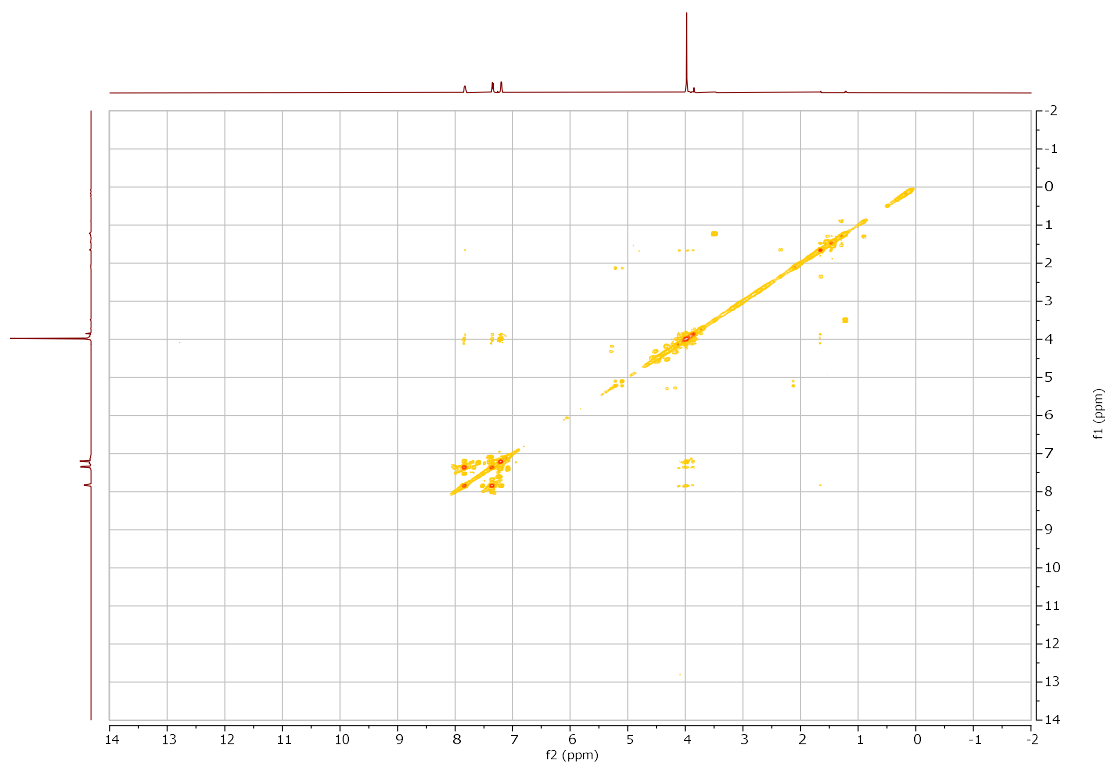
$^{19}\text{F}$  NMR spectrum of compound 19



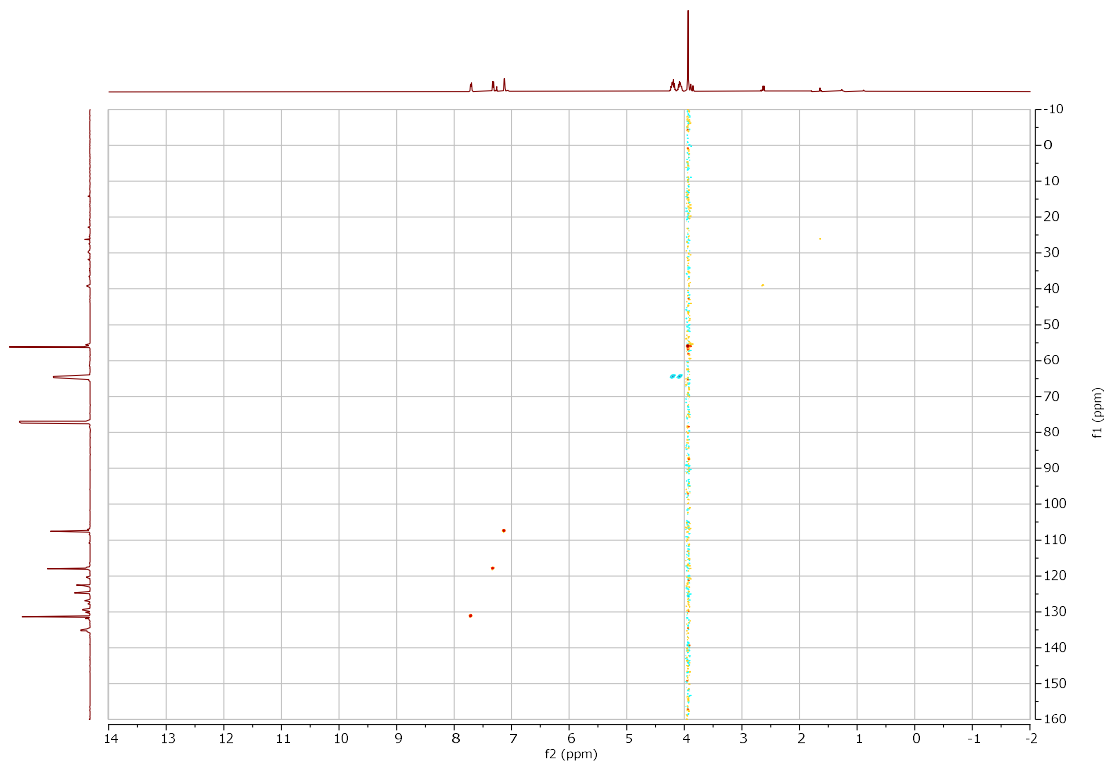
$^1\text{H}$  NMR spectrum of compound 19



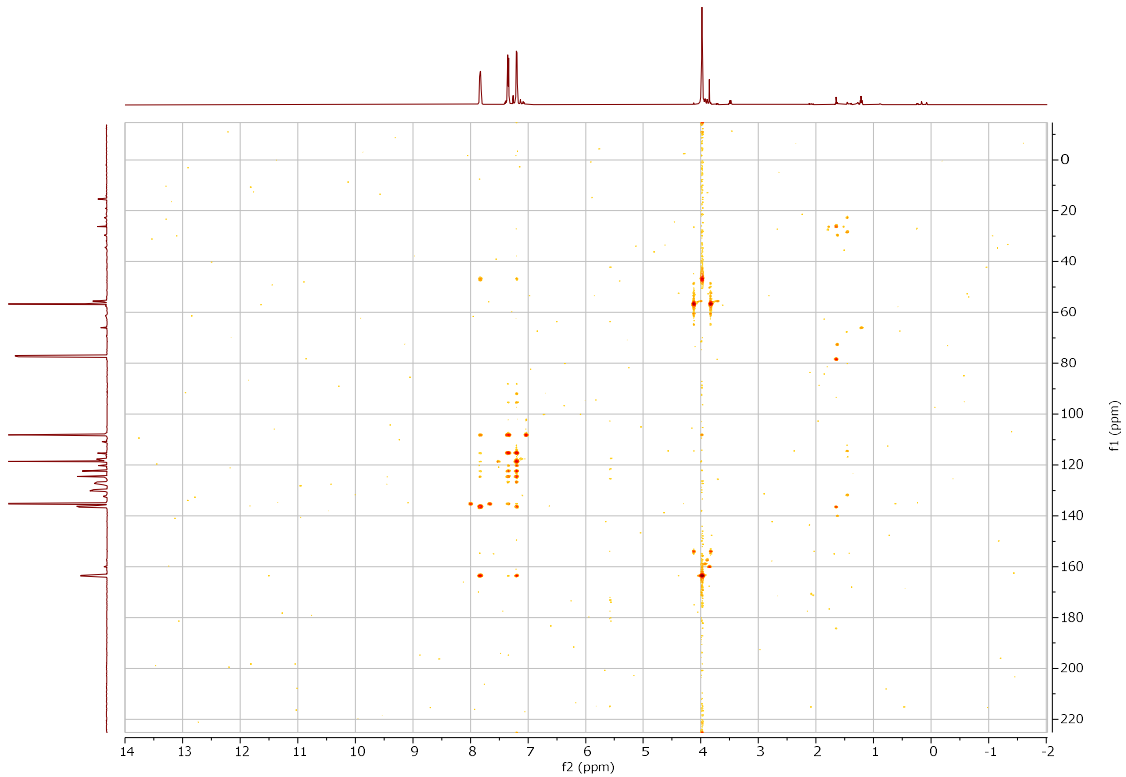
**$^{13}\text{C}(^1\text{H})$  NMR spectrum of compound 19**



**$^1\text{H}-^1\text{H}$  COSY NMR spectrum of compound 19**

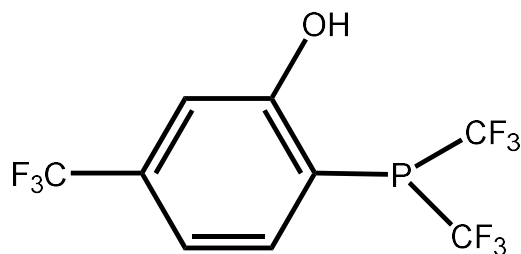


**$^{13}\text{C}$ - $^1\text{H}$  HSQC NMR spectrum of compound 19**



**$^{13}\text{C}$ - $^1\text{H}$  HMBC NMR spectrum of compound 19**

## Compound 20



**$^{31}\text{P}(^1\text{H})$  NMR spectrum of compound 20**

**$^{19}\text{F}$  NMR spectrum of compound 20**

**$^1\text{H}$  NMR spectrum of compound 20**

**$^{13}\text{C}(^1\text{H})$  NMR spectrum of compound 20**

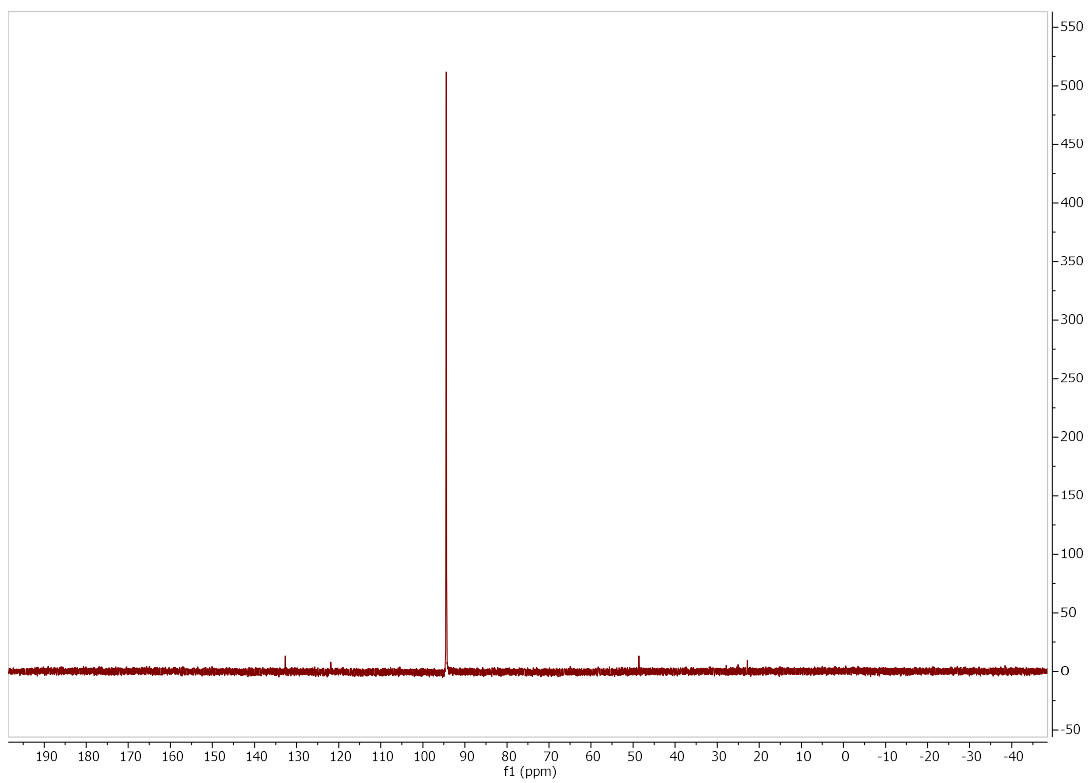
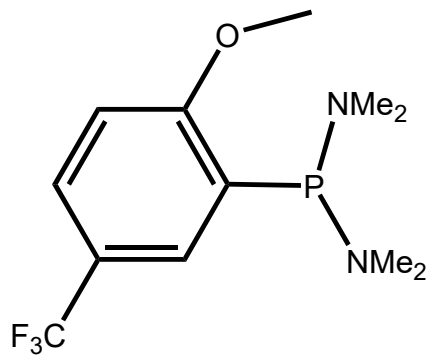
**$^1\text{H}-^1\text{H}$  COSY NMR spectrum of compound 20**

**$^{13}\text{C}-^1\text{H}$  HSQC NMR spectrum of compound 20**

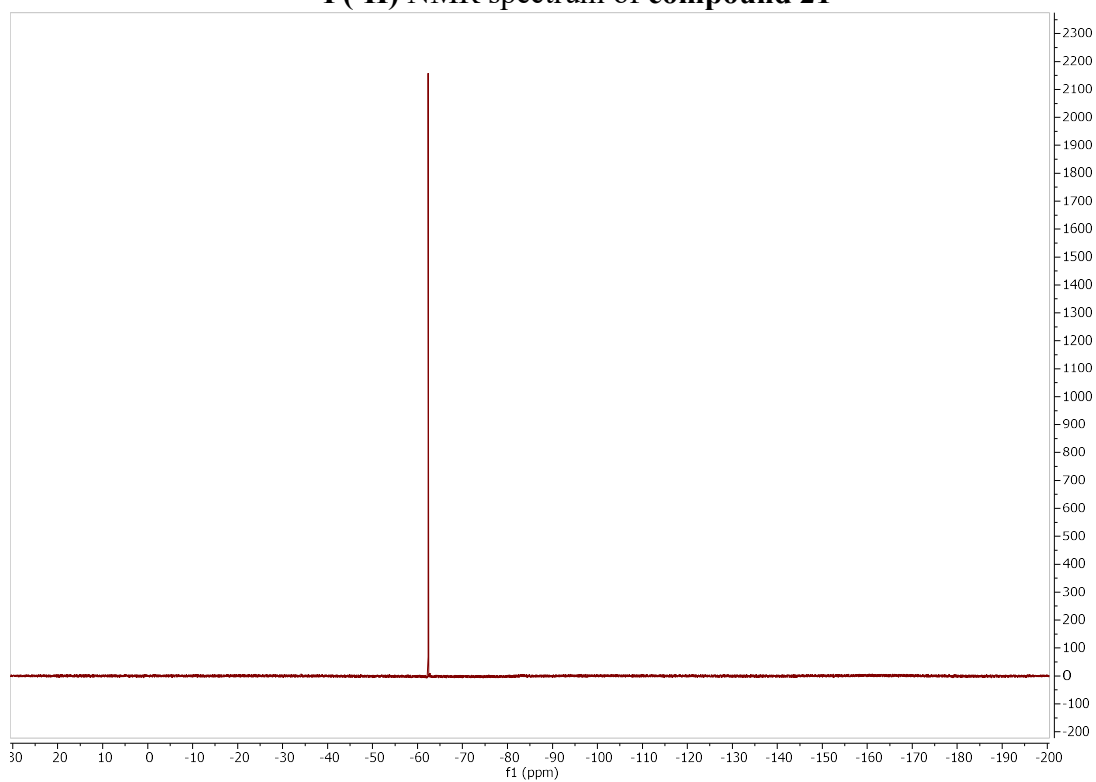
**$^{13}\text{C}-^1\text{H}$  HMBC NMR spectrum of compound 20**

# Compound 21

21



**$^{31}\text{P}(^1\text{H})$  NMR spectrum of compound 21**



**$^{19}\text{F}$  NMR spectrum of compound 21**

**$^1\text{H}$  NMR spectrum of compound 21**

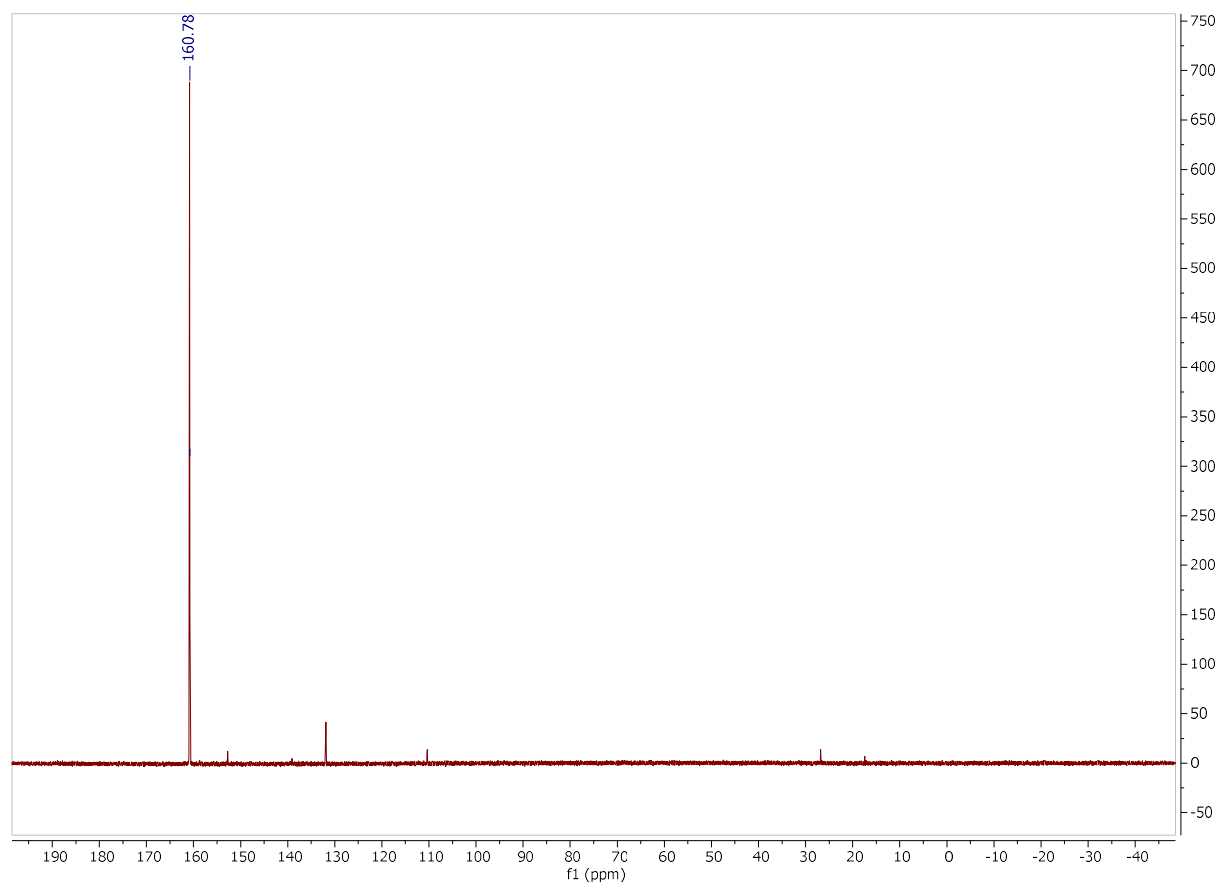
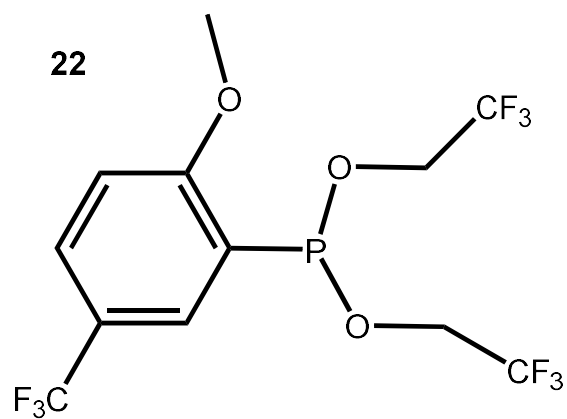
**$^{13}\text{C}(^1\text{H})$  NMR spectrum of compound 21**

**$^1\text{H}$ - $^1\text{H}$  COSY NMR spectrum of compound 21**

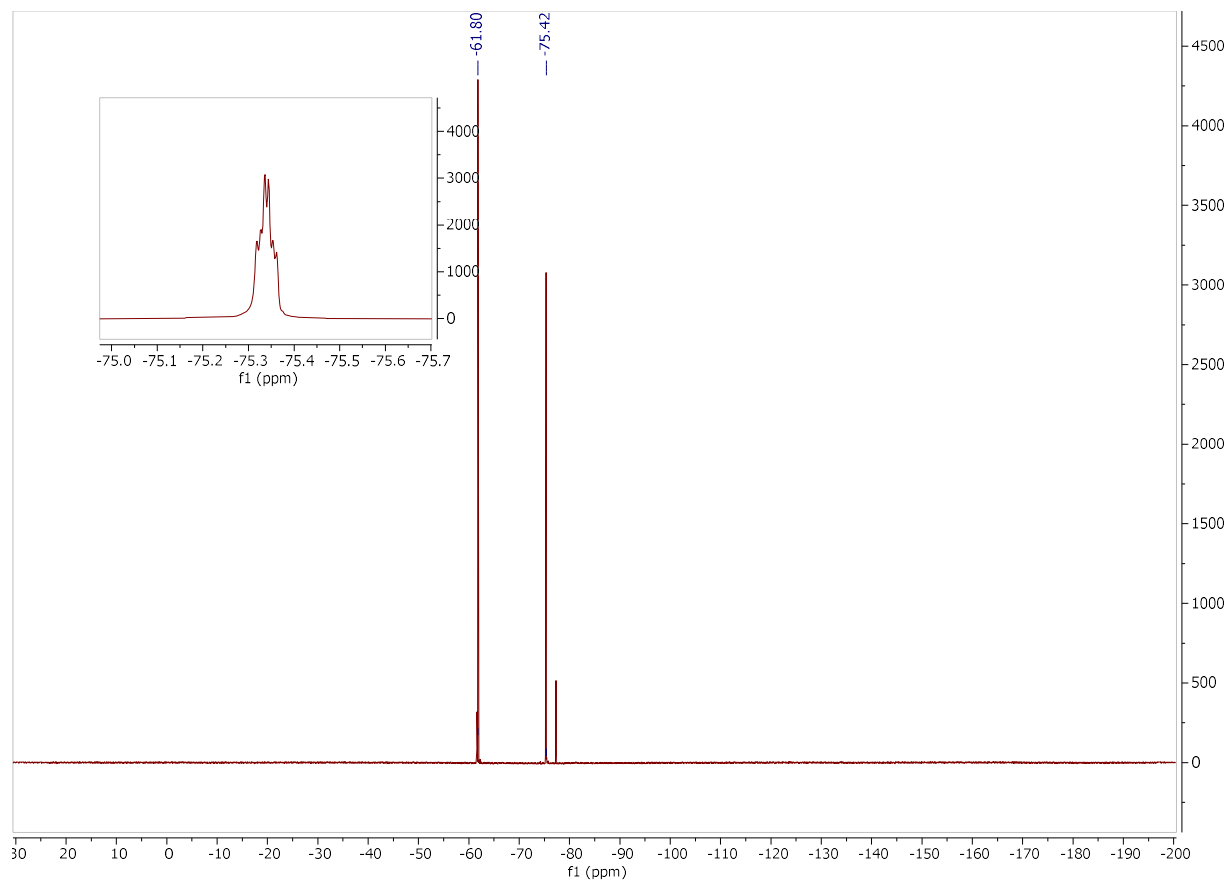
**$^{13}\text{C}$ - $^1\text{H}$  HSQC NMR spectrum of compound 21**

**$^{13}\text{C}$ - $^1\text{H}$  HMBC NMR spectrum of compound 21**

**Compound 22**

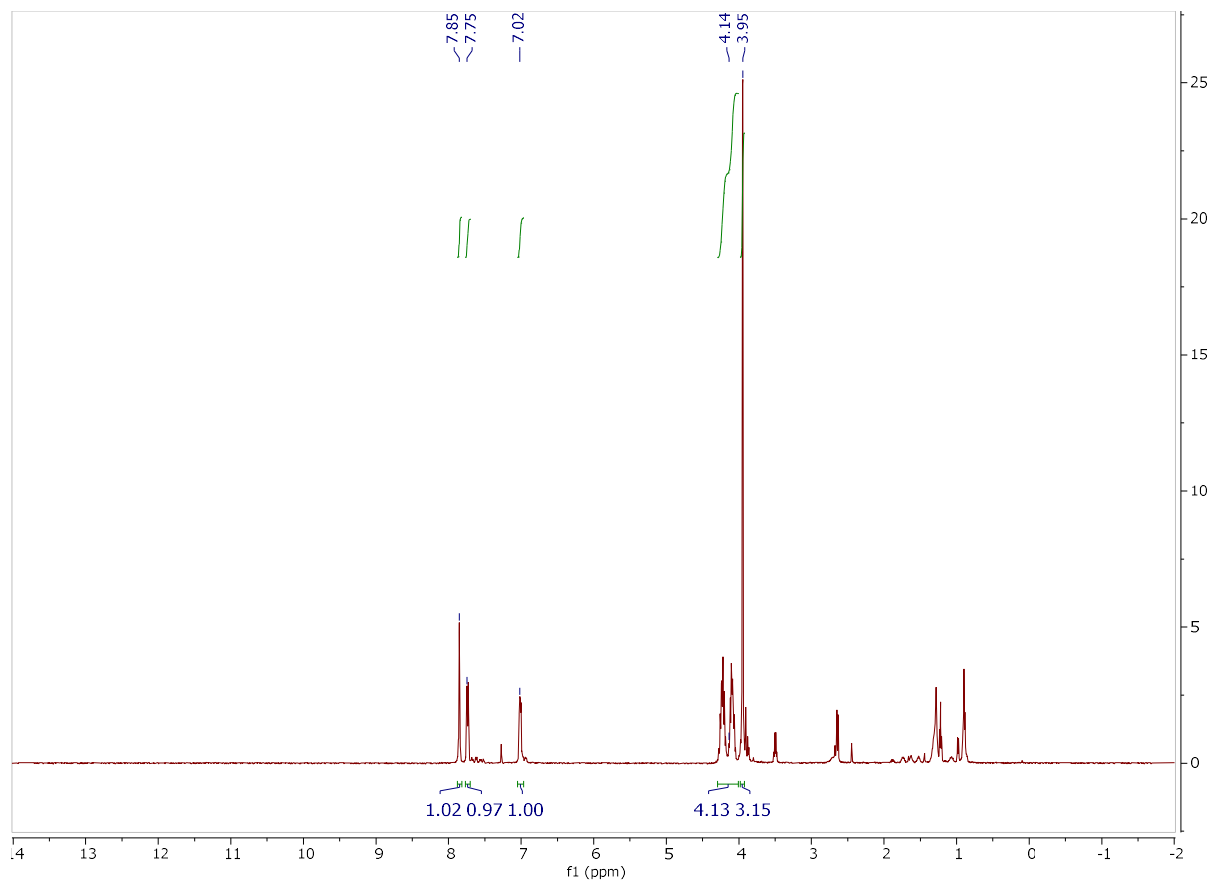


**<sup>31</sup>P(<sup>1</sup>H) NMR spectrum of compound 22**



**$^{19}\text{F}$  NMR spectrum of compound 22**





**$^1\text{H}$  NMR spectrum of compound 22**

**$^{13}\text{C}(^1\text{H})$  NMR spectrum of compound 22**

**$^1\text{H}$ - $^1\text{H}$  COSY NMR spectrum of compound 22**

**$^{13}\text{C}$ - $^1\text{H}$  HSQC NMR spectrum of compound 22**

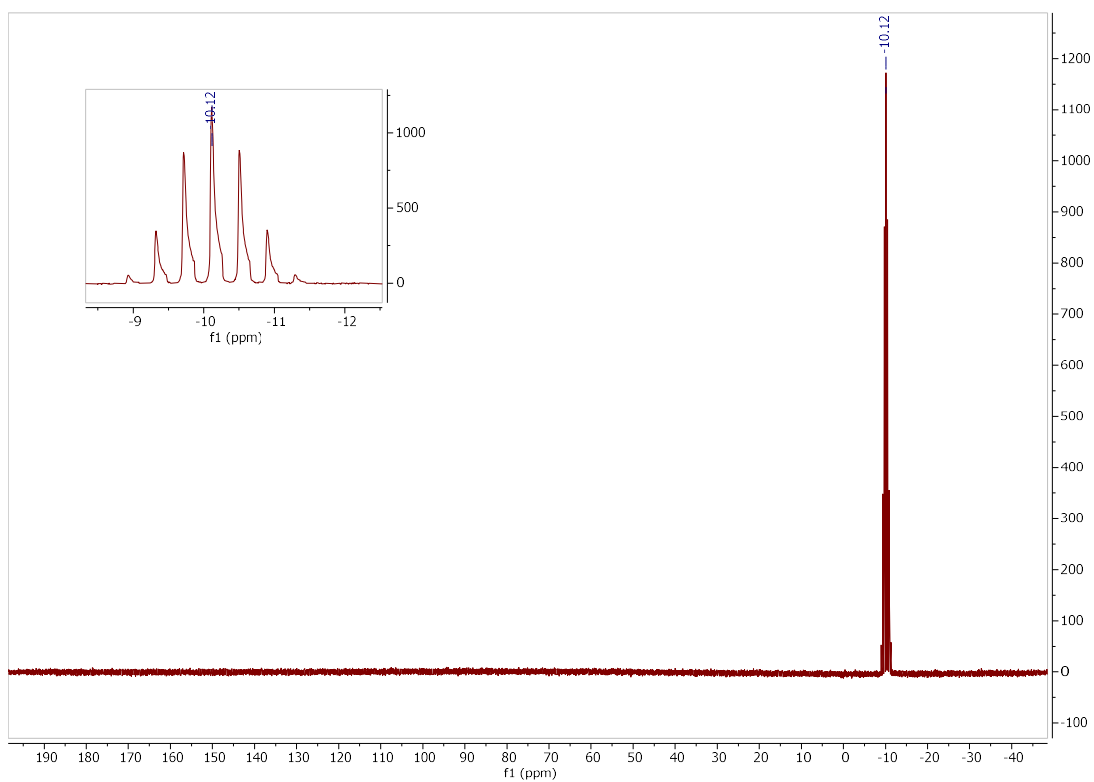
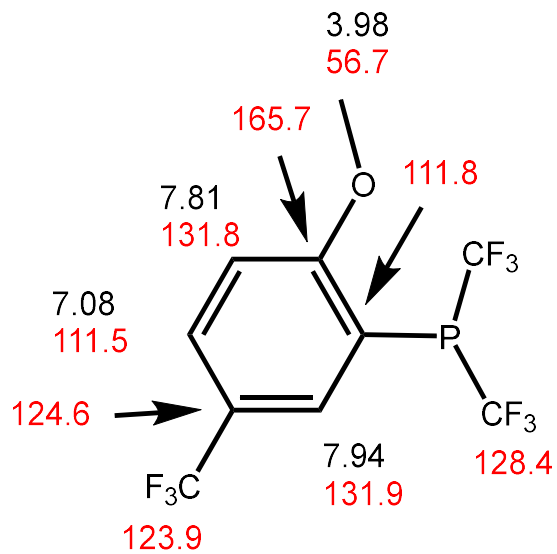
**$^{13}\text{C}$ - $^1\text{H}$  HMBC NMR spectrum of compound 22**

**Compound 23**

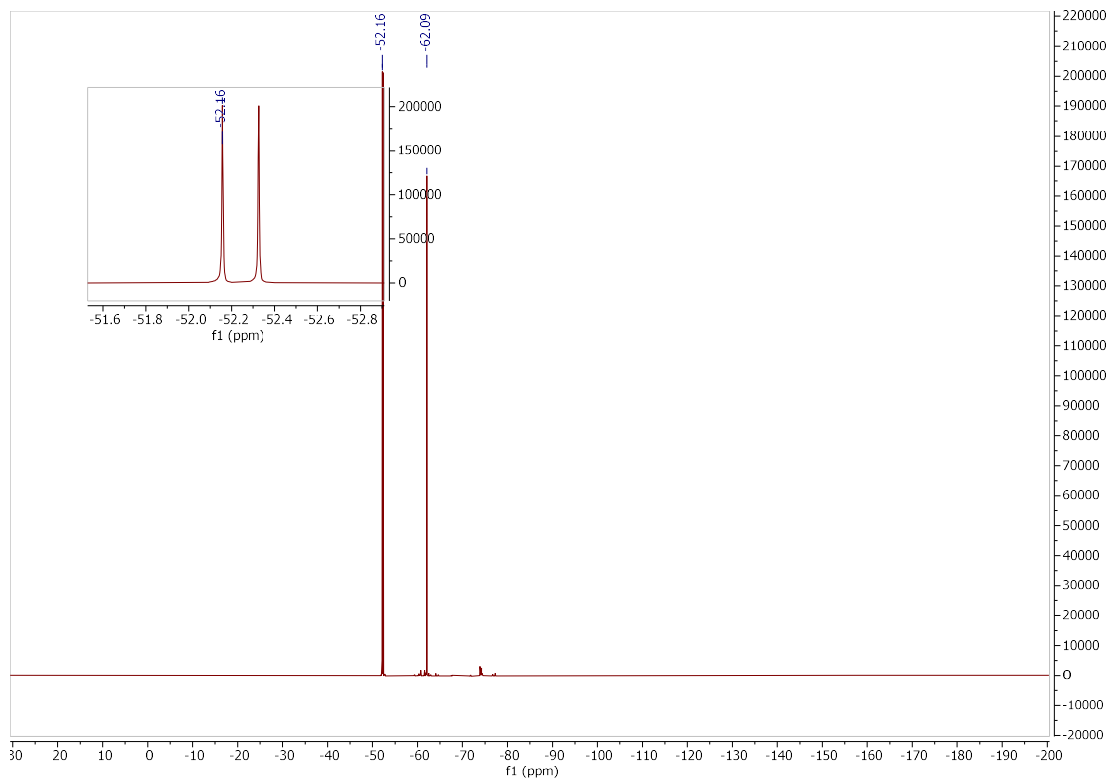
23

### Key HMBC Correlations

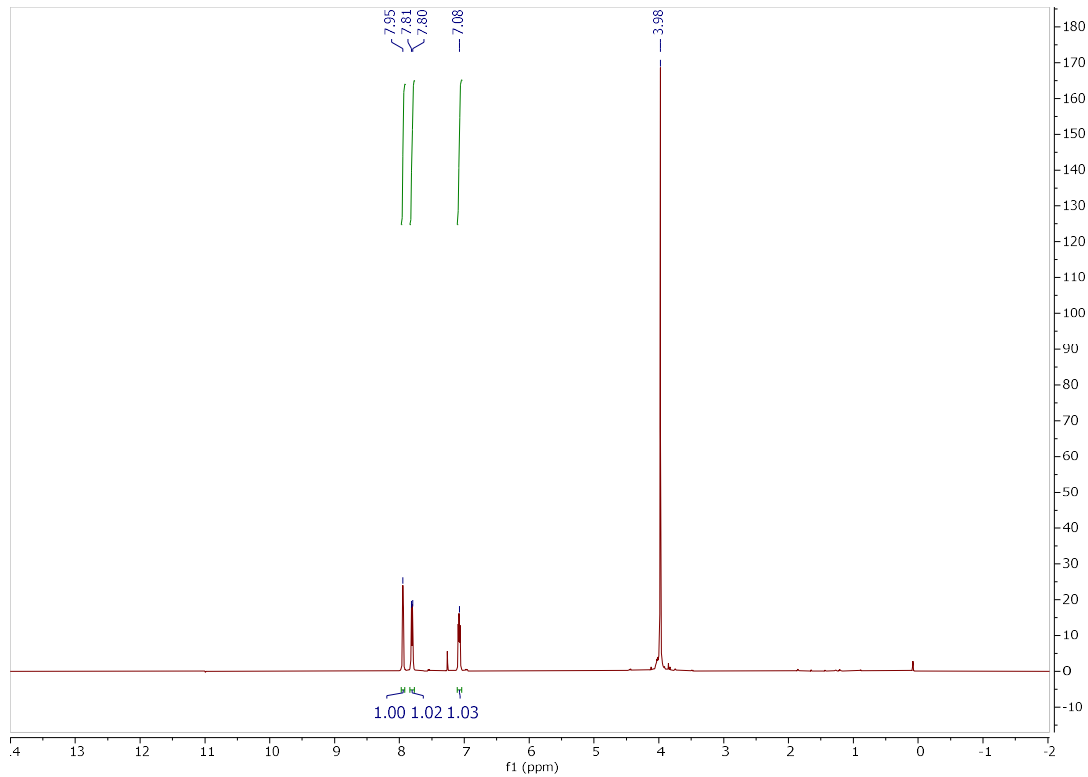
7.94: 165.7, 131.8, 124.6, 123.9,  
7.81: 165.7, 131.9, 123.9,  
7.08: 165.7, 131.8, 124.6,  
3.98: 165.7,



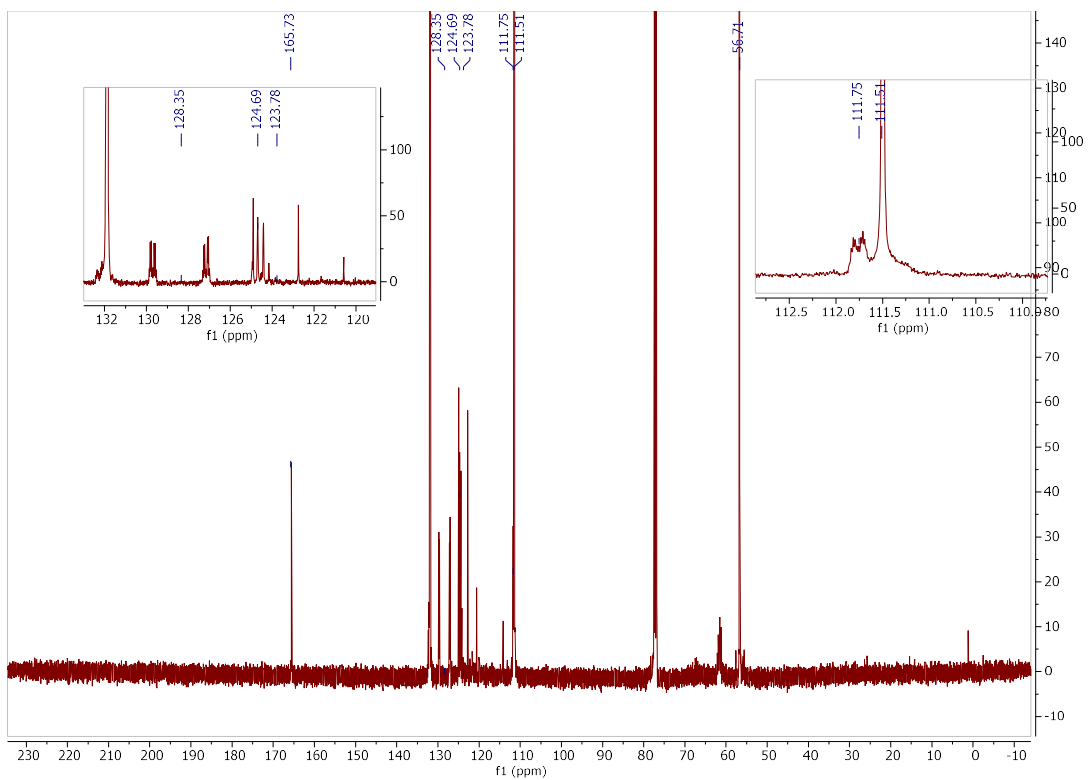
<sup>31</sup>P(<sup>1</sup>H) NMR spectrum of compound 23



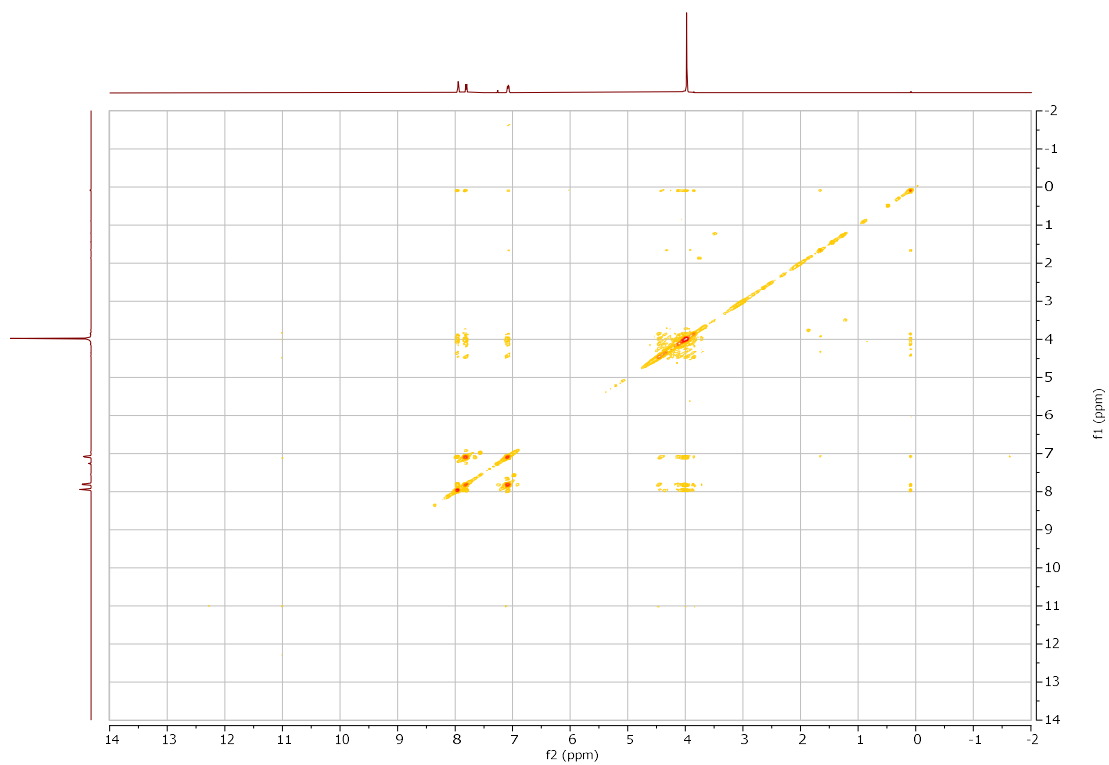
**$^{19}\text{F}$  NMR spectrum of compound 23**



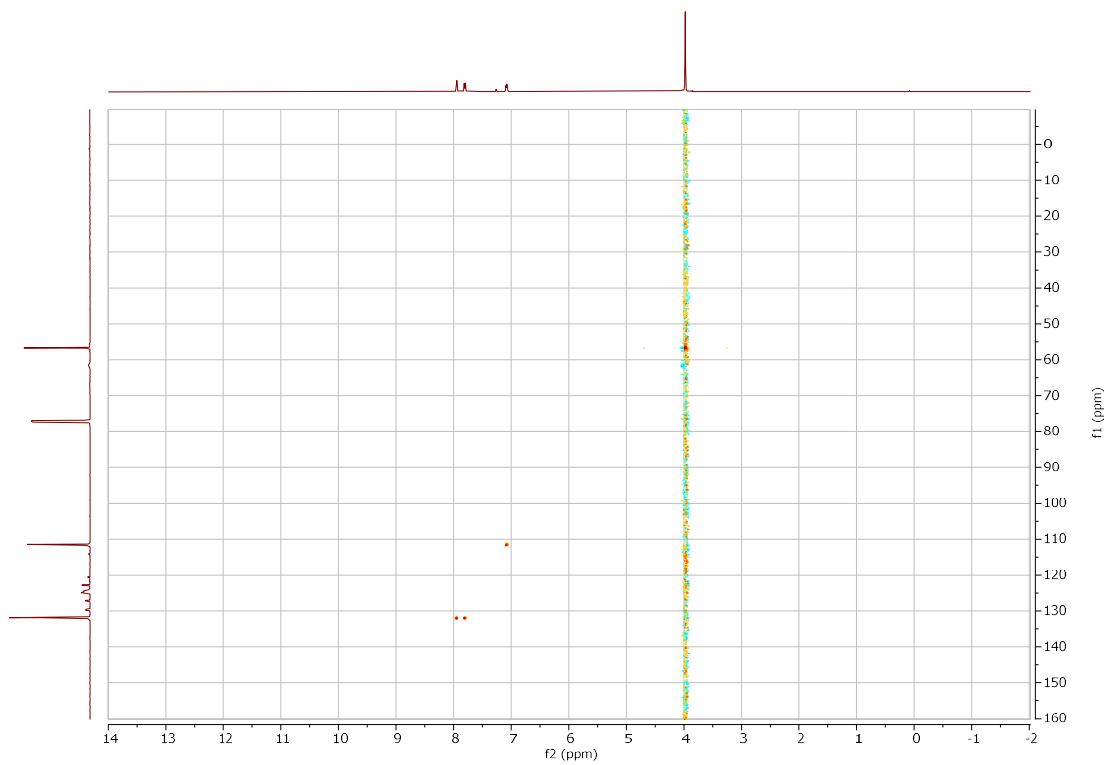
**$^1\text{H}$  NMR spectrum of compound 23**



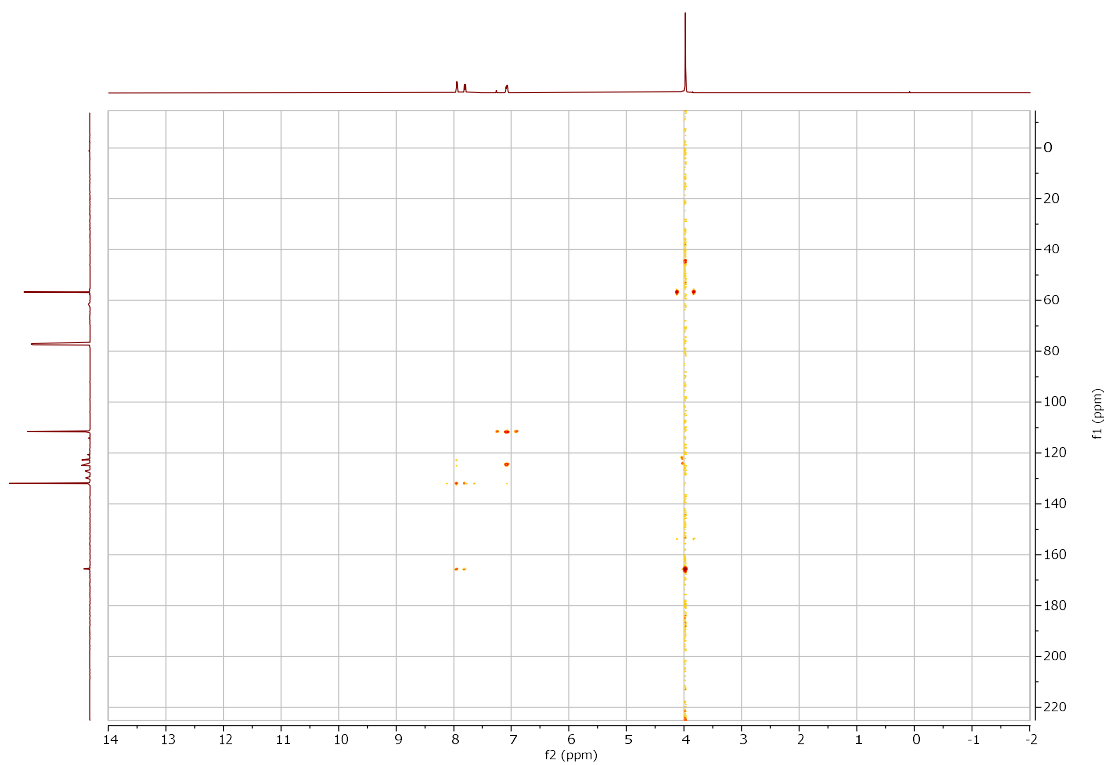
**$^{13}\text{C}(^1\text{H})$  NMR spectrum of compound 23**



**$^1\text{H}-^1\text{H}$  COSY NMR spectrum of compound 23**

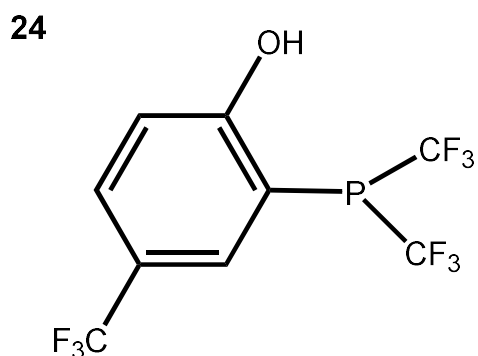


**$^{13}\text{C}$ - $^1\text{H}$  HSQC NMR spectrum of compound 23**



**$^{13}\text{C}$ - $^1\text{H}$  HMBC NMR spectrum of compound 23**

### Compound 24



$^{31}\text{P}(^1\text{H})$  NMR spectrum of compound 24

$^{19}\text{F}$  NMR spectrum of compound 24

$^1\text{H}$  NMR spectrum of compound 24

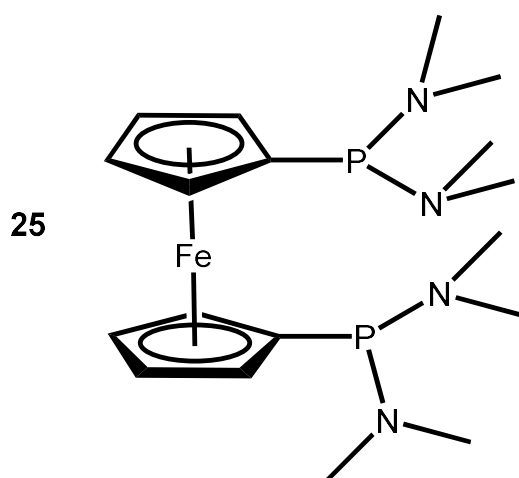
$^{13}\text{C}(^1\text{H})$  NMR spectrum of compound 24

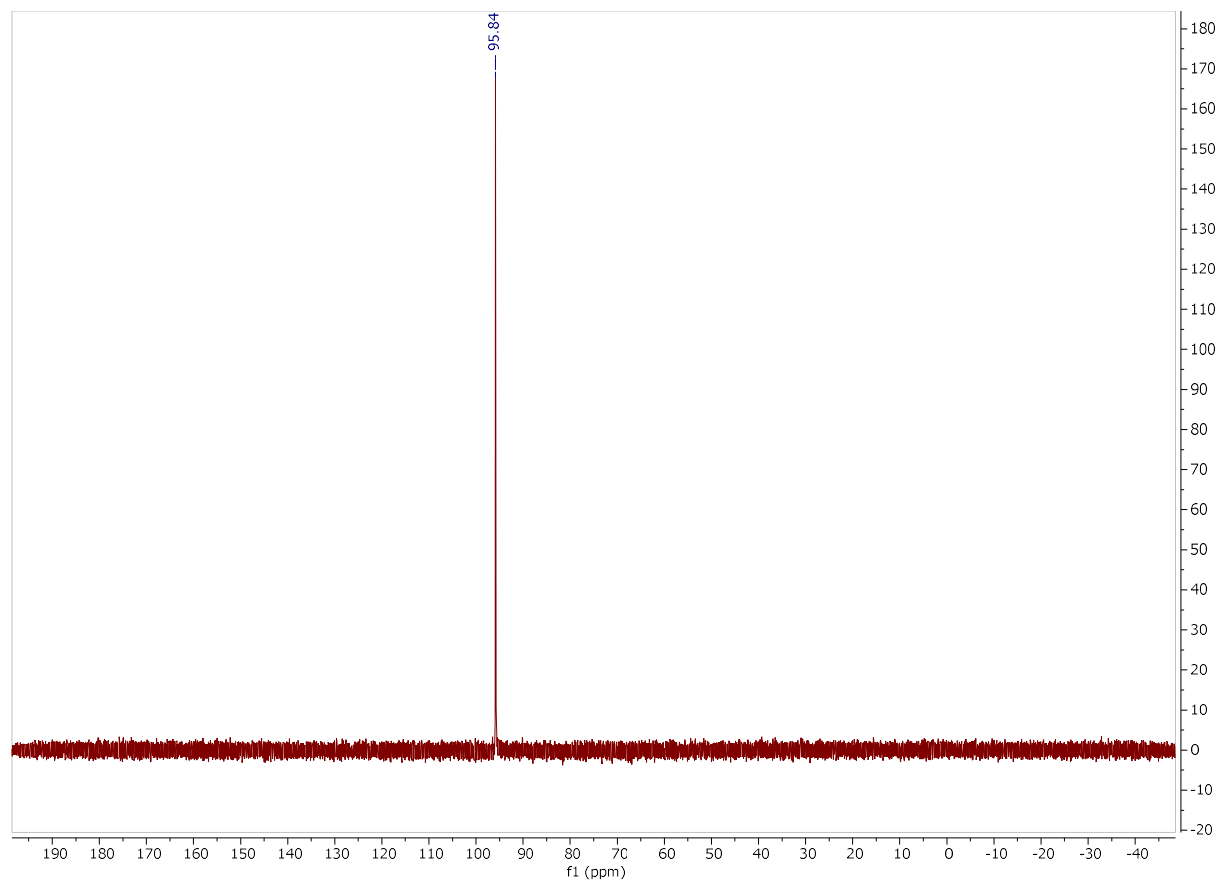
$^1\text{H}$ - $^1\text{H}$  COSY NMR spectrum of compound 24

$^{13}\text{C}$ - $^1\text{H}$  HSQC NMR spectrum of compound 24

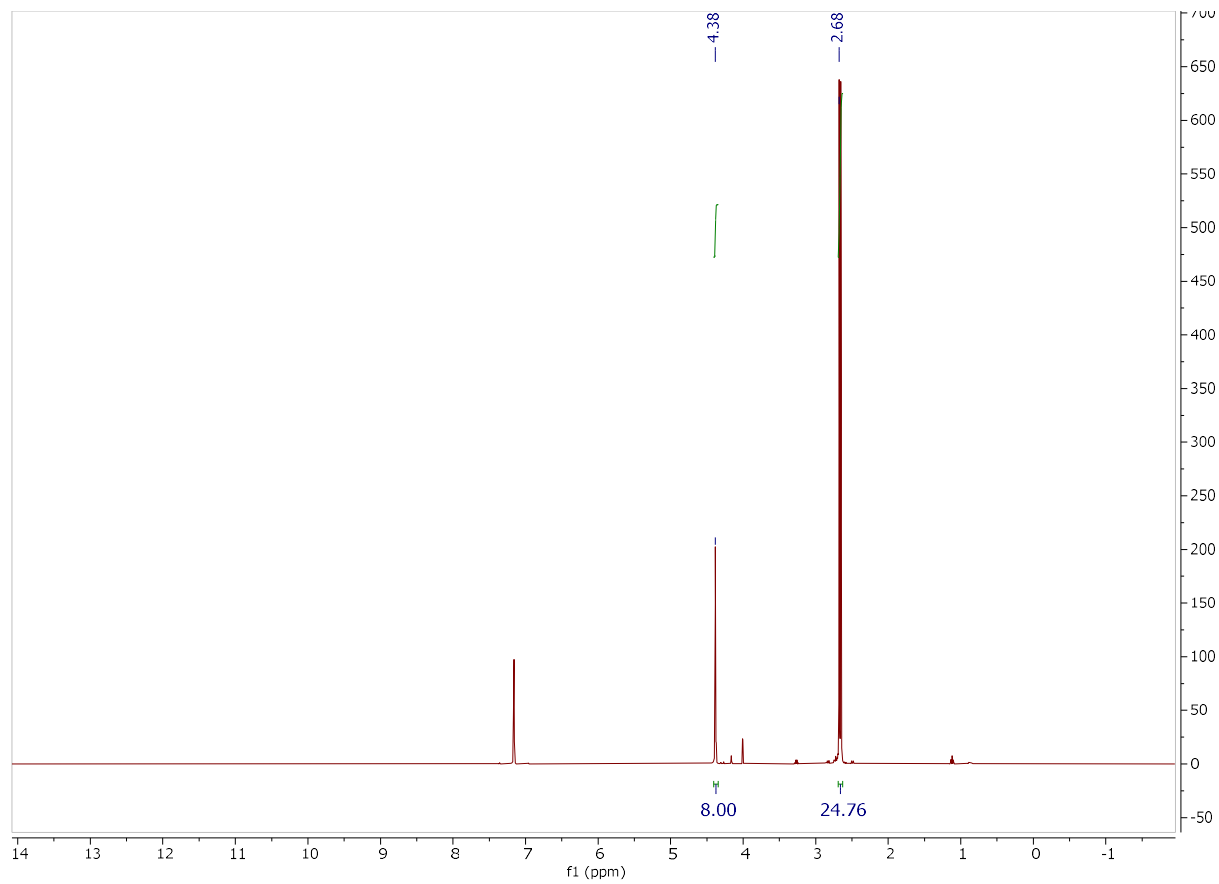
$^{13}\text{C}$ - $^1\text{H}$  HMBC NMR spectrum of compound 24

### Compound 25



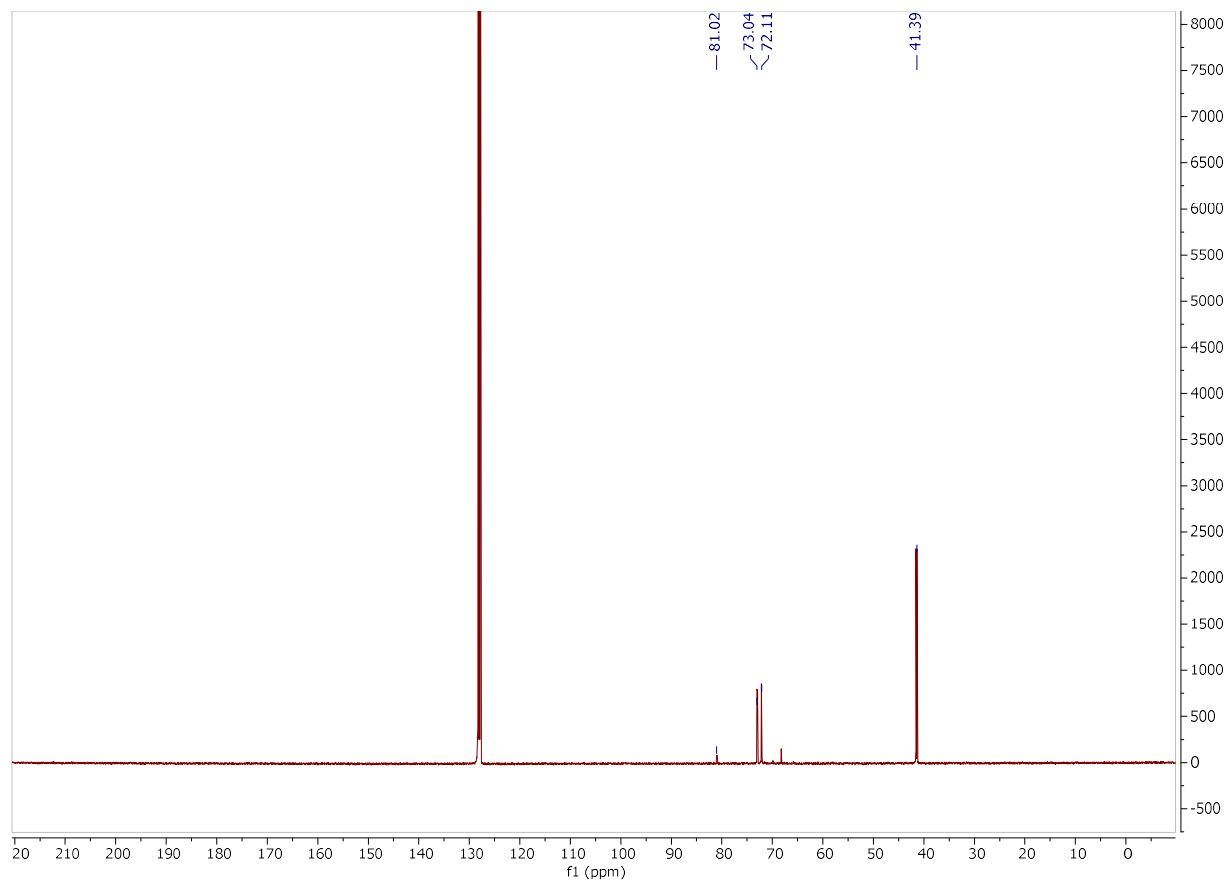


**$^{31}\text{P}$ ( $^1\text{H}$ ) NMR spectrum of compound 25**

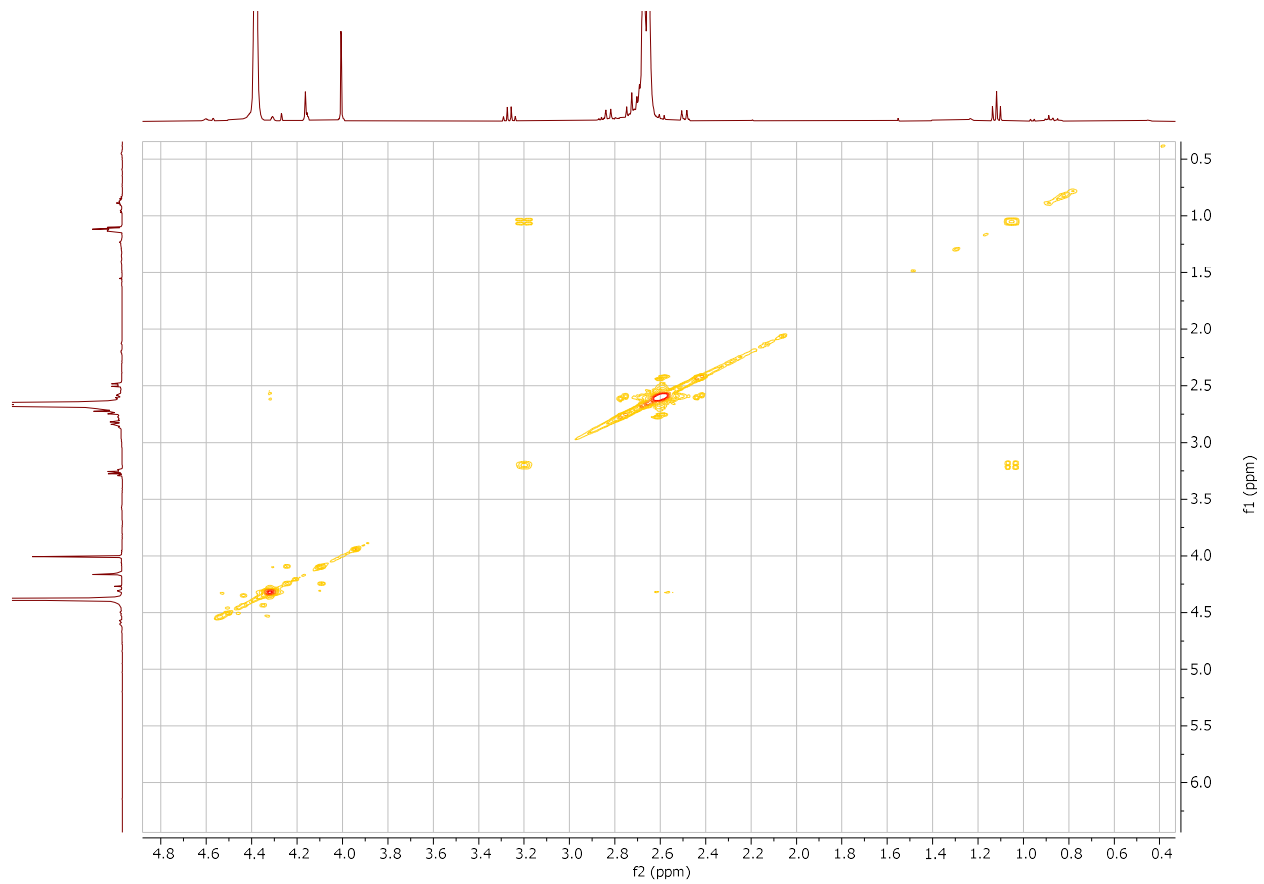


**$^1\text{H}$  NMR spectrum of compound 25**

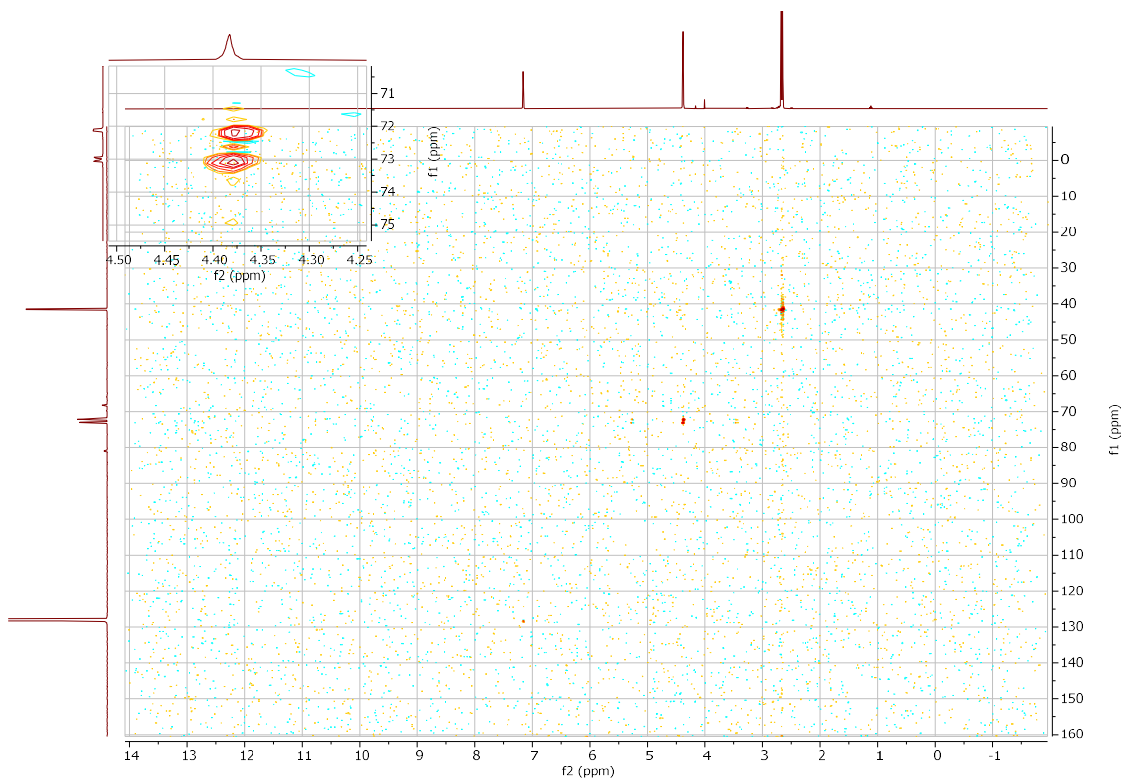




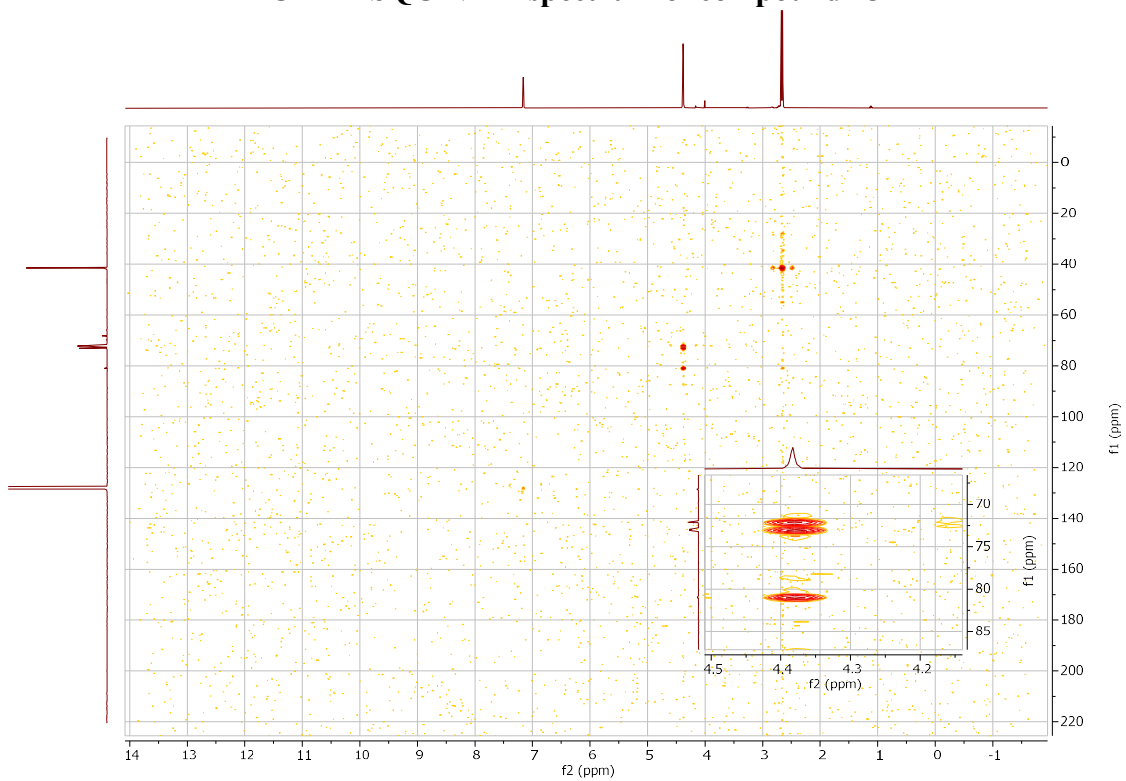
**$^{13}\text{C}$ ( $^1\text{H}$ ) NMR spectrum of compound 25**



**$^1\text{H}$ - $^1\text{H}$  COSY NMR spectrum of compound 25**

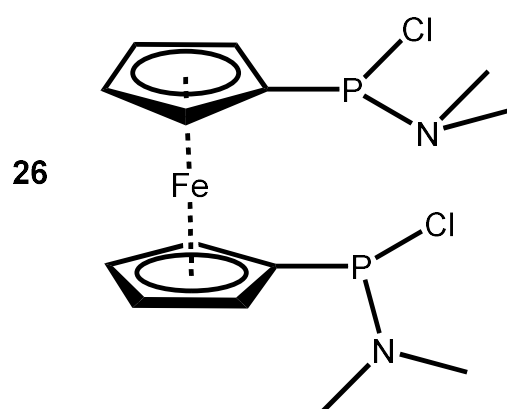


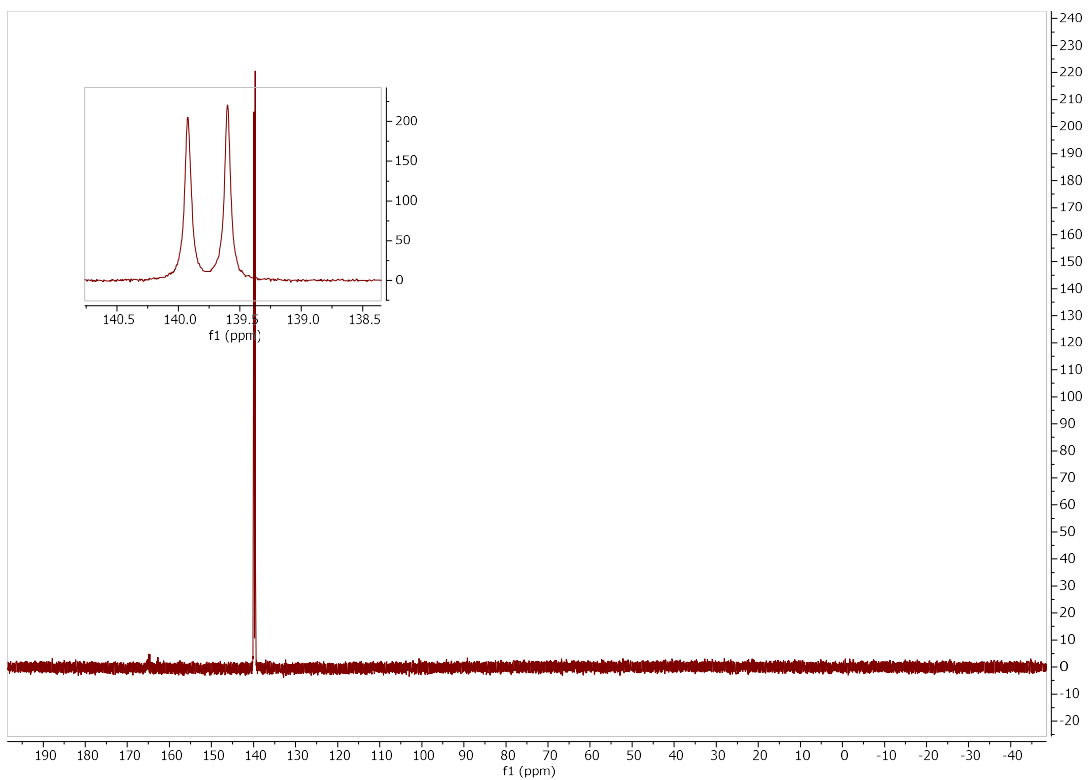
$^{13}\text{C}$ - $^1\text{H}$  HSQC NMR spectrum of compound 25



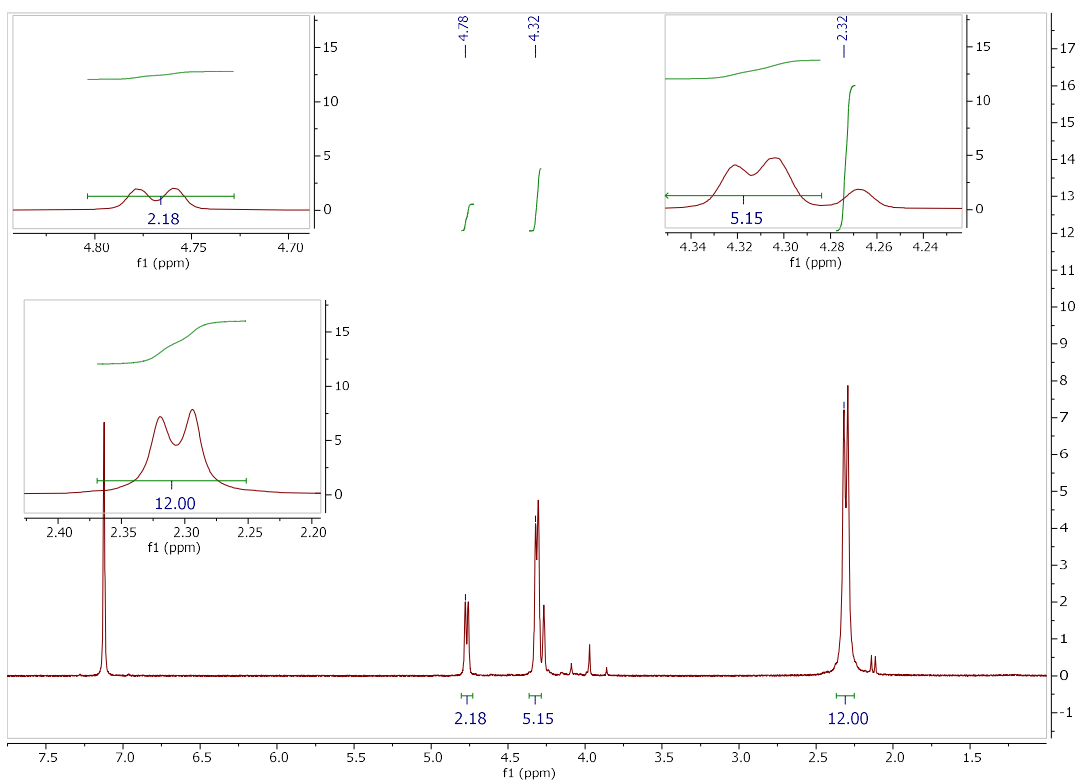
$^{13}\text{C}$ - $^1\text{H}$  HMBC NMR spectrum of compound 25

**Compound 26**





**$^{31}\text{P}(^1\text{H})$  NMR spectrum of compound 26**



**$^1\text{H}$  NMR spectrum of compound 26**

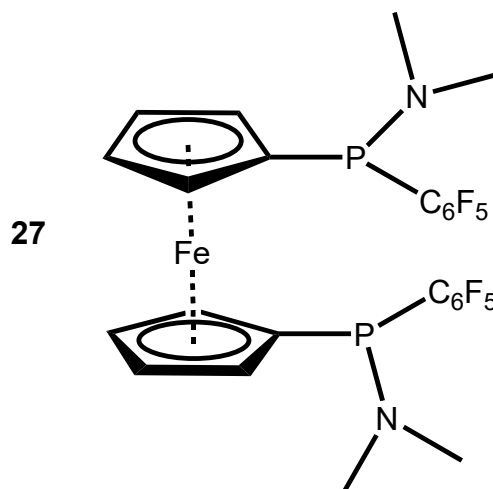
**$^{13}\text{C}(^1\text{H})$  NMR spectrum of compound**

**$^1\text{H}$ - $^1\text{H}$  COSY NMR spectrum of compound**

**$^{13}\text{C}$ - $^1\text{H}$  HSQC NMR spectrum of compound**

**$^{13}\text{C}$ - $^1\text{H}$  HMBC NMR spectrum of compound**

**Compound 27**



**$^{31}\text{P}(^1\text{H})$  NMR spectrum of compound 27**

**$^{19}\text{F}$  NMR spectrum of compound 27**

**$^1\text{H}$  NMR spectrum of compound 27**

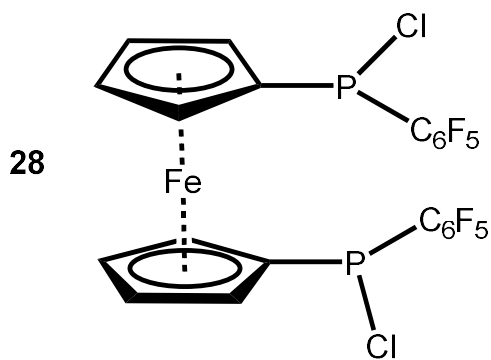
**$^{13}\text{C}(^1\text{H})$  NMR spectrum of compound 27**

**$^1\text{H}$ - $^1\text{H}$  COSY NMR spectrum of compound 27**

**$^{13}\text{C}$ - $^1\text{H}$  HSQC NMR spectrum of compound 27**

**$^{13}\text{C}$ - $^1\text{H}$  HMBC NMR spectrum of compound 27**

**Compound 28**



$^{31}\text{P}(^1\text{H})$  NMR spectrum of compound 28

$^{19}\text{F}$  NMR spectrum of compound 28

$^1\text{H}$  NMR spectrum of compound 28

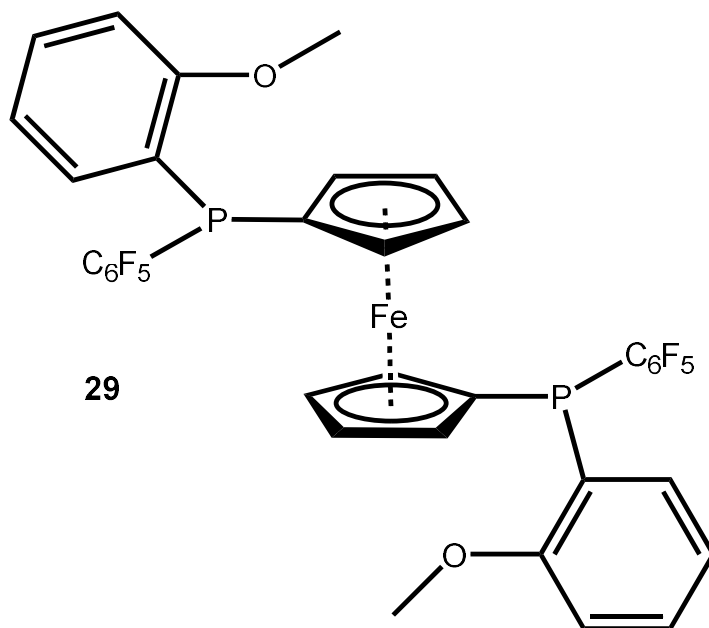
$^{13}\text{C}(^1\text{H})$  NMR spectrum of compound 28

$^1\text{H}$ - $^1\text{H}$  COSY NMR spectrum of compound 28

$^{13}\text{C}$ - $^1\text{H}$  HSQC NMR spectrum of compound 28

$^{13}\text{C}$ - $^1\text{H}$  HMBC NMR spectrum of compound 28

### Compound 29



**$^{31}\text{P}(^1\text{H})$  NMR spectrum of compound 29**

**$^{19}\text{F}$  NMR spectrum of compound 29**

**$^1\text{H}$  NMR spectrum of compound 29**

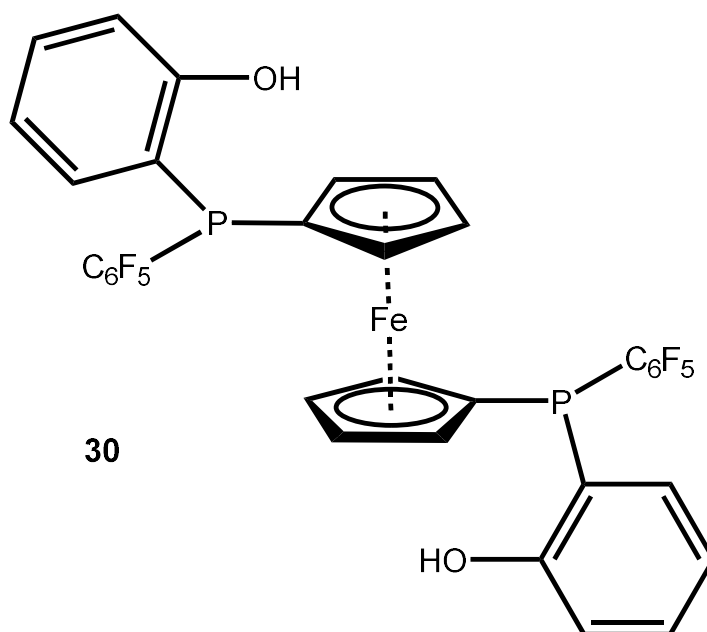
**$^{13}\text{C}(^1\text{H})$  NMR spectrum of compound 29**

**$^1\text{H}$ - $^1\text{H}$  COSY NMR spectrum of compound 29**

**$^{13}\text{C}$ - $^1\text{H}$  HSQC NMR spectrum of compound 29**

**$^{13}\text{C}$ - $^1\text{H}$  HMBC NMR spectrum of compound 29**

**Compound 30**



**$^{31}\text{P}(^1\text{H})$  NMR spectrum of compound 30**

**$^{19}\text{F}$  NMR spectrum of compound 30**

**$^1\text{H}$  NMR spectrum of compound 30**

**$^{13}\text{C}(^1\text{H})$  NMR spectrum of compound 30**

**$^1\text{H}$ - $^1\text{H}$  COSY NMR spectrum of compound 30**

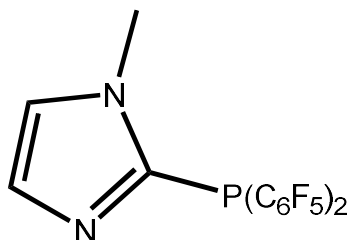
**$^{13}\text{C}$ - $^1\text{H}$  HSQC NMR spectrum of compound 30**

**$^{13}\text{C}$ - $^1\text{H}$  HMBC NMR spectrum of compound 30**



**Compound 31**

**31**



**<sup>31</sup>P(<sup>1</sup>H) NMR spectrum of compound 31**

**<sup>19</sup>F NMR spectrum of compound 31**

**<sup>1</sup>H NMR spectrum of compound 31**

**<sup>13</sup>C(<sup>1</sup>H) NMR spectrum of compound 31**

**<sup>1</sup>H-<sup>1</sup>H COSY NMR spectrum of compound 31**

**<sup>13</sup>C-<sup>1</sup>H HSQC NMR spectrum of compound 31**

**<sup>13</sup>C-<sup>1</sup>H HMBC NMR spectrum of compound 31**

1. Tolmachev, A. A.; Yurchenko, A. A.; Merculov, A. S.; Semenova, M. G.; Zarudnitskii, E. V.; Ivanov, V. V.; Pinchuk, A. M., Phosphorylation of 1-alkylimidazoles and 1-alkylbenzimidazoles with phosphorus(III) halides in the presence of bases. *Heteroatom Chemistry* **1999**, *10* (7), 585-597.
2. Clarkson, G. J.; Ansell, J. R.; Cole-Hamilton, D. J.; Pogorzelec, P. J.; Whittell, J.; Wills, M., Bis(diazaphospholidine) ligands for asymmetric hydroformylation: use of ESPHOS and derivatives based on ferrocene and diarylether backbones. *Tetrahedron: Asymmetry* **2004**, *15* (11), 1787-1792.